UNIVERSITAT DE BARCELONA

Targeted therapies in CLL

New drugs against CLL recurrent mutations

Neus Giménez Carabaza

TARGETED THERAPIES IN CLL
New drugs against CLL recurrent mutations

Neus Giménez Carabaza

Barcelona 2019

Doctoral Thesis

DOCTORAL PROGRAMME IN BIOMEDICINE

UNIVERSITAT DE **BARCELONA**

2016-2019

University of Barcelona - Faculty of Medicine

TARGETED THERAPIES IN CLL

New drugs against CLL recurrent mutations

Doctoral thesis presented by:

Neus Giménez Carabaza

Institut d'Investigacions Biomèdiques August Pi i Sunyer (IDIBAPS)

Experimental therapies in lymphoid neoplasms

<table>
<tr><td>Neus Gimenez Carabaza
Doctorand</td><td>Dolors Colomer Pujol
Thesis director</td><td>Elias Campo Güerri
Thesis director
Thesis tutor</td></tr>
</table>

Barcelona, 2019

INDEX

LIST OF TABLES AND FIGURES

FIGURES

TABLES

ABBREVIATIONS

LIST OF ABBREVIATIONS

ABC-DLBCL	Diffuse large B-cell lymphoma activated B-cell type
APC	Antigen presenting cell
Allo-HSCT	Allogenic hematopietic stem cell transplantation
ATM	Ataxia-telangiectasia mutated
BAKs	BCR associated kinases
BCL2	B-cell leukemia/lymphoma 2
BCR	B-cell receptor
BiTE®	Bi-specific T-cell engager
BL	Burkkit lymphoma
BM	Bone marrow
BMSC	Bone marrow stromal cell
BRAF	B-rapidly accelerated fibrosarcoma
BRAFi	BRAF inhibitors
BTK	Bruton's tyrosine kinase
cAMP	Cyclic adenosine monophosphate
CAR	Chimeric antigen receptor
CCL	C-C motif chemokine ligand
CDR	Common deleted region
CIT	Chemoimmunotherapy
CK	Complex karyotype
CLL	Chronic lymphocytic leukemia
CLL-IPI	CLL international prognostic index
CNS	Central nerve system
CTL	Cytotoxic T-lymphocyte
DAMPs	Danger-associated molecular patterns
DC	Dendritic cells
DLBCL	Diffuse large B-cell lymphoma
DUSP	Dual-specificity phosphatase
ERK	Extracellular signal-regulated kinase
Eμ-TCL1	*Eμ*-T-cell leukemia /lymphoma 1 transgenic mouse
Eμ-TCL1 AT	*Eμ*-T-cell leukemia /lymphoma 1 transgenic mouse adoptive transfer
EBV	Epstein-Barr virus
ECOG	Eastern cooperative oncology group
FasL	Fas ligand
FC	Fludarabine, cyclophosphamide
FCR	Fludarabine, cyclophosphamide, rituximab
FDA	Food and drug administration
FDC	Follicular dendritic cells
FISCH	Fluorescence *in situ* hybridization

FL	Follicular lymphoma
FSL-1	Diacylated lipoproteins
GC	Germinal center
GCB-DLBCL	Diffuse large B-cell lymphoma germinal center B-cell type
GTP	Guanosine triphosphate
HCC	Hepatocellular carcinoma
HCL	Hairy cell leukemia
HLA	Human leukocyte antigen
HMGCR	3-Hydroxy-3-methylglutaryl coenzyme A reductase
HSCT	Hematopoietic stem cell transplantation
I	Intermediate
ICAM	Intercellular adhesion molecule 1
Ig	Immunoglobulin
IGHV	Immunoglobulin variable regions of the heavy chain
IGLV	Immunoglobulin variable regions of the light chain
IL	Interleukin
IMID	Immunomodulatory drug
IPI	International prognostic index
IRAK	Interleukin 1 receptor associated kinase
ITGAL	Integrin alpha L
ITGB2	Integrin beta chain-2
iwCLL	International workshop on CLL
JAK-STAT3	Janus kinase/signal transducer and activator of transcription 3
LDT	Lymphocyte doubling time
LFA-1	Lymphocyte function-associated antigen 1
LN	Lymph node
LPS	Lipopolysaccharides
M-	Mutated
mAb	Monoclonal antibody
MALT	Extranodal marginal zone lymphoma of mucosa-associated lymphoid tissue
MAPK	Mitogen-associated protein kinase
MBL	Monoclonal B-cell lymphocytosis
MCL	Mantle cell lymphoma
MDR	Minimal deleted region
MDSC	Myeloid-derived suppressor cell
MEK	Mitogen-activated ERK kinase
MEKi	MEK inhibitors
ML	Memory-like
MYD88	Myeloid differentiation primary response 88
NF-κB	Nuclear factor kappa B

NGS	Next generation sequencing
NK	Natural killer
NL	Naive-like
NLC	Nurse-like cells
NOD	Non-obese diabetic
NSG	Non SCID Gamma
ODN	Oligodesoxinucleótidos
ORR	Overall response rate
OS	Overall survival
Pam3CSK4	Triacylated lipoproteins
PAMPs	Pathogen-associated molecular patterns
PB	Peripheral blood
PBMC	Peripheral blood mononuclear cell
PCM	Plasma cell myeloma or multiple myeloma
PD-1	Programmed cell death protein 1
PD-L1 / 2	Programmed cell death ligand 1 / 2
PDX	Patient-derived xenograft
PFS	Progression-free survival
PI3Kδ	Phosphoinositol-3-kinase δ isoform
RAS	Retrovirus-associated DNA sequences
R/R	Relapsed/Refractory
RTK	Receptor tyrosine kinase
SCID	Severe combined immunodeficiency
SF3B1	Splicing factor 3B subunit 1
SHM	Somatic hypermutations
SLL	Small lymphocytic lymphoma
SMI	Small molecules inhibitor
SMZL	Splenic marginal zone lymphoma
SOS	Son of seven less
SP	Spleen
TCL1	T-cell leukemia /lymphoma 1
TIR	Toll/interleukin-1 receptor
TLR	Toll like receptors
TME	Tumor microenvironment
TP53	Tumor protein 53
Treg	Regulatory T-cells
TRIF	TIR-domain-containing adapter-inducing interferon-β
TTFT	Time to first treatment
UM-	Unmutated
US	United states

V(D)J	Variable (diversity) join
VCAM1	Vascular cell adhesion protein 1
WES	Whole-exome sequencing
WHO	World health organization
WM	Waldenstrom's macroglobulinemia

INTRODUCTION

1. B-CELL LYMPHOID NEOPLASMS

B-cell lymphoid neoplasms are clonal expansions of B lymphocytes at various stages of differentiation in peripheral blood (PB), bone marrow (BM) and secondary lymphoid organs (spleen (SP), lymph nodes (LN) and extranodal tissues). Mature B-cell lymphoid neoplasms comprise over 90% of lymphoid neoplasms worldwide.[1]

The current World Health Organization (WHO) classification, revised in 2016, categorizes mature B-cell lymphoid neoplasms, in more than 35 distinct entities, primarily on the basis of morphology, immunophenotype, genetic alterations and clinical features.[2, 3]

Table 1. **2016 WHO classification of mature B-cell lymphoid neoplasms.**[3]

- Chronic lymphocytic leukemia (CLL) / small lymphocytic lymphoma (SLL)
- Diffuse large B-cell lymphoma (DLBCL)
    - Germinal center B-cell type (DLBCL-GCB)
    - Activated B-cell type (DLBCL-ABC)
- Plasma cell myeloma; multiple myeloma (PCM)
- Extranodal marginal zone lymphoma of mucosa-associated lymphoid tissue (MALT)
- Splenic marginal zone lymphoma (SMZL)
- Follicular lymphoma (FL)
- Mantle cell lymphoma (MCL)
- B-cell prolymphocytic leukemia
- Hairy cell leukemia (HCL)
- Monoclonal B-cell lymphocytosis (MBL)
- Splenic lymphoma/leukemia, unclassifiable
- Splenic diffuse red pulp small B-cell lymphoma
- Hairy cell leukemia-variant
- Lymphoplasmacytic lymphoma
    - Waldenstrom's Macroglobulinemia (WM)
- Monoclonal gammopathy of undetermined significance, IgM
- Monoclonal gammopathy of undetermined significance IgG/A
- Solitary plasmacytoma of bone
- Extraosseus plasmacytoma
- Monoclonal immunoglobulin deposition diseases
- Nodal marginal zone lymphoma
- Pediatric-type follicular lymphoma
- T-cell/histiocyte-rich large B-cell lymphoma
- Primary DLBCL of the central nervous system
- Primary cutaneous DLBCL, leg-type
- Epstein-Barr virus –positive DLBCL, NOS
- Epstein-Barr virus –positive mucocutaneus ulcer
- DLBCL associated with chronic inflammation
- Lymphomatoid granulomatosis
- Primary mediastinal (thymic) large B-cell lymphoma
- Intravascular large B-cell lymphoma
- Primary effusion lymphoma
- Anaplastic lymphoma kinase-positive large B-cell lymphoma
- Plasmablastic lymphoma
- Human herpes virus 8 DLBCL, NOS
- Burkitt lymphoma (BL)
- Burkkit-like lymphoma with 11q aberration
- High-grade B-cell lymphoma, with MYC and BCL2 and/or BCL6 rearrangements
- High-grade B-cell lymphoma, NOS
- B-cell lymphoma, unclassifiable, with features intermediate between DLBCL and classical Hodgkin lymphoma

1.1.   B-LYMPHOCYTES ROLE IN THE IMMUNE SYSTEM

The immune system is composed by the early innate and the later adaptive immunity.

The innate immunity consists of cellular and biochemical defense mechanisms that are in place even before infection and are poised to respond rapidly to infections. It is a first line non-specific defense against common structures of pathogens. The effector cells are natural killer cells, macrophages, neutrophils, dendritic cells, mast cells, basophils and eosinophils.

The adaptive (acquired) immunity is a second-line defense, which is specific to the pathogen presented, being the B and T lymphocytes the main players. B lymphocytes participate in a broad range of immunological functions, including antigen presentation, immune regulation, and provision of a cellular and humoral pre-immune repertoire, as well as immune memory.[4]

1.2. B-LYMPHOCYTES DEVELOPMENT AND DIFFERENTIATION

B-cell development is a sequential process that allows for the mature expression of the B-cell receptor (BCR). The BCR is composed of an immunoglobulin (Ig) molecule, usually IgM and IgD, and the heterodimer CD79a/CD79b.[5,6] Igs are generated following five main steps: V(D)J (variable(diversity)join) recombination, selection, clonal expansion, somatic hypermutations and class switching, Figure 1.[5]
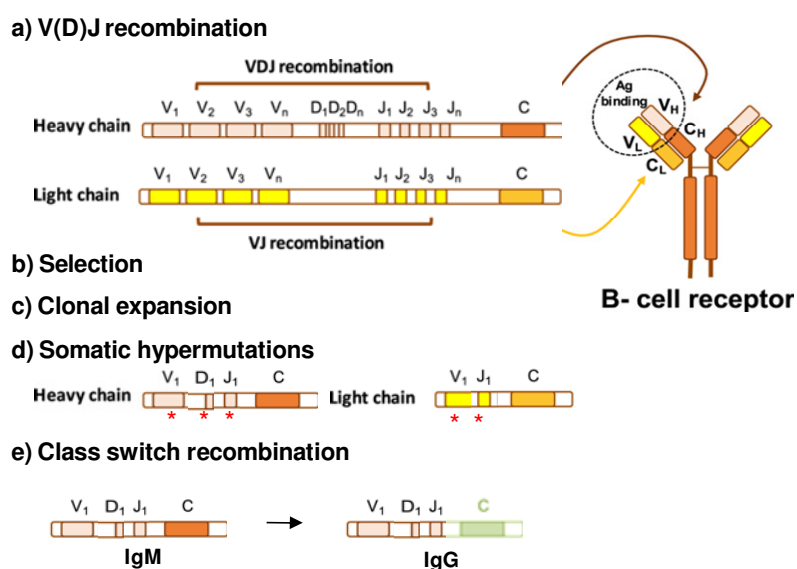
Figure 1. B-cell development. Recombination of V(D)J genetic regions of the heavy chain and VJ regions of the light chain allows generation of the variable regions of the heavy and light chain of the mature BCR. The high variability of the BCRs is in part due to the large number of V, D, and J gene regions of both Ig chains. The BCRs are selected for binding antigen (positive selection), and not to recognize autoantigens (negative selection). After clonal expansion in the germinal center (GC) and acquisition of somatic hypermutations they undergo to immunoglobulin (Ig) class switch recombination. The IgH constant regions μ (IgM) and δ (IgD) are substituted by either γ, ε, or α IgH, generating IgG, IgE, and IgA isotypes, which are involved in responses to viruses and bacteria (IgG), parasites (IgE), and mucosal microbes (IgA). V: variable; D: diversity; J: join, C: constant; H: heavy; L: light. Modified from *Hacken et al, Leukemia, 2019*.[5]

Hematopoietic stem cells, placed in the BM, undergo a differentiation process by randomly combining a V, a D and a J segment in the heavy chain (and later V/J in the light chain) from their Ig gene. Huge number of different antigen specific antibodies can be generated due to the multiple copies of each gene segment and their different possible recombinations.[6] Naive B cells that express functional BCR interact with CD4^{+} T cells and accessory cells, which aggregate to form follicles that become germinal centers (GCs) in the secondary lymphoid tissues. The B cells enter the dark zone of the GC, where they experience rapid proliferation and somatic hypermutation (SHM) in the genes encoding the Ig variable regions of the heavy chain (IGHV) and the light chain (IGLV). As they pass through the light zone, the B cells interact with follicular dendritic cells, macrophages and helper T cells. The BCR suffer a positive selection and may undergo Ig class-switch recombination, allowing the generation of BCRs that carry heavy chains of different isotypes than IgM and IgD. They are also screened no to recognize autoantigens (negative selection).[5, 7, 8]

1.3. ORIGIN OF B-CELL LYMPHOID NEOPLASMS

B-cell lymphoma pathogenesis is a multi-step process involving various genetic and epigenetic lesions, viruses, and distorted microenvironment antigenic interactions. When B cells undergo malignant transformation, they usually retain key features of their cell of origin.[2, 8]

As shown in Figure 2, most B-cell lymphomas are derived from GCs or post-GCs B cells. The vigorous proliferation of the B cells in the GCs and the SHM and class switching processes strongly increase the risk for a B cell to undergo malignant transformation.

Lymphomas are derived from errors occurring during these differentiation stages of B-cells, and they are subsequently classified based on the differentiation stage at which they seem to be "frozen". Since many products of the genes end up affecting convergent pathways, combinations of hits can lead to a phenotypically similar lymphomas, as the resulting deregulation of cellular processes is identical.[9]
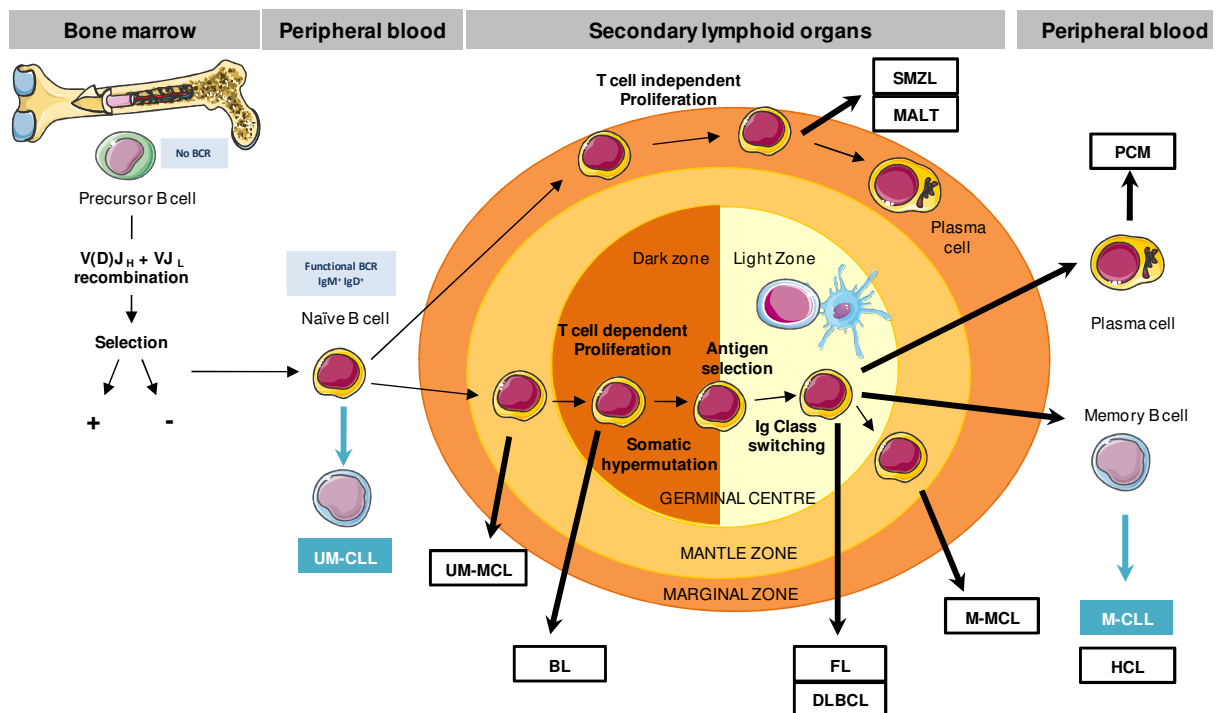
Figure 2. Cell of origin of mature B-cell lymphoid neoplasms. UM-CLL, chronic lymphocytic leukemia with no IGHV mutations; UM-MCL, mantle cell lymphoma with no IGHV mutations; MALT, mucosa-associated lymphoid tissue lymphoma; SMZL, splenic marginal zone lymphoma; FL, follicular lymphoma; BL, Burkitt lymphoma; DLBCL, diffuse large B-cell lymphoma; M-MCL, mantle cell lymphoma with IGHV mutations, M-CLL, chronic lymphocytic leukemia with IGHV mutations; PCM, multiple myeloma, HCL: hairy cell leukemia.[9]

2. CHRONIC LYMPHOCYTIC LEUKEMIA

2.1. CHARACTERISTICS AND EPIDEMIOLOGY

Chronic lymphocytic leukemia (CLL) is the most common leukemia in adults in the western countries. The incidence of CLL varies between individuals in different geographical regions and ranges from <0.01% of individuals in eastern Asia to 0.06% in Europe and the United States (US). The US National Cancer Institute estimated the number of new cases to be 6.3 per 10^5 men and 3.3 per 10^5 women per year.[10] The risk of developing CLL is about two-times higher for men than for women and increases with age. It typically occurs in elderly patients, being the median age at diagnosis of 70 years.[11, 12]

2.2. DIAGNOSIS AND CLINICAL PRESENTATION
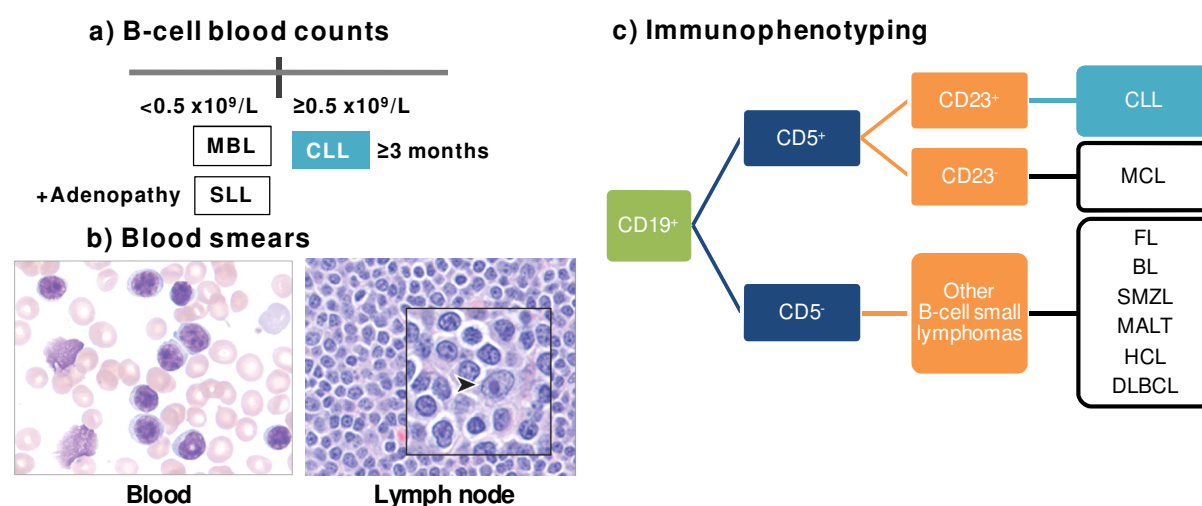
Figure 3. CLL diagnosis. CLL, chronic lymphocytic leukemia; MBL, monoclonal B-cell lymphocytosis; SLL, small lymphocytic lymphoma; MCL, mantle cell lymphoma; FL, follicular lymphoma; BL, Burkitt lymphoma; SMZL, splenic marginal zone lymphoma; MALT, mucosa-associated lymphoid tissue lymphoma; HCL: hairy cell leukemia; DLBCL, diffuse large B-cell lymphoma. Blood images are from *Nabhan and Rosen, Jama, 2014.*[11]

CLL diagnosis is based on the following markers[11-14] (summarized in Figure 3):

a) **B-cell blood counts** (in the PB)

- CLL: ≥5x10^6 B-cells/mL with the phenotype of CLL for at least 3 months.

- Monoclonal B-cell lymphocytosis (MBL): <5x10^6 B-cells/mL with the phenotype of CLL in the absence of lymphadenopathy. MBL progress to CLL is 1-2%/year.

- Small lymphocytic lymphoma (SLL): <5x10^6 B-cells/mL with the phenotype of CLL in the presence of lymphadenopathy. The diagnosis should be confirmed by histopathological evaluation of a LN biopsy.

b) Blood smears

B leukemia cells in the blood are small mature lymphocytes with a narrow border of cytoplasm and a dense nucleus lacking discernible nucleoli and having partially aggregated chromatin. Gumprecht nuclear shadows or smudge cells are also characteristic (Figure 3b). These cells may be admixed with larger or atypical cells, cleaved cells, or prolymphocytes.

c) Immunophenotyping

CLL B lymphocytes are identified as a clonal B-cell population carrying the cell surface antigens CD5, CD19 and CD23 (Figure 3c). Each clone of leukemia cells is restricted to expression of either kappa or lambda Ig light chains (Figure 4).[11]
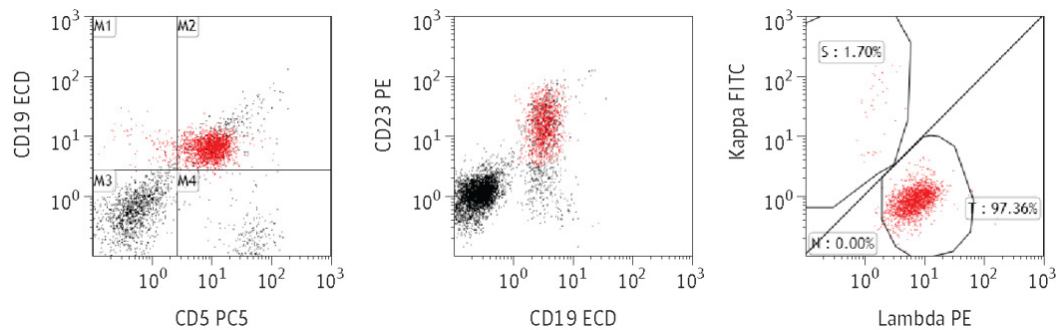
Figure 4. CLL immunophenotype. Images by flow cytometry from *Nabhan and Rosen, Jama, 2014*; in red a CLL clone.[11]

The levels of surface CD20 and CD79b are characteristically low compared to those found on normal B cells.[13]

2.2.1. Richter transformation

Analogous to other low-grade lymphoproliferations, CLL can transform into Richter syndrome, a large B-cell lymphoma with an aggressive behaviour that has an annual incidence of 0.5% among all patients with CLL.[14]

2.3. ORIGIN

The cellular origin of CLL is still controversial. CLL is a neoplasm of mature B lymphocytes but the earliest changes may already occur in hematopoietic stem cells primed for B-cell clonal differentiation, where common CLL genetic alterations have been found. The immunogenetic analyses of the BCR indicate that antigen selection may play a crucial role.[12]
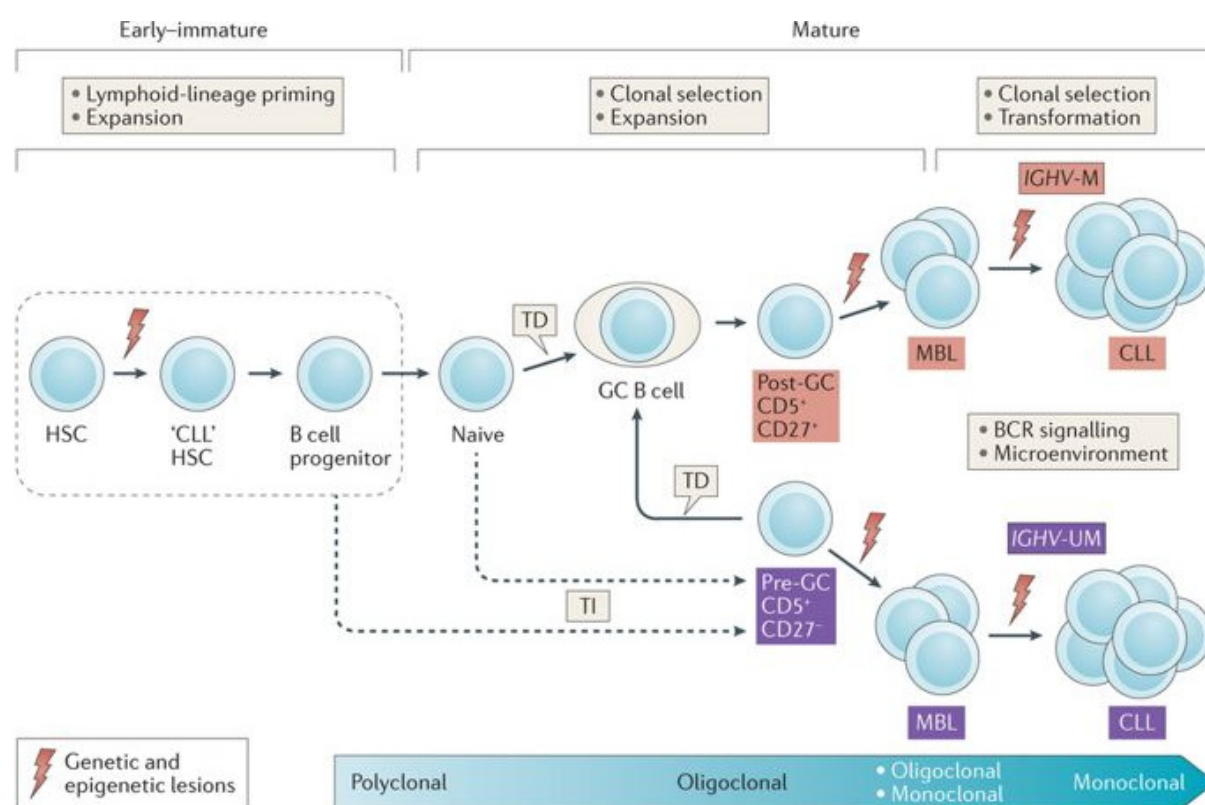
Figure 5. The cellular origin of CLL.[12]

As shown in Figure 2 and 5, there are two subtypes of CLL regarding their cell of origin. Gene expression profiling studies have suggested that unmutated IGHV (IGHV UM) emerges from a pre–GC CD5$^+$CD27$^-$ B cells prior to experiencing SHM, whereas mutated IGHV (IGHV M) derives from a CD5$^+$CD27$^+$ post–GC memory B cell.[15]

The pathogenesis of the two entities integrates genetic susceptibility, interactions between tumor cells and their microenvironment, and acquired genetic and epigenetic alterations, among others (Figure 6).[5, 16] The cut-off to distinguish between IGHV UM and IGHV M was established at 98% of sequence homology for IGHV genes compared to germline genes.[17]
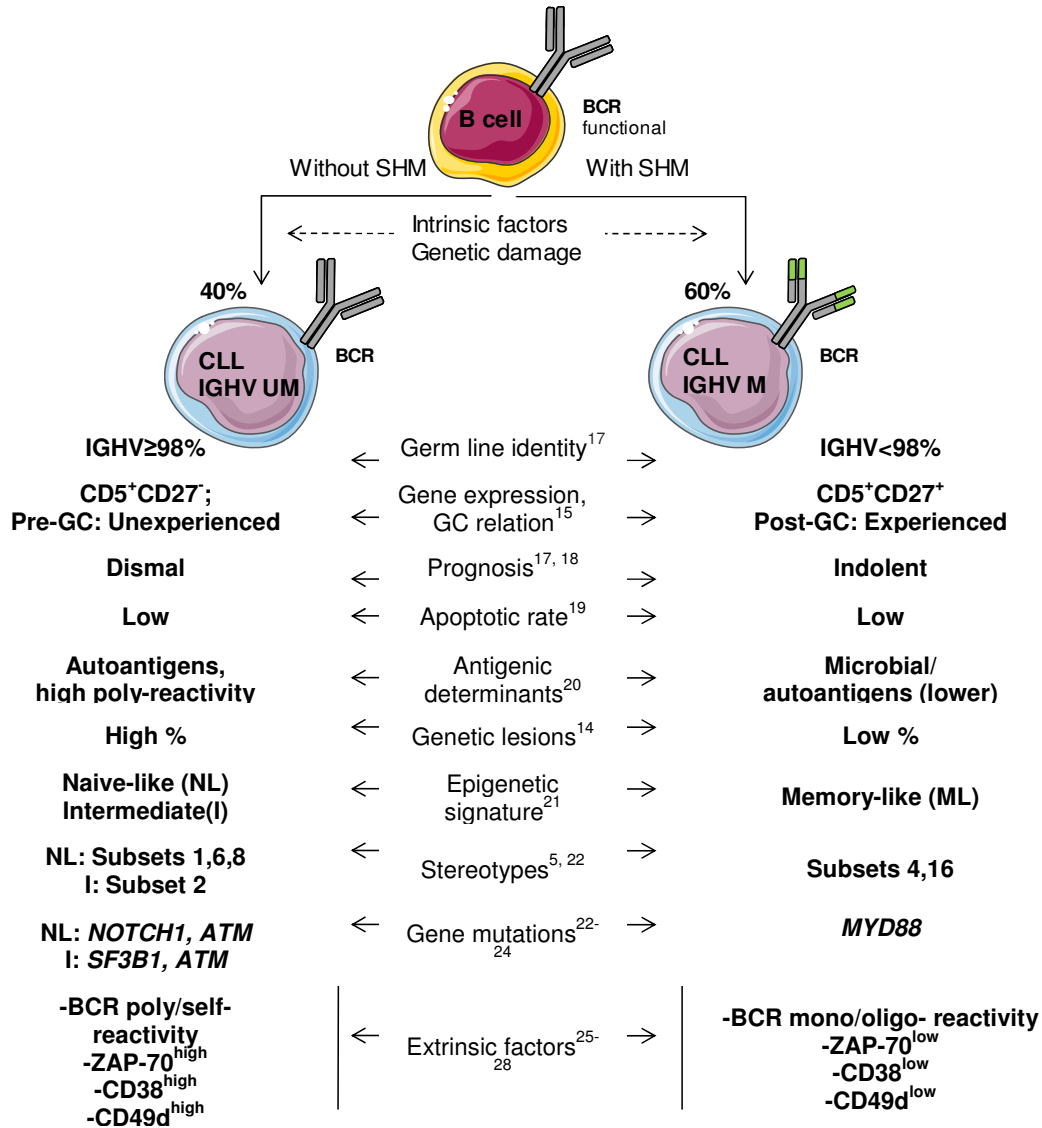
Figure 6. IGHV mutational status in CLL. CLL patients can be categorized into two main subsets (IGHV UM and IGHV M) based on the germline identity (IGHV M <98%).[17] This two subsets differ in many characteristics: the gene expression related to germinal center (GC) relation (IGHV UM is Pre-GC and CD5$^+$CD27$^-$),[15] the prognosis (IGHV UM is dismal[17, 18] with a low apoptotic rate)[19] and the antigenic determinants (IGHV UM is sensitive to autoantigens with high poly-reactivity while IGHV M is more sensitive to microbial)[20]. The risk of genetic lesions is higher in IGHV UM[14], which is related to gene mutations like *NOTCH1*, *ATM* and *SF3B1*.[22-24] The epigenetic signature of IGHV UM is naive-like or intermediate while IGHV M is memory-like.[21] Stereotype's subsets 1,2,6 and 8 are predominant in IGHV UM and subsets 4 and 16 in IGHV M.[5, 22] Regarding extrinsic factors, IGHV UM have BCR self-reactivity and have higher levels of ZAP-70, CD38 and CD49 than IGHV M.[25-28] SHM, Somatic hypermutations; BCR, B-cell receptor.

2.4. GENETICS

Genetic alterations in CLL include chromosomal and genomic alterations.

2.4.1. Chromosomal alterations

Approximately 80% of CLL patients carry at least one of the four common chromosomal alterations:[29] a deletion in the long arm of chromosome 13 (del13q14), trisomy 12, a deletion in the long arm of chromosome 11 (del11q22-q23) or a deletion in the short arm of chromosome 17 (del17p13).[16] The *tumor protein 53* (*TP53*) gene is located on the short arm of chromosome 17[30-32] whereas the *ataxia-telangiectasia mutated (ATM)* gene is located in the long arm of chromosome 11.[29, 33]

2.4.2. Somatic mutations

The application of whole-exome sequencing (WES) techniques has established that CLL harbors a high genetic variability. Although a common mutation is not described, there are many genes recurrently mutated at low frequency and only a few genes mutated in up to 15% of patients.[24, 34, 35] The mutated genes tend to cluster in different pathways that fall into 7 core signaling pathways (Figure 7): NOTCH signaling,[36-38] inflammatory pathways (e.g., *MYD88-Myeloid differentiation primary response 88-*),[34, 39] BCR signaling and differentiation, WNT signaling, DNA damage genes (e.g., *TP53*[24] and *ATM*),[33] chromatin modification, and mRNA processing (e.g., *SF3B1- Splicing factor 3B subunit 1-*).[35, 40]
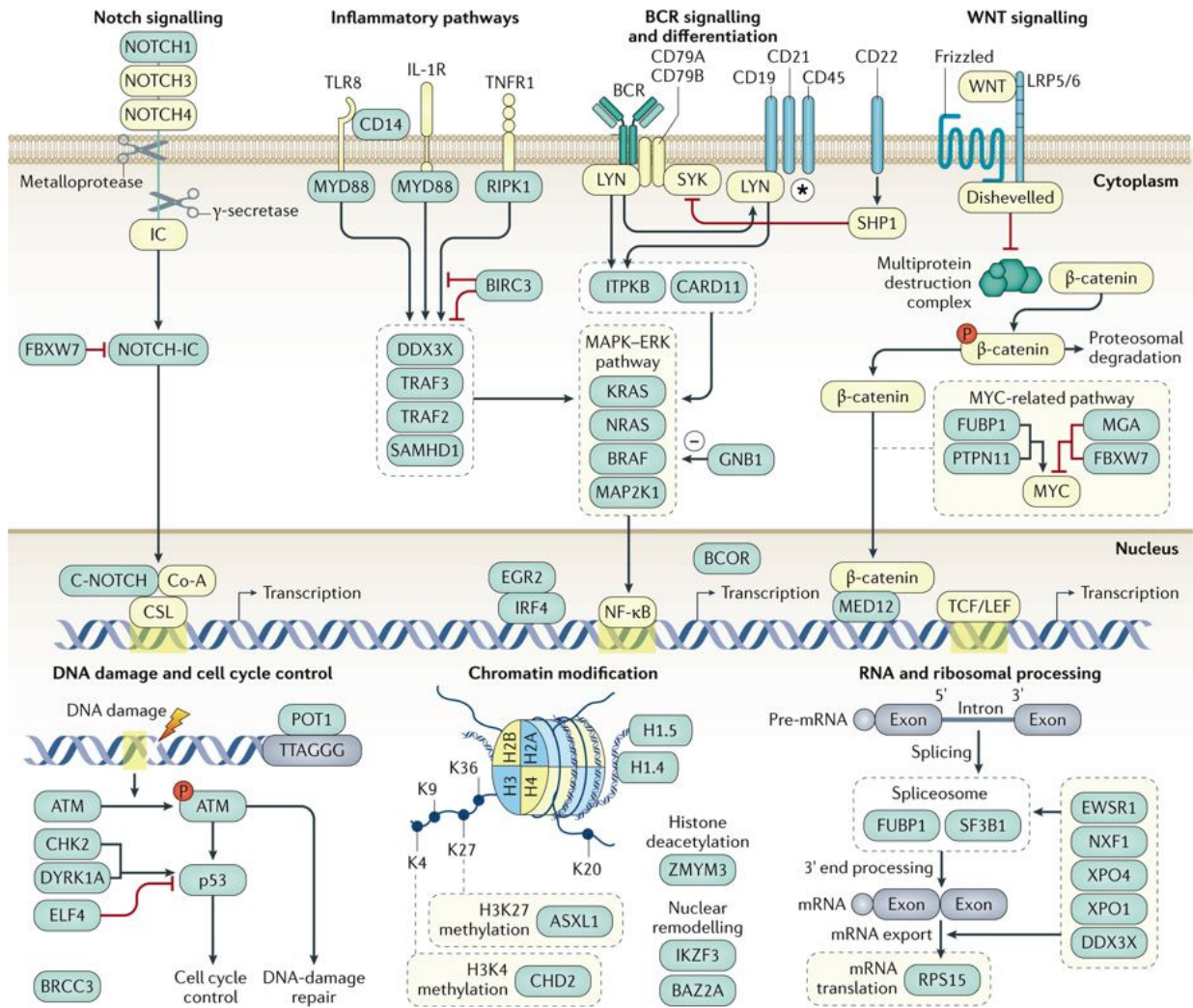
Figure 7. Significantly mutated genes and associated gene pathways in CLL. The most recurrently mutated genes in CLL, and its core signaling pathways. From *Kipps et al, Nature Reviews Disease Primers, 2018.*[10]

These results highlight the molecular heterogeneity of CLL and may provide new biomarkers and potential therapeutic targets for its diagnosis and management.[23, 24]

The frequency of mutations is related with the IGHV mutational status. As shown in Figure 8, there are mutations i) only present in IGHV M cells (e.g., *MYD88*), ii) only present in IGHV UM cells (e.g., *BRAF -B-rapidly accelerated fibrosarcoma-*) and iii) present in both subsets (e.g.,*SF3B1*).[23, 24, 41]
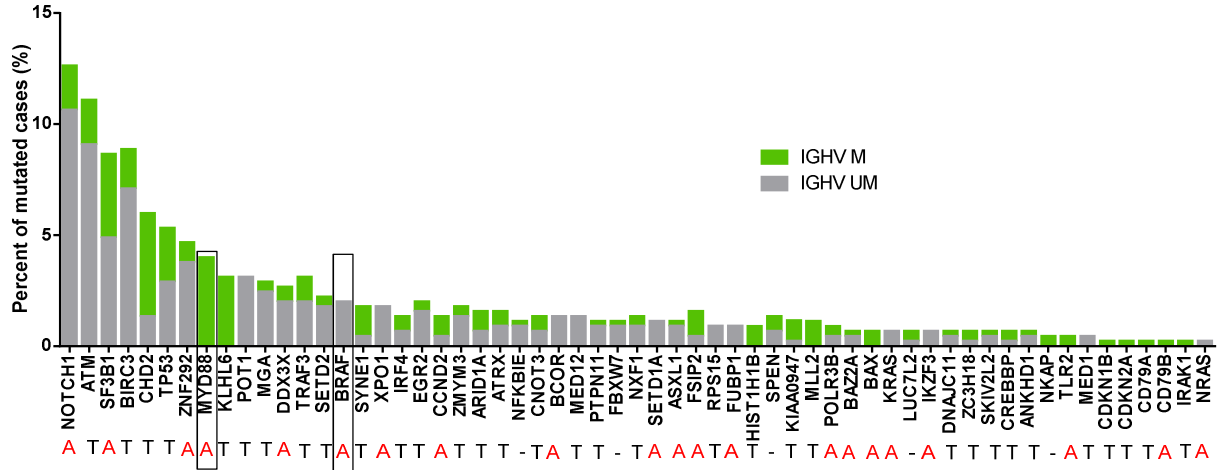
Figure 8. Repertoire of mutations in CLL. Frequency of the most common somatic mutations in CLL according to the IGHV mutational status. A: activating, T: truncating. Data are taken from *Puente et al, Nature, 2015*.[24]

Furthermore, most of these mutations are subclonal.[23, 24, 42] Figure 9 shows the subclonal diversity of the CLL driver mutations. Small subclonal mutations in *TP53, NOTCH1, NFκBIE*, and *protection of telomeres 1* (*POT1)*, among others, appear to have the same prognostic value as mutations in larger clones.[23, 42-44]
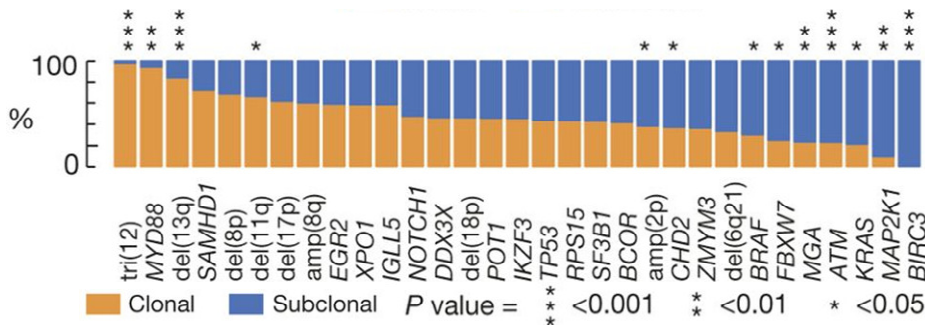
Figure 9. CLL mutational clonal al subclonal diversity. The proportion in which a recurrent driver is found as clonal (orange) or subclonal (blue) across 583 CLL samples. Modified from *Landau,et al. Nature 2015*.[23]

2.5. EPIGENETICS

B-cell differentiation process implies epigenomic changes. As observed in other cancers, the CLL epigenome shows global hypomethylation combined with local hypermethylation. Furthermore, Queiros *et al*,[21] have identified that IGHV UM CLL has an epigenetic signature reflecting that originates from a cell that has matured outside of the GC and maintains a naive-like signature, whereas IGHV M CLL has a memory-like signature. These studies also identified a third subtype with an intermediate methylation profile between the naive-like and memory-like, suggesting that it could originate in a not-yet-identified normal B cell.

Methylation profiling showed substantial intra-tumoral heterogeneity, which is associated with increased genetic complexity owing to the acquisition of subclonal mutations, thus linking genomic and methylomic evolution in CLL. In support of this notion methylation evolution is associated with an adverse clinical outcome, Figure 10.[21, 45]
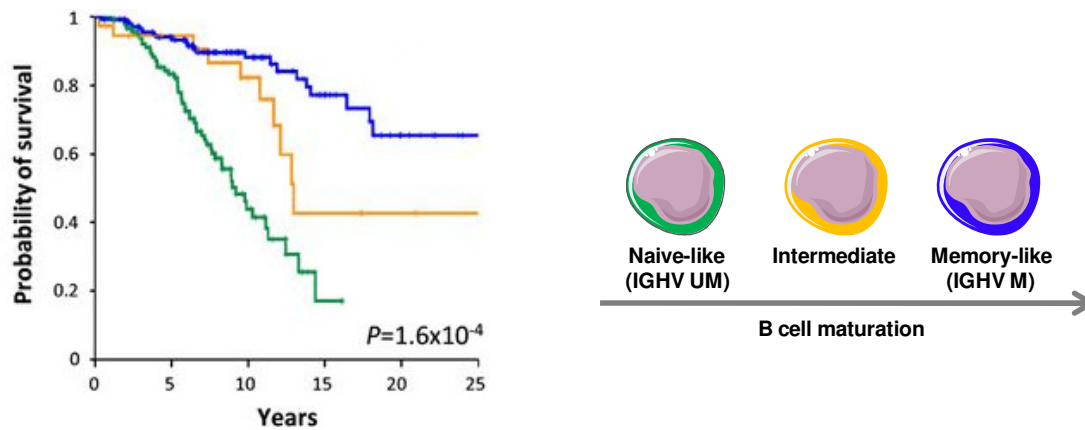
Figure 10. Epigenetic classification correlates with survival and B-cell maturation. Kaplan–Meier survival curve according to the epigenetic classification (n=295). Left image from *Queiros et al, Leukemia 2015*.[21]

2.6. PROGNOSIS

2.6.1. Prognostic Factors

CLL clinical evolution is very heterogeneous, with patients having an indolent behavior and others following a rapid evolution.[12] Thus, there have been numerous efforts to guide clinicians to a more accurate prognostic of this disease.[46] Table 2 shows a plethora of prognostic markers that help stratify CLL patients.[47]

Table 2. Factors suggestive of poorer prognosis in CLL.[48]

Host factor	Biochemical abnormalities and cell surface markers	Genetic abnormalities / IGHV UM
- Male sex	- Elevated serum thymidine kinase	- del17p13 /*TP53* mutation
- Age ≥ 60	- Serum β2-microglobulin and soluble CD23	- del11q22-q23
- ECOG ≥ 1	- Lymphocyte doubling time <6 months	- *BIRC3/NOTCH1/SF3B1* mutations
- Heritable risk	- CD49d$^+$, CD38$^+$, ZAP70$^+$	- IGHV UM

2.6.1.1. Host factor

Being a male older than 60 years old is a bad prognostic factor. The Eastern Cooperative Oncology Group (ECOG) score, also called the WHO score, considers a worse prognosis when the ECOG score is >1 (with 0 denoting perfect health and 5 death of the patient).[49] In addition, first-degree relatives of CLL patients have an increased risk up to 8.5-fold of developing the disease,[6] identifying nearly 40 loci of single nucleotide polymorphisms (SNPs) associated with familial CLL.[10]

2.6.1.2. Biochemical abnormalities and cell surface markers

Serum levels of β2-microglobulin, thymidine kinase and soluble CD23 have all been described as independent bad-prognosis markers in CLL.[50]

Lymphocyte doubling time (LDT), defined as the period needed for lymphocytes to double in number the amount found at diagnosis, correlates with increased progression-free survival (PFS) and overall survival (OS) if it is higher than 12 months. An increase in the lymphocyte count of >50% in two months or LDT during less than 6 months is a recommended criteria of active disease and indication for treatment.[48, 51]

Multiple studies have proven the prognostic value of CD49d, a protein that mediates cell-cell interaction, prolonging cell survival.[52, 53] ZAP70, an intracellular kinase, and CD38, a transmembrane enzyme implicated in cell metabolism. All these proteins are bad-prognosis markers regarding PFS and OS. ZAP70 and CD38 expression correlates with IGHV UM cases.[25, 26, 48, 54-56]

2.6.1.3. Mutational status of the IGHV genes and genetic abnormalities

IGHV mutational status has a remarkable impact on CLL survival and it is used as a prognostic marker[17, 18] (how will the disease develop naturally) and as a predictive marker (how will de disease develop with the treatment).[57] IGHV M cases present a more indolent clinical course (Figure 11a)[17, 18] and a better response to chemotherapy (Figure 11b).[57]
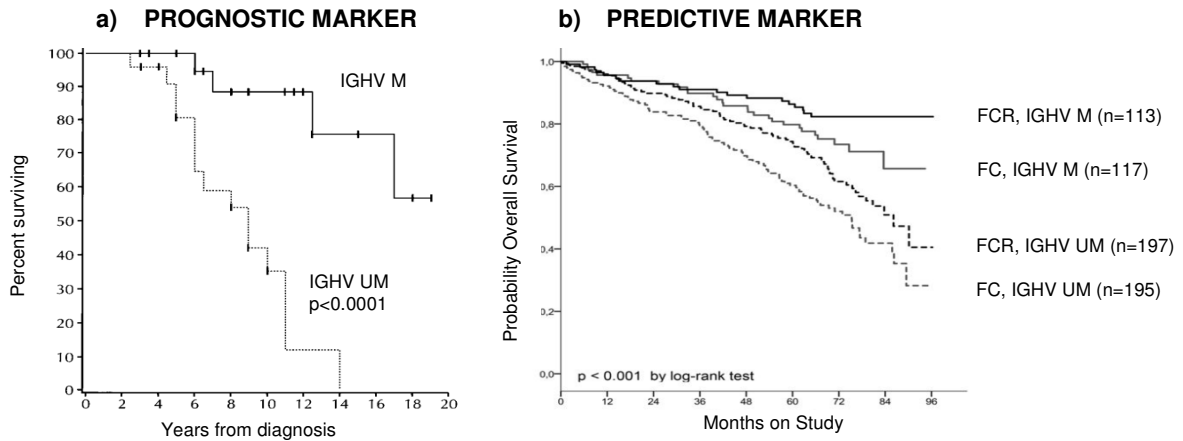
Figure 11. IGHV mutational status as a prognostic and predictive marker. IGHV UM cases have a shorter a) OS (from *Damle et al, Blood 1999*)[17], which is maintained also after b) chemotherapy (FC) or chemoimmunotherapy (FCR) treatment (from *Fischer et al Blood 2016*).[57]
FC: fludarabine, cyclophosphamide; FCR: fludarabine, cyclophosphamide, rituximab.

Genetic alterations including chromosomal and genomic alterations are described as important prognostic factors in CLL.[16, 29]

The most frequent chromosomal aberration is the del13q14, found in up to 50% cases and associated with a good prognosis.[29] The following-most-frequent aberration is the del11q22-q23 (~18 % of patients),[29] which is associated with aggressive clinical course and reduced OS[16]. Del17p13[58] and trisomy 12 are associated with rapid disease progression and short OS, as shown in Figure 12a. [16,48]
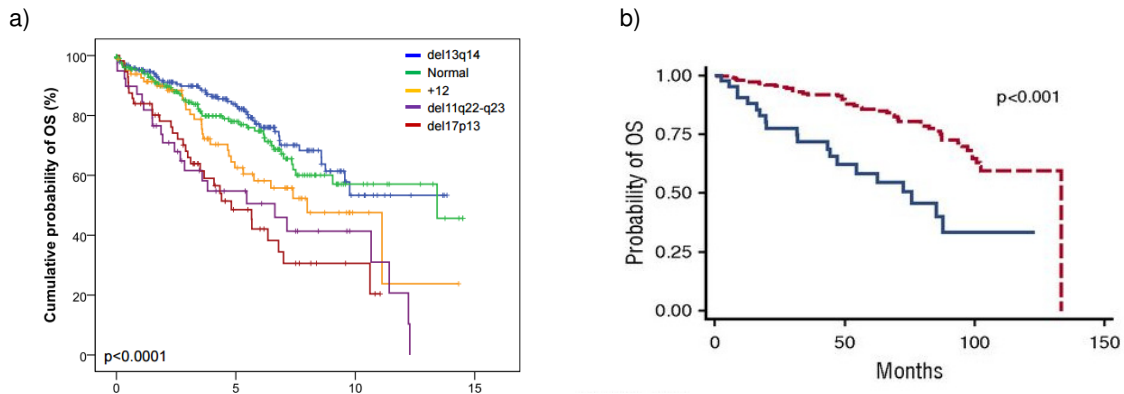
Figure 12. The four common chromosomal alterations. Implication in Overall Survival (OS) of a) each chromosomal alterations (from *Rossi et al, Blood, 2013).*[16] and b) Complex karyotype (defined by the presence of ≥ 3 alterations by cytogenetic analysis; from *Gian Matteo Rigolin, Blood, 2017).*[59]

Complex Karyotype (CK), defined by the presence of ≥3 chromosome aberrations by cytogenetic analysis, is associated with an unfavorable outcome (Figure 12b).[59]

The presence of *TP53* aberrations and IGHV mutations status guide treatment decisions[32, 60-62] and *NOTCH1* mutations may predict for impaired responses to rituximab.[63, 64] Mutations in *TP53*, *NOTCH1*, *SF3B1* and *BIRC3* genes are also associated with worse outcome, as shown in Figure 13.[30, 34, 35, 42]
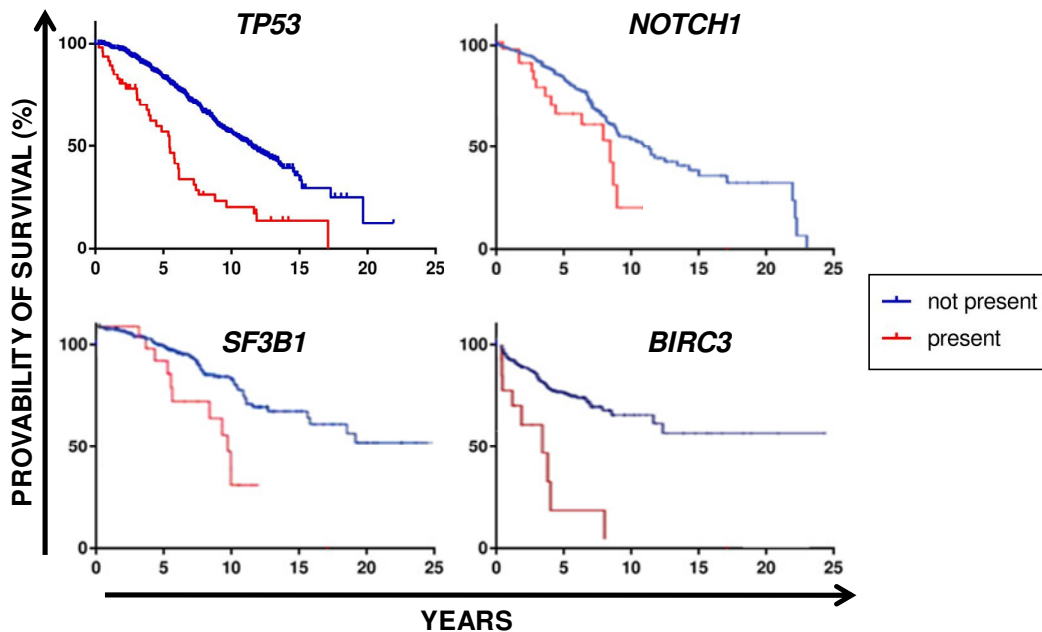
Figure 13. Clinical relevance of recurrent mutations. *TP53* from *Eric Conference 2018*; *NOTCH1* from *Puente et al, Nature, 2011*;[34] *SF3B1* from *Quesada et al, Nat Genet, 2011*;[35] *BIRC3* from *Rossi et al Blood, 2012*.[30]

2.6.2. Prognostic Staging

Although many different prognostic factors are being described, not all of them are currently used for the prognostic staging in CLL. Two prognostic staging systems exist: a) Rai[65, 66] and Binet[67] (established by physical examination and blood counts) and b) International Prognostic Index (IPI; based on clinical stage and various biological and genetic markers).[68]

2.6.2.1.   Rai and Binet staging systems

The Rai[65, 66] and Binet[67] staging systems are established by physical examination and blood counts, respectively, (Figure 14).
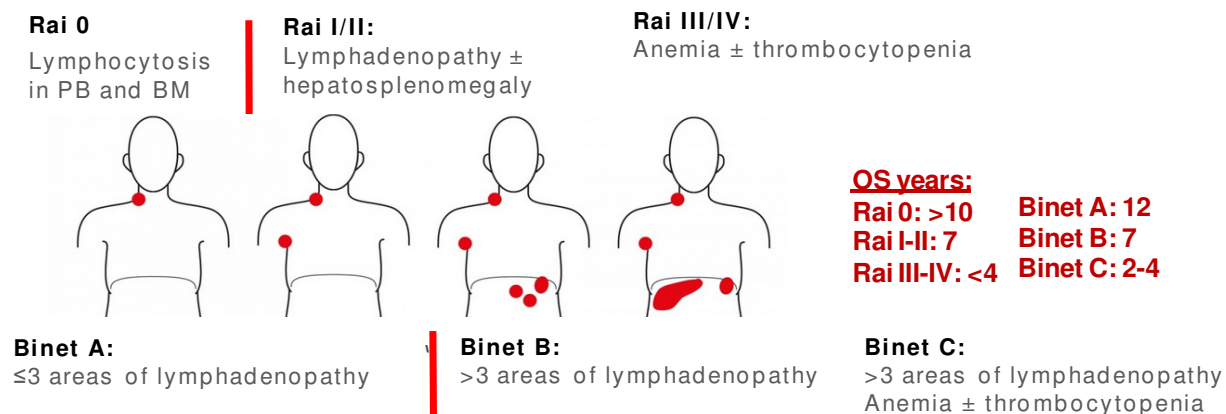
Figure 14. Rai and Binet staging systems for CLL. Rai ranges from 0-IV and it is based mostly on lymphocytosis. Binet ranges from A-C and it is based on the number of affected lymphoid tissues. They also consider whether the patient has anemia or thrombocytopenia. Data from *Nabhan and Rosen, JAMA, 2014.*[11]

2.6.2.2.   International Prognostic Index

In 2016, the International Prognostic Index (IPI), originally designed as a prognostic factor model for aggressive non Hodking's Lymphoma, was adapted to CLL (CLL-IPI). The CLL-IPI is a comprehensive prognostic score based on five widely available parameters (including genetics, biology and clinical variables: TP53 status, IGHV mutational status, β2-microglobulin, clinical stage and age (Table 3).[68]

Table 3. CLL-IPI score multivariable model. Data from the patients represented in Figure 17. n=1214.[11, 68]

	Adverse factors	Regression coefficient	Hazard ratio (95%CI)	p value	Assigned risk score
TP53 status	Deleted/ mutated	1,434	4,2	<0,0001	4
IGHV mutational status	Unmutated	0,950	2,6	<0,0001	2
β₂-microglobulin	>3,5mg/L	0,678	2,0	<0,0001	2
Clinical stage	Rai I-VI or Binet B-C	0,464	1,6	<0,0001	1
Age	>65 years	0,555	1,7	<0,0001	1

After risk score assignment, patients can be classified in four risk categories: low, intermediate, high and very high (Figure 15a). Significantly different 10-year OS was observed for the different groups (Figure 15b).[68]

Category	Risk score	Median OS	OS at 10 years	Treatment advise
Low	0-1	NR	79%	Do not treat
Intermediate	2-3	105 months	39%	Do not treat except if is symptomatic
High	4-6	75 months	22%	Treatment indicated except if is asymptomatic
Very high	7-10	29 months	4%	Do not use chemotherapy. If treatment is required, use novel agents/clinical trials
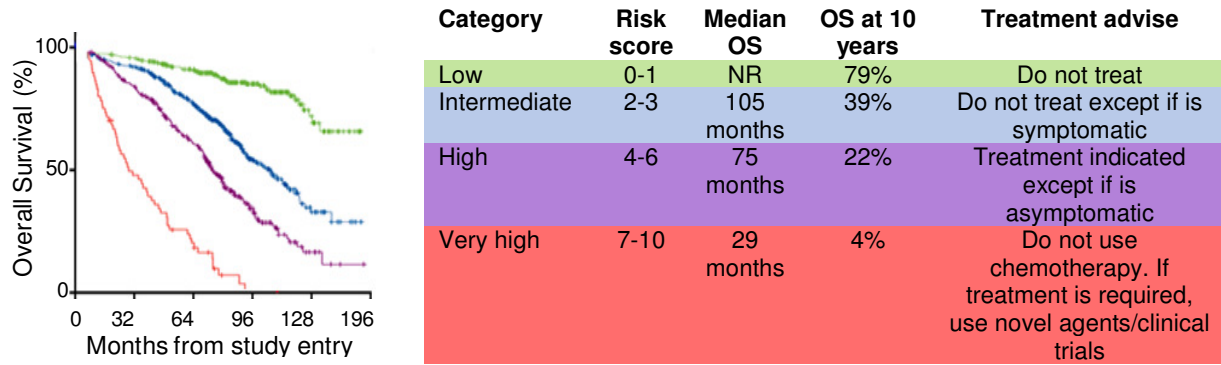
Figure 15. Overall survival (OS) according to the CLL-IPI risk groups. n=1214. Similar results were obtained with different studies (n total= 3472) from 5 study groups in US and Europe.[11, 68]

3. CLL MICROENVIRONMENT

CLL cells circulate between PB and tissues, mainly BM and LN, where they interact with follicular dendritic cells (FDC), T cells and other stromal cells by a complex network of adhesion molecules, cell surface ligands, chemokines, cytokines and their respective receptors (Figure 16).[20] These crucial interactions between CLL cells and tumor microenvironment (TME) increase the expression of downstream targets of the BCR signaling, nuclear factor kappa B (NF-κB) activation, cytokines and antiapoptotic and proliferation-related markers.[69, 70] TME provides crucial contributions to the licensing of cancer hallmark capabilities and disease progression.[20]
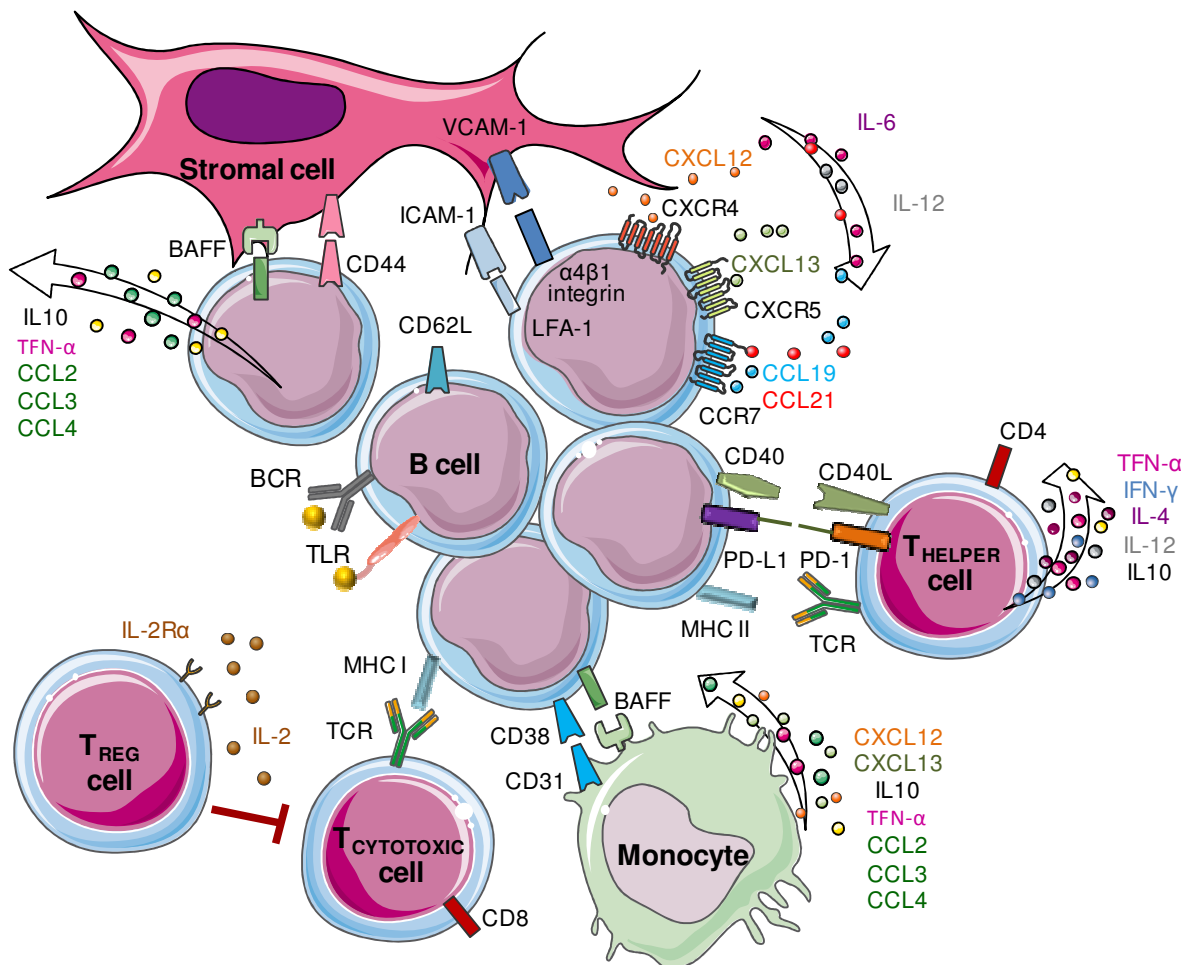
Figure 16. Crosstalk between CLL cells and surrounding microenvironment. Contact between CLL cells and stromal cells, T cells and monocytes is established and maintained by chemokine/cytokine receptors, adhesion molecules and ligand-receptor interactions. CLL cells migrate to tissues attracted by the chemokines CXCL12 (nurse-like cells (NLC) and stromal cells secretion), CXCL13 (FDC secretion) and CCL19/CCL21 (high endothelial venules secretion), which interact with the CLL receptors CCR7, CXCR4 and CXCR5, respectively. Adhesion molecules (α4β1 integrin, lymphocyte function-associated antigen 1 (LFA-1), among others) and their ligands (vascular cell adhesion protein 1 (VCAM1), intercellular adhesion molecule 1 (ICAM), among others) facilitate tumor cells migration and homing. Survival and proliferation stimuli are mainly provided by T cells, particularly through CD40L and the secretion of several cytokines and NLC and stromal cells. The presence of environmental and/or self-antigens in the niches may trigger BCR and TLRs (Toll like receptors pathway) activation, which amplify the responsiveness of CLL cells to the signals and factors that are provided by its microenvironment.[6, 20]

In turn, CLL cells can use different strategies to expand and recruit various types of suppressive tumor-infiltrating lymphocytes, like regulatory T (Treg) cells, tolerogenic dendritic cells (DCs), tumor-derived macrophages and myeloid suppressor cells. Tumor cells organize this favorable niche by secreting soluble factors, direct contact with surrounding cells, and release of extracellular vesicles (Figure 17).[20, 71]

Activated CLL cells secrete chemokines (C-C motif chemokine ligands: CCL3, CCL4, and CCL22) and angiogenic factors that attract TME cells.[71] In addition, tumor cells can secrete suppressive factors (IL-10 and TGF-β), express immune inhibitory molecules (FasL-Fas ligand- and PD-L1 -Programmed cell death ligand-).[72] Direct contact of CLL with T cells induce abnormal synapses impairing their antitumor response triggering to an exhausted phenotype.[73-75] Survival signals delivered by macrophages and stromal cells also require their direct contact with CLL cells that activate different pathways both in CLL and stromal cells including LYN and NF-κB.[76, 77] Tumor-released extracellular vesicles carrying noncoding RNA and proteins enhance T cells, monocytes, and stromal cells proinflammatory signals.[78]

Figure 17. Tumor microenvironment is changed by CLL cells.[79]

The importance of TME in CLL cells can be observed in cell cultures and xenograft mice models. Purified CLL cells rapidly die *in vitro,* and their surveillance increase when cocultured with NLC, stromal or T cells.[80] In the same way, xenograft models require autologous T cells to be developed.[81]

Alterations of immune system in CLL are the result of infection-related mechanisms, chemotherapy and leukemia-driven re-shaping of cell functions occurring in the microenvironment. Infections remain a major cause of morbidity and mortality in CLL patients.[82] Resistance to targeted drugs and chemotherapy is also linked to extrinsic survival signals from the stromal and immune TME.[83, 84] So CLL treatment needs to interfere the dynamic co-evolution of tumor cells and the reprogrammed stroma.[79]

4. MOUSE MODELS OF CLL

CLL mouse models can be classified into two categories: genetically engineered and xenotransplantation models.

4.1. GENETICALLY ENGINEERED CLL MOUSE MODELS

The most used CLL genetically engineered mouse models are summarized in Table 4.

Table 4. Features of genetically engineered CLL mouse models. Adapted from *Simonetti et al, Blood 2014.*[85]

Mouse model	Disease penetrance	Time to CLL[a]	IG gene	Key findings
Mouse models mimicking the spectrum of deletions of chromosomal region 13q14				
mir-15a/16-1[-/-] **mir-15a/16-1[floxed]** **CD19-Cre mice**	20%	12-18	UM	Germ-line mutations interfering with the mir-15a/16-1 expression is observed in a small fraction of CLL patients. The loss of the mir-15a/16-1 cluster led to an earlier entry into the cell cycle and an up-regulation of BCL2 protein levels compared with wild-type B cells.
14qC3-MDR^{-/-}/MDR[floxed]	22%	6-18	UM	MDR[-/-/floxed] mice show a higher penetrance of the phenotype and a more aggressive disease course compared with mir-15a/16-1-deleted mice. CDR^{-/-}causes embryonic lethality and CDR[floxed] leads to CLL development: tumor cell infiltrates in spleen, BM and non-lymphoid organs. CDR^{+/-} leads to a more aggressive disease than MDR^{+/-}.
CDR[floxed]	50%			
CD19-Cre				
Mouse models mimicking the deregulated expression of genes in human CLL				
***E*μ-TCL1 transgenic mice[86]**	100%	15	UM	*E*μ-TCL1 mice develop an overt leukemia and massive infiltrations of monoclonal CD5^{+} B cells in lymphoid and non-lymphoid tissues.
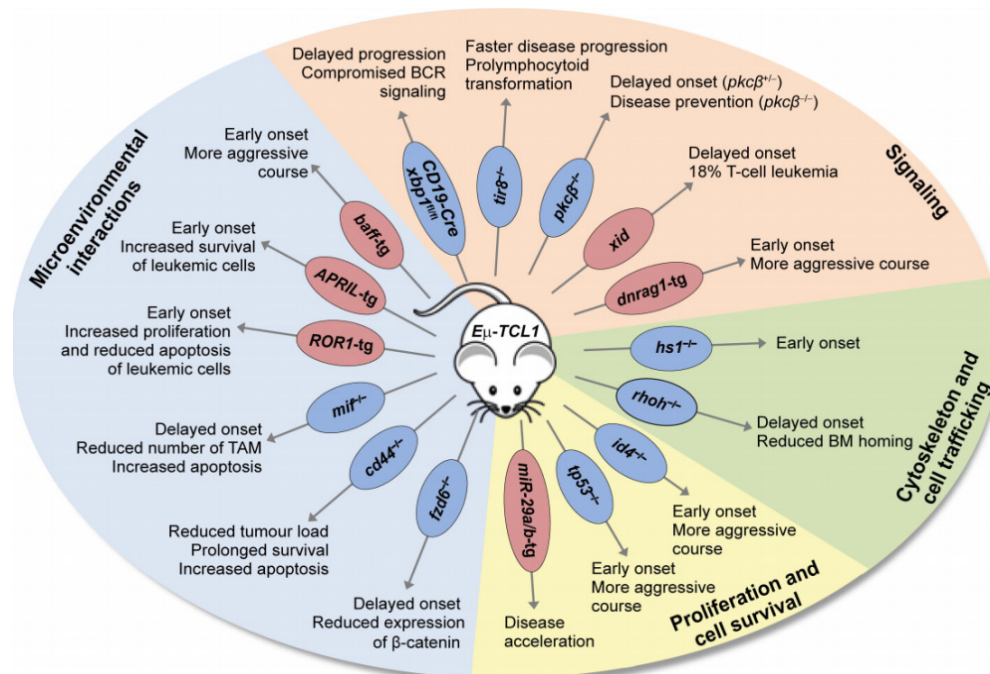
*Some of the models showed in the Figure are IGHV M, as are generated by crossing *E*μ-TCL1 mice with other mice with the alteration of interest (that can be IGHV M).

***SF3B1* M /** ***ATM* deleted[87]**	30-50%	24	UM	CLL-like cells were detected in PB/BM mononuclear cells and splenocytes.

[a]Time (months) of appearance of circulating leukemic cells. UM: unmutated. MDR: minimal deleted region; CDR: common deleted region. *E*μ-TCL1 *(T*-cell leukemia /lymphoma 1); PB/BM: peripheral blood and bone marrow.

4.1.1. Eµ-TCL1 transgenic

The T-cell leukemia/lymphoma 1 transgenic mouse (Eµ-TCL1) currently represents the most widely accepted animal model for CLL, as shown in Table 4, as it is the one with the highest penetrance and the best approach to TME.[86] The Eµ-TCL1 is based on the exogenous expression of the human TCL1 gene under the IGHV promoter control and IGH enhancer (Eµ) in vivo, which results in the clonal expansion of $CD19^+CD5^+IgM^+$ B cells in PB. These mice develop a progressive CLL-like clonal disease with many characteristics of human CLL, like leukemia, lymphadenopathy, splenomegaly and hepatomegaly.[85] Somatic mutations in the IGHV and IGLV are absent in this model (IGHV UM).[86, 88]

TCL1 is a co-activator of the serine/threonine kinase AKT and activates the NF-κB pathway.[89] In CLL, high TCL1 expression is associated with aggressive features (IGHV UM, ZAP70^{high}, del11q22-q23, and overall worse disease outcome.[88] As a result of animal studies, it has been suggested that TCL1 is involved in the initiation of human CLL.[86]

As the development of CLL in the Eµ-TCL1 mouse occurs late, approximately after 15 months, and has a heterogenous course of disease, adoptive transfer of murine CLL cells isolated from leukemic Eµ-TCL1 mice into syngeneic wild-type animals are performed to allow treatment studies in more homogenous and faster disease development animal cohorts: Eµ-TCL1 adoptive transfer model (Eµ-TCL1 AT)[86] (Figure 18).
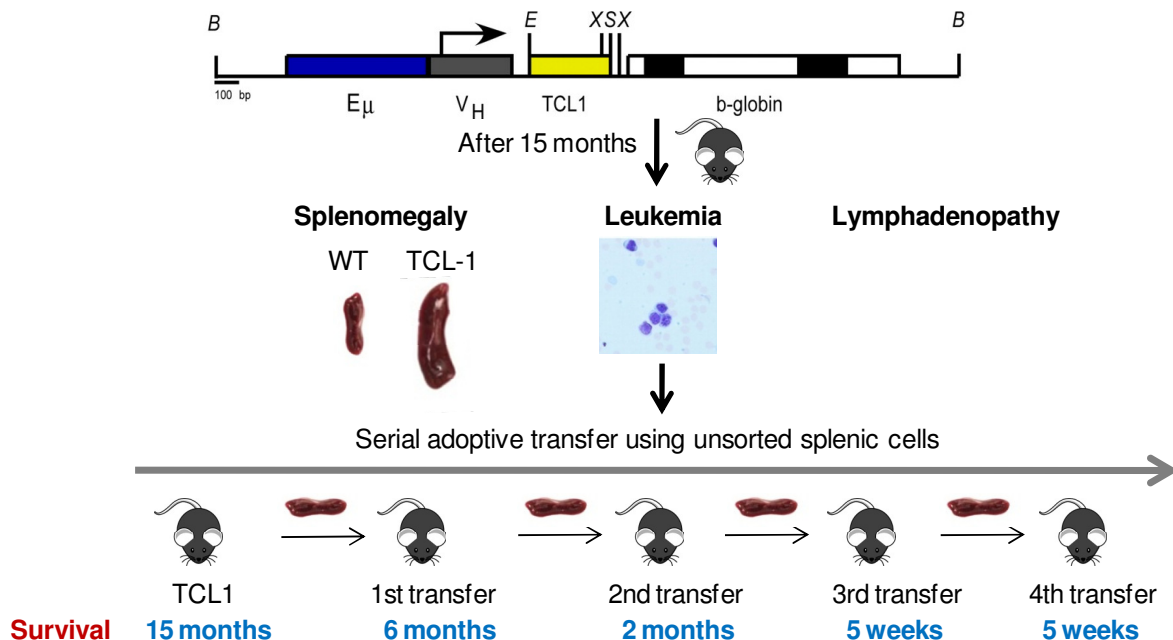
Figure 18. Eµ-TCL1 transgenic mouse model. From a transgenic mouse that has adopted the *TCL1* gene and shows human CLL-like disease phenotype, splenocytes are transferred into syngeneic wild-type animals, which develop the disease faster. *TCL1* gene image is from *Bichi et al,Proc Natl Acad Sci,* 2002.[86]

4.2. XENOTRANSPLANTATION MODELS

Xenotransplantation of human tumor cells into immunodeficient mice has been a powerful preclinical tool in several hematological malignancies, with the notable exception of CLL. For several decades, this possibility was hampered by the inefficient and/or short-term engraftment of CLL cells into available animals. All initial attempts to xenotransplant human primary CLL cells have been hampered by the lack of mice immunodeficient enough to prevent the rejection of human leukemic cells, although some models of cell lines or primary CLL cells in immunodeficient mice have been described, Table 5.[90]

Table 5. Xenograft models of cell lines and primary CLL cells. Data from *Bertilaccio et al, Leukemia, 2013.*[90]

Model	CLL source	Description
Human/mouse radiation chimera	Human tumor cells	Transplantation of CLL PBMCs into peritoneal cavity of irradiated Balb/c or BNX mice, radio-protected with bone marrow from SCID mice[91]
NOD/SCID	Human tumor cells	Transplantation of CLL PBMCs NOD/SCID mice and combining intravenously and intraperitoneally injection[92]
NOD/SCID-IL2rg$^{-/-}$	Human tumor cells	Co-transferring of CLL PBMCs intravenously with allogeneic APCs (CD14$^+$ or CD19$^+$ cells)[93]
NOD/SCID-IL2rg$^{-/-}$	Human tumor cells	Transplantation of hematopoietic stem cells purified from CLL patients into newborn mice (by facial vein)[94]
NSG	Human tumor cells	Co-transferring of CLL PBMCs intravenously via the retro-orbital plexus with activated autologous T-cells[95]
Nude	Cell lines: EBV-CLL (1) EBV-CLL (3)	EBV (1): trisomy 12; EBV (3): 11q+[96]
Nude or SCID	Cell line: MO1043	CD19$^+$, CD20$^+$, CD5$^+$, HLA-DR$^+$, IgK$^+$ Trisomy 12[97]
Nude	Cell line: JVM-3	CD19$^+$, CD20$^+$, CD5$^-$, HLA-DR$^+$, IgK$^+$, Trisomy 12[98]
Balb/c-Rag2$^{-/-}$IL2rg$^{-/-}$	Cell line: MEC-1	CD19$^+$, CD20$^+$, CD5$^-$, HLA-DR$^+$, IgK$^+$, sIgM$^+$, sIgD$^+$, CD23$^+$, CD38$^+$, del(17), del(12)[99]

APC, antigen presenting cell; BNX, Balb/c or beige/nude/Xid; IL, interleukin; NOD, non-obese diabetic; PBMC, peripheral blood mononuclear cell; SCID, severe combined immunodeficiency; NSG, non-SCID gamma; HLA, human leukocyte antigen, EBV: Epstein-Barr virus.

Nowadays, a new strategy for xenotransplantation in immunodefient mice is the cotransfer of CLL PBMCs (either intravenous or intrabone) and autologous T lymphocytes and allogeneic antigen presenting cells (APCs), which elicited an increase CLL cell survival and proliferation *in vivo*. A direct correlation between T-cell levels in mouse blood and leukemic cell proliferation was seen, as in animals without T-cell expansion, CLL cell proliferation did not occur.[81]

CLL xenograft models may become useful tools not only to evaluate innovative therapeutic strategies, but also to help designing patient-specific treatment options.[90]

Recently, a novel Richter syndrome patient-derived xenograft (PDX) model to study genetic architecture, biology, and therapy responses of this CLL aggressive evolution syndrome.[100]

5. CLL THERAPEUTIC STRATEGIES

Therapeutic options for CLL include watchful waiting, chemotherapy, immunotherapy, novel molecularly targeted therapy and alo-transplantation (Figure 19).[101]
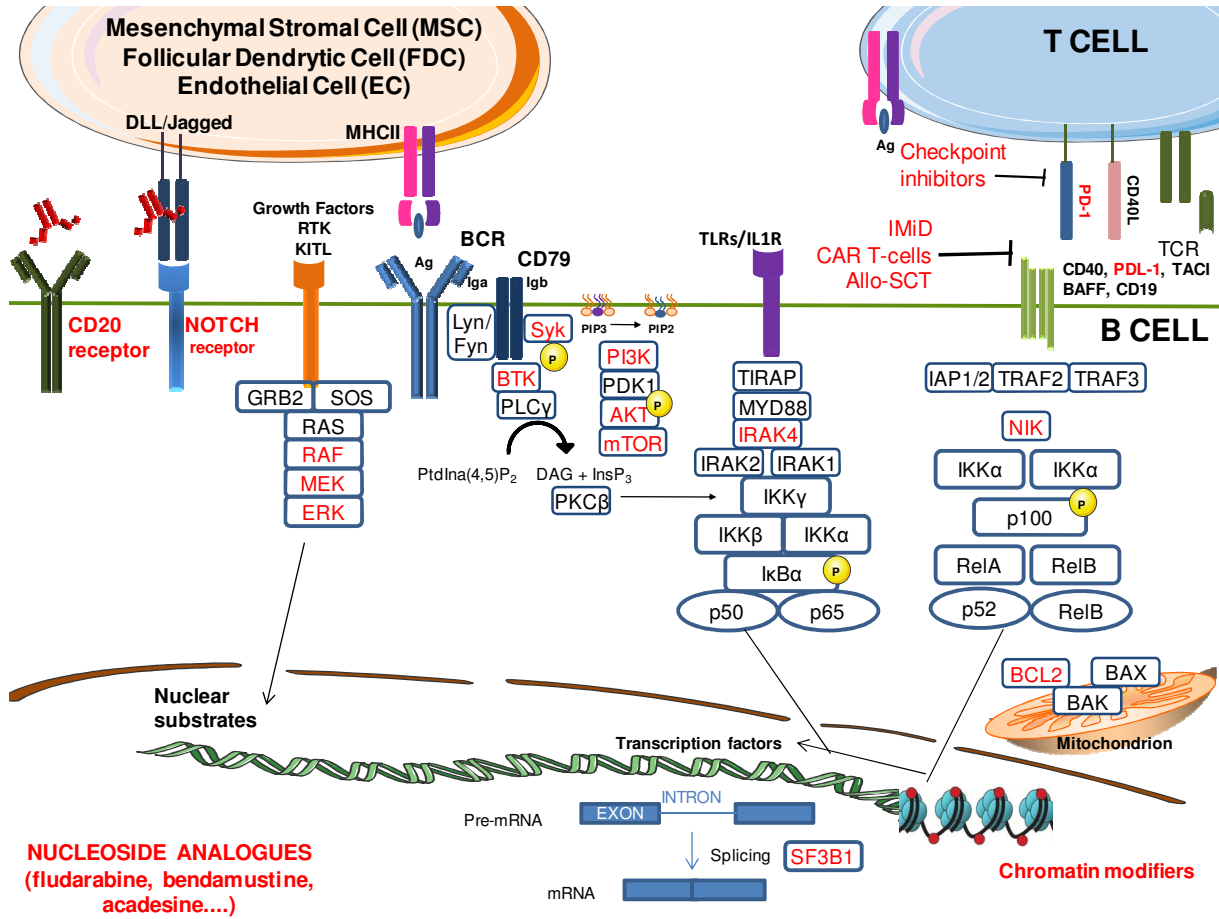
Figure 19. Therapeutic strategies for CLL. Red symbols and letters indicate studied therapeutics for CLL. Some of these compounds have not reached clinical testing or approval by the regulatory bodies and are therefore not broadly covered in the manuscript.

5.1. CURRENT TREATMENT OF CLL PATIENTS

Given the number of choices, the treatment selection need to be based on good clinical judgment and an appropriate use of diagnostic tools.[102] Only those patients who meet the 2018 international workshop on CLL (iwCLL) criteria for initiation of therapy (Table 6) should be treated.[103]

Table 6. Updated 2018 iwCLL guidelines to initiate CLL therapy.[47, 103]

Any <u>one</u> of the following criteria should be met to initiate CLL therapy

- Progressive marrow failure, hemoglobin <10gm/dL or platelet count <100x10^9/L
- Massive (≥6cm below the left costal margin) or progressive or symptomatic splenomegaly
- Massive (≥10cm in longest diameter) or progressive or symptomatic lymphadenopathy
- Progressive lymphocytosis with an increase of ≥50% over a 2-month period or LDT of <6 months
- Autoimmune complications of CLL, that are poorly responsive to corticosteroids
- Symptomatic extranodal involvement
- Disease-related symptoms, including:
    - o Unintentional weight loss of ≥10% within the previous 6 months
    - o Significant fatigue
    - o Fever ≥38ºC for 2 or more weeks without evidence of infection
    - o Night sweats for ≥1 month without evidence of infection

The CLL-IPI score (see chapter 2.6.2.2. "International Prognostic Index") can also be used to determine the treatment criteria: Low: do not treat, Intermediate: do not treat except if the disease is really symptomatic, High: treatment indicated except if the disease is asymptomatic and Very High: do not use chemotherapy if treatment is required, but rather novel agents or clinical trials, Figure 15.[68]

5.1.1. Asymptomatic patients

Many patients with CLL experience and indolent course of the disease for many years and do not require therapy at initial diagnosis.[104] There are certain subsets of patients having survival rates without treatment that are similar to the normal population.[105, 106]

In early stage (Rai stage <3, Binet stage A or B) asymptomatic CLL patients who do not meet the iwCLL 2018 criteria to initiate therapy the standard of care is observation ("wait and see") , rather than immediate treatment.[103]

5.1.2. Symptomatic patients

Patients with more advanced stage CLL or those who demonstrate symptoms or progressive disease have a median survival without treatment between 18 months and three years.[103] Treatment of the underlying CLL is indicated for patients who meet the 2018 iwCLL criteria for initiation of therapy. Hence, treatment decision for CLL requires careful evaluation of different factors including: del17p13/*TP53* alterations, IGHV mutational status, del13q, trisomy 12, age, patient fitness status, and disease stage.[102, 103]
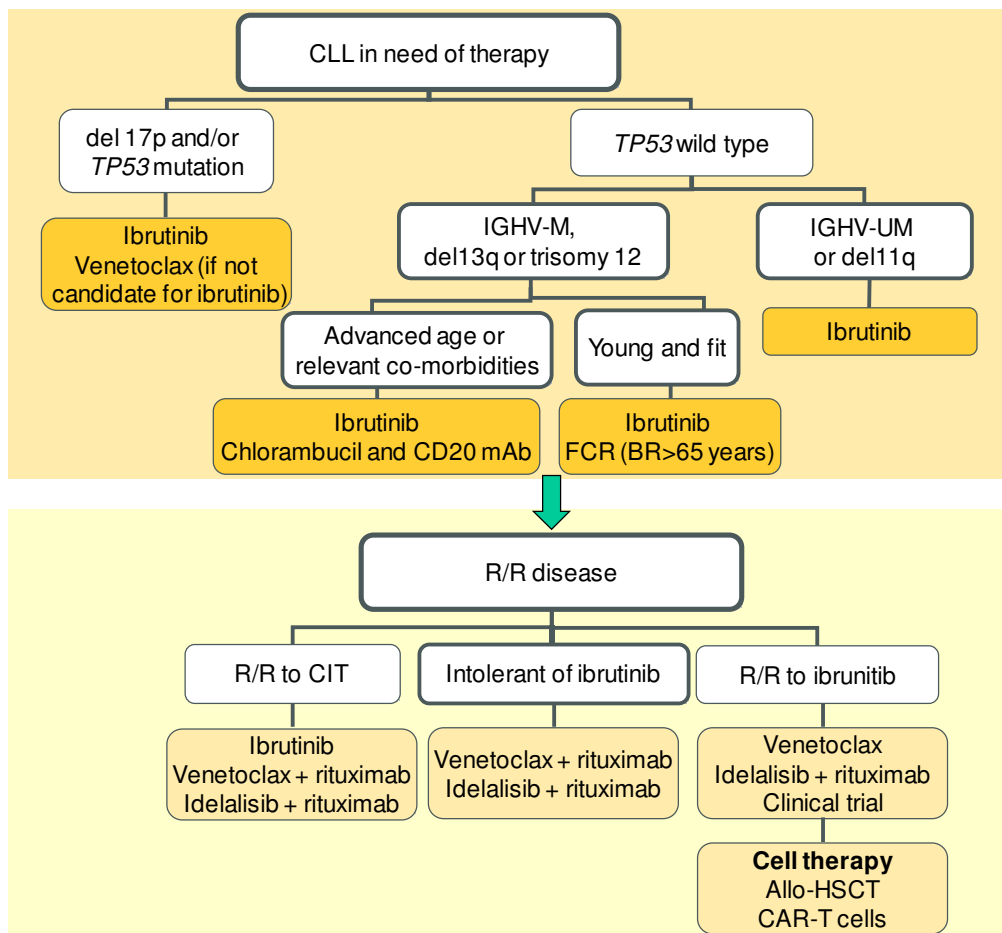
Figure 20. Therapeutic algorithm for patients with CLL. Data from *Bosch and la-Fabera, Nature Reviews.Clinical Oncology, 2019.*[14] FCR: fludarabine, cyclophosphamide, rituximab; BR: bendamustine, rituximab; mAb: monoclonal antibody; CIT: chemoimmunotherapy; Allo-HSCT: allogenic haematopoietic stem cell transplantation; CAR: chimeric antigen receptor.

5.1.2.1. First-line treatment

The *TP53* and IGHV mutational status are the most important prognostic and predictive biomarkers in CLL and are used for treatment decision. *TP53* aberrations should be ascertained checking del17p13 by FISH (fluorescence *in situ* hybridization) and *TP53* mutations by Sanger sequencing or next-generation sequencing. It is important to obtain both tests, since patients can harbor a *TP53* mutation on DNA sequencing in the absence of del17p13 by FISH; and these patients have similar poor outcomes.[29, 58, 107]

- **Patients with del17p13 and/or *TP53* mutation**

TP53 is a DNA damage regulator and is the target of the genotoxic effect of chemotherapy. Upon chemotherapy-induced DNA damage, *TP53* is activated and cells undergo apoptosis. Conversely, when *TP53* is nonfunctional, because of deletion or mutation, the apoptosis in response to chemotherapy cannot be triggered. Patients with *TP53* alterations, even at subclonal level,[108] have a short PFS and OS when treated with chemoimmunotherapy regimens such as FCR and BR.[109, 110] Thus, these patients are candidates for therapies with mechanisms of action not requiring the presence of an intact and functional DNA repair machinery. Ibrutinib (a Bruton's tyrosine kinase (BTK) inhibitor) in previously untreated CLL patients with *TP53* alterations showed an ORR of 97% and the 2-year OS of 84%.[111] The excellent response rates and outcomes make ibrutinib the treatment of choice in this group of patients.[47] In patients who are not eligible to receive ibrutinib (for example, owing to specific comorbidities, drug interactions or patient choice), venetoclax (a BCL2 (B-cell leukemia/lymphoma 2) antagonist) is an excellent alternative.[112] Combination of ibrutinib and venetoclax is proposed for high-risk and older patients with CLL.[113]

- **Patients without del17p13 or *TP53* aberrations and IGHV mutated**

In young fit patients IGHV M or carrying del13q or trisomy 12, the standard of care for first line therapy is chemoimmunotherapy combination (<u>FCR regimen</u>) with fludarabine (purine analogue), cyclophosphamide (alkylating agent), and rituximab (monoclonal antibody (mAb) anti-CD20) with an overall response rate (ORR) of 94%.[114] IGHV M patients who receive FCR experience a long PFS (that can exceed 10 years).[57, 115, 116] Bendamustine, a dual alkylator/purine analogue agent, is also indicated for this group of patients, in combination with the anti-CD20 antibody rituximab (<u>BR</u>) with a ORR of 89%.[117] FCR treatment is only recommended in young (<65 years) and fit patients who are able to tolerate this intensive regimen.[57, 109] A follow-up of FCR treatment show that after ~13 years the risk of secondary myeloid neoplasms was ~5% and of Richter's transformation was ~8%.[109]

In patients with advanced age or relevant comorbidities, therapy with chlorambucil and ofatumumab (a CD20 mAb) significantly improved ORR compared to chlorambucil monotheraphy (82% vs 69%).[118] Moreover, a new CD20 mAb, obinutuzumab, has been approved in combination with chlorambucil after demonstrating significantly higher ORR (78% vs. 65%) and longer PFS (29 months vs. 15 months) compared to chlorambucil and rituximab.[119, 120]

A growing consensus exist on the use of ibrutinib in the front-line setting, regardless of *TP53* and IGHV mutational status, age or comorbidities.[101, 121-124]

5.1.2.2. Second-line treatment - Relapsed/Refractory disease

All patients who have relapsed CLL should undergo a comprehensive assessment of their disease status, including a BM aspirate and/or biopsy, and a computed tomography scan of the chest, abdomen, and pelvis. Also, all patients should have a FISH and *TP53* mutation status re-analysis prior to starting therapy.[47] Although the *TP53* disruption status may not impact treatment choice given that all novel agents have excellent efficacy in this group of patients, the frequency of follow-up, monitoring for progression of disease, and the anticipated PFS benefit will be different in patients with *TP53* disruption compared to patients with intact *TP53*.[47]

In patients with relapsed/refractory (R/R) disease after chemoimmunotherapy, the most recommended options are ibrutinib or venetoclax plus rituximab, whereas idelalisib (a phosphoinositol-3-kinase δ isoform (PI3Kδ) inhibitor) plus rituximab can be considered as the third option.[125-128]

Patients with R/R disease who are intolerant to ibrutinib can be salvaged with venetoclax plus rituximab or idelalisib plus rituximab.[125, 127]

Finally, patients progressing after ibrutinib can be treated with venetoclax plus rituximab or idelalisib plus rituximab, or included in clinical trials, and subsequently considered for allogeneic hematopoietic stem cell transplantation (HSCT), which demonstrated the potential of inducing a durable T-cell response against a CLL clone.[47] Considering the median age of diagnosis in CLL, HSCT is not eligible due to the significant treatment-related mortality. Nonetheless, many still consider HSCT as the choice for young patients with high-risk disease.[129]

In R/R patients there is an spectrum of lesions that appears while treatment, and may have clinical impact and determine treatment response, like *TP53*, *ATM* and *NOTCH1* mutations (Figure 21).[64, 129, 130] Furthermore, some novel agents induce *de novo* mutations that predict resistance to them, like *BTK* or phospholipase Cγ2 (*PLCγ2*) induced by ibrutinib.[131-133]
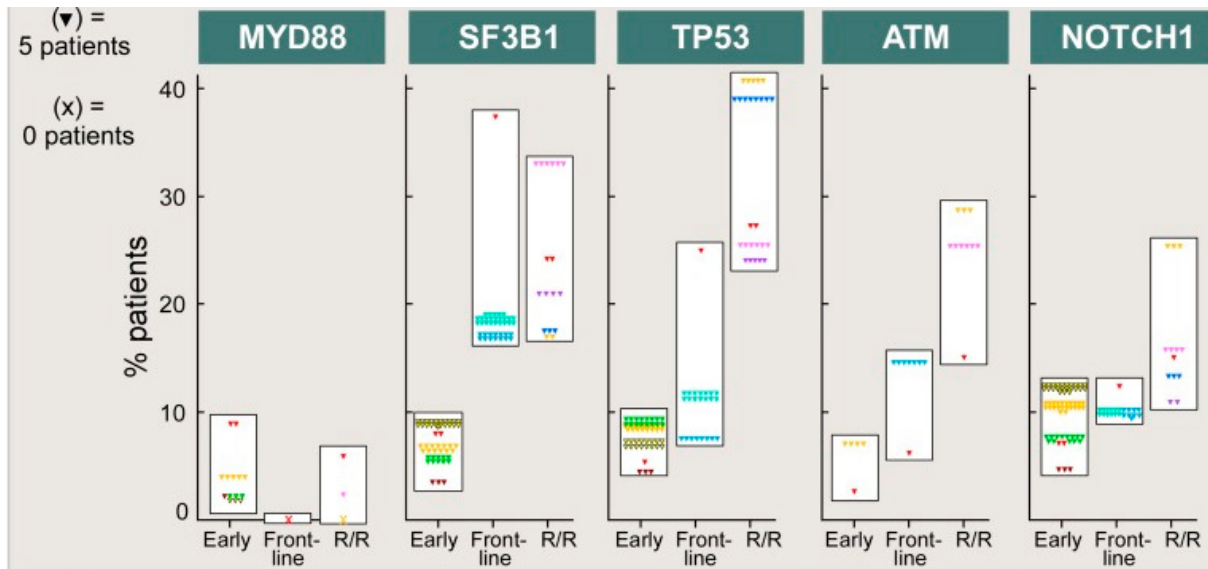
Figure 21. Frequency of gene mutations depending on the course of the disease. "Early" (newly diagnosed and untreated patients); "Frontline" (untreated patients requiring therapy); and "R/R" (relapsing or refractory patients). *SF3B1*, *TP53*, *ATM* and *NOTCH1* mutations have a dependency on disease course, but not *MYD88*.[130]

5.2. OTHER STRATEGIES IN CLL

Apart from the first- and second-line treatments of choice, there is a large number of therapeutic options that could be used in CLL management.

5.2.1. Immunotherapy

New anti-CD20 antibodies, immunomodulatory agents, check-point inhibitors and cellular therapies are being studied for CLL relapsed patients (Figure 22).[101]
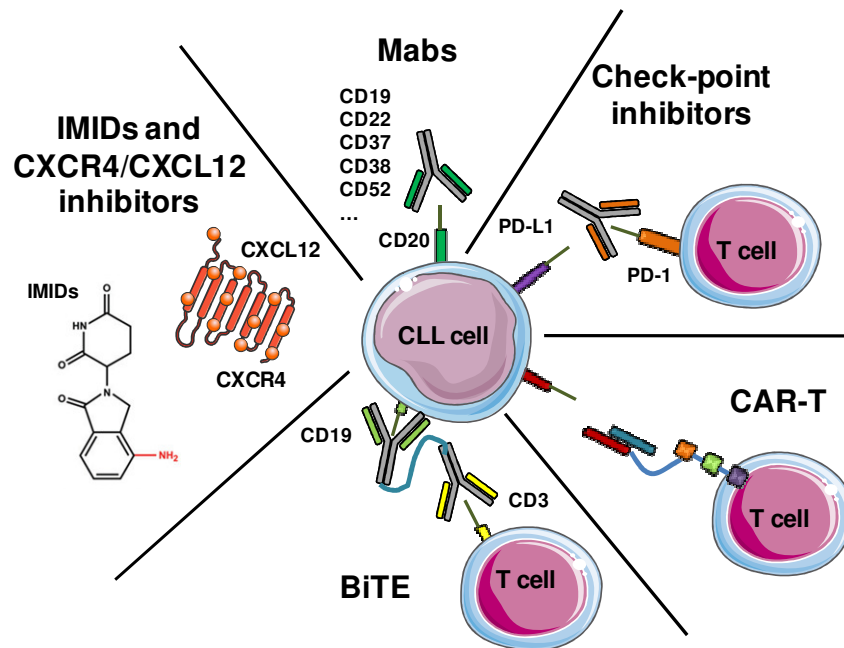
Figure 22. Mechanism of action of immunotherapies available in CLL.

5.2.1.1. Adoptive cellular therapy (CAR-T cells)

Genetically engineered autologous T cells -chimeric antigen receptor (CAR) T cells- are native T cells engineered *ex vivo* to recognize a tumor specific antigen (like CD19 for CLL) in conjunction with a co-stimulatory motif.[134] These cells are expanded and re-infused to generate a T cell-mediated cytotoxic response. Although CAR-T cells induce B-cell aplasia since normal CD19-expressing B cells are also eliminated, CAR-T cells are available to the patients in clinical trials, and are postulated as the alternative to HSCT.[129]

5.2.1.2. Check-point inhibitors

The discovery that malignant cells can evade the host immune system by inhibiting T cells has led to the development of immune checkpoint inhibitors.[135] Programmed cell death protein 1 (PD-1) and its ligands PD-L1 and PD-L2 have been identified as the most important axis in the maintenance of a malignant pro-survival microenvironment. CLL cells upregulate PD-L1 expression and suppress host T cell effector responses, exacerbating the development of an exhausted T-cell phenotype, which overexpresses the PD-1 receptor and rendered incapable of attacking the malignant clone. A clinical trial has demonstrated synergy of ibrutinib and nivolumab in CLL (an anti-PD-1 monoclonal antibody).[129]

5.2.1.3. Monoclonal antibodies

Apart from the CD20 antibodies approved in CLL (rituximab, ofatumumab and obinutumab), some newer CD20 glycoengineered, like ublituximab,[129] are being tested in R/R CLL.

Monoclonal antibodies against different antigens rather than CD20 are also being tested in CLL clinical trials, like otlertuzumab (anti-CD37)[136] and alemtuzumab (anti-CD52).[137] CD37 is almost exclusively expressed on mature human B cells arguing for its role as a prime target molecule for CLL immunotherapy. The exact function of CD37 has not yet been elucidated, although it seems to be important for T-cell-dependent B-cell responses, and may be involved in both pro- and antiapoptotic signaling.[138] In contrast, CD52 is not restricted to B cells and is expressed also by T cells, granulocytes, monocytes, macrophages, natural killer and dendritic cells, and it is implicated in costimulatory signals for T-cell activation and proliferation.[139] Although alemtuzumab was approved for CLL front-line therapy, unfortunately the license of this drug has been withdrawn and it is only available through an international compassionate use program.[140]

5.2.1.4. IMIDs and CXCR4/CXCL12 inhibitors

Lenalidomide, a thalidomide analog, is an immunomodulatory drug (IMID), which interferes with CLL microenvironment: with NLC and endothelium survival support signals. It also restores functional immune synapse between T and CLL cells and down-regulates the immunosuppressive axis PD-1/PD-L1.[129] Lenalidomide is active alone, in CLL R/R patients, or in combination with rituximab or ibrutinib.[20, 102]

The CXCR4/CXCL12 signaling axis is involved in chemotaxis and CLL–NLC and CLL–BMSC (bone marrow stromal cell) interactions.[141] Plerixafor, a CXCR4 antagonist, in combination with rituximab, is in a phase I clinical trial in relapsed CLL patients.[142] Also NOX-A12, a CXCL12 RNA oligonucleotides, is in a phase II trial in combination with bendamustine and rituximab in relapsed CLL patients.[129]

5.2.1.5. Bi-Specific T-cell Engager (BiTE®)

Blinatumomab is a recombinant fusion single-chain antibody with bi-specific properties, composed of an anti-CD3 fragment linked to an anti-CD19 fragment. This novel antibody can opsonize CD19$^+$ cells and promotes direct immune synapse formation with T cells. This construct, a bi-specific T-cell engager (BiTE®), has received FDA (food and drug administration) approval for R/R acute lymphoblastic leukemia. Studies in indolent non-Hodgkin's lymphoma and diffuse large B-cell lymphoma (DLBCL) are ongoing with encouraging results.[129]

5.2.2. Novel kinase inhibitors

Apart from the approved inhibitors, several BTK inhibitors (e.g., acalabrutinib,[143-145] tirabrutinib,[146, 147] CC-292,[148, 149] and zanubrutinib,[150] new generation PI3K inhibitors (e.g.,umbralisib,[151] duvelisib,[152, 153] pilarilib,[154] buparlisib[155]) and new generation SYK inhibitors (e.g., entospletinibfre)[156] are emerging.

6. TOLL LIKE RECEPTORS PATHWAY

Toll-like receptors (TLRs) are the most well-known molecular pattern recognition receptors, which can recognize and respond to a unique repertoire of distinct molecules: pathogen-associated molecular patterns (PAMPs) and danger-associated molecular patterns (DAMPs).[157] When engaging with PAMPs or DAMPs, TLRs transduce the signaling to initiate innate and adaptive immune responses. TLRs are present in vertebrates, as well as in invertebrates. The TLRs thus appear to be one of the most ancient, conserved components of the immune system. In recent years TLRs were identified also in the mammalian nervous system. Members of the TLRs family were detected on glia, neurons and on neural progenitor cells in which they regulate cell-fate decision.[158]

TLRs constitute the 3rd essential signal for naive B-cell activation, along with BCR triggering and interaction with T cells.[159] In case of pathological overstimulation of the immune system, such as autoimmune diseases, B cells react to self-antigens using the BCR and TLRs.[160] A total of 13 TLRs have been identified, among which TLRs 1–10 are expressed in human despite the function of TLR10 is still unclear.[157] The expression of TLRs can be found in a variety of immune cells and non-immune cells, as shown in Table 7.[161]

Table 7. TLRs immune expression in different cell types and its PAMPs and DAMPs.[161-164]

TLR	Immune expression	PAMPs/DAMPs
TLR1/2	Cell surface: monocytes, macrophages, dendritic-/B-cells	Triacylated lipoproteins (Pam3CSK4), Peptidoglycans, Lipopolysaccharides
TLR2/6	Cell surface: monocytes, macrophages, dendritic-/B-cells	Diacylated lipoproteins (FSL-1)
TLR3	Endosome: B-, T-, natural killer- and dendritic- cells.	dsRNA (poly(I:C)), tRNA, siRNA
TLR4	Cell surface/endosomes: monocytes, macrophages, dendritic-/mast- cells, intestinal epithelium	Lipopolysaccharde (LPS), Paclitaxel
TLR5	Cell surface: monocytes, macrophages, dendritic-/B-cells	Flagellin
TLR7	Endosomes: monocytes, macrophages, dendritic-/B-cells	ssRNA, Imidazoquinolines (R848), Guanosine analogs (Loxoribine)
TLR8	Endosomes: monocytes, macrophages, dendritic-/mast- cells	ssRNA, Imidazoquinolines (R848)
TLR9	Endosomes: monocytes, macrophages, dendritic-/B-/T-cells	CpG DNA, CpG ODN (oligodesoxinucleótidos)
TLR10	Endosomes: monocytes, macrophages, dendritic cells	Not well described

While TLR1, TLR2, and TLR4–6 are mainly found on the cell surface, TLR3 and TLR7–9 are primarily expressed in the endosomes.[165] The molecular pathways of TLRs signal transduction can be simply categorized into two cascades; one is through the main adaptor protein, MYD88 and the other is through the TRIF (TIR-domain-containing adapter-inducing interferon-β) protein.[157] The TLRs pathway eventually activates the NF-κB and Janus kinase/signal transducer and activator of transcription 3 (JAK-STAT3) pathways to promote survival, activation, cytokine secretion and expansion of immune cells (Figure 23).[34, 166] It also activates the mitogen-associated protein kinase (MAPK), which drives the expression of pro-inflammatory genes.[157]

Figure 23. The TLRs signaling pathway and its ligands. TLRs are located on either plasma or endolysosomal membranes. Signaling downstream of TLRs is mediated by MYD88- and/or TRIF-dependent pathways, leading to the activation of NF-κB, IRF5, and the MAPK pathways, inducing the expression of proinflammatory cytokines. Modified from *Balka and De Nardo, J Leukoc Biol, 2019.*[167]

The ligation of TLRs ligands results in the recruitment of MYD88 to the Toll/interleukin-1 receptor (TIR) domain and subsequently induces Interleukin 1 receptor associated kinase 4 (IRAK4) and kinase 1 and 2 (IRAK1/2) binding to form the Myddosome (Figure 23).[167] TLR3 and partially TLR4 signaling is through the adaptor protein TRIF, to activate interferon regulatory factors and NF-κB.[168]

TLRs activation is one of the first defensive mechanisms used by the host to induce innate and subsequent adaptive immune responses to fight the invading pathogens and repair the damaged tissues.[169] However, dysregulated TLRs signaling could disrupt the immune homeostasis in the host by sustained pro-inflammatory cytokines and chemokines secretion. This often contributes to the development of many inflammatory and autoimmune diseases. Thus, there is a growing interest in modulating TLRs activity as a strategy to prevent uncontrolled infection and limit inflammation, and for its possible beneficial effects in chronic inflammatory diseases, autoimmune diseases and cancer.[168]

6.1. RECURRENT MUTATIONS IN TLRs-PATHWAY

Gain-of-function mutations in TLRs pathway activate downstream signaling in absence of cognate ligands for TLRs, transduced to a constitutive activation of classical NF-κB signaling, resulting in increased cellular proliferation and survival.[170, 171] The enhanced activity of TLRs conferred by these mutations triggers an increased production of cytokines which results in the recruitment of myeloid cells and T lymphocytes, creating a favorable microenvironment.[172] These mutations are found in many lymphoid neoplasms, like DLBCL or CLL. Mutations are found in different proteins of the pathway, like *TLRs, MYD88* and *IRAK1*, among others in CLL.[173] *TLRs* linked to *MYD88* are more frequently mutated than those linked to *TRIF*.[174] Activating mutations of *MYD88*, particularly L265P, occur in about 30% of activated B cell-like (ABC) DLBCLs, a subtype of DLBCL that responds poorly to standard chemotherapy[175] and in extranodal subtypes of DLBCL such as primary DLBCL of the central nerve system (CNS; 70%), cutaneous DLBCL, leg-type (54%) and testicular DLBCL.[170] This mutation also occurs in ~90% of Waldenström macroglobulinemia (WM) cases and in significant portions of CLL patients.[170, 171]

6.1.1. *MYD88 mutations in CLL*

MYD88 mutations reach up to 2% to 5% in CLL and are strikingly enriched among patients expressing IGHV M.[176] *MYD88* mutated (*MYD88* M) patients are significantly younger (Figure 24a), have a trend to male predominance, a lower frequency of Binet stage A, and almost absence of adverse cytogenetic alterations or mutations in *TP53, NOTCH1, SF3B1, ATM*, and *BIRC3* and lower percentage of cases with high expression of CD38 than in patients with *MYD88* unmutated (*MYD88* UM).[173] *MYD88* M cases are not assigned to a common stereotyped BCR subset.[176] The OS of IGHV M CLL patients *MYD88* M showed a significant better OS than *MYD88* UM (Figure 24b), there is no correlation in time to first treatment (TTFT).[173]
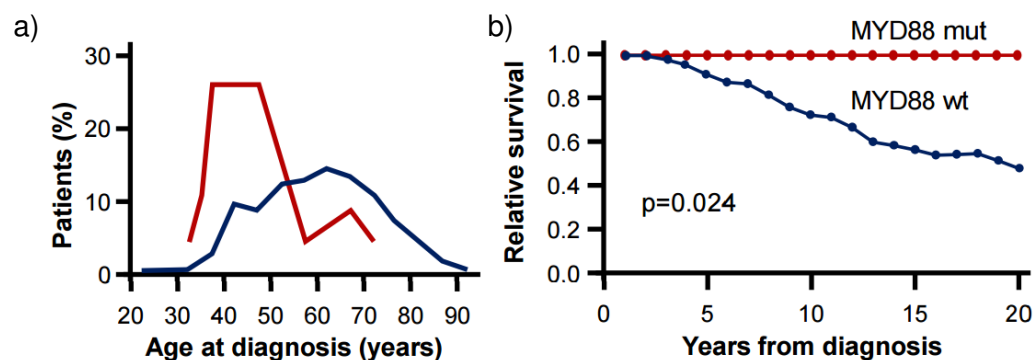
Figure 24. Age distribution and outcome of patients according to *TLR/MYD88* mutations. Images from *Martinez Trillo et al, Blood, 2014.*[173]

6.2. TOLL-LIKE RECEPTORS PATHWAY STIMULATION

As shown in Table 7 and Figure 23, specific ligands are described to stimulate the different TLRs, ranging from virus or bacteria to endogenous ligands.

TLRs stimulation can have anti-tumor effects by acting on immune cells or directly on tumor cells, thereby improving the anti-tumoral immune response and/or leading to tumor cell apoptosis. In contrast, TLRs stimulation can have pro-tumoral effects, so it's not very clear the TLRs stimulation effects in cancer, Table 8.[177]

Table 8. Pro- and anti-tumoral effects of TLRs expression and/or stimulation.
HCC: hepatocellular carcinoma; MDSC: myeloid-derived suppressor cell; Treg: regulatory T-cells; NK: natural killer; CTL: cytotoxic T-lymphocyte. Data from *Dajon et al, Immunobiology, 2017.*[177]

Anti-tumoral effect		
TLR	**Tumor type**	**Mechanism**
TLR1/2	- Colon cancer	- ↑Tumor cell apoptosis; ↓ Tumor cell proliferation
	- HCC and lung cancer	- ↑Cytotoxic immune cells; ↓MDSC, Treg
TLR3	- Head/neck cancer, pharyngeal and colon carcinoma, melanoma, HCC	- ↑Tumor cell apoptosis + pro-apoptotic protein; ↓Surviving + anti-apoptotic proteins
	- HCC, colon cancer, lung cancer	- ↑Cytotoxic immune cells (NK, CD8$^+$ T cells); ↓Immunosuppressive immune cells
TLR4	- Skin cancer, mammary cancer, HCC, lung cancer	- ↑IFN-γ; ↓ Immunosuppressive immune cells (Treg) + tumor cell proliferation + angiogenic factors
	- Breast cancer, melanoma	- ↑Cytotoxic immune cells (CTL, NK cells)
TLR5	- Breast cancer, colorectal cancer, lung cancer	- ↑Necrosis areas + neutrophil infiltration
	- Melanoma	- ↑Cytotoxic immune cells (CTL)
TLR7	- Pancreatic cancer, T-cell lymphoma, HCC, breast cancer, melanoma	- ↑Cytotoxic immune cells (CTL, NK cells, T cells)
	- CLL	- ↑Sensitivity to cytotoxic effectors (↑ in T cell proliferation)
TLR 9	- Neuroblastoma, glioma, CLL	- ↑Tumor cell apoptosis; ↓Tumor cell proliferation
	- Ovarian and lung cancer	- ↑Cytotoxic immune cells (NK, CD8$^+$T cells, M1) + granulocytes; ↓Immunosuppressive immune cells (Treg, M2)

Pro-tumoral effect		
TLR	**Tumor type**	**Mechanism**
TLR2	- Head/neck carcinoma, lymphoma, HCC, breast and intestinal cancer	- ↑Pro-inflammatory factors; ↑ immunosuppressive immune cells (MDSC)
TLR4	- Breast, lung, head, neck and prostate cancer and HCC	- ↑IL6 + IL8 + TGFβ + VEFG + Tumor cell proliferation ↓Tumor cell apoptosis
	- Colon cancer	- ↑IL6; ↓ Cytotoxic immune cells (NK + T cells)
TLR5	- Gastric, salivary and gland cancer	- ↑IL8 + Tumor cell proliferation
	- Sarcoma cancer	- ↑IL6 + MDSC
TLR7	- Myeloma, CLL	- ↑IL6
	- Pancreatic cancer	- ↑Inflammation + tumor cell proliferation + pro-tumoral molecules; ↓ Anti-tumoral molecules
	- Lung cancer	- ↑MDSC + Anti-apoptotic molecules
TLR9	- Esophageal and prostate cancer and myeloma	- ↑Pro-inflammatory cytokines + tumor cell proliferation; ↓Tumor cell apoptosis
	- Ovarian and breast cancer	- Inflammation- and stem-cell-related markers

Recently, a new activity for TLR8 activation has been described: blocking the induction of T-cell senescence in naive/effector T cells from tumor-derived endogenous cyclic adenosine monophosphate (cAMP), resulting in enhanced anti-tumor immunity.[72] Although TLRs stimulation can confer anti- or pro-tumoral effects, it is clear that it's important to study their role in cancer treatments.[177]

6.3. TOLL-LIKE RECEPTORS PATHWAY INHIBITION

Because of the overactive TLRs signaling in several autoimmune diseases and as some B-cell lymphomas carry activating mutations in this pathway, there is strong interest in developing inhibitors/antagonists of this pathway. TLRs inhibition can be achieved through two major strategies: (1) blocking the binding of the agonists to the corresponding ligands (i.e., antibodies, lipid A analogs, small molecules inhibitors (SMIs) and oligonucleotides) and (2) inhibiting the intracellular signaling of the TLRs pathways (i.e., SMIs) (Figure 25).

Although significant efforts have been made in developing different kinds of new TLRs inhibitors/antagonists, only limited numbers of them have undergone clinical trials, and none have been approved for clinical uses to date. Nevertheless, these findings and continuous studies of TLRs inhibition highlight the pharmacological regulation of TLRs signaling.[168]
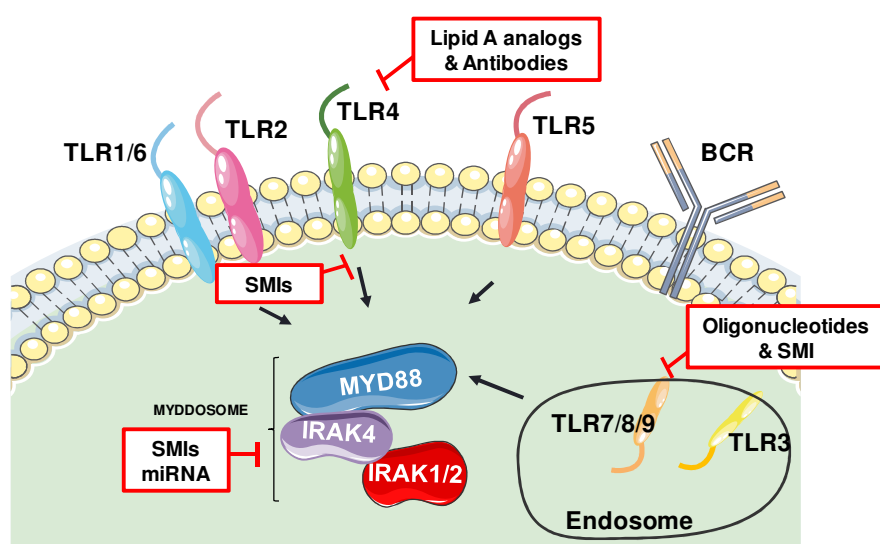
Figure 25. Potential drug targets of TLRs pathway. Data from Gao W *et al, Front Physiol. 2017.*[168]

As MYD88 is the most commonly mutated gene in B-cell lymphomas, lot of effort has been made to develop MYD88 inhibitors, but unfortunletly, itself is not a promising target, because it is difficult to develop inhibitors for adaptor proteins. IRAK4 is essential for its signaling, but not IRAK1.[171] IRAK4 inhibitors are being studied for autoimmune disorders and other malignancies that depend on TLRs signaling. Kelly *et al*,[172] evaluated the *in vitro* and *in vivo* effects of ND2158, an IRAK4 competitive inhibitor, in blocking TLR-mediated responses in ABC-DLBCLs *MYD88* M. This agent promoted killing of ABC-DLBCL lines harboring *MYD88* L265P mutation, by down-modulating survival signals, including NF-κB and autocrine IL-6/IL-10 engagement of the JAK–STAT3 pathway. In ABC-DLBCL xenograft models, IRAK4 inhibition suppressed tumor growth as a single agent, and in combination with ibrutinib or venetoclax. As such, they have proposed that inhibitors of IRAK4 kinase activity could have a therapeutic impact in lymphomas with *MYD88* mutations.[171, 172]

7. RAS-BRAF-MAPK-ERK PATHWAY

The starting point of the RAS-BRAF-MAPK-ERK pathway is the binding of a ligand (e.g., a growth/differentiation factor, cytokine or hormone) to the receptor tyrosine kinase (RTK). Ligand binding causes the dimeri formation and leads to phosphorylation of their cytoplasmic domains, which activate RAS (retrovirus-associated DNA sequences). Following, RAS activates BRAF (encoded by *MAPKKK-mitogen associated kinase kinase kinase*),[178] a member of the kinase RAF family.[179] BRAF facilitates phosphorylation of the protein kinase MEK (mitogen-activated ERK kinase; encoded by *MAPKK*). MEK activates ERK (extracellular signal-regulated kinase), the final kinase in the cascade (encoded by *MAPK*) which translocate to the nucleus activating transcription factors.[178] This pathway plays a key role in regulating embryogenesis, cell proliferation, differentiation, migration, and survival.[180] This cascade is under control of feedback loops (Figure 26), which effects can be rapid or delayed. The rapid feedback mechanisms refer to activated ERK which inhibits phosphorylation of their upstream factors (MEK, RAF, SOS (son of sevenless) and RTKs).[181] The delayed feedback mechanisms are the *de novo* expression of DUSPs (dual-specificity phosphatase) proteins, which dephosphorylate ERK.[182] In short, the feedback loops play an essential role in maintaining cellular homeostasis in physiological conditions.[183]
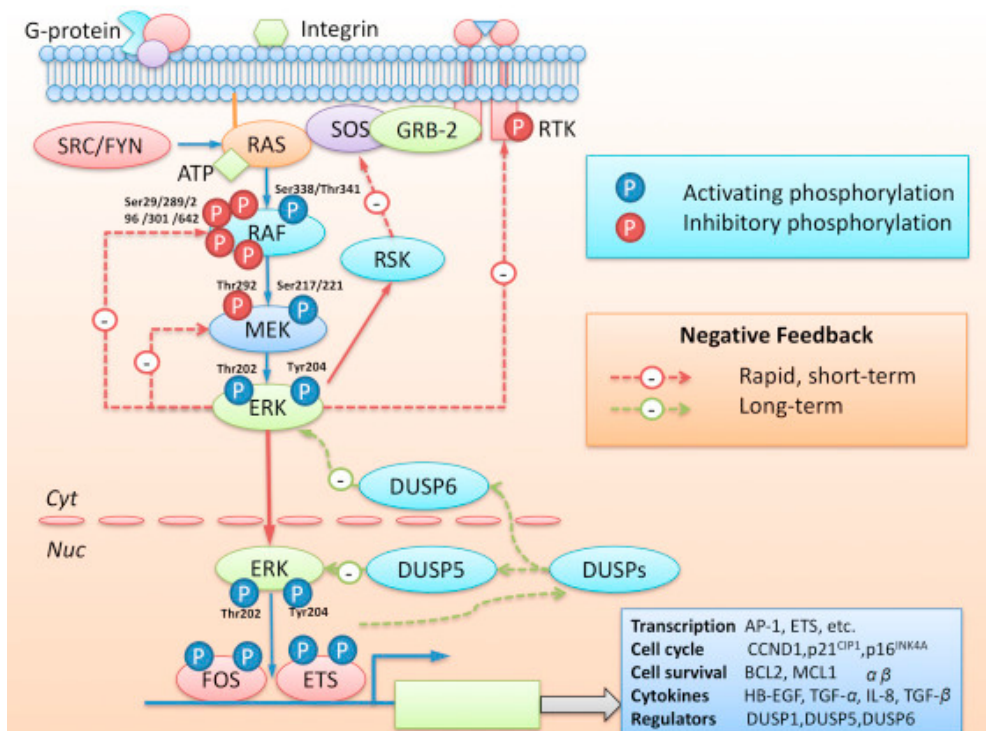
Figure 26. Activation and feedback regulation of the MAPK pathway. The MAPK pathway is activated in human tumors by upstream receptor tyrosine kinases (RTK) or by mutations in RAS, BRAF, and MEK1. RTKs activate RAS by recruiting adaptor proteins and exchange factors. RAS activation promotes the formation of RAF dimers, which activate MEK-ERK cascade through phosphorylation. ERK pathway activity is regulated by negative feedback at multiple levels, including the transcriptional activation of DUSP proteins that negatively regulate the pathway. ERK also phosphorylates and thus regulates CRAF and MEK activity directly. ERK, phosphorylates SOS, inhibiting its activity and thus negatively regulating RAS. From *Liu F, Acta Pharm Sin B.*[183]

7.1.   RECURRENT MUTATIONS IN RAS-BRAF-MAPK-ERK PATHWAY

Malfunction in MAPK signaling leads to the occurrence and progression of cancers (Table 9), mainly by somatic mutations.[184]

RAS has been identified as an oncogene and is mutationally activated in approximately one-third of all cancers, like pancreas, colon, thyroid or melanoma.[185] *BRAF* mutations have been widely identified in tumors of all human cancers.[186] This mutation is highly prevalent in hairy cell leukemia (HCL) and melanoma.[187] The most common mutation of *BRAF* is *BRAF^{V600E}*, which is a point mutation at valine 600 to yield glutamic acid, which lead to overactivity of its down-stream effectors MEK and ERK.[180] *MEK* mutations have been mainly identified in melanoma.[188] Generally, all of the upstream mutations can lead to ERK protein hyperactivation, which is related to modulation of anti-apoptotic molecules such as BCL2, linked to drug resistance in some types of cancers.[183]

Table 9. MAPK mutations in different cancers. Data from *Liu F, Acta Pharm Sin B.*[183]

Cancer type	Mutation type and rate (%)	Major mutation site
Prostate cancer	- *KRAS* (90%)	- G12D, G13D, G12V, G12S, G12C
Non-small cell lung cancer	- *NRAS* (35%)	- Q61K, Q61R, C186F, Q61L, Q61K
Colorectal cancer	- *KRAS* (45%)	- G12D, G12V, G13D, G12C, A146T, F566L
	- *BRAF* (12%)	- V600E
Pancreatic cancer	- *KRAS* (90%)	- G12D, G12V, G12R, G12C
Melanoma	- *NRAS* (15%)	- Q61R, Q61L, Q61K, Q61H
	- *BRAF* (66%)	- V600E
	- *MEK* (6%)	- Q56P, V60E, C121S, G128V, P124L, V154L
Bladder cancer	- *KRAS* (50%)	- G12V, G12D, G12C
Acute myeloid leukemia	- *NRAS* (30%)	- G12D, G13D, G12V, Q61H, A59E, A164T
Ovarian cancer	- *BRAF* (30%)	- V600E, A747V, G464E, V226M
Papillary thyroid cancer	- *RAS* (60%)	- KRAS:G12R, NRAS:Q61R
	- *BRAF* (35%–70%)	- V600E
Hairy cell leukemia (HCL)	- *BRAF* (100%)	- V600E

Surprisingly, the *BRAF^{V600E}* mutation is very rare in hematologic malignances excluding HCL.[35, 189] In CLL, constitutive activation of MAPK signaling has been reported in about half of cases, which hints at a critical role of MAPK signaling in cell survival.[190]

7.2.   RAS-BRAF-MAPK-ERK PATHWAY INHIBITION

As the abnormal activation of the RAS-BRAF-MAPK-ERK signaling pathway plays a major role in many tumors a number of studies have been focused on the inhibitors of the core protein kinases RAS, RAF, MEK and ERK (Figure 27) and some of them are being used in the clinics.[191]

To develop RAS inhibitors is a significant challenge and, until now, there are not clinically effective molecules so far.[192]

BRAF and MEK inhibitors have shown clinical benefits in cancers harboring oncogenic mutations in this pathway. However, patients treated with RAF or MEK inhibitors frequently develop drug resistance.[193, 194] The BRAF inhibitors (BRAFi) vemurafenib (specific for $BRAF^{V600E}$ mutated cases) and dabrafenib (specific for mutations in $BRAF^{600}$) were the first selective BRAFi clinically approved for the treatment of melanoma with $BRAF$ mutations. MEK1 and MEK2 inhibitors (MEKi), may have antitumor activities against melanoma patients with/without NRAS mutations.

ERK inhibitors have gained an increasing interest with the difficulties faced by RAF and MEK inhibitors.[183, 191] Some ERK inhibitors are being used in clinical trials, like ulixertinib (Phase II), which was used in acute myeloid leukemia, solid tumors and melanoma.[183, 195]
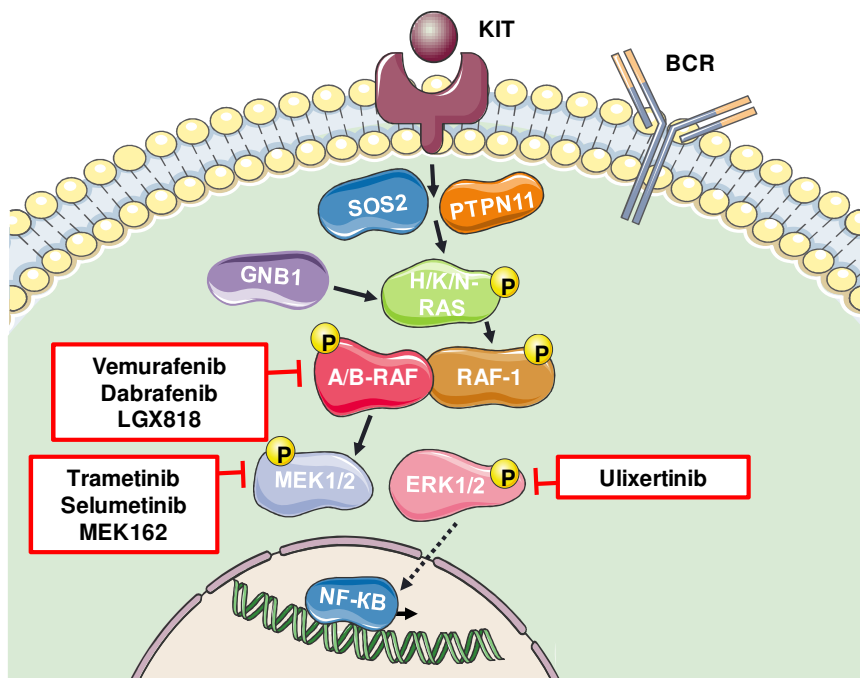
Figure 27. Potential drug targets of RAS-BRAF-MAPK-ERK signaling pathway tested in the clinics. Data from *McCain, P T. 2013.*[178]

AIMS

GENERAL OBJECTIVES

The main goal of this dissertation is to explore new therapeutic approaches targeting CLL cells and their interactions with their microenvironment. CLL is a very heterogeneous incurable disease with a very high dependency on microenvironment.

Following this line of investigation, the **first objective** of this thesis is to analyze CLL cells response, with and without microenvironment signals, to specific inhibitors against major recurrent mutations. On the other hand, the **second objective** of this thesis is to validate new targetable molecules (found by systems biology) implicated in the tumor microenvironment crosstalk in CLL.

SPECIFIC OBJECTIVES

1. To study the TLRs pathway in CLL blocking IRAK4 (a key kinase in the TLRs signal transduction), with a new inhibitor (ND2158).
    1.1. To characterize the TLRs pathway in CLL cells.
    1.2. To analyze the cytotoxic effect of ND2158 on primary CLL cells.
    1.3. To establish the molecular basis of ND2158 effects on human CLL cells and tumor microenvironment.
    1.4. To study the antitumor effect of ND2158 *in vivo.*
    1.5. To assess potential therapeutic combinations of ND2158 with currently approved CLL drugs.
2. To analyze the clinical impact of mutations in the RAS-BRAF-MAPK-ERK pathway in CLL and the possibility to target them.
    2.1. To characterize the MAPK pathway in CLL cells.
    2.2. To analyze the cytotoxic effect of MAPK pathway inhibitors in primary CLL cells.
    2.3. To establish the molecular basis related to drug response.
    2.4. To analyze the clinical impact of mutations in the MAPK pathway.
3. To find new compounds on reprofiling drugs to target CLL by systems biology.
    3.1. To generate an *in silico* model of CLL and select the target candidates.
    3.2. To analyze the effectivity of the selected compounds and their mechanism of action.
    3.3. To assess potential therapeutic combinations of selected compounds with currently approved CLL drugs.

RESULTS

Article 1: Targeting IRAK4 disrupts inflammatory pathways and delays tumor development in chronic lymphocytic leukemia

Giménez N*, Shulz R*, Higashi M, Aymerich M, Villamor N, Delgado J, Juan M, Lopez-Guerra M, Campo E, Rosich L[+], Seiffert M[+], Colomer D[+]

ABSTRACT

Interleukin-1 receptor-associated kinase 4 (IRAK4) plays a critical role in Toll-like receptor (TLR) signal transduction and innate immune responses. Recruitment and subsequent activation of IRAK4 upon TLR stimulation is mediated by the myeloid differentiation primary response 88 (MYD88) adaptor protein. Around 3% of chronic lymphocytic leukemia (CLL) patients have activating mutations of *MYD88*, a driver mutation in this disease. Here, we studied the effects of TLR activation and the pharmacological inhibition of IRAK4 with ND2158, an IRAK4 competitive inhibitor, as a therapeutic approach in CLL. Our in vitro studies demonstrated that ND2158 preferentially killed CLL cells in a dose-dependent manner. We further observed a decrease in NF-κB and STAT3 signaling, cytokine secretion, proliferation and migration of primary CLL cells from *MYD88*-mutated and –unmutated cases. In the *Eμ*-TCL1 adoptive transfer mouse model of CLL, ND2158 delayed tumor progression and modulated the activity of myeloid and T cells. Our findings show the importance of TLR signaling in CLL development and suggest IRAK4 as a therapeutic target for this disease.

*Equally contribution

[+]Share senior authorship

ARTICLE

Chronic lymphocytic leukemia

Targeting IRAK4 disrupts inflammatory pathways and delays tumor development in chronic lymphocytic leukemia

Neus Giménez[1,2] · Ralph Schulz[3,4] · Morihiro Higashi[1] · Marta Aymerich[5] Neus Villamor[5] · Julio Delgado[6] · Manel Juan[7] · Mònica López-Guerra[1,5] · Elias Campo[5,8] · Laia Rosich[1] · Martina Seiffert[3] Dolors Colomer[1,5,8]

Abstract

Interleukin-1 receptor-associated kinase 4 (IRAK4) plays a critical role in Toll-like receptor (TLR) signal transduction and innate immune responses. Recruitment and subsequent activation of IRAK4 upon TLR stimulation is mediated by the myeloid differentiation primary response 88 (MYD88) adaptor protein. Around 3% of chronic lymphocytic leukemia (CLL) patients have activating mutations of *MYD88*, a driver mutation in this disease. Here, we studied the effects of TLR activation and the pharmacological inhibition of IRAK4 with ND2158, an IRAK4 competitive inhibitor, as a therapeutic approach in CLL. Our in vitro studies demonstrated that ND2158 preferentially killed CLL cells in a dose-dependent manner. We further observed a decrease in NF-κB and STAT3 signaling, cytokine secretion, proliferation and migration of primary CLL cells from *MYD88*-mutated and -unmutated cases. In the *Eμ*-TCL1 adoptive transfer mouse model of CLL, ND2158 delayed tumor progression and modulated the activity of myeloid and T cells. Our findings show the importance of TLR signaling in CLL development and suggest IRAK4 as a therapeutic target for this disease.

Introduction

Toll-like receptors (TLRs) are the most well-known molecular pattern recognition receptors. They constitute the third essential signal for naïve B-cell activation,

These authors contributed equally: Neus Giménez, Ralph Schulz

These authors contributed equally: Laia Rosich, Martina Seiffert, Dolors Colomer

✉ Martina Seiffert
m.seiffert@dkfz.de

✉ Dolors Colomer
dcolomer@clinic.cat

[1] Experimental Therapeutics in Lymphoid Malignancies Group, Institut d'Investigacions Biomèdiques August Pi i Sunyer (IDIBAPS), CIBERONC, Barcelona, Spain

[2] Anaxomics Biotech, Barcelona, Spain

[3] Division of Molecular Genetics, German Cancer Research Center (DKFZ), Heidelberg, Germany

[4] Faculty of Biosciences, Heidelberg University, Heidelberg, Germany

[5] Hematopathology Unit, Department of Pathology, Hospital Clinic, IDIBAPS, CIBERONC, Barcelona, Spain

[6] Department of Hematology, Hospital Clinic, IDIBAPS, CIBERONC, Barcelona, Spain

[7] Department of Immunology, Hospital Clinic, HSJD-HCB Immunotherapy Platform, IDIBAPS, Barcelona, Spain

[8] University Barcelona, Barcelona, Spain

along with B-cell receptor (BCR) triggering and interaction with T cells [1]. In case of pathological over-stimulation of the immune system, such as autoimmune diseases, B cells react to self-antigens using the BCR and TLRs [2]. Continuous TLR activation and subsequently, induction of chronic inflammation are also thought to be involved in malignant B-cell transformation, regulating both tumor cells and tumor-infiltrating innate and adaptive immune cells, including monocytes and T cells [3–5]. Thus, there is a growing interest in modulating TLR activity as a strategy to prevent uncontrolled infection and limit inflammation, and for its possible

beneficial effects in chronic inflammatory diseases, autoimmune diseases, and cancer [6].

TLR signaling is mediated by the adaptor molecule myeloid differentiation primary response 88 (MYD88) which recruits and activates interleukin-1 receptor-associated kinase 4 (IRAK4), accounting for almost all biological functions of MYD88 [7]. The TLR pathway eventually activates the nuclear factor kappa B (NF-κB) and Janus kinase/signal transducer and activator of transcription 3 (JAK-STAT3) pathways to promote survival, activation, and expansion of immune cells [8, 9].

A crucial role for TLRs has recently emerged in the pathogenesis of chronic lymphocytic leukemia (CLL), a malignancy that is characterized by a progressive accumulation of mature $CD19^+CD5^+$ B cells [10]. Approximately 3% of CLL cases harbor recurrent activating *MYD88* mutations [9, 11, 12]. These mutations are the most frequent in young CLL patients and are associated with a mutated status of the variable region of the immunoglobulin heavy chain (IGHV) locus [11, 12]. *MYD88* mutations are predominantly clonal and considered as drivers of CLL, highlighting the relevance of TLR signaling in CLL development and evolution [13, 14]. The enhanced activity of TLRs conferred by these mutations triggers an increased production of cytokines [9], which results in the recruitment of myeloid cells and T lymphocytes, creating a favorable microenvironment [15]. Previous findings suggest a therapeutic potential for IRAK4 inhibitors for the activated B-cell-like (ABC) subtype of diffuse large B-cell lymphoma (DLBCL) presenting with *MYD88* mutations, as well as for autoimmune disorders and other malignancies that depend on TLR signaling [8, 16–18]. Herein, we aimed to evaluate the in vitro and in vivo effects of ND2158, an IRAK4 competitive inhibitor, in blocking TLR-mediated responses in CLL cells and different subsets of immune cells that constitute the CLL microenvironment. The presented results enhance the understanding of this therapeutic approach and suggest new avenues for the development of novel TLR/MYD88-mediated cancer immunotherapy strategies.

Materials and methods

Human samples

Peripheral blood mononuclear cells (PBMCs) from CLL patients (with ≥90% tumor B cells) and healthy donors were isolated, cryopreserved and stored within the Hematopathology collection registered at the Biobank (Hospital Clinic-IDIBAPS; R121004-094). Clinical and biological data of each patient are detailed in Supplementary Table 1. *MYD88* mutations were analyzed in previous sequencing studies [9, 19, 20].

Mouse models

Eμ-TCL1 (TCL1) mice on C57BL/6 background were kindly provided by Dr. Carlo Croce (Ohio State University) [21]. *Nr4a1*[GFP] mice and *Myd88*^{−/−} mice were a kind gift from Dr. Markus Feuerer (DKFZ, Heidelberg) [22] and Prof. Dr. Hermann-Josef Gröne (DKFZ, Heidelberg) [23], respectively. Adoptive transfer (AT) of TCL1 leukemia in C57BL/6N wild-type mice (Janvier Labs, Saint-Berthevin, France) was performed as described before [24].

In vitro TLR stimulation

Primary CLL cells or B cells from TCL1 splenocytes were cultured with TLR ligands (0.5 μg/mL Pam3CSK4-TLR1/2, 10^8 cells/mL HKLM-TLR2, 1 μg/mL poly(I:C)LMW-TLR3, 1 μg/mL *Salmonella typhimurium* flagellin-TLR5, 1 μg/mL FSL1-TLR2/6, 1 μg/mL Imiquimod-TLR7, 1 μg/mL ssRNA40-TLR8, and 5 μM ODN2006-TLR9) alone or with a TLR agonist mix (Pam3CSK4, HKLM, FSL1 and ODN2006) from Human TLR1-9 Agonist Kit[TM] (InvivoGen, San Diego, CA, USA). TLR4 was not assessed due to its broad recognition pattern of microbial components. For all incubations, cells were first incubated with 10 μg/mL of polymyxin B (Sigma-Aldrich, St. Louis, MO, USA) for 20 min in order to neutralize unspecific TLR stimulation. Specific ligands for TLR10 have not yet been univocally identified. Monocytes were stimulated via TLR4 using lipopolysaccharides (LPS; Sigma-Aldrich).

Statistical analysis

Statistical data analysis was performed using Prism 6.01 Graphpad software. Statistical analyses were performed using two-tailed nonparametric tests assuming equal variances of data. Wilcoxon matched-pairs signed-rank test was used for paired comparisons. For independent comparisons, the Mann−Whitney test was used instead. The Wilcoxon signed-rank test was used to compare sample medians to a hypothetical value. Sample size was determined based on expected variance of read-out. No samples or animals were excluded from the analyses. No randomization or blinding was used in animal studies. The statistical test used for each data set is indicated in the figure legends. Statistical significance was considered when *P* value < 0.05.

Results

MYD88-mutated CLL cases harbor an inflammatory phenotype

As the TLR pathway has been described to have a central role in *MYD88*-mutated CLL cases [9], we first analyzed the

mRNA expression of the TLR repertoire in CLL cells. By using gene expression data generated previously [19], we compared *MYD88*-mutated cases (*n* = 18, all IGHV-mutated) with *MYD88*-unmutated cases (*n* = 249 IGHV-mutated and *n* = 143 IGHV-unmutated). The TLR expression profiles in the three subgroups were very similar, with high expression levels of *TLR1*, *TLR7* and *TLR10*, and intermediate levels of *TLR2*, *TLR4*, *TLR6*, *TLR8* and *TLR9*. CLL cells expressed low levels of *TLR3* and *TLR5* (Fig. 1a).

To characterize the impact of *MYD88* mutations on the transcriptome of CLL cells, we compared gene expression profiles (GEP) of 18 *MYD88*-mutated CLL cases with 398 cases without mutation in this gene and further restricted this analysis to CLL IGHV-mutated cases (*n* = 249), as all 18 cases with *MYD88* mutations were among this group. Several gene sets related to cytokines and inflammation, such as NF-κB pathway and STAT signaling, were the most enriched in the *MYD88*-mutated subgroup compared to *MYD88*-unmutated cases (Fig. 1b, Supplementary Fig. S1, and Supplementary Table 3). Accordingly, we observed significantly higher mRNA expression levels for CCL3, TNFα, and IL6 in *MYD88*-mutated compared to -unmutated cases (Fig. 1c, left panel). In line with this, primary CLL cells from *MYD88*-mutated patients analyzed in cell culture supernatants by Luminex® Bead Panel secreted higher levels of CCL2, CCL3, and CCL4 in vitro compared with *MYD88*-unmutated CLL cases (Fig. 1c, right panel). IL1β, TNFα, IL10, and IL6 secretion levels were under the limit of detection.

TLR stimulation modulates cytokine secretion, intracellular signaling, and CLL cell proliferation

We next analyzed the functionality of TLRs in CLL by stimulating primary CLL cells from *MYD88*-mutated and -unmutated cases with various TLR agonists in an attempt to distinguish the contribution of each TLR to cell signaling. CLL cells (CD19$^+$CD5$^+$ cell content: 95.1% ± 2.6%) were cultured with TLR agonists and levels of CCL2 (MCP1), CCL3 (MIP1α), CCL4 (MIP1β), TNFα, IL1β, IL6, IL10, IL1RA, IFNγ and IL12-p70 were analyzed in cell culture supernatants using Luminex® Bead Panel. All cytokines, besides IFNγ and IL12-p70, were detectable and upregulated by TLR stimulation (Fig. 2a). Except Poly(I:C)LMW and Imiquimod which barely induced cytokine secretion in CLL cells, all other TLR agonists triggered a strong cytokine response, with TLR1 and -2 agonists being the strongest inductors in most CLL cases. This suggests activity for TLR1, -2, -5, -6, -8 and -9, but not TLR3 and -7 in CLL cells.

We further analyzed the effect of the different TLR agonists on NF-κB and STAT3 signaling by immunoblot analysis. The highest levels of phosphorylated IκBα$^{pS32/36}$ and STAT3^{pY705} were observed in CLL cells after stimulation with Pam3CSK4,

HKLM, FSL1 and ODN2006 (TLR1, -2, -6 and -9 agonists) (Supplementary Fig. S2). As responses to TLR agonists were heterogeneous among cases, we tested the combination of these four TLR agonists (named as "mix") to achieve a full activation of the pathway in all cases. We observed higher phosphorylation levels of IκBα and STAT3 (Fig. 2b, Supplementary Fig. S3), and higher cytokine levels in CLL cell culture supernatants (Fig. 2c) upon stimulation with this mix compared to individual TLR agonists. We further detected a stronger induction of CLL cell proliferation, analyzed by CFSE dilution, by the TLR mix (up to eightfold of unstimulated cells) compared to single TLR agonists (2- to 7-fold) (Fig. 2d). For all analyzed responses to TLR stimulation, no differences between *MYD88*-mutated and -unmutated CLL cases were observed. We also analyzed responses to TLR agonist mix in IGHV-unmutated CLL cases and obtained similar results as with IGHV-mutated CLL cells (Supplementary Fig. S4). Therefore, we used the TLR agonist mix for further analyses to achieve a complete activation of TLR signaling in CLL cells.

The IRAK4 inhibitor ND2158 decreases viability and proliferation in CLL cells

To evaluate the potential of IRAK4 inhibition for CLL, cells from 37 CLL patients were exposed to increasing concentrations of the IRAK4 inhibitor ND2158. Treatment with 10−100 μM ND2158 significantly reduced cell viability compared to untreated samples in a dose-dependent manner (Fig. 3a). This effect was higher in CLL cells compared to B or T lymphocytes from healthy donors (Fig. 3a and Supplementary Fig. S5). There was no difference in the effect of ND2158 on CLL cells from *MYD88*-mutated and -unmutated cases, as previously reported [25]. Comparable results were obtained by analyzing intracellular ATP levels of ND2158-treated and untreated CLL cells of the same cases (Supplementary Fig. S6). ND2158 reduced viability of CLL cells also in co-cultures with monocytes that protect CLL cells from spontaneous apoptosis in vitro and are therefore considered to model the tissue microenvironment of CLL (Supplementary Fig. S7).

We further tested the cytotoxic activity of ND2158 for CLL cells that were stimulated with TLR agonists and confirmed significantly lower levels of cell viability in treated versus untreated samples, for both *MYD88*-mutated and -unmutated cases after 2 and 6 days of incubation (Fig. 3b).

CLL cell proliferation induced by TLR agonists after 6 days was impaired by ND2158 treatment and no difference between *MYD88*-mutated and -unmutated cases was observed (Fig. 3c). Similar results were obtained using single TLR agonists to stimulate CLL cells (Supplementary Fig. S8). These results were validated by analyzing incorporation of EdU in proliferating cells and by Ki-67 stainings (Supplementary Fig. S9).
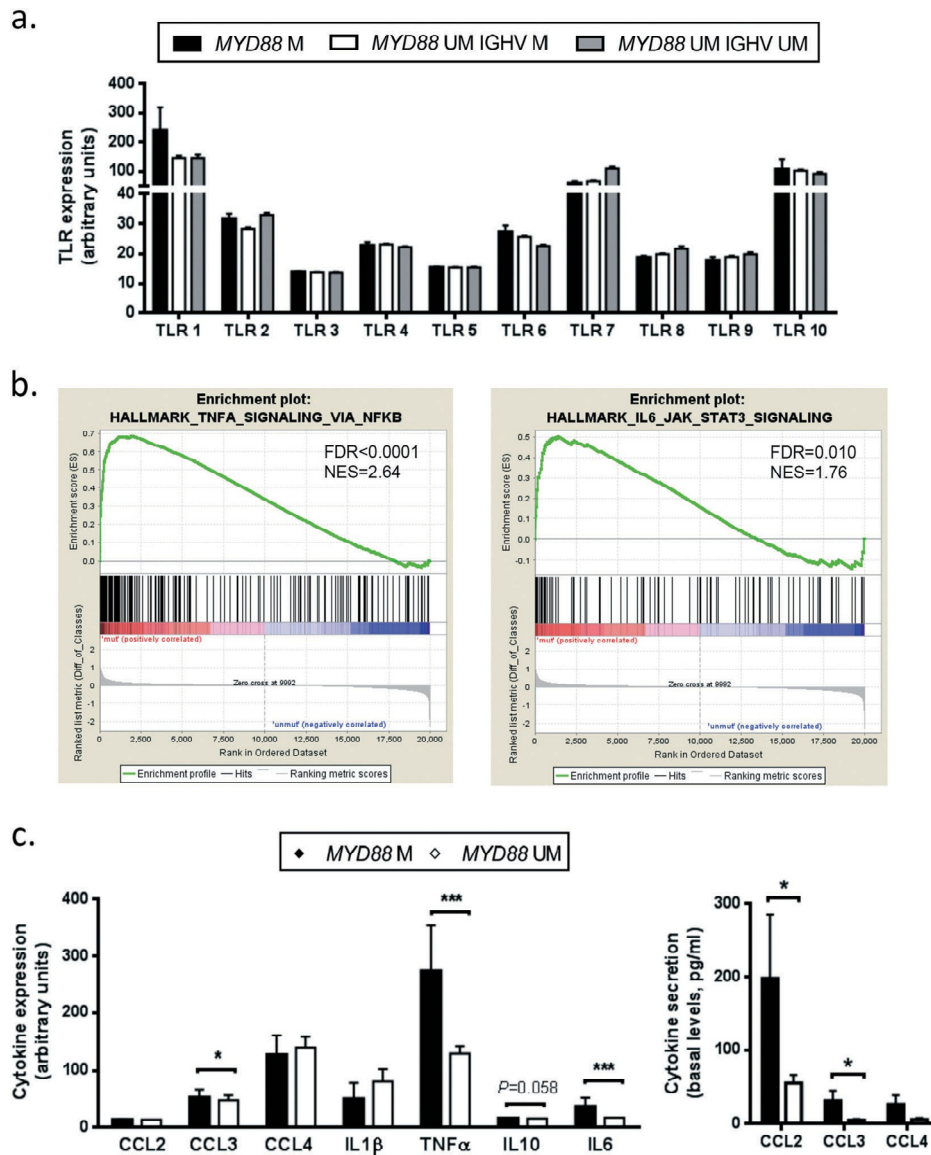
Fig. 1 *MYD88*-mutated CLL cases harbor an inflammatory phenotype. a TLR gene expression profile in CLL cells comparing *MYD88*-mutated ($n = 18$ IGHV-mutated) and *MYD88*-unmutated cases ($n = 249$ IGHV-mutated and $n = 143$ IGHV-unmutated). b Gene set enrichment analysis comparing *MYD88*-mutated ($n = 18$) versus *MYD88*-unmutated ($n = 249$) CLL cases (all IGHV-mutated). c Left panel: Cytokine transcript levels of *MYD88*-mutated ($n = 18$) and *MYD88*-unmutated CLL cases ($n = 249$ IGHV-mutated CLL samples) analyzed by gene expression profile. Right panel: Cytokine secretion of CLL cells from *MYD88*-mutated ($n = 6$) and *MYD88*-unmutated ($n = 9$) cases (all IGHV-mutated) was analyzed after 48 h of culture by flow cytometry using Luminex®Bead Panel. Bars represent the mean ± SEM of all samples analyzed. Wilcoxon signed-rank test was used for statistical analysis. *$P < 0.05$, ***$P < 0.001$. Gene sets with false discovery rate (FDR) q value < 0.05 and a normalized enrichment score (NES) ≥ 1.5 were considered to be significantly enriched in the mutated group. M mutated, UM unmutated

ND2158 downregulates NF-κB and STAT3 signaling in TLR-stimulated CLL cells

Using a DNA-binding ELISA-based assay, we analyzed p65 and p52 NF-κB activity in nuclear extracts from *MYD88*-mutated and *MYD88*-unmutated CLL samples. At baseline, we observed a higher DNA-binding activity of p65, as reported previously [9], but not of p52 in *MYD88*-mutated compared to -unmutated CLL cells (Supplementary Fig. S10). After TLR stimulation, we observed a marked increase of p65

Targeting IRAK4 disrupts inflammatory pathways and delays tumor development in chronic lymphocytic…
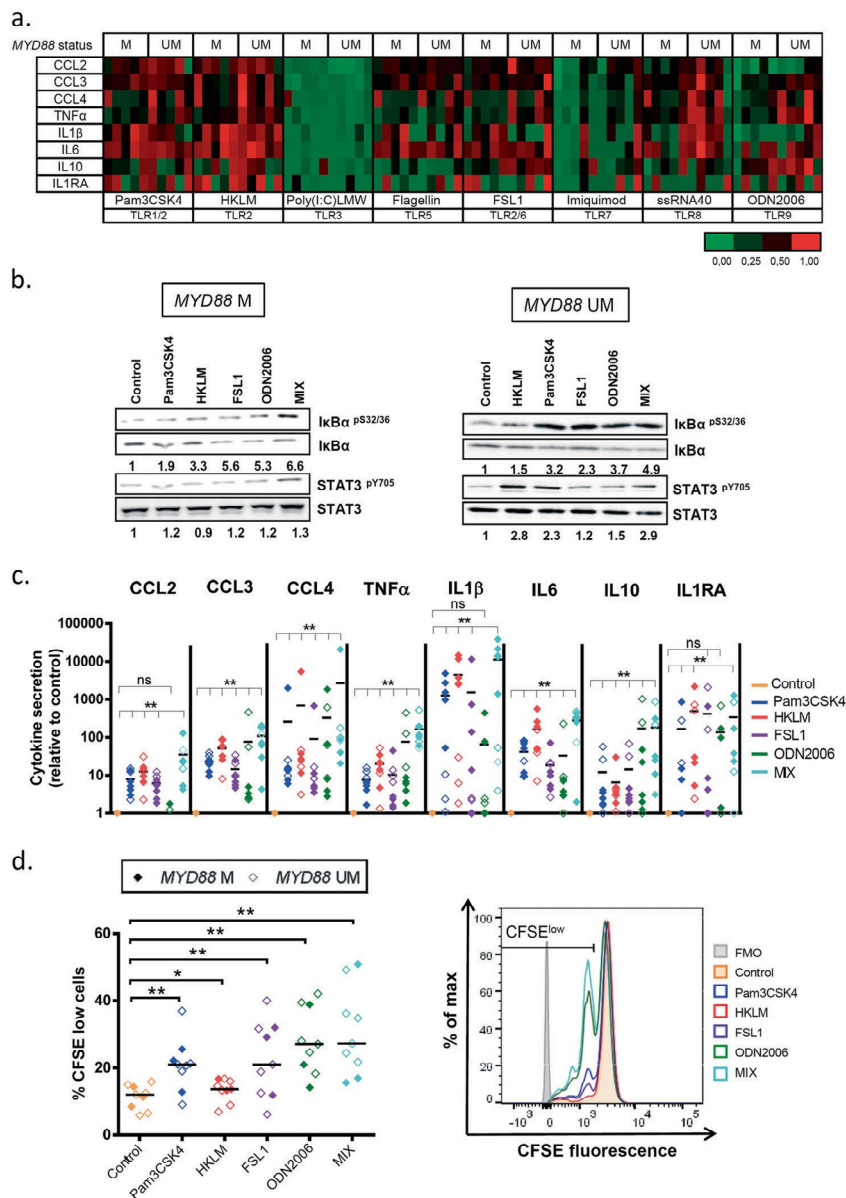
Fig. 2 TLR stimulation increases cytokine secretion, NF-κB and STAT3 signaling and proliferation of CLL cells. CLL cells were cultured with single TLR agonists or the TLR agonist mix (Pam3CSK4, HKLM, FSL1 and ODN2006). a Heatmap representing cytokine secretion in CLL supernatants after 48 h of TLR stimulation of *MYD88*-mutated and *MYD88*-unmutated cases (n = 5 each) analyzed by flow cytometry Luminex® Bead Panel. The level of secretion of each cytokine is represented relative to each control. b Western blot analysis of IκBα[pS32/36] and STAT3[pY705] phosphorylation and total levels of IκBα and STAT3 in CLL cell extracts after 3 h of single or TLR agonist mix stimulation. Analysis of α-tubulin was used as loading control. A representative *MYD88*-mutated (#07) and *MYD88*-unmutated (#25) CLL case are shown. Ratios of phosphorylated and total protein levels were calculated and provided numbers are as fold changes relative to the untreated control sample. c Cytokine secretion after 48 h of TLR

stimulation was assessed in cell culture supernatants of *MYD88*-unmutated (n = 3) and *MYD88*-mutated (n = 5) CLL cases by flow cytometry Luminex® Bead Panel. Data are presented as fold change relative to unstimulated control. Wilcoxon signed-rank test was used for statistical analysis. d Left panel: Percentage of proliferating CD19^{+} CLL cells after single or TLR agonist mix stimulation for 6 days measured by CFSE dilution (n = 3 *MYD88*-mutated; n = 6 *MYD88*-unmutated). Right panel: Flow cytometry histogram of a representative *MYD88*-unmutated CLL case (#51) shows proliferating cells (gated on viable CD19^{+} cells) after 6 days of TLR and IL15 stimulation. A decrease in CFSE signal is indicative for cells that have divided. Wilcoxon matched-paired signed-rank test was used for statistical analysis. Horizontal bars represent population means. n.s. not significant, $P \geq 0.05$, *$P < 0.05$, **$P < 0.01$. M mutated, UM unmutated, FMO fluorescence-minus-one.

67

DNA binding which was blocked by 10 µM ND2158 (Fig. 4a, left panel). No modulation of p52 binding was observed after TLR stimulation and ND2158 treatment (Fig. 4a, left panel). Accordingly, we observed by immunofluorescence microscopy that TLR agonist stimulation of both *MYD88*-mutated and -unmutated CLL cells promoted p65 translocation to the nucleus, reflecting NF-κB signaling activity (Fig. 4a, right panel). This effect was reversed by ND2158 treatment, and p65 was mainly located in the cytoplasm (Fig. 4a, right panel). Furthermore, high levels of phosphorylated STAT3^{pY705} were observed in protein extracts of CLL cells from *MYD88*-mutated and -unmutated cases after TLR stimulation, which were decreased after ND2158 treatment (Fig. 4b, Supplementary Fig. S11). In addition, we observed a significant, 5- to 7-fold decrease in the secretion of all analyzed cytokines (CCL2, CCL3, CCL4, TNFα, IL1β, IL6, and IL1RA), except for IL10, by ND2158 treatment of TLR-stimulated CLL cells compared to untreated cells (Fig. 4c). This negative impact of ND2158 on cytokine secretion was further confirmed in CLL cells that were stimulated with single TLR agonists (Supplementary Fig. S12).

We next analyzed the effect of ND2158 on VCAM-1-mediated adhesion and migration of CLL cells triggered by CXCL12, a key chemokine for CLL cell homing to lymphoid tissues [26]. We observed that cell migration considerably increased after TLR activation and that it was significantly reduced by ND2158 to a similar level as nonstimulated cells (Fig. 4d). The observed effects were comparable in cases with or without *MYD88* mutation.

We further analyzed the functional impact of ND2158 in IGHV-unmutated CLL cases and obtained similar results as with IGHV-mutated cases (Supplementary Fig. S13), validating effectivity of ND2158 in both CLL subtypes.

ND2158 reduces viability, proliferation, and cytokine secretion of TCL1 leukemia cells in vitro

To corroborate the in vitro results obtained with primary CLL cells, we tested the effect of ND2158 on splenocytes from leukemic TCL1 mice. Upon in vitro TLR stimulation with the agonist mix, 10 µM ND2158 induced a significant reduction in cell viability in CD19$^+$CD5$^+$ leukemia cells after 3 and 6 days of treatment (Fig. 5a, left panel), which was also confirmed by a decrease in intracellular ATP levels in the presence of 10 and 30 µM ND2158 (Supplementary Fig. S14a). Further, ND2158 decreased the number of proliferating leukemia cells upon TLR stimulation at 3 and 6 days (Fig. 5a, right panel, and Supplementary Fig S14b, c for single TLR agonist stimulation), suggesting comparable activity of ND2158 for human and murine CLL cells.

We next analyzed cytokine secretion and activation of CD19-sorted B cells from spleens of leukemic TCL1 mice after ex vivo TLR stimulation. We observed significantly decreased secretion of CCL3, CCL4, TNFα, and IL6 in ND2158-treated versus untreated samples (Fig. 5b, left panel). In line with results from human CLL cells, ND2158 was not able to reduce the levels of TLR-induced IL10 secretion. Levels for IFNγ, IL12-p70, CCL2, and IL1β were below the detection threshold. Furthermore, ND2158 treatment reduced the expression of the B-cell activation markers CD25, CD40, CD69, and CD86 that were upregulated upon TLR stimulation (Fig. 5b, right panel).

ND2158 affects monocyte function in vitro

Since monocytes rely for their activity on TLR-mediated signals and have been shown to support CLL cell survival [27, 28], we investigated the effect of ND2158 on these cells. Monocytes isolated from leukemic TCL1 mice or C57BL/6N wild-type mice were analyzed after ex vivo stimulation with LPS, a commonly used TLR agonist for these cells. An increase in the secretion of CCL3, CCL4, TNFα, IL6, and IL10 was observed after LPS stimulation, which was decreased after ND2158 treatment (Fig. 5c, left panel). Moreover, monocyte activation marker CD54 was upregulated after LPS stimulation and this effect was inhibited with ND2158 (Fig. 5c, right panel). These data suggest that ND2158 impairs monocyte activity and might, therefore, be able to disrupt tumor-supporting abilities of monocytes.

ND2158 treatment delays tumor progression in the TCL1 adoptive transfer model

In order to assess the in vivo efficacy of ND2158, we used the TCL1 AT mouse model of CLL. Splenocytes from leukemic TCL1 mice were transplanted into syngeneic immunocompetent C57BL/6N mice, assigned and treated as shown in Fig. 6a and Supplementary Fig. S15. Three weeks after the start of treatment, mice receiving ND2158 showed a significant decrease in absolute counts of CD19$^+$CD5$^+$ leukemia cells in PB compared to vehicle-treated controls (Fig. 6b, left panel). A similar trend was observed for absolute counts of CD19$^+$CD5$^+$ cells in the spleen (Supplementary Fig. S16). Mice were sacrificed after 23 days of treatment and effects in tumor-affected tissues were analyzed. ND2158 treatment reduced spleen weight (Fig. 6b, right panel) and tumor load in spleen, peritoneal cavity and lymph nodes (Fig. 6c, left panel). In addition, the expression of programmed death-ligand 1 (PD-L1), an inhibitory signal for T cells, was decreased on tumor cells in the peritoneal cavity and lymph nodes after ND2158 treatment (Fig. 6c, right panel). These data show that ND2158 is able to control leukemia progression in mice, along with a decrease in immunosuppressive features of the tumor.

Targeting IRAK4 disrupts inflammatory pathways and delays tumor development in chronic lymphocytic...

Fig. 3 ND2158 exerts preferential cytotoxicity for CLL cells. a Viability was analyzed by flow cytometry after 48 h of incubation of cells in culture at ND2158 concentrations from 10 to 100 µM in *MYD88*-mutated IGHV-mutated ($n = 6$), *MYD88*-unmutated IGHV-mutated ($n = 16$) CLL samples, and in $CD19^+$ B cells and $CD3^+$ T cells from healthy donors ($n = 10$). Percentage of viable cells was measured by Annexin-V and normalized to untreated control. b Viability of ND2158-treated CLL cells was analyzed after TLR stimulation for 2- ($n = 12$) and 6 days ($n = 6$). c Left panel: Percentage of proliferating $CD19^+$ CLL cells after TLR stimulation and ND2158 treatment for 6 days measured by CFSE dilution ($n = 5$ *MYD88*-mutated; $n = 7$ *MYD88*-unmutated). Right panel: Flow cytometry histogram of a representative *MYD88*-unmutated CLL case (#51) shows proliferating cells (gated on viable $CD19^+$ cells) after 6 days of TLR and IL15 stimulation and ND2158 treatment. A decrease in CFSE signal is indicative for cells that have divided. Wilcoxon signed-rank test was used for statistical analysis. Horizontal bars represent population means. *$P < 0.05$, **$P < 0.01$, ***$P < 0.001$, ****$P < 0.0001$. M mutated, UM unmutated
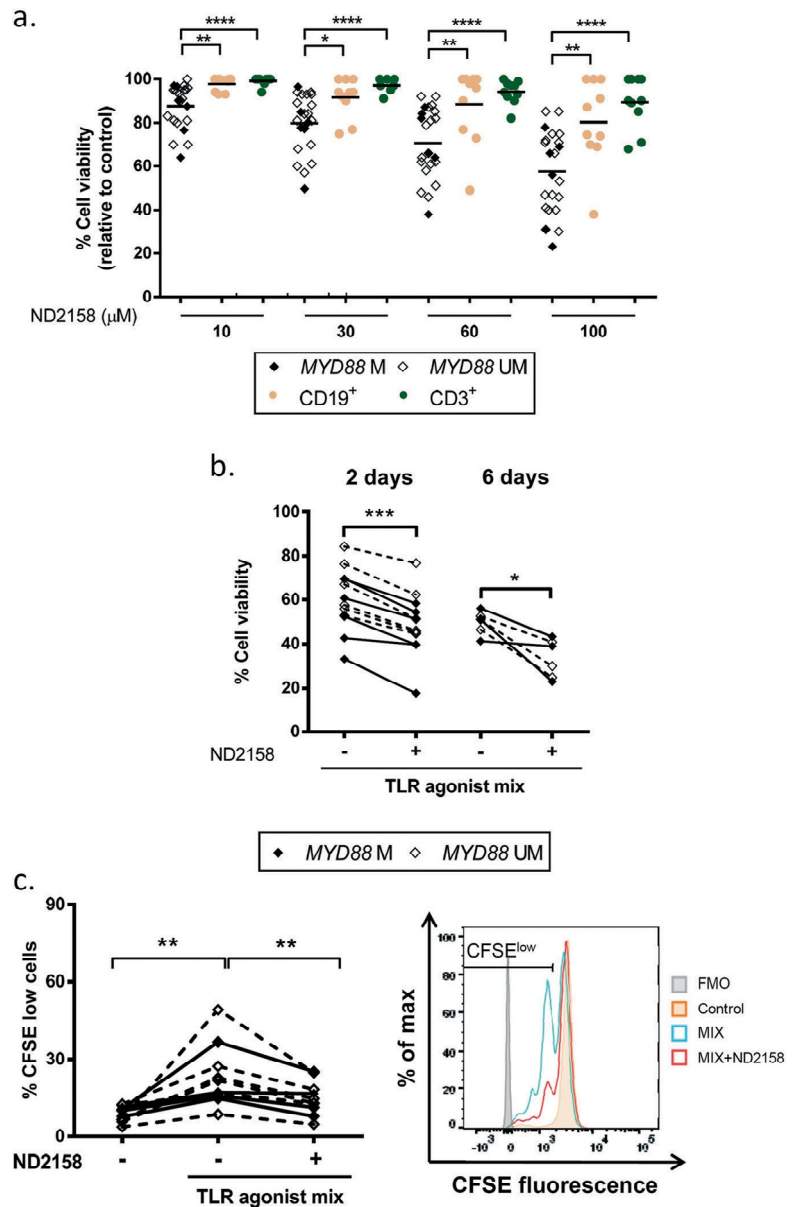
ND2158 reduces tumor-supporting monocytes in mice

We further analyzed effects of ND2158 treatment on the immune microenvironment of mice after TCL1 AT. Thereby, we observed a significantly lower number of $CD11b^+CX3CR1^+F4/80^+$ monocytes in ND2158-treated animals compared to the control group, and this affected both $Ly6C^{high}$ (inflammatory) and $Ly6C^{low}$ (patrolling) monocytes (Fig. 7a, left panel). In addition, the expression of chemokine receptor CCR2, which is important for CCL2-induced recruitment of $Ly6C^{high}$ monocytes in this model [29],

was significantly lower in these cells in ND2158-treated mice compared to vehicle-treated mice (Fig. 7a, right panel), which might indicate an impact of this drug on monocyte recruitment.

ND2158 treatment impairs $CD8^+$ T-cell proliferation and function

$CD8^+$ T cells have been shown to control tumor progression in the TCL1 AT model [24]. Therefore, we analyzed the effects of ND2158 on $CD8^+$ T cells in tumor-bearing mice.

N. Giménez etal.
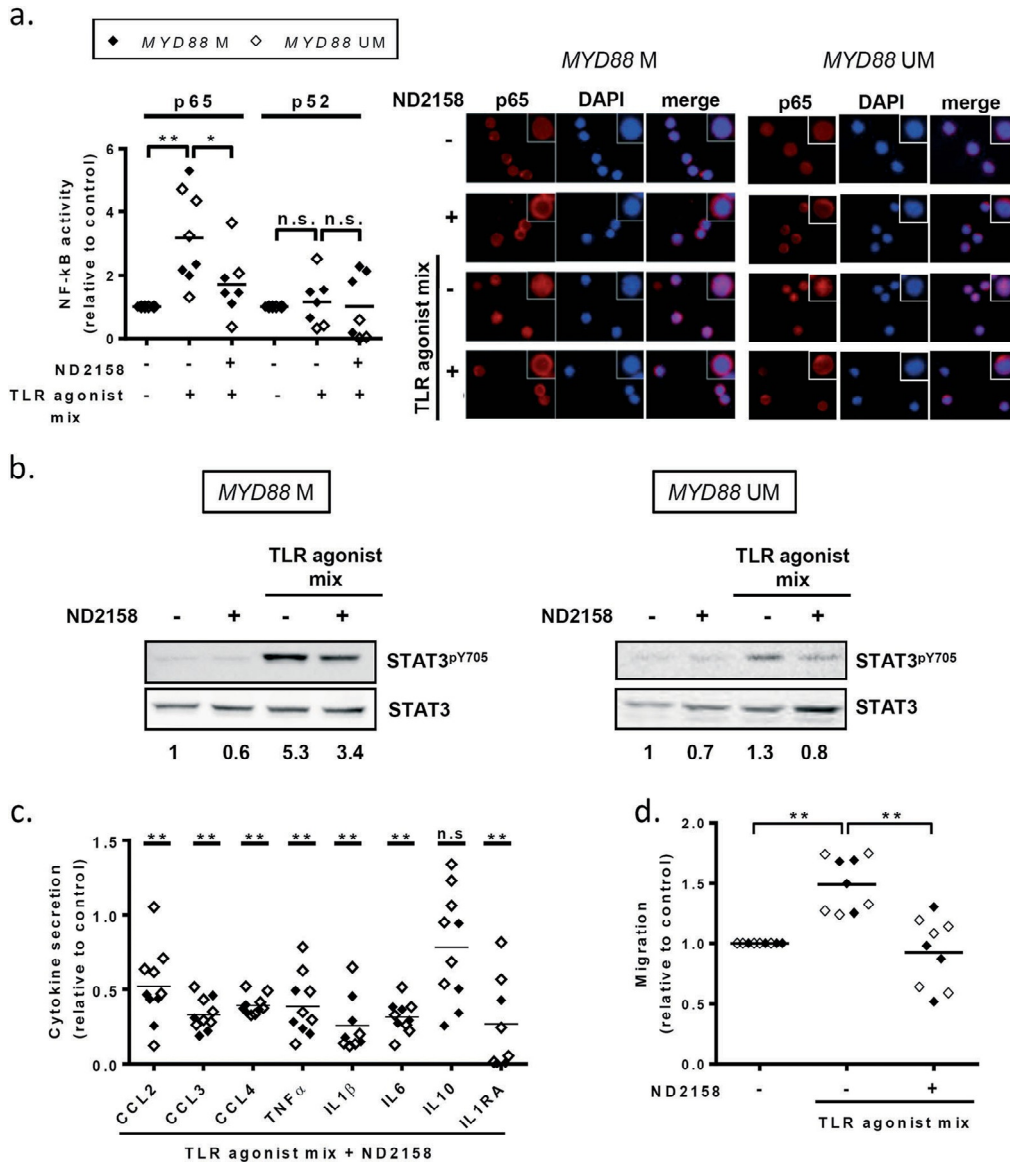
Fig. 4 Impact of ND2158 on CLL cell signaling, cytokine release and migration. CLL cells were stimulated in vitro with TLR agonist mix for 30 min, before 10 μM ND2158 was added to the culture. a Left panel: Binding of p65 or p52 to NF-κB consensus sequence was analyzed using nuclear extracts from CLL cells of MYD88-mutated ($n = 4$) and MYD88-unmutated ($n = 4$) samples via a DNA-binding ELISA-based assay 3 h after treatment. Values are represented relative to untreated samples. Right panel: p65 translocation to the nucleus was analyzed by immunofluorescence microscopy in a representative MYD88-mutated (#7) and MYD88-unmutated (#19) CLL case 3 h after treatment. p65 was stained with anti-NF-κB p65 antibody (clone D14E12) for 30 min, and incubated with an Alexa546-conjugated secondary antibody (red), and DAPI (blue) was used to stain the nuclei. b Western blot analysis for STAT3^{pY705} of CLL cell extracts of a representative MYD88-mutated (#1) and MYD88-unmutated CLL case (#19) 3 h after treatment. Ratios of phosphorylated and total

protein levels were calculated and provided numbers are fold changes relative to the untreated control sample. c Cytokine secretion in supernatants from CLL cells ($n = 4$ MYD88-mutated; $n = 6$ MYD88-unmutated) exposed to TLR agonist mix prior treatment with ND2158 for 48 h was analyzed by a multiplexed sandwich immunoassay based on flow cytometry using Luminex® Bead Panel. Values are presented relative to untreated control. Asterisks indicate statistical significance level relative to control. d Migration of TLR-stimulated CLL cells treated with ND2158 for 3 h ($n = 4$ MYD88-mutated; $n = 5$ MYD88-unmutated) towards CXCL12 was analyzed by transwell assays. Values are presented as the ratio of migrating cells and total viable cells, relative to the untreated control. Wilcoxon matched-pairs signed-rank test was used for statistical analysis. Horizontal bars represent population means. n.s. not significant; $P ≥ 0.05$, $*P < 0.05$, $**P < 0.01$. M mutated, UM unmutated.

Interestingly, ND2158-treated mice showed significantly lower absolute numbers of antigen-experienced CD8 $^+$CD44$^{\text{int-high}}$CD127$^{\text{low}}$ effector T cells in the spleen (Fig. 7b, left panel), and a lower proportion of Ki-67$^+$ cells within this population (Fig. 7b, right panel) compared to vehicle-treated animals, suggesting a lower proliferative capacity and therefore expansion of these cells by ND2158 treatment. Although no difference in absolute numbers of CD8$^+$CD44$^{\text{high}}$CD127-$^{\text{high}}$ memory T cells was observed, significantly less Ki-67$^+$ cells were detected in this subset as well (Fig. 7b and Supplementary Fig. S17a). Furthermore, a significant increase in the percentage of CD8$^+$ effector cells expressing the inhibitory receptors TIGIT, CD160, CD244 and LAG3 was observed in ND2158-treated mice compared to vehicle-treated animals (Fig. 7c and Supplementary Fig. S17b). We further detected a higher expression level of the immune checkpoint protein PD-1 on these cells (Fig. 7c and Supplementary Fig. S17b). Even though the percentage of PD-1 $^+$CD8$^+$ effector T cells was similar in both treatment groups (Supplementary Fig. S17c), these cells expressed higher levels of the immune checkpoint protein PD-1 in ND2158-treated mice (Fig. 7c), which has been linked to terminal exhaustion of CD8$^+$ T cells [30]. In addition, we observed a lower percentage of CD8$^+$ effector T cells expressing CXCR3, a protein important for T-cell trafficking and function, and a significantly lower expression of the costimulatory receptor CD28 on these cells in ND2158-treated mice compared to controls (Fig. 7c and Supplementary Fig. S17b). These findings thus suggest a more exhausted and less functional phenotype of CD8$^+$ effector T cells in ND2158-treated mice.

To further follow this hypothesis, we performed in vitro experiments using anti-CD3-stimulated T cells from human PBMCs and murine splenocytes and observed a significant inhibition of proliferation of CD8$^+$ T cells (Fig. 8a and Supplementary Fig. S18a), associated with lower expression of activation markers CD25, CD28 and CD137 in ND2158-treated samples compared to controls (Fig. 8b and Supplementary Fig. S18b). In addition, ND2158 significantly reduced the induction of the effector molecule granzyme B after T-cell stimulation (Fig. 8c and Supplementary Fig. S18b). We further quantified T-cell receptor (TCR) activity using transgenic $Nr4a1^{\text{GFP}}$ mice, in which GFP expression is a measure of TCR signaling strength [22]. Upon anti-CD3 stimulation of $Nr4a1^{\text{GFP}}$ splenocytes, we observed a considerable inhibition of GFP expression in ND2158-treated CD8$^+$T cells compared to controls (Fig. 8d, left panel and Supplementary Fig. S18c) indicating a decrease in TCR signaling.

As MYD88/IRAK4-mediated signals are not known to be of central relevance for T-cell expansion and function, we next tested whether the inhibitory effect of ND2158 on CD8$^+$ T cells was dependent on this signaling complex by using anti-CD3 stimulated splenocytes from $Myd88^{-/-}$ mice. As ND2158 inhibited proliferation, activation and granzyme B

production to a similar degree in $Myd88^{-/-}$ and wild-type CD8$^+$ T cells (Fig. 8d, right panel and Supplementary Fig. S19), we suggest that the activity of ND2158 on CD8$^+$ T cells might be independent of MYD88 and IRAK4.

Taken together, our results indicate impaired activation and proliferative capacity of CD8$^+$ T cells in the presence of ND2158. This effect most likely contributes to the enhanced CD8$^+$ T-cell exhaustion induced by ND2158 in the TCL1 AT mouse model, and thus might be a possible explanation for the only moderate effect of this drug on tumor progression in the mice.

Discussion

CLL is a malignancy of antigen-experienced mature B lymphocytes, in which microenvironmental signals play a critical role in ontogeny and evolution [31]. Among these extracellular triggers that are known to drive CLL, auto-antigens and bacterial components which can be recognized by B cells via BCR and TLR collaboration have been described [32, 33]. Moreover, CLL patients are often associated with an increased frequency and severity of infections and autoimmune complications [34]. MYD88 is a critical adaptor protein of the TLR signaling pathway [2] and activating mutations of *MYD88* have been observed in about 3% of CLL patients [9, 12]. Our results confirm that CLL cases with mutations in *MYD88* are significantly enriched in gene expression signatures related to cytokines and inflammation, such as NF-κB and STAT3 signaling, as well as high basal cytokine secretion, which is in accordance with previous reports in CLL [12] and DLBCL [8]. CLL cells were shown to have a similar expression pattern of TLRs as normal B cells [35–38] and we did not observe differences between *MYD88*-mutated or unmutated CLL cases, indicating that the TLR signaling framework is of similar relevance in both groups. Previous studies suggested the involvement of TLR signaling in CLL cell survival [37] and its contribution to NF-κB activity and an inflammatory micromilieu in CLL [39]. In addition, response to TLR stimulation in CLL cells was shown to be dependent on biological and clinical features of patients [40, 41]. To avoid heterogeneous responses when activating TLR signaling in CLL cells, we used a mix of TLR agonists that stimulates TLR1, TLR2, TLR6, and TLR9, and showed that it reliably triggered activation of the NF-κB and JAK-STAT signaling pathways, secretion of cytokines, and enhanced CLL cell migration and proliferation in vitro in all CLL samples, highlighting the relevance of TLR signaling in CLL pathobiology. In the last years, several IRAK4 inhibitors have been developed and tested for the treatment of cancer and other diseases related to IRAK overexpression [42]. ND2158 has been described as a highly selective and bioavailable small molecule IRAK4 inhibitor, which exhibited robust activity
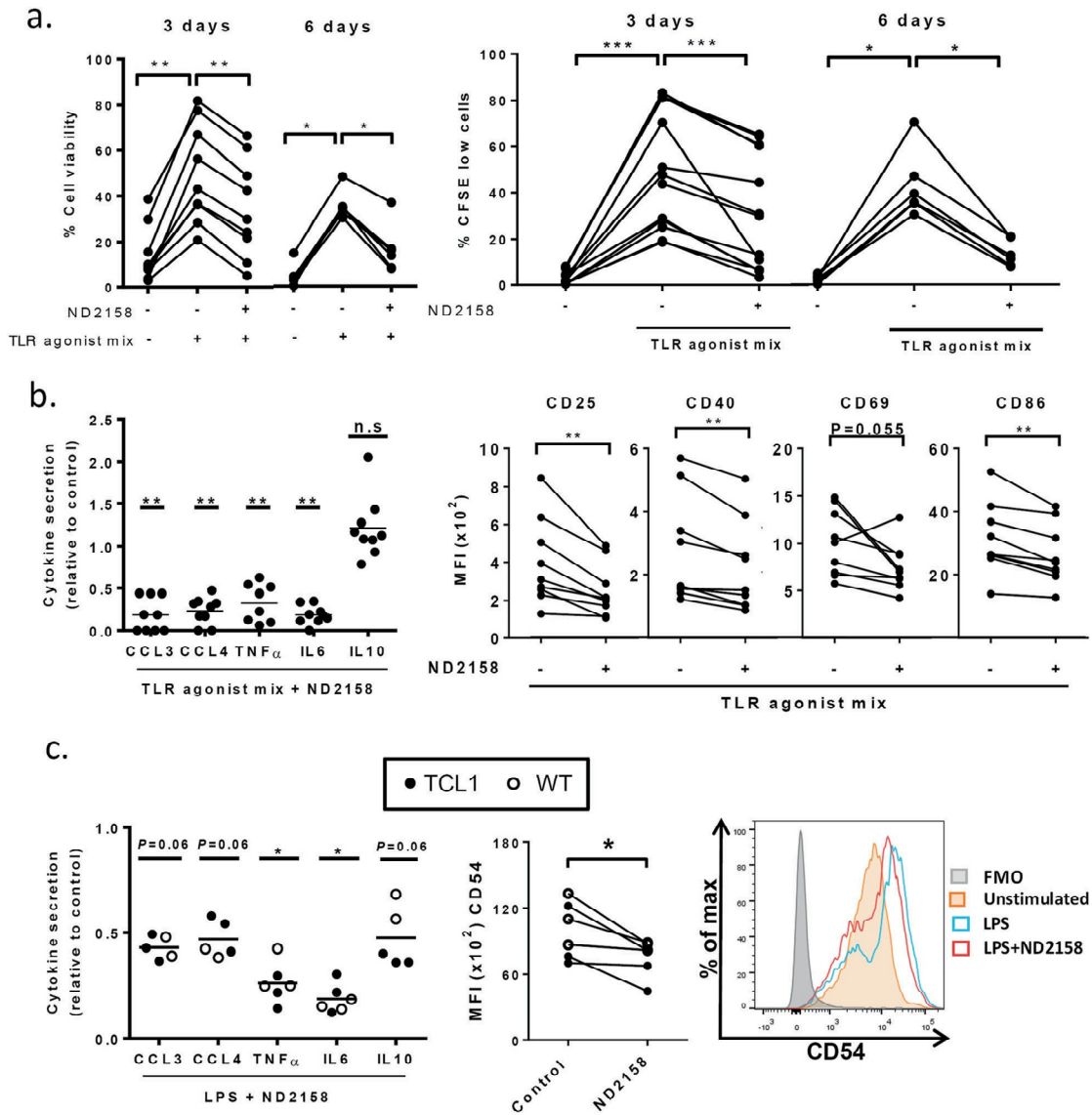
Fig. 5 Impact of ND2158 on *Eμ*-TCL1 CLL cells and monocytes from mice. Cells were stimulated with TLR agonist mix (B cells) or LPS (monocytes) for 30 min before 10 μM ND2158 treatment. a Left panel: Total splenocytes of 1-year-old leukemic TCL1 mice were treated as described above, and viability of CD19$^+$CD5$^+$ CLL cells was analyzed after 3 days ($n = 9$) and 6 days ($n = 6$) by flow cytometry using fixable viability dye. Right panel: Percentage of proliferating CD19$^+$CD5$^+$ CLL cells was measured by CFSE dilution after 3 and 6 days ($n = 6$). b MACS-sorted B cells from spleens of 1-year-old leukemic TCL1 mice ($n = 9$) were cultured for 6 h. Left panel: Cytokine secretion data acquired as above are shown relative to untreated control. Cytokine secretion was analyzed by flow cytometry using

Luminex® Bead Panel. Right panel: CD25, CD40, CD69 and CD86 expression on CD19$^+$CD5$^+$ CLL cells was analyzed by flow cytometry. c MACS-sorted monocytes from 1-year-old wild-type (WT; $n = 3$) and TCL1 mice ($n = 3$) were cultured for 6 h. Left panel: Cytokine secretion data acquired as above are shown relative to untreated control. Asterisks indicate statistical significance level relative to control. Horizontal bars represent population means. Right panel: Median fluorescence intensity (MFI) of CD54 on murine monocytes was analyzed. Wilcoxon matched-pairs signed-rank test was used for statistical analysis. n.s. not significant; $P \geq 0.05$, *$P < 0.05$, **$P < 0.01$, ***$P < 0.001$.

Targeting IRAK4 disrupts inflammatory pathways and delays tumor development in chronic lymphocytic. . .

Fig. 6 ND2158 delays CLL progression in the TCL1 adoptive transfer mouse model. a Treatment schedule of ND2158 in TCL1 AT model. BID twice a day, i.p. intraperitoneally. b Left panel: Absolute tumor cell count (CD19$^+$CD5$^+$) in peripheral blood (PB) over time as analyzed by flow cytometry. Right panel: Spleen weight of vehicle- ($n = 7$) and ND2158-treated ($n = 7$) mice. Representative examples of spleens are shown. c Left panel: Tumor load (CD19$^+$CD5$^+$ cells out of CD45$^+$ cells) in spleen (SP), peritoneal cavity (PC), lymph nodes (LN), and bone marrow (BM) as acquired by flow cytometry. Right panel: Median fluorescence intensity (MFI) of PD-L1 in CLL cells from PC and LN. Horizontal bars represent population means. Mann−Whitney test was used for statistical analysis. *$P < 0.05$, **$P < 0.01$
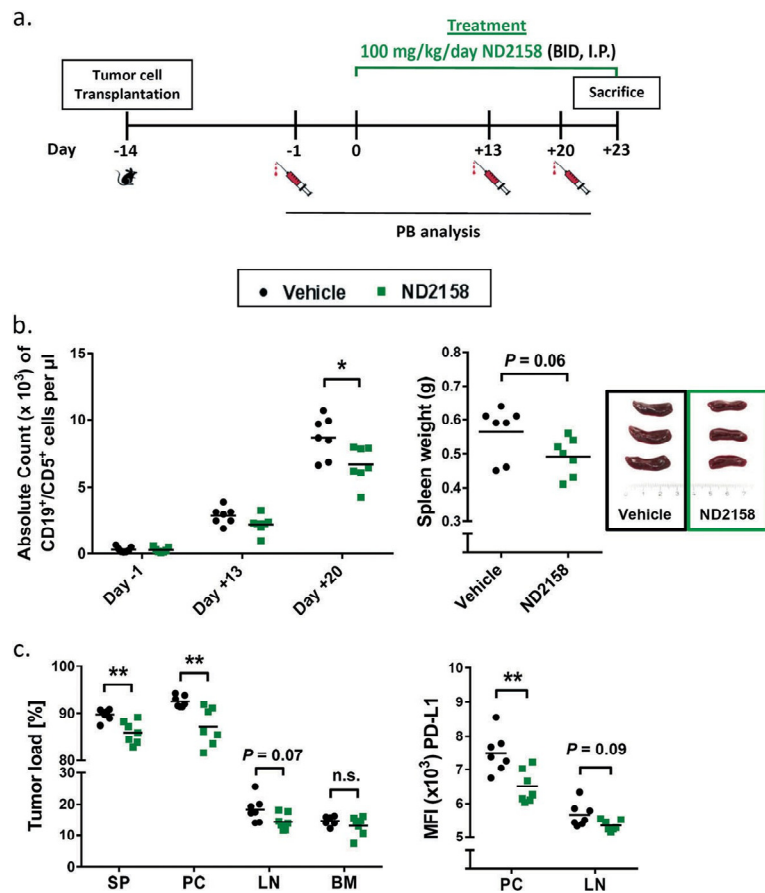
against the ABC subtype of DLBCL presenting with *MYD88* mutations in preclinical mouse models [16].

In CLL samples, ND2158 reduced cell viability independently of the *MYD88* mutational status, at concentrations that did not impact on normal B- and T-cell survival. ND2158 further inhibited TLR agonist-induced NF-κB and STAT3 activity, which play a cooperative role in CLL cell survival [43] and reduced viability, proliferation, adhesion−migration, and cytokine release of CLL cells which were enhanced upon TLR activation. As ND2158 also reduced the release of inflammatory factors by monocytes, which are known to support CLL progression [44], we hypothesized that its combined activity on CLL cells and myeloid bystander cells will be of benefit for the treatment of CLL. To test the therapeutic potential of ND2158, we used the TCL1 AT mouse model of CLL that mirrors many features of human disease, including alterations in the tumor microenvironment [27, 29]. Treatment of leukemic TCL1 AT mice with ND2158 slowed down leukemia progression and led to lower tumor load in secondary lymphoid organs compared to control mice. This was accompanied with a decrease in monocyte numbers, as well as in their activation and cytokine

secretion. Previous studies have shown that depletion of monocytes using clodronate-liposomes delays CLL in the TCL1 AT model, as well as in a xenotransplantation approach using the MEC-1 CLL cell line [27, 45]. Thus, the reduction and functional impairment of monocytes by ND2158 and its impact on the inflammatory milieu might reduce microenvironment-mediated support of CLL cells, and likely contributes to the observed delay in tumor progression.

Surprisingly, ND2158 further negatively impacted on CD8$^+$ T-cell activity and expansion, both in vivo and in vitro. The fact that we only see a moderate effect on tumor load in our treatment study could be due to the potential negative effect of the drug on CD8$^+$ T cells. In treated mice, this led to lower numbers of CD8$^+$ effector T cells with reduced expression of proliferation and activation markers, and higher expression of exhaustion markers, including the inhibitory receptor PD-1, when compared to control mice. Our data further suggest that the activity of ND2158 on CD8$^+$ T cells is independent of MYD88/IRAK4. An unbiased analysis of ND2158's activity on kinases showed that besides effectively targeting IRAK4 (100% inhibition at 10 µM), ND2158 also inhibits

Targeting IRAK4 disrupts inflammatory pathways and delays tumor development in chronic lymphocytic...
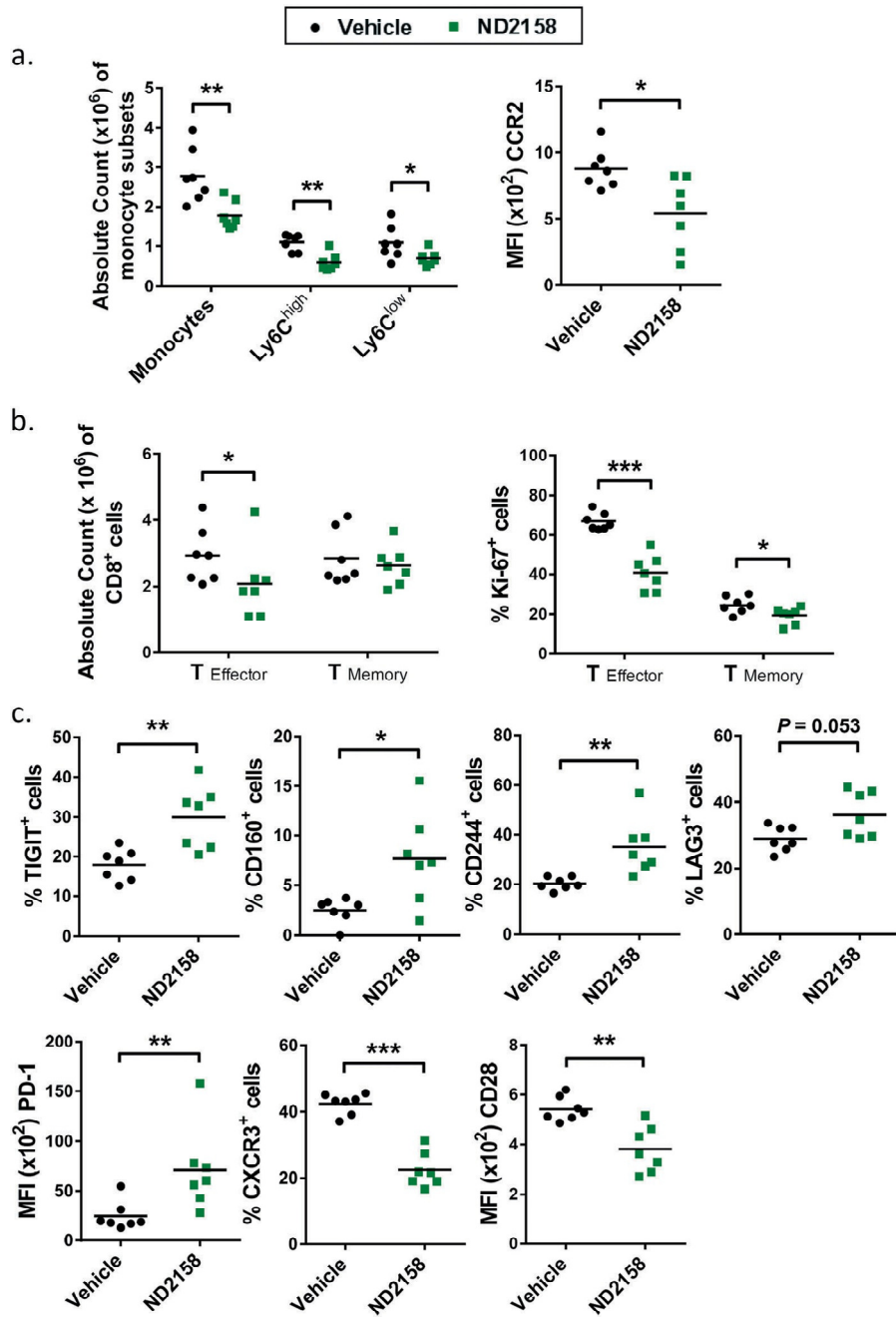
Fig. 7 ND2158 impacts on the tumor microenvironment in the TCL1 adoptive transfer model. a Left panel: Absolute counts of monocytes in the spleen (SP) of vehicle- ($n = 7$) and ND2158-treated ($n = 7$) mice. Right panel: CCR2 protein expression (MFI) on Ly6C^{+} monocytes in the spleen acquired by flow cytometry. b Left panel: Absolute numbers of CD8^{+} effector and memory T cells in the spleen acquired by flow cytometry. Right panel: Percentage of Ki-67^{+}CD8^{+} effector and memory T cells in the spleen of vehicle- and ND2158-treated mice analyzed by flow cytometry. c Protein expression analysis of inhibitory receptors and activation markers on CD8^{+} effector T cells by flow cytometry. Data are shown as percentage of TIGIT^{+}, CD160^{+}, CD244^{+}, LAG3^{+}, and CXCR3^{+} CD8^{+} effector T cells for bimodal populations or as MFI of costimulatory receptor CD28 as unimodal population. MFI of PD-1 was analyzed for PD-1^{+}CD8^{+} effector T cells. Horizontal bars represent population means. Mann–Whitney test was used for statistical analysis. *$P < 0.05$, **$P < 0.01$, ***$P < 0.001$. MFI median fluorescence intensity, FMO fluorescence-minus-one.

Targeting IRAK4 disrupts inflammatory pathways and delays tumor development in chronic lymphocytic...

Fig. 8 ND2158 impairs proliferation and function of CD8$^+$ T cells in vitro. Cells were stimulated with an anti-CD3 antibody for 30 min followed by treatment with 10 μM ND2158. a Left panel: Human PBMCs from healthy donors ($n = 6$) were stained with CFSE and percentage of proliferating cells was measured in viable CD8$^+$ T cells after 3 days by flow cytometry. Right panel: A representative histogram of the CFSE signal is shown. b Protein expression of CD25, CD28 and CD137 was analyzed after 24 h of treatment in viable CD8$^+$ T cells by flow cytometry. Quantification of data is shown in the upper row; corresponding representative histograms are shown in the bottom row. Data are shown as percentage of CD25$^+$ or CD137$^+$ CD8$^+$ T cells for bimodal populations, or as MFI of CD28 on CD8$^+$ T cells as unimodal population. c Percentage of granzyme B$^+$ viable CD8$^+$ T cells was analyzed after 24 h of treatment by flow cytometry. Quantification of data is shown on the left; corresponding representative dot plots are shown on the right. Wilcoxon matched-pairs signed-rank test was used for statistical analysis. d Left panel: GFP expression was analyzed by flow cytometry in splenocytes from *Nr4a1*^{GFP} transgenic mice ($n = 4$) in viable CD8$^+$ T cells 3 h after treatment with ND2158. Right panel: Splenocytes from wild-type (WT) C57BL/6 ($n = 4$) and *Myd88*$^{-/-}$ mice ($n = 4$) were stained with CFSE and percentage of proliferating cells was analyzed in viable CD8$^+$ T cells after 48 h as described above. *$P < 0.05$
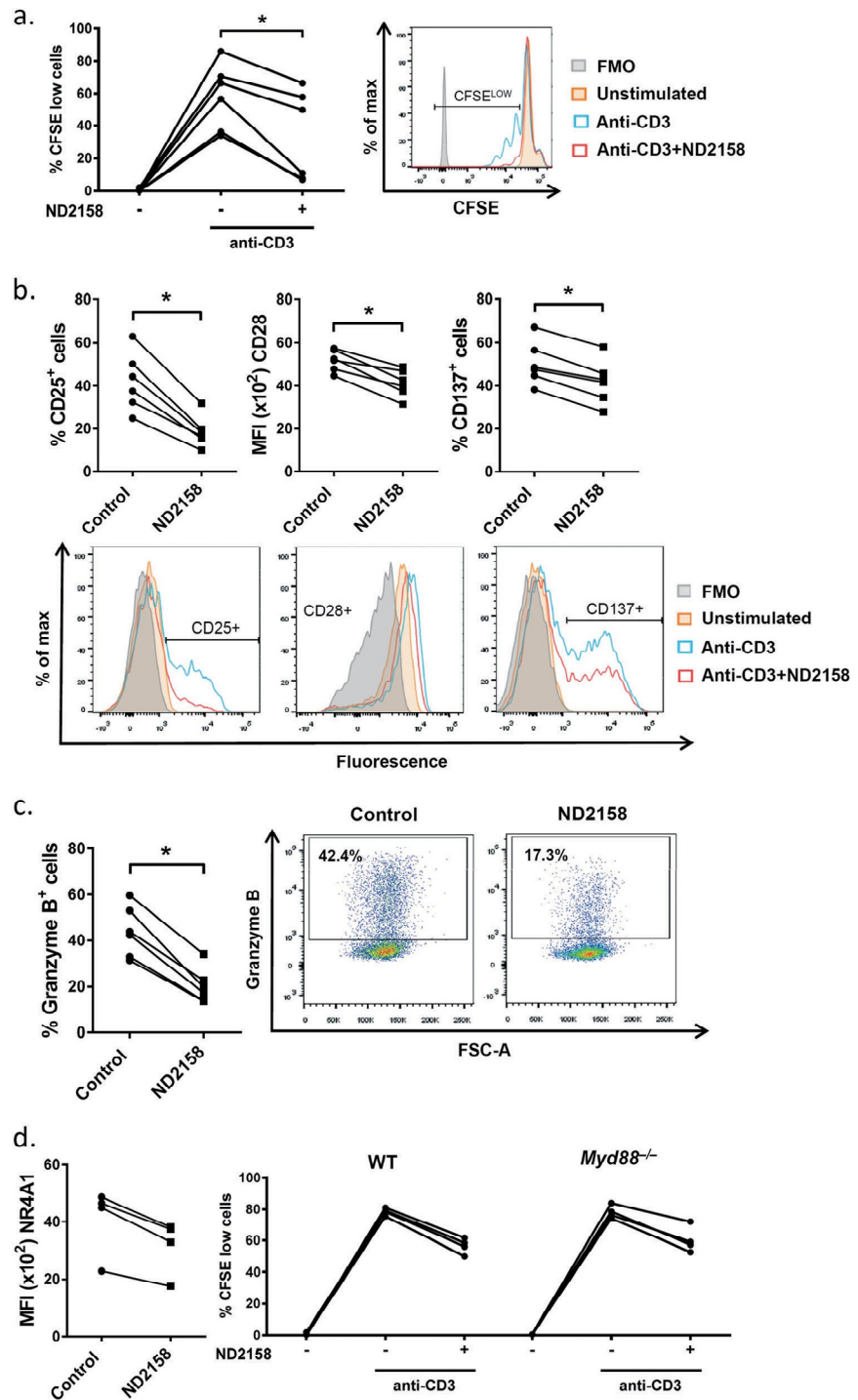
other kinases with lower efficacy, including enzymes that are of functional relevance in T cells (e.g. > 70% inhibition of DYRK1, TXK and LCK at 10 μM) [16].

Our previous work showed that leukemia development in the TCL1 mouse model is controlled by an oligoclonally expanded CD8$^+$ effector T-cell population that gradually

shows features of functional exhaustion [24]. As ND2158 treatment of mice inhibits CD8$^+$ effector T-cell expansion and increases their exhaustion, an inferior tumor control by these cells is expected. The results of this treatment study suggest that ND2158 enhances CD8$^+$ effector T-cell exhaustion by inhibiting their proliferation. Therefore, the positive antitumor effects of ND2158 on tumor cells and monocytes seems to be counteracted by its negative impact on the T-cell compartment, which might at least partly explain the modest effects ND2158 has in controlling leukemia development in the TCL1 mouse model.

In agreement with previous studies [16, 46], we also observed a superior antitumor activity when combining the IRAK4 inhibitor ND2158 with ibrutinib or venetoclax (Supplementary Fig. S20). In addition, to overcome the negative impact of ND2158 on T cells, we propose to consider its combination with drugs that improve T-cell function and avoid their rapid exhaustion. As we observed increased expression of several inhibitory receptors on CD8$^+$ T cells in ND2158-treated mice, including PD-1 and TIGIT, blocking these receptors with antibodies might be a successful strategy to overcome the loss of T-cell function and improve therapy outcome. More importantly, the development of more selective inhibitors for IRAK4 and therefore the reduced negative impact on T cells should be considered to improve therapeutic targeting of the TLR pathway in CLL and other diseases. Ideally, such drugs should not compromise the patients' immune system, and decrease their risk of infections, which is a frequent adverse effect in treated CLL patients [16, 47].

In summary, our data suggest IRAK4 as a novel treatment target for CLL. Inhibition of IRAK4 blocks survival and proliferation of CLL cells. In addition, it impacts on the tumor-supportive inflammatory milieu, by reducing cytokine secretion in malignant and bystander cells. In light of our findings in the TCL1 mouse model, combining the IRAK4 inhibitor ND2158 with immune checkpoint therapy might result in enhanced treatment efficacies.

Compliance with ethical standards

References

1. Ruprecht CR, Lanzavecchia A. Toll-like receptor stimulation as a third signal required for activation of human naive B cells. Eur J Immunol. 2006;36:810–6.
2. Rawlings DJ, Schwartz MA, Jackson SW, Meyer-Bahlburg A. Integration of B cell responses through Toll-like receptors and antigen receptors. Nat Rev Immunol. 2012;12:282–94.
3. Pradere JP, Dapito DH, Schwabe RF. The Yin and Yang of Toll-like receptors in cancer. Oncogene. 2014;33:3485–95.
4. Huang L, Xu H, Peng G. TLR-mediated metabolic reprogramming in the tumor microenvironment: potential novel strategies for cancer immunotherapy. Cell Mol Immunol. 2018;15:428–37.
5. Ntoufa S, Vilia MG, Stamatopoulos K, Ghia P, Muzio M. Toll-like receptors signaling: a complex network for NF-κB activation in B-cell lymphoid malignancies. Semin Cancer Biol. 2016; 39:15–25.
6. Hennessy EJ, Parker AE, O'Neill LA. Targeting Toll-like receptors: emerging therapeutics? Nat Rev Drug Discov. 2010; 9:293–307.
7. Lin SC, Lo YC, Wu H. Helical assembly in the MyD88-IRAK4-IRAK2 complex in TLR/IL-1R signalling. Nature. 2010; 465:885–90.
8. Ngo VN, Young RM, Schmitz R, Jhavar S, Xiao W, Lim KH, et al. Oncogenically active MYD88 mutations in human lymphoma. Nature. 2011;470:115–9.
9. Puente XS, Pinyol M, Quesada V, Conde L, Ordóñez GR, Villamor N, et al. Whole-genome sequencing identifies recurrent mutations in chronic lymphocytic leukaemia. Nature. 2011; 475:101–5.
10. Puente XS, Jares P, Campo E. Chronic lymphocytic leukemia and mantle cell lymphoma: crossroads of genetic and microenvironment interactions. Blood. 2018;131:2283–96.
11. Baliakas P, Hadzidimitriou A, Agathangelidis A, Rossi D, Sutton LA, Kminkova J, et al. Prognostic relevance of MYD88 mutations in CLL: the jury is still out. Blood. 2015;126:1043–4.
12. Martínez-Trillos A, Pinyol M, Navarro A, Aymerich M, Jares P, Juan M, et al. Mutations in TLR/MYD88 pathway identify a subset of young chronic lymphocytic leukemia patients with favorable outcome. Blood. 2014;123:3790–6.
13. Nadeu F, Clot G, Delgado J, Martín-García D, Baumann T, Salaverria I, et al. Clinical impact of the subclonal architecture and

mutational complexity in chronic lymphocytic leukemia. Leukemia. 2018;32:645−53.

1. Landau DA, Carter SL, Stojanov P, McKenna A, Stevenson K, Lawrence MS, et al. Evolution and impact of subclonal mutations in chronic lymphocytic leukemia. Cell. 2013;152:714−26.

2. Burger JA, Quiroga MP, Hartmann E, Bürkle A, Wierda WG, Keating MJ, et al. High-level expression of the T-cell chemokines CCL3 and CCL4 by chronic lymphocytic leukemia B cells in nurselike cell cocultures and after BCR stimulation. Blood. 2009;113:3050−8.

3. Kelly PN, Romero DL, Yang Y, Shaffer AL, Chaudhary D, Robinson S, et al. Selective interleukin-1 receptor-associated kinase 4 inhibitors for the treatment of autoimmune disorders and lymphoid malignancy. J Exp Med. 2015;212:2189−201.

4. Liu X, Hunter ZR, Xu L, Chen J, Chen JG, Tsakmaklis N, et al. Targeting myddosome assembly in Waldenstrom macroglobulinaemia. Br J Haematol. 2017;177:808−13.

5. Li Z, Younger K, Gartenhaus R, Joseph AM, Hu F, Baer MR, et al. Inhibition of IRAK1/4 sensitizes T cell acute lymphoblastic leukemia to chemotherapies. J Clin Invest. 2015;125:1081−97.

6. Puente XS, Beà S, Valdés-Mas R, Villamor N, Gutiérrez-Abril J, Martín-Subero JI, et al. Non-coding recurrent mutations in chronic lymphocytic leukaemia. Nature. 2015;526:519−24.

7. Quesada V, Ramsay AJ, Rodríguez D, Puente XS, Campo E, López-Otín C. The genomic landscape of chronic lymphocytic leukemia: clinical implications. BMC Med. 2013;11:124.

8. Bichi R, Shinton SA, Martin ES, Koval A, Calin GA, Cesari R, et al. Human chronic lymphocytic leukemia modeled in mouse by targeted TCL1 expression. Proc Natl Acad Sci USA. 2002;99:6955−60.

9. Moran AE, Holzapfel KL, Xing Y, Cunningham NR, Maltzman JS, Punt J, et al. T cell receptor signal strength in Treg and iNKT cell development demonstrated by a novel fluorescent reporter mouse. J Exp Med. 2011;208:1279−89.

10. Adachi O, Kawai T, Takeda K, Matsumoto M, Tsutsui H, Sakagami M, et al. Targeted disruption of the MyD88 gene results in loss of IL-1- and IL-18-mediated function. Immunity. 1998;9:143−50.

11. Hanna BS, Roessner PM, Yazdanparast H, Colomer D, Campo E, Kugler S, et al. Control of chronic lymphocytic leukemia development by clonally-expanded CD8. Leukemia . 2019;33:625−37.

12. Improgo MR, Tesar B, Klitgaard JL, Magori-Cohen R, Yu L, Kasar S, et al. MYD88 L265P mutations identify a prognostic gene expression signature and a pathway for targeted inhibition in CLL. Br J Haematol. 2019;184:925−36.

13. Davids MS, Burger JA. Cell trafficking in chronic lymphocytic leukemia. Open J Hematol. 2012;3(S1).pii:-3.

14. Hanna BS, McClanahan F, Yazdanparast H, Zaborsky N, Kalter V, Rößner PM, et al. Depletion of CLL-associated patrolling monocytes and macrophages controls disease development and repairs immune dysfunction in vivo. Leukemia. 2016;30:570−9.

15. Seiffert M, Schulz A, Ohl S, Döhner H, Stilgenbauer S, Lichter P. Soluble CD14 is a novel monocyte-derived survival factor for chronic lymphocytic leukemia cells, which is induced by CLL cells in vitro and present at abnormally high levels in vivo. Blood. 2010;116:4223−30.

16. McClanahan F, Riches JC, Miller S, Day WP, Kotsiou E, Neuberg D, et al. Mechanisms of PD-L1/PD-1-mediated CD8 T-cell dysfunction in the context of aging-related immune defects in the Eμ-TCL1 CLL mouse model. Blood. 2015;126:212−21.

17. Barber DL, Wherry EJ, Masopust D, Zhu B, Allison JP, Sharpe AH, et al. Restoring function in exhausted CD8 T cells during chronic viral infection. Nature. 2006;439:682−7.

18. Ten Hacken E, Burger JA. Microenvironment interactions and B-cell receptor signaling in chronic lymphocytic leukemia:

implications for disease pathogenesis and treatment. Biochim Biophys Acta. 2016;1863:401−13.

19. Lau CM, Broughton C, Tabor AS, Akira S, Flavell RA, Mamula MJ, et al. RNA-associated autoantigens activate B cells by combined B cell antigen receptor/Toll-like receptor 7 engagement. J Exp Med. 2005;202:1171−7.

20. Chiorazzi N, Ferrarini M. B cell chronic lymphocytic leukemia: lessons learned from studies of the B cell antigen receptor. Annu Rev Immunol. 2003;21:841−94.

21. Riches JC, Gribben JG. Understanding the immunodeficiency in chronic lymphocytic leukemia: potential clinical implications. Hematol Oncol Clin North Am. 2013;27:207−35.

22. Rozková D, Novotná L, Pytlík R, Hochová I, Kozák T, Bartůnková J, et al. Toll-like receptors on B-CLL cells: expression and functional consequences of their stimulation. Int J Cancer. 2010;126:1132−43.

23. Arvaniti E, Ntoufa S, Papakonstantinou N, Touloumenidou T, Laoutaris N, Anagnostopoulos A, et al. Toll-like receptor signaling pathway in chronic lymphocytic leukemia: distinct gene expression profiles of potential pathogenic significance in specific subsets of patients. Haematologica . 2011;96:1644−52.

24. Muzio M, Scielzo C, Bertilaccio MT, Frenquelli M, Ghia P, Caligaris-Cappio F. Expression and function of toll like receptors in chronic lymphocytic leukaemia cells. Br J Haematol. 2009;144:507−16.

25. Grandjenette C, Kennel A, Faure GC, Béné MC, Feugier P. Expression of functional toll-like receptors by B-chronic lymphocytic leukemia cells. Haematologica . 2007;92:1279−81.

26. Herishanu Y, Pérez-Galán P, Liu D, Biancotto A, Pittaluga S, Vire B, et al. The lymph node microenvironment promotes B-cell receptor signaling, NF-kappaB activation, and tumor proliferation in chronic lymphocytic leukemia. Blood. 2011;117:563−74.

27. Tromp JM, Tonino SH, Elias JA, Jaspers A, Luijks DM, Kater AP, et al. Dichotomy in NF-kappaB signaling and chemoresistance in immunoglobulin variable heavy-chain-mutated versus unmutated CLL cells upon CD40/TLR9 triggering. Oncogene. 2010;29:5071−82.

28. Ntoufa S, Vardi A, Papakonstantinou N, Anagnostopoulos A, Aleporou-Marinou V, Belessi C, et al. Distinct innate immunity pathways to activation and tolerance in subgroups of chronic lymphocytic leukemia with distinct immunoglobulin receptors. Mol Med. 2012;18:1281−91.

29. Genung NE, Guckian KM. Small molecule inhibition of interleukin-1 receptor-associated kinase 4 (IRAK4). Prog Med Chem. 2017;56:117−63.

30. Liu FT, Jia L, Wang P, Wang H, Farren TW, Agrawal SG. STAT3 and NF-κB cooperatively control in vitro spontaneous apoptosis and poor chemo-responsiveness in patients with chronic lymphocytic leukemia. Oncotarget. 2016;7:32031−45.

31. Hanna BS, Öztürk S, Seiffert M. Beyond bystanders: myeloid cells in chronic lymphocytic leukemia. Mol Immunol. 2019;110:77−87. pii:S0161-5890:30577-1.

32. Galletti G, Scielzo C, Barbaglio F, Rodriguez TV, Riba M, Lazarevic D, et al. Targeting macrophages sensitizes chronic lymphocytic leukemia to apoptosis and inhibits disease progression. Cell Rep. 2016;14:1748−60.

33. Dadashian EL, McAuley EM, Liu D, Shaffer AL, Young RM, Iyer JR, et al. TLR signaling is activated in lymph node-resident CLL cells and is only partially inhibited by ibrutinib. Cancer Res. 2019;79:360−71.

34. Voo KS, Bover L, Harline ML, Weng J, Sugimoto N, Liu YJ. Targeting of TLRs inhibits CD4+ regulatory T cell function and activates lymphocytes in human peripheral blood mononuclear cells. J Immunol. 2014;193:627−34.

Supplementary information

Isolation and culture of primary human cells

Peripheral blood mononuclear cells (PBMCs) from patients diagnosed with CLL according to the World Health Organization criteria [1] and from healthy donors were used in this study. IGHV gene mutational status was assessed according to the European Research Initiative on CLL guidelines [2]. The ethical approval for this project including the informed consent of the patients was granted following the guidelines of the Hospital Clinic Ethics Committee and the Declaration of Helsinki.

Thawed cells were cultured in fresh RPMI-1640 (Gibco, Carlsbad, CA, USA) supplemented with 10% fetal bovine serum (FBS), 2 mM glutamine and 4% penicillin-streptomycin (Life Technologies) and cultured in a humidified atmosphere at 37ºC containing 5% carbon dioxide. CD14$^+$ monocytes from healthy donor PBMCs were isolated via magnetic activated cell sorting (MACS) using human CD14 MicroBeads (MiltenyiBiotec Inc., Auburn, CA, USA), according to manufacturer's protocol.

Gene expression analysis

Total RNA was isolated from these samples using TRIzol reagent (Life Technologies, Eugene, OR, USA) according to manufacturer's instructions. RNA integrity was examined with the Bioanalyzer 2100 (Agilent Technologies, Santa Clara, CA, USA) and only high quality samples were hybridized to AffymetrixGeneChip HT HG-U219 perfect-match-only array plate, following Affymetrix standard protocols. The Expression Console software (Affymetrix, Santa Clara, CA, USA) was used to get the summarized expression values by the Robust Multi-array Analysis. Expression array data have been submitted to the European Genome-Phenome Archive under accession number EGAS00001000772.

The gene expression profile (GEP) of *MYD88*-mutated cases versus those without mutations was compared using the gene set enrichment analysis (GSEA) package version 3.0. A respective analysis was performed including only IGHV-mutated patients. An enrichment of gene set signatures was evaluated using the Hallmark gene sets collection version 6.1 with a two class analysis, 1000 permutations of gene sets and weighted metrics. Gene sets with false discovery rate (FDR) q-value <0.05 were considered to be significantly enriched in the mutated group.

Isolation and culture of cell suspensions from murine spleen

Spleens from age- and sex-matched leukemic TCL1, C57BL/6 wild-type (WT) control mice, *Nr4a1*^{GFP} transgenic mice, *Myd88*^{−/−} mice and vehicle- or ND2158-treated TCL1 AT mice were isolated and homogenized with a gentle MACS Dissociator (MiltenyiBiotecInc.). Single cell suspensions were obtained after erythrocyte lysis by incubation with Red blood cell lysis buffer (BioLegend, San Diego, CA, USA) [3] and filtration through 70 µm nylon sieves (BD Falcon™, Franklin Lakes, NJ, USA). For *in vitro* stimulation experiments, purified B cells, monocytes or total splenocytes were cultured in RPMI-1640 supplemented with 10% FBS and 1% penicillin/streptomycin and cultured in a humidified atmosphere at 37ºC containing 5% carbon dioxide. Purified B cells and monocytes were isolated from total splenocytes via MACS using mouse CD19 MicroBeads (MiltenyiBiotec Inc.), or the EasySep™ Mouse Monocyte Isolation Kit (StemCell Technologies, Vancouver, Canada), respectively, according to manufacturer's protocols. Human PBMCs and murine splenocytes from C57BL/6, *Myd88*^{−/−} and *Nr4a1*^{GFP} transgenic mice for CD8$^+$ T cell experiments were cultured in RPMI-1640 supplemented with 10% fetal calf serum, 1% L-Glutamine, 1% non-essential aminoacids, 10 mM HEPES, 1 mM sodium pyruvate, 1x (55 µM) 2-mercaptoethanol and 1% penicillin/streptomycin.

Cytokine measurements

Milliplex MAP Human Cytokine Magnetic Bead Panel (Merck-Millipore, Billerica, MA, USA), a multiplexed sandwich immunoassay based on flow-cytometry Luminex® technology, was used to measure CCL2/MCP1, CCL3/MIP1α, CCL4/MIP1β, TNFα, IL1β, IL6, IL10, IL1RA, IFNγ and IL12-p70 in supernatants from PBMCs of CLL primary cases seeded at 2×10^6 cells/mL for 48 h. B cells and monocytes from spleens of leukemic TCL1 AT mice were cultured at 2×10^6 cells/mL for 48 h and concentrations of CCL2/MCP1, CCL3/MIP1α, CCL4/MIP1β, TNFα, IL1β, IL6, IL10, IFNγ and IL12-p70 in the culture supernatants were determined by using the fluorescence-activated cell sorter analysis (Luminex® 100 System) Milliplex MAP Mouse Cytokine Magnetic Bead Panel (Merck-Millipore). Data was analyzed with the Luminex® Xponent software.

Western blot analysis

Whole protein extraction and Western blot analysis were carried out as previously described [4]. Membranes were probed with antibodies against $I\kappa B\alpha^{pS32/36}$, $I\kappa B\alpha$, $STAT3^{pY705}$ and STAT3 (Cell Signaling Technology, Danvers, MA, USA). Antibody binding was detected using secondary peroxidase-labeled anti-mouse and anti-rabbit (Sigma-Aldrich) antibodies and enhanced chemiluminescent substrate (ECL; ThermoScientific, Rockford, IL, USA). Chemiluminescence was detected using a mini-LAS4000 Fujifilm device (Fujifilm, Minato, TY, Japan). As two different membranes for the detection of phosphorylated proteins and total proteins were used, densitometry studies were performed by normalizing values to α-tubulin (Sigma-Aldrich) bands in each membrane, and then, calculating the ratio between normalized phosphorylated and total protein values using the Image Gauge software (Fujifilm). Subsequently, these values were normalized to results of untreated control samples. Results of α-tubulin analysis have been removed from the main figures, but the original blots including α-tubulin are shown in the supplementary figures.

In vitro cell proliferation assays

Cells were labeled with 0.5 µM carboxyfluoresceinsuccinimidyl ester (CFSE; Life Technologies) and seeded in 96-well plates at a density of 10^5 cells/200 µl. B cells were cultured in RPMI-1640 medium which was supplemented with 15 ng/ml recombinant human or murine IL15 (R&D systems, Minneapolis, MN, USA) as described before [5, 6]. When specified, cells were incubated with TLR agonists and/or ND2158. For T cell proliferation assay, PBMCs were stimulated for 30 min with 1 µg/ml anti-CD3 antibody before ND2158 addition.

The percentage of dividing cells was determined as the percentage of live human B (CD19^{+}) or T cells (CD3^{+}CD8^{+}) or as the percentage of live tumor cells (CD45^{+}CD19^{+}CD5^{+}) showing a decrease in CFSE signal compared to non-stimulated cells.

For 5-ethynyl-2′-deoxyuridine (EdU) incorporation, cells were cultured in medium as indicated above supplemented with 10 µM EdU (Life Technologies, Carlsbad, USA) for 6 days. For EdU detection, cells were washed and stained for surface molecules in FACS buffer as described in the Immunostainings section. Cells were fixed with 4% PFA in PBS for 15 min at room temperature, washed twice with 1% BSA in PBS and permeabilized using 0.1% Triton X-100 in PBS for 30 min at room temperature. After washing with 1% BSA in PBS, cells were incubated with 100 µl Click-iT™ reaction cocktail (9% of 10X Click-iT™ Cell Reaction Buffer, 2% of 100 mM $CuSO_4$, 0.5% Fluorescent dye Alexa Fluor® 488 azide, 1% of 10X Reaction Buffer Additive in H_2O; all from Life Technologies, Carlsbad, USA) for 30

min at room temperature in the dark. Cells were washed twice and resuspended in 1% BSA in PBS before acquisition. The percentage of proliferating cells was determined as percentage of EdU$^+$ live tumor cells (CD45$^+$CD19$^+$CD5$^+$).

Ki-67 staining of human CLL cells was performed as described in the Immunostainings section. The percentage of proliferating cells was determined as percentage of Ki-67$^+$ live tumor cells (CD45$^+$CD19$^+$CD5$^+$).

For all the assays, Fluorescence-minus-one (FMO) was used as a negative control. Data analysis was performed using FlowJo v 10.0.7 software (FlowJo, Ashland, OR, USA).

Analysis of cytotoxicity

ND2158 was provided by Nimbus Therapeutics (Cambridge, MA, USA). Human PBMCs from healthy donors or from 37 CLL patients with ≥90% tumor B cells were incubated for 48 h with ND2158 at doses ranging from 10 to 100 µM. Cell death was quantified by flow cytometry after staining with Annexin-V-FITC and propidium iodide (PI) (eBiosciences, San Diego, CA, USA). B and T lymphocytes from healthy donor samples were identified by staining with anti-CD3 and -CD19 antibodies (Becton Dickinson) and cytotoxicity determined by Annexin-V-PB (Life-Technologies). Percentage of viable cells was defined as Annexin-V$^-$ cells. Viability of TCL1 splenocytes was determined by Fixable Viability Dye eFluor 780 (Via780; eBiosciences), as the percentage of CD45$^+$CD19$^+$CD5$^+$Via780$^-$ cells. Fixable Viability Dye eFluor 780 (eBiosciences) was added 1:1000 diluted for live/dead cell discrimination.

CellTiter-Glo luminescent cell viability assay

Viable cells in culture were determined using the CellTiter-Glo® Luminescent Cell Viability Assay (Promega, Madison, WI, USA), based on quantitation of intracellular ATP levels, following manufacturer's instructions. Primary CLL cells were incubated with 10 µM or 30 µM ND2158 for 48 h assay performance. Data is presented relative to untreated control.

NF-κB DNA-binding assay

Nuclear extracts were generated from primary CLL cells and assayed for NF-κB p65 and p52 activity using the Nuclear Extract Kit and the TransAM NF-κB Chemiluminescence kit (Active Motif, Carlsbad, CA, USA), respectively. Two micrograms of nuclear extracts were incubated for 3 hours according to the manufacturer's protocol in 96-well plates coated with an oligonucleotide containing the NF-κB consensus DNA-binding site. DNA binding of NF-κB subunits was detected by incubating with an antibody against p65 or p52 followed by a horseradish peroxidase-conjugated secondary antibody (ELISA-based method). The acquisition and quantification of the signal were done on a LAS4000 device (Fujifilm).

Immunofluorescent microscopy

For immunofluorescent staining, CLL cells were washed in PBS, fixed in 4% paraformaldehyde and attached to poly-L-lysine-coated cover glass slides overnight at 4ºC. After washing the slides with PBS, bound cells were permeabilized with 0.1% saponine in PBS, washed twice in PBS, incubated with anti NF-κB p65 antibody (clone D14E12; Cell Signaling Technology) for 30 min, washed twice in PBS, and incubated with an Alexa546-conjugated secondary antibody (Invitrogen, Carlsbad, CA, USA). The cells were washed three times in PBS and mounted in anti-fading mounting reagent including DAPI (Sigma-Aldrich). Stained cells were imaged using a fluorescent microscope (Eclipse 50i; Nikon, Corp., Tokyo, Japan) equipped with a CCD camera (CoolCube1, MetaSystems Hard & Software GmbH, Altlussheim, Germany) and a precentered fiber illuminator as light source. Oil immersion objective lens of 100x was used for imaging of cells.

Chemotaxis assay

CLL cells were washed twice and maintained in serum-starved in FBS-free RPMI during the whole experiment. When indicated, TLR agonist mix was added 30 min before ND2158 treatment. Three hours after treatment cells were diluted to 5×10^6 cells/mL with 0.5% bovine serum albumin (BSA; Sigma-Aldrich) in PBS. One hundred microliters of the cell suspension (5×10^5 cells) were added to the top chamber of a Transwell culture polycarbonate insert with 6.5 mm diameter and 5 µm pore size (Corning, Corning, NY, USA). Transwell inserts had been previously coated with VCAM-1 (Peprotech, Rocky Hill, NJ, USA) overnight, washed twice with PBS, and transferred to 24-well culture plates containing 600 µL of RPMI with 0.5% BSA with or without 200 ng/mL of human recombinant CXCL12 (Peprotech) per well. After 3 h of incubation, 100 µL from each lower chamber of the transwell plate were

collected in triplicate and viable cells counted on a cytometer for 12 s under a constant flow rate of 500 µL/min. Values are presented as the ratio of migrating cells and total viable cells, relative to the untreated control. The untreated condition shows CXCL12-induced migration of unstimulated CLL cells which was also reduced by ND2158 treatment in some cases.

TCL1 Adoptive Transfer (AT) mouse model

Eight-week-old female C57BL/6N wild-type mice (Janvier Labs, Saint-Berthevin, France) were injected intravenously with 1×10^7 splenocytes from leukemic $E\mu$-TCL1 mice. Splenocytes used for the adoptive transfer had a purity of 96% CD19$^+$CD5$^+$ cells. After 13 days, mice were assigned to treatment arms based on tumor load in peripheral blood and injected intraperitoneally twice daily (BID) with 50 mg/kg ND2158 in 1% β-cyclodextrin (n=7) or 1% β-cyclodextrin (vehicle; n=7). Tumor progression was monitored by blood withdrawal and quantification of CD19$^+$CD5$^+$ cells as described below, until mice were euthanized after 23 days of treatment. Spleens were weighed, and single cell suspensions were obtained from peripheral blood, bone marrow, inguinal lymph node, spleen and peritoneal cavity. Bone marrow cells were flushed out from one femur with 5 mL of PBS with 2% FBS followed by filtration through 70 µm nylon sieves. Single cell suspensions from one inguinal lymph node were obtained by manual dissociation with a 3 mL syringe plunger in 5 mL of PBS with 2% FBS over a 70 µm nylon sieve. Single cell suspensions from peritoneal cavity were obtained by flushing peritoneal cavity with 3 mL of PBS with 2% FBS. Tumor load in the affected organs was determined via flow cytometry as absolute number or percentage of CD5$^+$CD19$^+$ cells. The total viable spleen cell count and the percentage of splenic monocyte or CD8$^+$ T cell populations out of total viable CD45$^+$ cells, analyzed by flow cytometry, were used for the calculation of absolute cell counts: (Total viable spleen cell count/100) x Percentage (%) of cell population of interest. Cell counting was performed on an automated Vi-CELL XR hemocytometer (Beckman Coulter, High Wycombe, UK). Whole blood from treated mice was stained by incubation for 30 min at 4ºC with a 1:200 diluted antibody cocktail. Erythrocyte lysis and cell fixation were done using the 1-step Fix/Lyse Solution (eBioscience). 123count eBeads™ Counting Beads (eBioscience) were added before cell acquisition to determine the absolute cell counts per µL. Absolute cell numbers in blood were calculated according to the formula: absolute count (cells/µL) = (cell count x bead volume x bead concentration)/(bead count x cell volume). All *in vivo* experiments were performed at the German Cancer Research Center (DKFZ) according to local animal experimental ethics committee guidelines and after approval by the Regierungspräsidium Karlsruhe.

Immunostainings for flow cytometry

At experimental endpoints, single cell suspensions of all analyzed tissues were washed with FACS buffer (PBS containing 2% FBS) and incubated with the respective surface marker antibody cocktails for 30 min at 4°C in the dark. BD Horizon™ Fixable Viability Stain 700 (BD Biosciences, Franklin Lakes, NJ, USA), Fixable Viability dye eFluor 506 (eBioscience) or Fixable Viability Dye eFluor 780 (eBioscience) was added at 1:1000 dilution for live/dead cell discrimination. Cells were then washed twice with FACS buffer, fixed in 100 µl IC fixation buffer (eBioscience) for 30 min at room temperature and washed with FACS buffer again. Cells were kept at 4°C in the dark until acquisition. For intracellular staining, fixed cells were permeabilized in 200 µl of 1x Permeabilization buffer (eBioscience) for 5 min at room temperature and then incubated with intracellular marker antibody cocktail in 1x Permeabilization buffer for 30 min at room temperature in the dark. For nuclear Ki-67 stainings, cells were fixed and permeabilized in 200 µl Foxp3/Transcription Factor Fixation/Permeabilization buffer (eBioscience) for 30 min at room temperature followed by incubation with an anti-mouse or anti-human Ki-67 antibody in 1x Permeabilization buffer for 30 min at room temperature in the dark. Cells were washed twice with FACS buffer and cells were kept at 4°C in the dark until acquisition.

In vitro T cell stimulation

Human PBMCs and murine splenocytes were incubated with 1 µg/ml anti-human CD3e (Clone UCHT1; Biolegend) and 1 µg/ml anti-mouse CD3e (Clone 145-2C11; eBioscience) antibody, respectively. For detection of granzyme B and cytokines, cells were restimulated with 0.5x PMA/ionomycin stimulation cocktail (eBioscience) in the presence of 1x protein transport inhibitor cocktail (eBioscience) for 4 h before harvesting the cells. T cell activation was assessed after 24 h of stimulation.

Flow cytometry sample acquisition and data analysis

Samples were acquired either on a FACS-Canto II flow cytometer (BD Biosciences) using FACS-DIVA 6.1.1 software, a BD LSR Fortessa flow cytometer using the BD FACSDiva software version 8.0.2 or an Attune focusing acoustic cytometer (Life Technologies). Data analyses were performed using FlowJo10.0.7 software. Bimodal populations were quantified as percentage of protein-expressing cells, whereas for unimodal populations mean fluorescence intensities (MFI) were analyzed. MFI were recorded and normalized by subtracting the MFI of the respective FMO control.

Gating strategies for analyzed immune subsets in the spleen were as follows: cell debris and doublets were excluded from the analysis and only live cells were selected for further analysis. Murine splenic monocytes were identified as $CD45^+Lineage^-Ly6G^-$ $CD11b^+CX3CR1^+F4/80^+$ cells. Lineage markers included CD19, CD3, NK1.1 and TER-119. Within this population, inflammatory monocytes were defined as $Ly6C^{high}$ and patrolling monocytes as $Ly6C^{low}$ cells. Splenic cytotoxic T cells were identified as $CD45^+CD3^+CD8^+$ cells. Identification of $CD8^+$ T cells subsets was based on the expression of CD127 and CD44, with $CD8^+$ effector T cells identified as $CD127^{low}/CD44^{int-high}$ cells and $CD8^+$ memory T cells as $CD127^{high}CD44^{high}$ cells.

References

1.   Swerdlow SH, Campo E, Pileri SA, Harris NL, Stein H, Siebert R, et al. The 2016 revision of the World Health Organization classification of lymphoid neoplasms. Blood. 2016;127:2375-90.

2.   Ghia P, Stamatopoulos K, Belessi C, Moreno C, Stilgenbauer S, Stevenson F, et al. ERIC recommendations on IGHV gene mutational status analysis in chronic lymphocytic leukemia. Leukemia. 2007;21:1-3.

3.   Hoyer KK, French SW, Turner DE, Nguyen MT, Renard M, Malone CS, et al. Dysregulated TCL1 promotes multiple classes of mature B cell lymphoma. Proc Natl Acad Sci U S A. 2002;99:14392-7.

4.   Giménez N, Martínez-Trillos A, Montraveta A, Lopez-Guerra M, Rosich L, Nadeu F, et al. Mutations in RAS-BRAF-MAPK-ERK pathway define a specific subgroup of patients with adverse clinical features and provide new therapeutic options in chronic lymphocytic leukemia. Haematologica. 2018; e-pub ahead of print 27 September 2018; doi: 10.3324/haematol.2018.196931.

5.   Mongini PK, Gupta R, Boyle E, Nieto J, Lee H, Stein J, et al. TLR-9 and IL-15 Synergy Promotes the In Vitro Clonal Expansion of Chronic Lymphocytic Leukemia B Cells. J Immunol. 2015;195:901-23.

6.   Gupta R, Yan XJ, Barrientos J, Kolitz JE, Allen SL, Rai K, et al. Mechanistic Insights into CpG DNA and IL-15 Synergy in Promoting B Cell Chronic Lymphocytic Leukemia Clonal Expansion. J Immunol. 2018;201:1570-85.

SUPPLEMENTARY TABLES

Case	Gender/ Age at diagnosis	[a]Tumor cells	[b]Binet/ Rai stage	[c]IGHV	Previous treatment	[d]Cytogenetic alterations	*MYD88* status	[e]Other Recurrent mutations	ICGC
01	M/45	98	C/IV	M	No	del(13q)	L265P	*KLHL6*	3
02	M/49	96	C/IV	M	No	del(13q)	L265P	*CHD2*	181
03	F/43	96	A/I	UM	Flu	-	M	-	553
04	M/56	95	B/III	M	No	del(13q), Try12	M232T	*SF3B1*	564
05	M/37	93	B/II	M	No	-	L265P	-	629
06	M/43	90	B/II	M	Cl	del(13q)	L265P	-	633
07	M/57	94	B/II	M	Cl	-	V209F	-	1534
08	F/53	94	B/II	UM	Flu,R-FCM,B-R	del(13q) del(11q)	UM	*IKZF3,POT1, SF3B1*	13
09	M/70	95	B/II	UM	No	del(13q)	UM	*ATM, SF3B1*	10
10	M/59	95	A/0	UM	No	-	UM	*ATM,NFKBI, ZNF292,ZMYM3*	16
11	M/69	96	BII	UM	RCHOP,FC,Cl	Try12	UM	-	24
12	M/53	97	C/IV	UM	R-FCM	del(13q)	UM	*TLR2,POT1, ZNF292*	44
13	M/52	97	B/II	UM	Yes	del(13q)	UM	-	63
14	M/64	93	B/II	M	No	Try12, t(14;18)	UM	-	64
15	M/52	94	B/I	UM	No	del(17p)	UM	-	75
16	M/47	86	C/IV	UNKN	multiple	del(13q), der(11)t(11; 13)	UM	-	79
17	M/58	98	B/II	UM	multiple	del(11q)	UM	-	101
18	M/62	98	C/IV	M	B	del(13q)	UM	-	115
19	M/66	95	C/IV	M	No	del(13q)	UM	-	159
20	M/65	94	A/I	UM	No	del(13q)	UM	-	186
21	M/58	93	A/I	M	No	-	UM	*PTPN11*	191
22	M/56	93	A/0	M	No	-	UM	-	273
23	M/61	96	C/III	UM	No	del(11q)	UM	*BIRC3(DEL), MED12*	278
24	M/78	94	A/II	UM	No	del(13q)	UM	-	316
25	F/43	95	A/0	M	No	del(13q)	UM	-	344
26	M/44	97	B/II	UM	No	del(13q)	UM	*XPO1*	350
27	F/48	91	A/0	M	No	del(13q)	UM	-	361
28	F/54	91	CIII	UM	No	del(11q), del(13q)	UM	-	384
29	M/62	97	B/II	UM	No	del(11q), del(13q)	UM	*ATM*	442
30	F/41	99	C/IV	UM	Cl,Flu	del(13q)	UM	-	540
31	M/69	98	A/0	M	No	-	UM	-	561
32	F/69	98	A/0	M	C	-	UM	*CHD2*	569
33	F/52	92	B/II	M	No	Try12	UM	-	642
34	M/54	96	B/II	M	FCM, R-FCM	del(13q)	UM	-	680
35	M/59	95	B/II	M	No	del(13q)	UM	*NFKBIA*	684
36	M/53	88	A0	M	No	-	UM	*SF3B1*	758
37	M/66	98	B/III	UM	No	del(11q)	UM	*ATM, BIRC3(DEL)*	761
38	M/57	98	A/0	M	No	del(13q)	UM	-	815
39	F/56	94	A/0	M	No	del(13q)	UM	-	1103
40	F/54	92	B/II	M	No	T(14;18)	UM	-	1291
41	F/63	97	C/IV	M	No	del(13q)	UM	*NFKB2*	1323
42	M/83	60	A0	M	No	del(11q) del(13q) del(17p)	UM	-	1339
43	M/78	96	A/0	M	No	del(13q)	UM	-	1481
44	F/64	91	A/0	UM	Cl	del(11q)	UM	-	-
45	F/47	86	A/I	UM	FCM	-	UM	-	77
46	M/56	98	C/IV	UM	No	-	UM	*NOTCH1*	11
47	M/58	96	B/II	UM	FCM; R-FCM	del(13q)	UM	*BRAF*	27
48	M/55	79	A/0	UM	No	t(5;14)(q34; q11.2)	UM	*NOTCH1*	15
49	M/60	79	B/II	UM	No	del(11q)	UM	*ATM, BIRC3,SF3B1*	306
50	M/62	95	A/0	UM	No	Try12	UM	*ATM, BIRC3,NOTCH*	723
51	M/55	91	A/0	M	No	N	UM	-	-

Table S1. Clinical and biological characteristics of CLL patients.

M, male; F, female; ND, not determined; M, mutated; UM, unmutated; del, deletion; T, treated; U, untreated; FCM, Fludarabine, Cyclophosphamide, Mitoxantrone; CHOP, Cyclophosphamide, Doxorubicin, Vincristine, Prednisone;FC, Fludarabine, Cyclophosphamide; Cl,Chlorambucil; Flu, Fludarabine; R, Rituximab; C, Cyclophosphamide; B, bendamustine; UNKN, unknown.
[a]Percentage of tumoral cells was quantified by flow cytometry labeling CD5+/CD19+ cells and light chain restriction. Try2: Trisomy12.
[b]According to Rai and Binet's classification: Early (Rai 0, Binet A), intermediate (Rai I/II, Binet B) and advanced (Rai III/IV, Binet C).
[c]IGHV gene was sequenced following RT-PCR, and aligned to NCBI IgBlast. Mutated status was assigned when >2% deviation from germline IGHV sequence was present. [d] Cytogenetic alterations were assessed by FISH. [e]Recurrent mutations were identified by exome-sequencing analysis within the ICGC project.

Table S2. Flow cytometry antibodies.

Antibody	Fluorophore	Clone	Vendor
Anti-mouse CD45	AF700	30-F11	Biolegend
Anti-mouse CD19	PE-Cy7 or FITC	eBio1D3	eBioscience
Anti-mouse CD5	APC	53-7.3	Biolegend
Anti-mouse MHC-II I-A/I-E	AF700 or FITC	M5/114.15.2	eBioscience
Anti-mouse CD25	FITC or PerCP-Cy5.5	PC61	Biolegend
Anti-mouse CD40	PE	1C10	eBioscience
Anti-mouse CD86	PerCP-Cy5.5	GL-1	Biolegend
Anti-mouse CD69	PE-Dazzle	H1.2F3	Biolegend
Anti-mouse CD11b	PE-Cy7	M1/70	eBioscience
Anti-mouse F4/80	APC or PE	BM8	Biolegend
Anti-mouse CD54	PE	YN1/1.7.4	Biolegend
Anti-mouse Ly6G	FITC	1A8	Biolegend
nti-mouse Ly6C	APC-Cy7	HK1.4	Biolegend
Anti-mouse PD-L1	PerCP-eFluor710	MIH5	eBioscience
Anti-mouse CD3e	V450	500A2	BD Biosciences
Anti-mouse CD90.2	APC-Cy7	30-H12	Biolegend
Anti-mouse CD4	APC-Cy7	RM4-5	Biolegend
Anti-mouse CD8a	BV605	53-6.7	Biolegend
Anti-mouse CD127	PE-Cy7	A7R34	Biolegend
Anti-mouse CD44	AF700	IM7	eBioscience
Anti-mouse CD28	PE	37.51	Biolegend
Anti-mouse PD-1	PE	RMPI-30	Biolegend
Anti-mouse CD137	APC	17B5	Biolegend
Anti-mouse CXCR3	FITC	CXCR3-173	eBioscience
Anti-mouse LAG3	PE	eBioC9B7W	eBioscience
Anti-mouse TIGIT	PE-Dazzle	1G9	Biolegend
Anti-mouse CD160	PerCP-Cy5.5	7H1	Biolegend
Anti-mouse Granzyme B	V450	NGZB	eBioscience
Anti-mouse Ki-67	FITC	SolA15	eBioscience
Anti-human CD14	FITC	M5E2	Biolegend
Anti-human PD-L1	PE	MIH1	eBioscience
Anti-human CD54	PE-Vio770	Not indicated	MiltenyiBiotec
Anti-human CD5	FITC or APC	UCHT2	Biolegend
Anti-human CD8a	PE-Dazzle or BV605	RPA-T8	Biolegend
Anti-human CD25	BV605	BC96	Biolegend
Anti-human CD28	PerCP-Cy5.5	CD28.2	Biolegend
Anti-human CD137	PE	4B4-1	Biolegend
Anti-human Granzyme B	FITC	GB11	Biolegend
Anti-human CD19	PE	SJ25C1	BD Biosciences
Anti-human CD3	FITC	SK7	BD Biosciences
Anti-human Ki-67	PE-Cy7	Ki-67	Biolegend

Table S3. Gene set enrichment analysis of *MYD88*-mutated compared to *MYD88*-unmutated CLL cases.

	MYD88 M (n=18) vs. *MYD88* UM (n=398)		*MYD88* M IGHV M (n=18) vs. *MYD88* UM IGHV M (n=249)	
	[a]FDR	[b]NES	[a]FDR	[b]NES
TNFα signaling via NFκB	<0.0001	2,66	<0.0001	2.64
IL6 JAK STAT3 signaling	0.008	1,71	0.010	1.76
Inflammatory response	0.050	1,52	0.022	1.57
Apoptosis	0.039	1,51	0.012	1.69
IL2 STAT5 signaling	0.038	1,49	0.044	1.47
Hypoxia	0.131	1,30	0.021	1.59

[a]False discovery rate q-value (FDR)
[b]Normalized enrichment score (NES) ≥1.5 were considered to be significantly enriched in the mutated group.
M, mutated; UM, unmutated.

SUPPLEMENTARY FIGURES
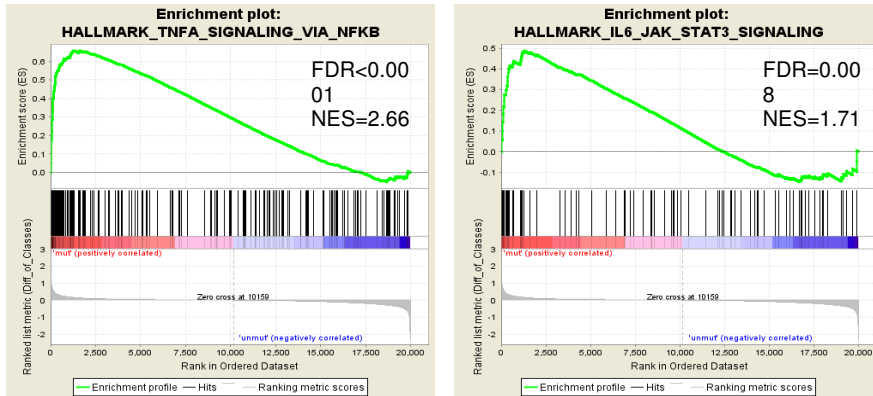
Figure S1. Gene set enrichment analysis of *MYD88*-mutated and *MYD88*-unmutated CLL cases. Enrichment plots for two gene sets that are significantly enriched in *MYD88*-mutated cases (n=18) compared to *MYD88*-unmutated CLL cases (n=398). Gene sets with false discovery rate (FDR) q-value <0.05 and a normalized enrichment score (NES) ≥1.5 were considered to be significantly enriched in the mutated group.

a.
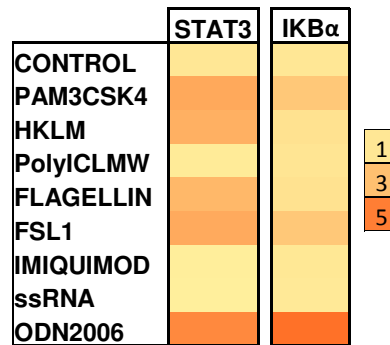
b.
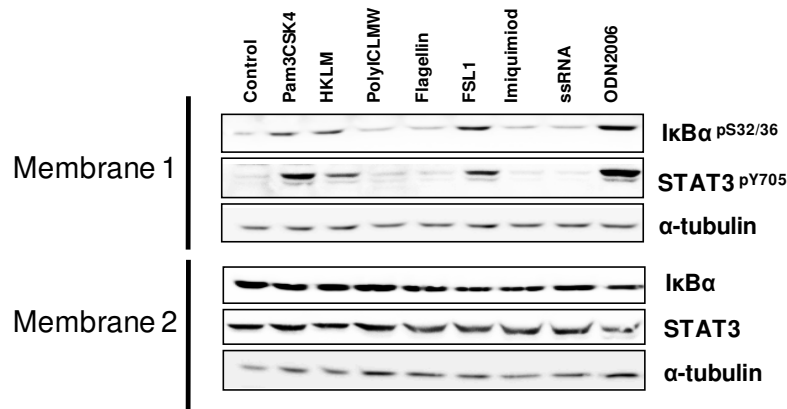
Figure S2. TLR stimulation activates NF-κB and STAT3 signaling. Western blot analysis of IκBα$^{pS32/36}$ and STAT3^{pY705} phosphorylation levels in CLL cells after stimulation with TLR ligands for 3 h. **a)** Heatmap representing the mean rations of TLR-stimulated over untreated samples that were calculated from obtained densitometry values from 4 Western blots (3 *MYD88*-unmutated and 1 *MYD88*-mutated CLL samples). **b)** A representative *MYD88*-unmutated, IGHV-mutated CLL case (#31) is shown. α-tubulin levels were used as loading control.
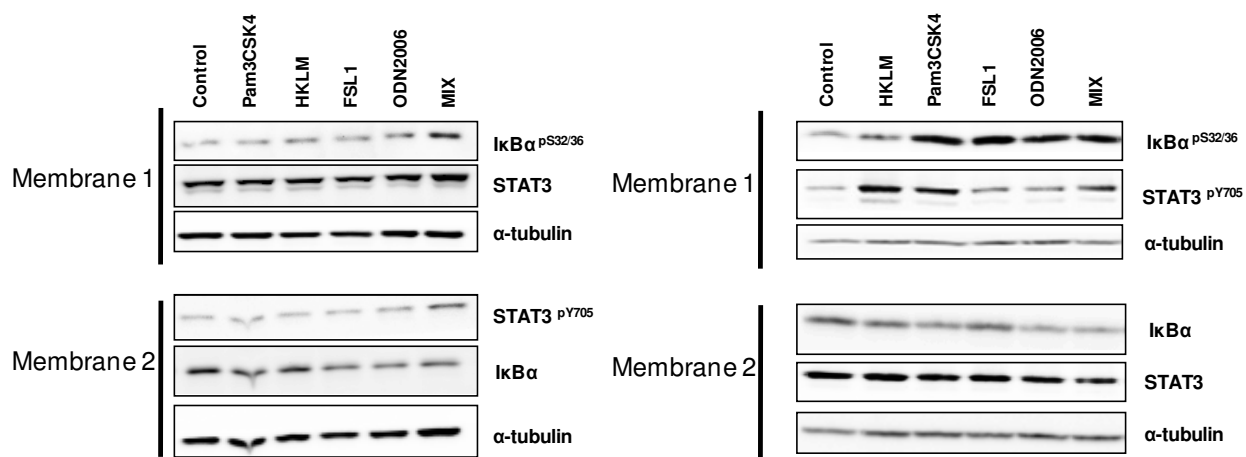
Figure S3. Western blot results from Figure 2b including α-tubulin levels which was used as a loading control in each membrane.

a.
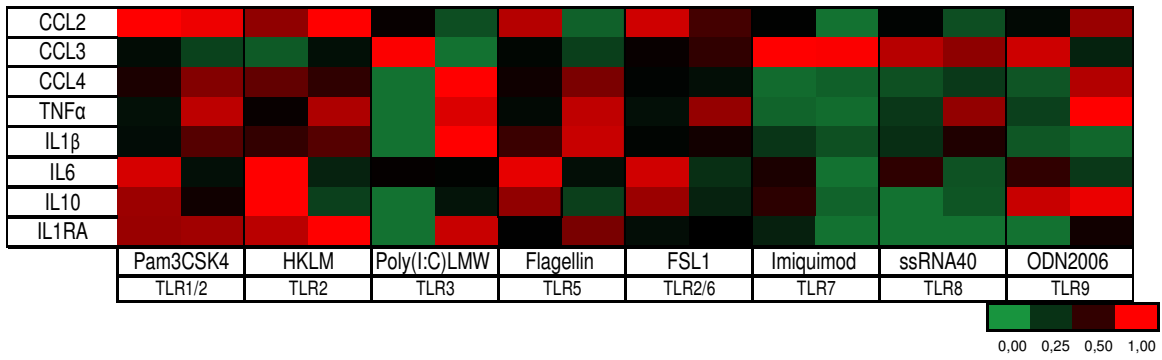
b.
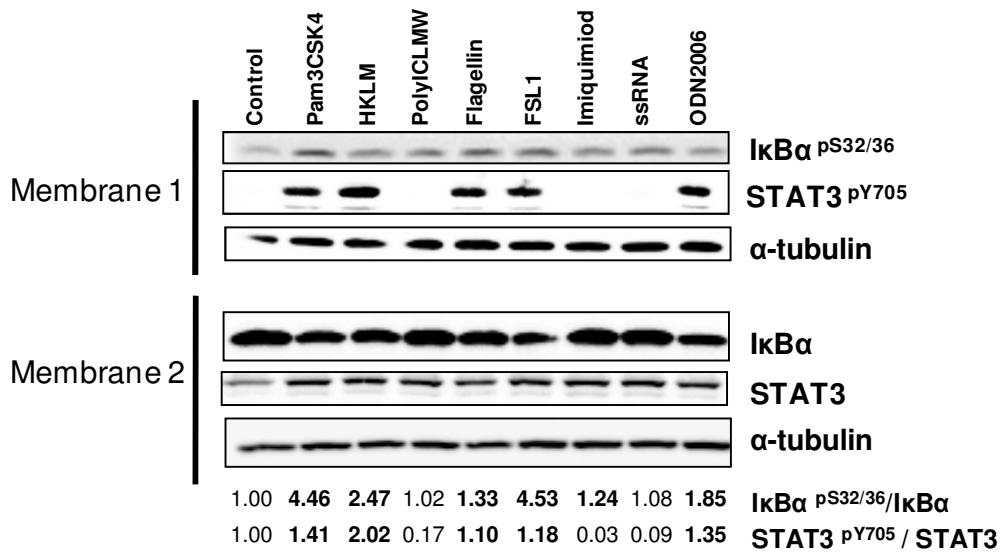
c.
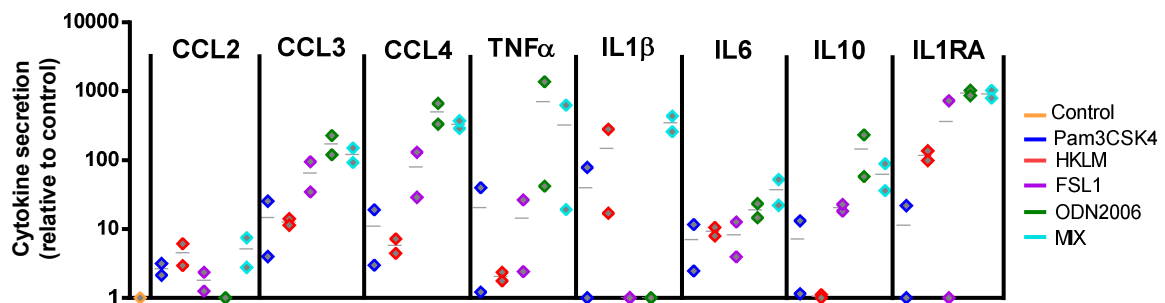
Figure S4. TLR stimulation increases cytokine secretion, NF-κB and STAT3 signaling of IGHV-unmutated CLL cells. CLL cells were cultured with single TLR agonists or TLR agonist mix (Pam3CSK4, HKLM, FSL1 and ODN2006). **a)** Heatmap representing cytokine levels in CLL culture supernatants after 48 h of TLR stimulation (n=2) analyzed by flow cytometry Luminex® Bead Panel. The level of secretion of each cytokine is presented relative to untreated control. **b)** Western blot analysis of IκBα[pS32/36] and STAT3[pY705] phosphorylation and total levels of IκBα and STAT3 in IGHV-unmutated CLL cell extracts after 3 h of single or TLR agonist mix stimulation. α-tubulin was used as loading control. A representative IGHV-unmutated CLL case (#11) is shown. Ratios of phosphorylated and total protein levels were calculated and are provided as fold changes relative to the untreated control sample. **c)** Cytokine secretion after 48 h of TLR stimulation was assessed in cell culture supernatants by flow cytometry Luminex® Bead Panel (n=2). Data is presented as fold change relative to unstimulated control.

a.

b.
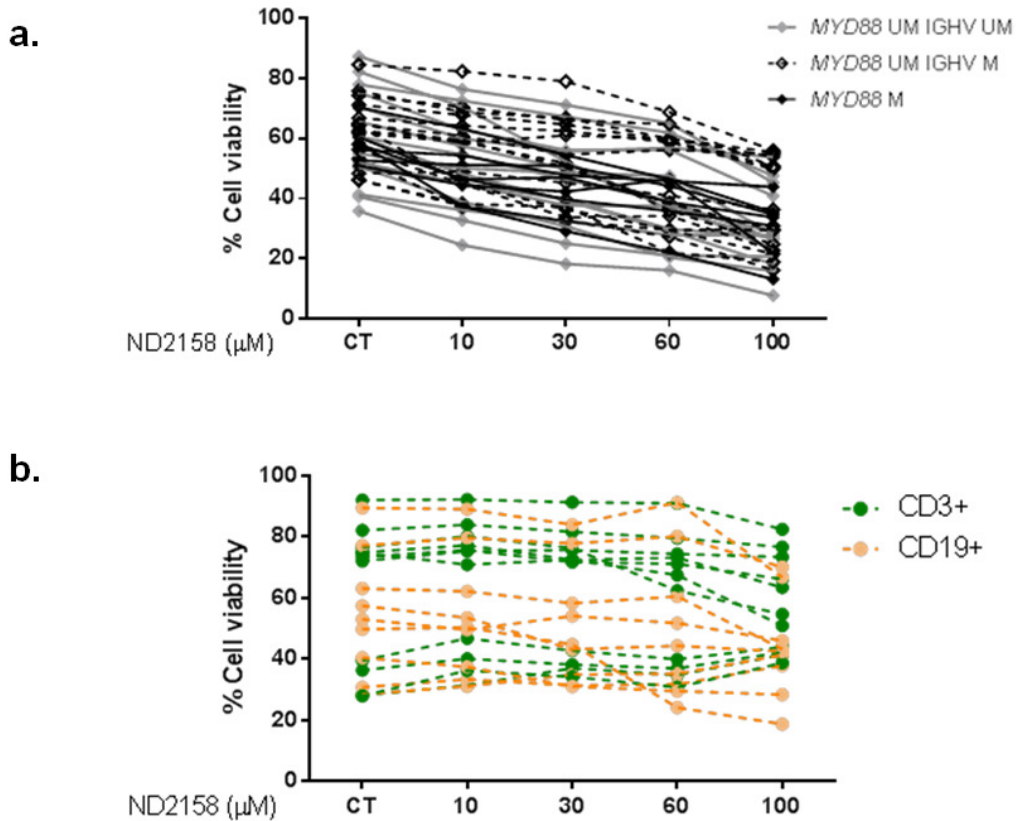
Figure S5. ND2158 decreases viability of CLL cells. Viability of CD19+CD5+ CLL cells in **a)** *MYD88*-mutated IGHV-mutated (n=6), *MYD88*-unmutated IGHV-mutated (n=16) CLL samples, and **b)** CD19+ B cells and CD3+ T cells from healthy donors (n=10) was analyzed by flow cytometry after 48 h of incubation with the indicated concentrations of ND2158. Percentage of viable cells was measured by staining with Annexin-V. M, mutated; UM, unmutated.
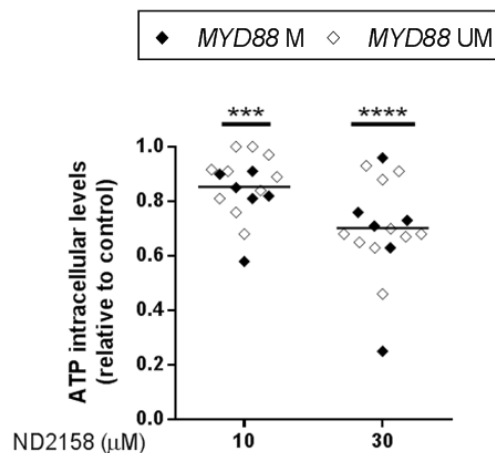
Figure S6. ND2158 exerts cytotoxicity in CLL cells. Intracellular ATP levels in CLL cells from *MYD88*-mutated (n=6) and *MYD88*-unmutated (n=10) patients (all IGHV-mutated) were measured after 48 h of incubation with 10 or 30 μM ND2158 using CellTiter-Glo® Luminescent Cell Viability Assay, and are depicted relative to untreated control. Wilcoxon signed-rank test was used for statistical analysis. Asterisks indicate statistical significance level relative to control. ***$P<0.001$, ****$P<0.0001$. M, mutated; UM, unmutated.
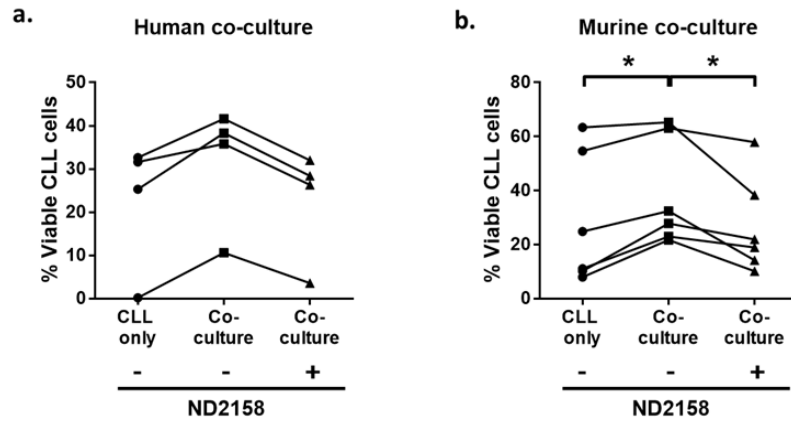
Figure S7. Effect of ND2158 on viability of CLL cells in co-cultures with monocytes. a) Human monocytes were isolated by MACS from healthy donor PBMC samples and cultured with MACS-sorted human CLL cells. ND2158 (10 µM) or DMSO as control was added to co-cultures and cells were harvested after 4 days. Viable (Annexin V⁻/7-AAD⁻) CD19⁺CD5⁺ CLL cells were quantified by flow cytometry. **b)** Bone marrow-derived myeloid cells were isolated from murine femurs and differentiated to macrophages in RPMI-1640 containing 30% L929 conditioned medium for 4 days. At day 4, malignant B cells isolated by MACS from the spleen of mice with TCL1 leukemia were added to bone marrow-derived macrophages and treated with 10 µM ND2158 or DMSO. Viable (Annexin V⁻/7-AAD⁻) CD19⁺CD5⁺ CLL cells were quantified by flow cytometry after 48 h of co-culture. Wilcoxon matched pairs signed-rank test was used for statistical analysis. *$P<0.05$.
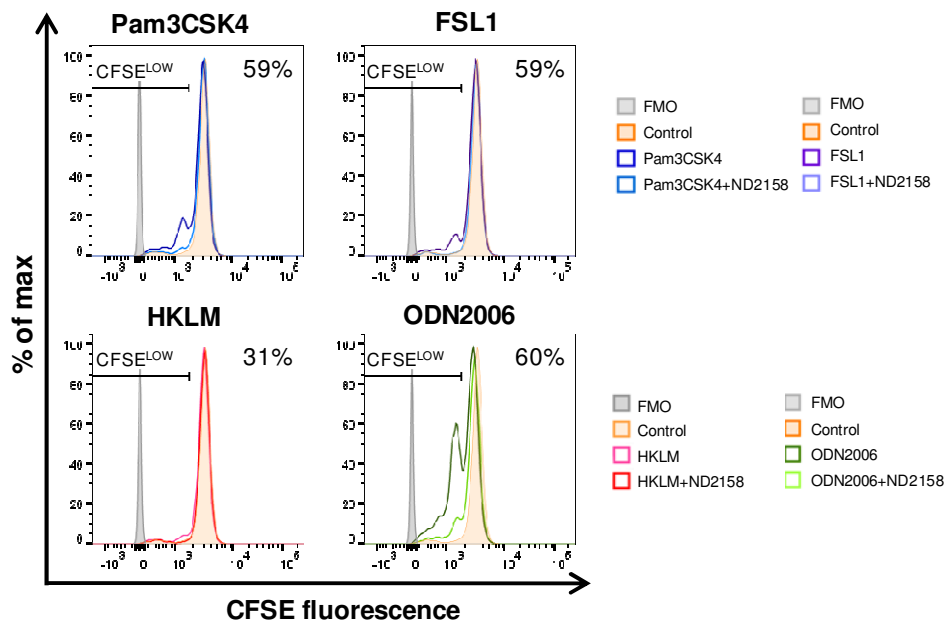
Figure S8. Anti-proliferative effect of ND2158 on TLR-stimulated CLL cells *in vitro*. CLL cells were exposed to TLR agonists and IL15 for 30 min before adding 10 µM ND2158. Proliferation of cells was analyzed by CFSE dilution assay after 6 days of incubation. Histograms of a representative *MYD88*-unmutated, IGHV-mutated CLL case (#51) are shown.

a.

b.
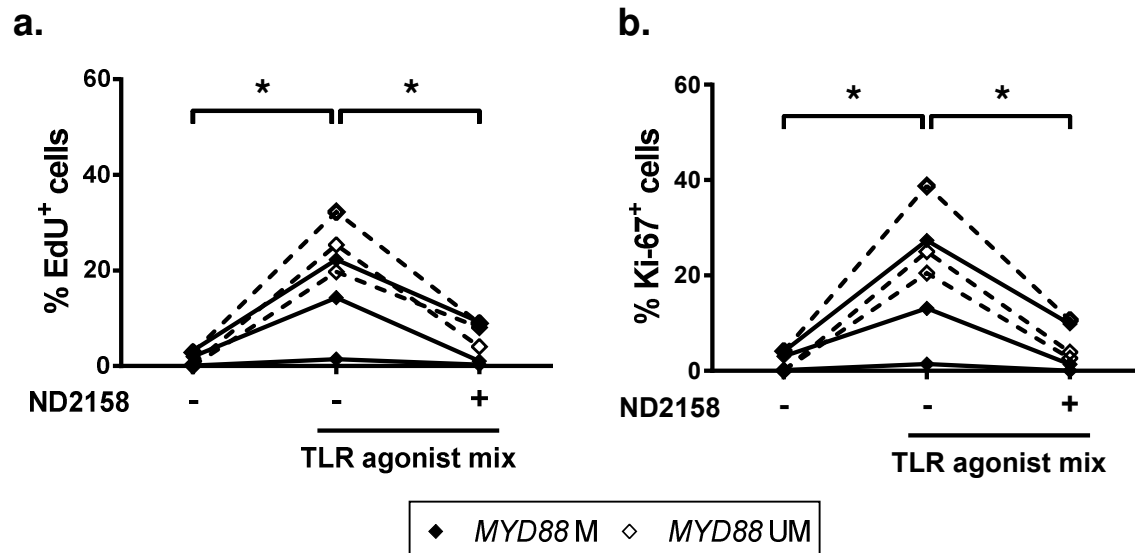
Figure S9. Percentage of proliferating CD19$^+$CD5$^+$ CLL cells after TLR stimulation and 10 µM ND2158 treatment for 6 days measured by **a)** EdU incorporation or **b)** Ki-67$^+$ staining (n=6). Wilcoxon matched pairs signed rank test was used for statistical analysis. *P<0.05. M, mutated; UM, unmutated.
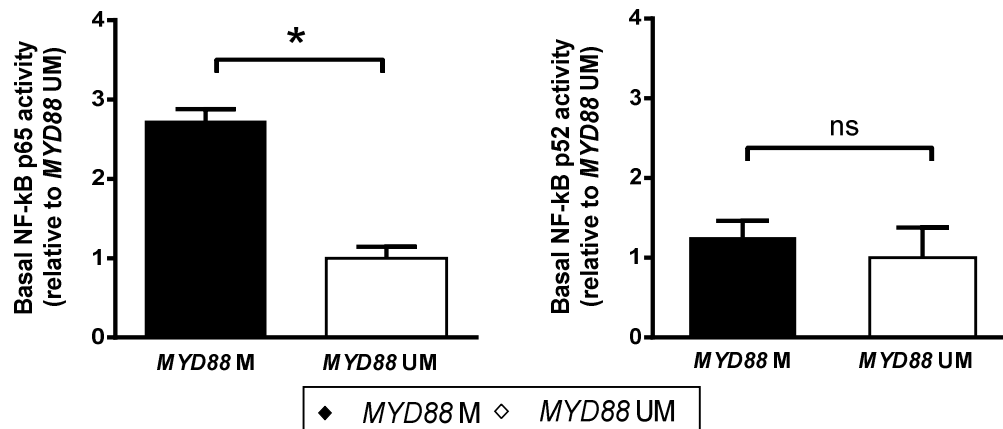
Figure S10. NF-κB basal levels in *MYD88*-mutated and *MYD88*-unmutated CLL cases. Basal levels of p65 and p52 NF-kB subunits in nuclear extracts of *MYD88*-mutated (n=4) and *MYD88*-unmutated cases (n=4) were determined by NF-κB DNA-binding assay to plate-bound NF-kB consensus sequence oligos after 3 h of incubation. Obtained values for NF-kB binding are presented relative to *MYD88*-unmutated mean values. Results are expressed as mean ± SD. Mann-Whitney test was used for statistical analysis. ns, not significant; P≥0.05, *P<0.05. M, mutated; UM, unmutated.
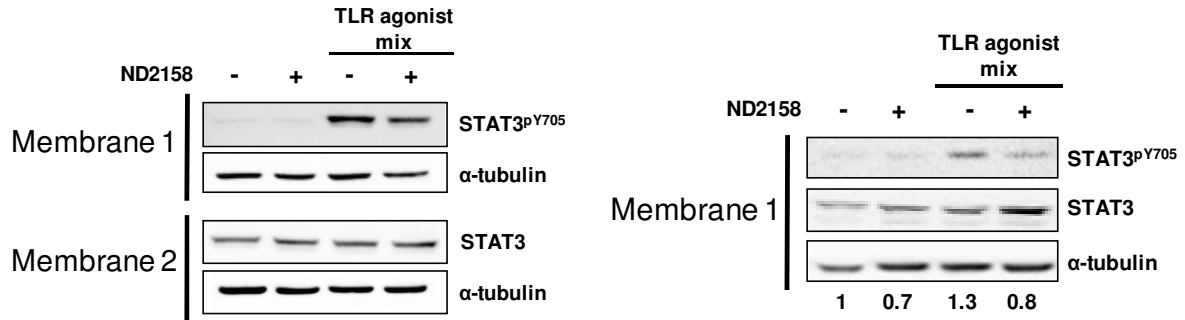
Figure S11. Western blot results from Figure 4b including α-tubulin levels which was used as a loading control in each membrane.
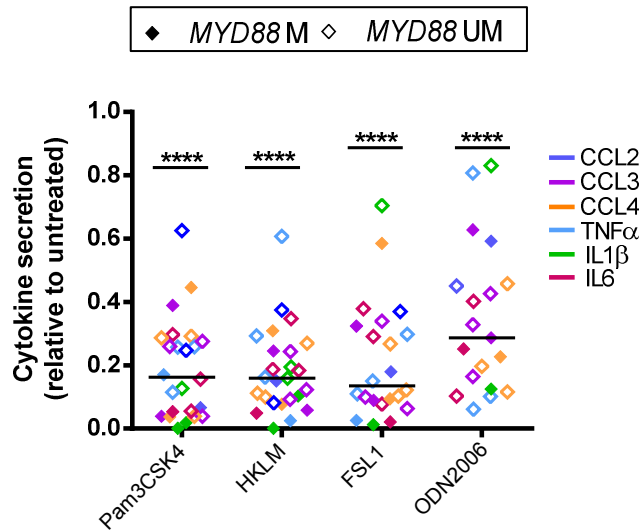
Figure S12. Inhibition of cytokine secretion by ND2158 in TLR-stimulated CLL cells *in vitro*. Cells were exposed to TLR agonists for 30 min before adding 10 µM ND2158. Cytokine levels of CCL2, CCL3, CCL4, TNFα, IL1β and IL6 in supernatants from *MYD88*-mutated (n=2) and *MYD88*-unmutated (n=3) CLL cases after 48 h of culture were analyzed. Values are depicted relative to untreated control. Wilcoxon signed-rank test was used for statistical analysis. ****$P<0.0001$.
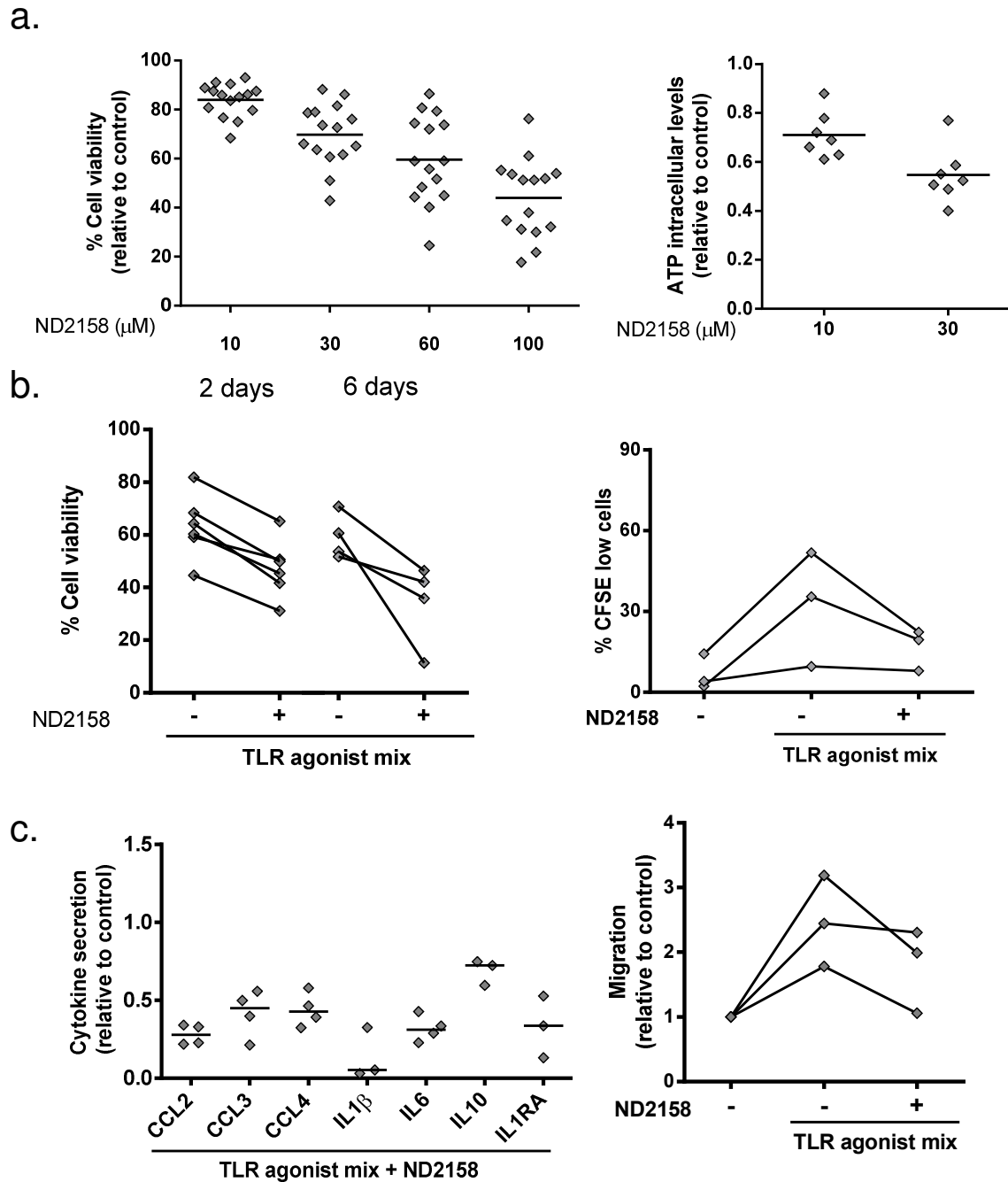
Figure S13. Impact of ND2158 on IGHV-unmutated CLL cells. a) Left panel: Viability of IGHV-unmutated CLL cells (n=15) was analyzed by flow cytometry after 48 h of incubation with the indicated concentrations of ND2158. Percentage of viable cells was measured by staining with Annexin-V and normalized to untreated control. **Right panel:** Intracellular ATP levels after 48 h of 10 µM and 30 µM ND2158 treatment relative to untreated control (n=7). **b) Left panel**: Viability of ND2158-treated CLL cells was analyzed after TLR stimulation for 2 (n=6) and 6 days (n=4). **Right panel**: Percentage of proliferating CD19$^+$ CLL cells after TLR stimulation and ND2158 treatment for 6 days measured by CFSE dilution (n=3). **c)** Cytokine levels in supernatants from 4 samples exposed to TLR agonist mix prior treatment with ND2158 for 48 h was analyzed by a flow cytometry using Luminex® Bead Panel. Values are presented relative to untreated control. **d)** Migration of TLR-stimulated CLL cells treated with ND2158 (n=3) towards CXCL12 was analyzed by transwell assays after 3 h of incubation. Values are presented as the ratio of migrating cells and total viable cells, relative to the non-stimulated, untreated control.
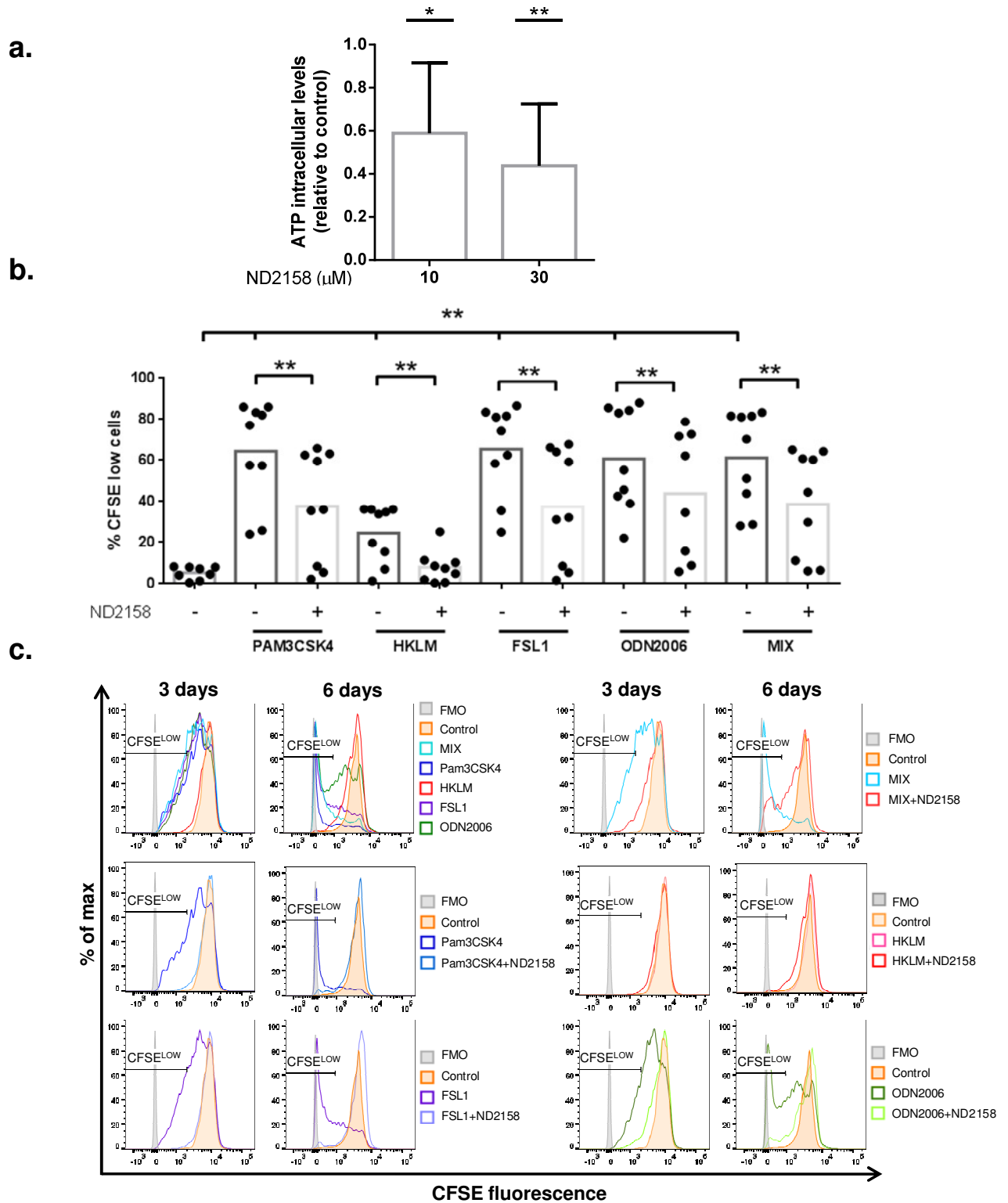
Figure S14. ND2158 blocks proliferation of leukemic B cells from TCL1 mice. a) Intracellular ATP levels of TCL1 splenocytes after 48 h of incubation with TLR agonist mix and 10 µM and 30 µM ND2158 relative to untreated controls (n=6). Results are expressed as mean ± SEM. Wilcoxon signed-rank test was used for statistical analysis. **b)** Quantification of flow cytometry data of TCL1 splenocytes showing percentages of viable CD45⁺CD19⁺CD5⁺ cells with a decrease in CFSE staining, indicative of new cell generations, after 3 days of incubation with TLR ligands or the TLR agonist mix, and treatment with 10 µM ND2158 or without treatment (n=9). **c)** CFSE histograms of one representative sample of TCL1 splenocytes treated as described above; non-stimulated cells were used as control. *$P<0.05$, **$P<0.01$. FMO, fluorescence-minus-one.
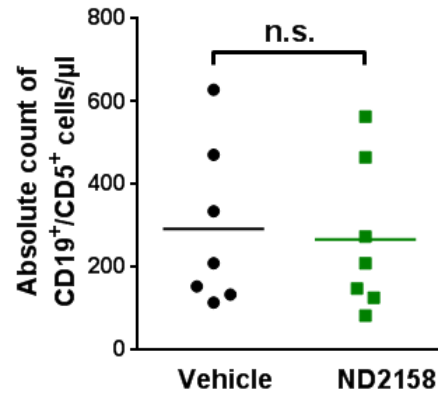
Figure S15. Assignment of mice to treatment arms based on number of leukemic cells in blood. Absolute counts of CD19+CD5+ CLL cells in the peripheral blood of TCL1 AT mice assigned to vehicle (n=7) or ND2158 (n=7) treatment groups 13 days after tumor transplantation and 1 day before treatment start. Mann-Whitney test was used for statistical analysis. n.s., not significant; $P \geq 0.05$.
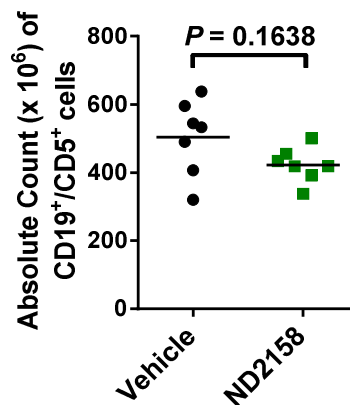
Figure S16. Absolute tumor cell count in the spleen of TCL1 adoptive transfer mice after treatment with ND2158. After 23 days of treatment, absolute count of tumor cells (CD19+CD5+) in the spleen of vehicle- (n=7) and ND2158-treated (n=7) mice was analyzed.
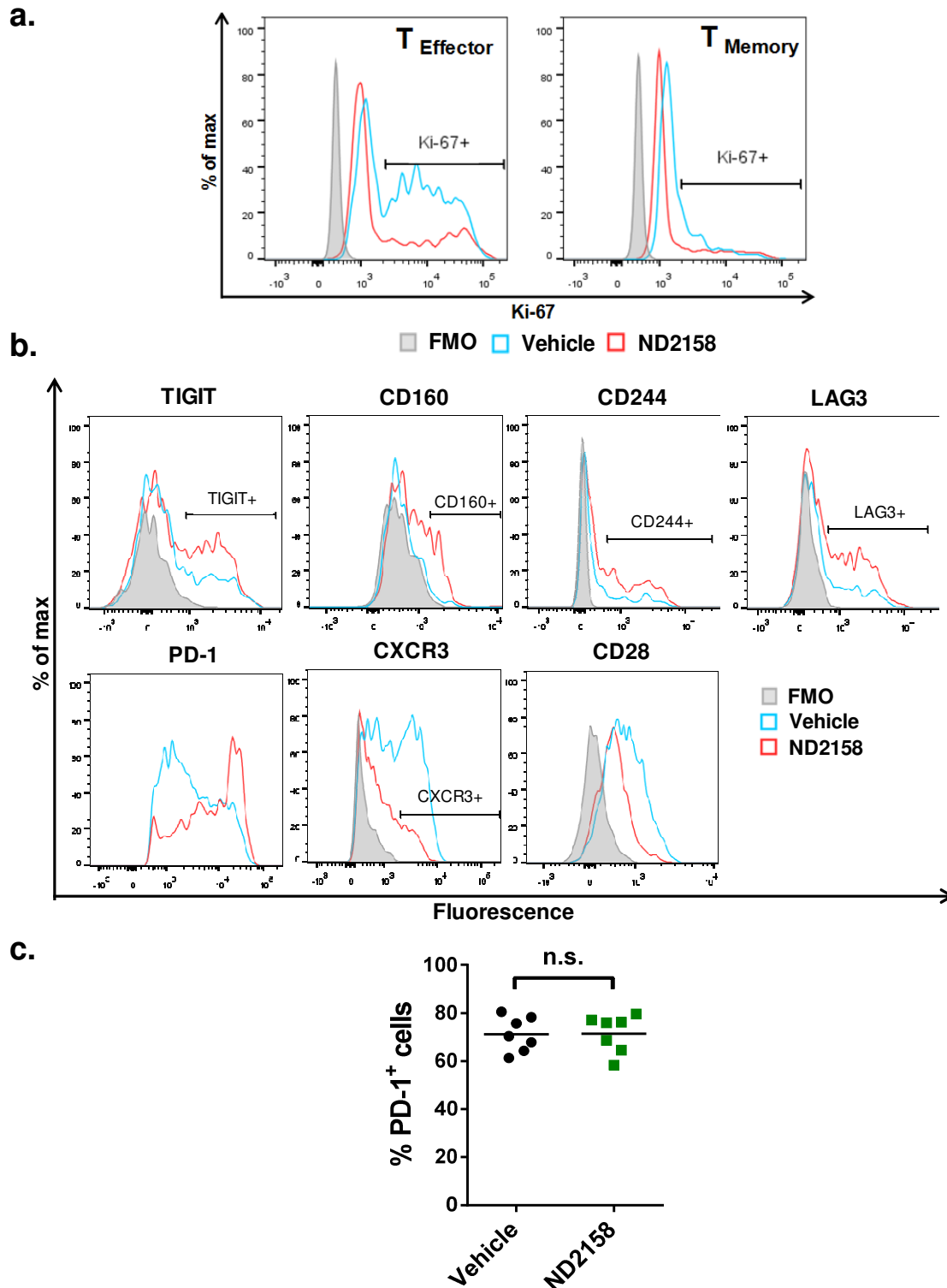
Figure S17. Effects of ND2158 treatment on CD8+ T cells in the TCL1 AT mouse model.
a) Representative flow cytometry histograms of Ki-67+ levels in CD8+ effector and CD8+ memory T cells from the spleen of vehicle- (n=7) or ND2158-treated (n=7) mice. **b)** Representative flow cytometry histograms of TIGIT, CD160, CD244, LAG3, PD-1, CXCR3 and CD28 –expression in splenic CD8+ effector T cells from ND2158 or vehicle-treated mice. **c)** Percentage of PD-1-expressing CD8+ effector T cells in the spleen of vehicle- (n=7) or ND2158-treated (n=7) mice as determined by flow cytometry. Mann-Whitney test was used for statistical analysis. n.s, not significant; $P{\geq}0.05$, $*P{<}0.05$, $**P{<}0.01$. MFI, median fluorescence intensity; FMO, fluorescence-minus-one.
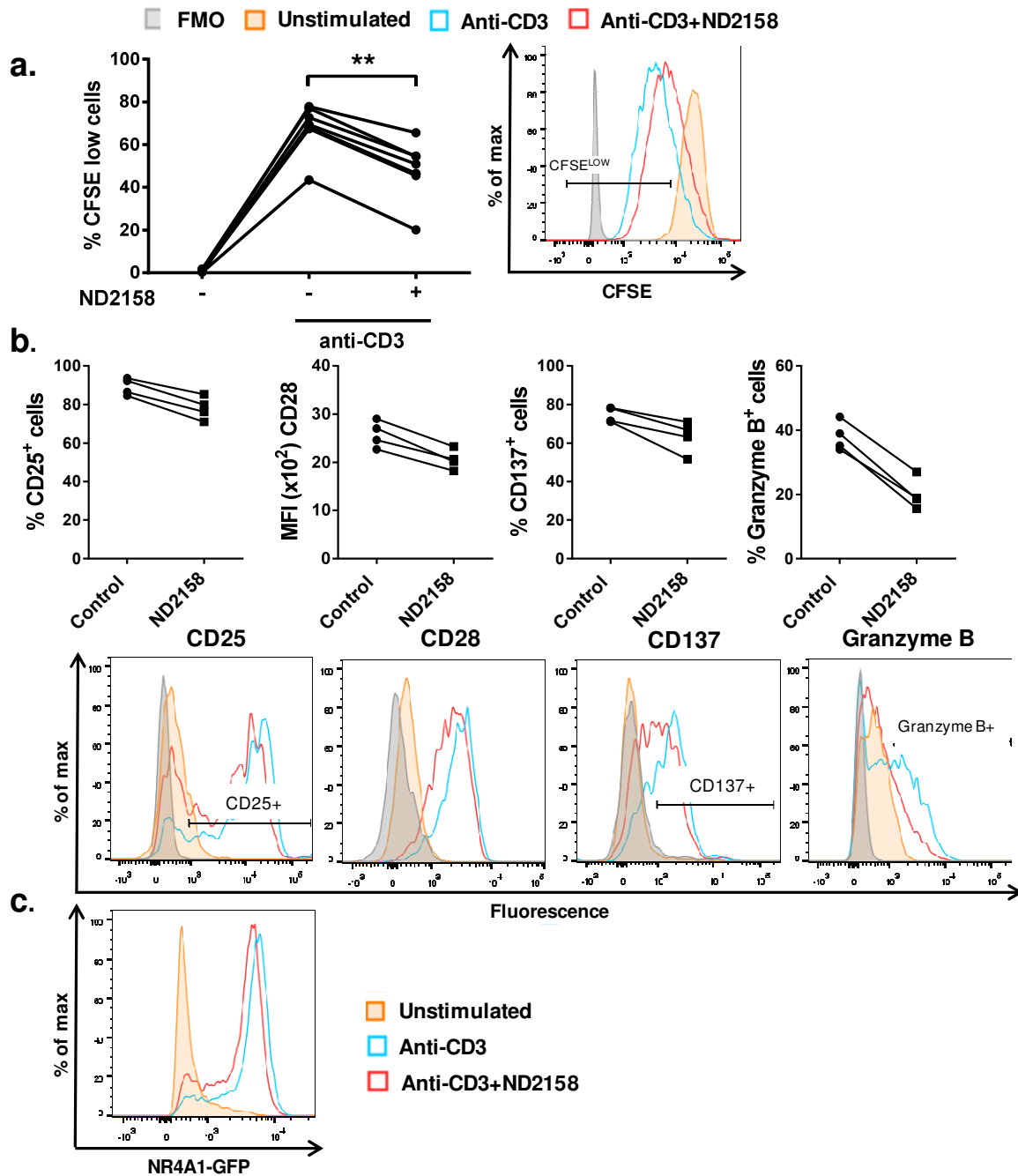
Figure S18. ND2158 impairs CD8+ T cell proliferation, activation and T cell receptor signaling *in vitro*. a) Splenocytes from WT C57BL/6 mice (n=8) were stained with CFSE and stimulated with an anti-CD3 antibody 30 min before adding 10 μM ND2158. **Left panel**: Percentage of proliferating cells as measured by CFSE dilution was analyzed in viable CD8+ T cells after 2 days. Wilcoxon matched pairs signed-rank test was used for statistical analysis. **Right panel**: a representative histogram is shown. **b)** Splenocytes from WT C57BL/6 (n=4) mice were stimulated with an anti-CD3 antibody 30 min before adding 10 μM ND2158. Protein expression was analyzed after 24 h in viable CD8+ T cells by flow cytometry. Granzyme B expression was analyzed after restimulation with PMA and ionomycin and addition of a protein transport inhibitor 4 h before harvesting the cells. Quantifications are shown in the upper row; corresponding representative histograms are shown in the bottom row. Data are shown as percentage for bimodal populations or as MFI of CD8+ T cells for unimodal populations. **c)** Representative histogram of GFP fluorescence from splenocytes of *Nr4a1*^{GFP} transgenic mice (n=4). GFP expression was analyzed by flow cytometry in viable CD8+ T cells after 3 h. **$P<0.01. MFI, median fluorescence intensity; FMO, fluorescence-minus-one.
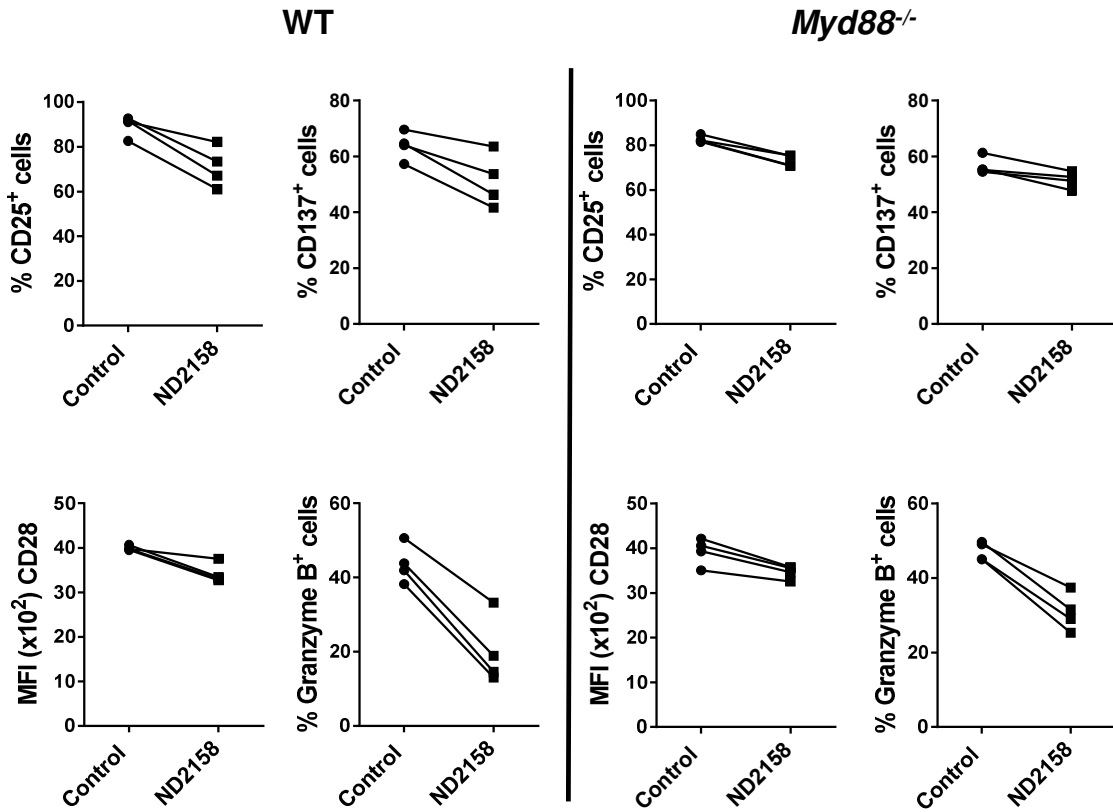
Figure S19. ND2158 impairs activation of *Myd88*-deficient CD8$^+$ T cells *in vitro*. Splenocytes from WT C57BL/6 (n=4) and *Myd88$^{-/-}$* mice (n=4) were stimulated with anti-CD3 antibody 30 min before 10 µM ND2158 was added. Protein expression of CD25, CD137, CD28 and granzyme B was analyzed after 24 h in viable, single CD8$^+$ T cells from WT (**Left panel**) or *Myd88$^{-/-}$* mice (**Right panel**) by flow cytometry. Granzyme B expression was analyzed after restimulation with PMA and ionomycin and addition of a protein transport inhibitor 4 h before harvesting the cells. Data are shown as percentage of CD25$^+$, CD137$^+$ or granzyme B$^+$ CD8$^+$ T cells for bimodal populations, or as MFI of CD28 of CD8$^+$ T cells as unimodal population. MFI, median fluorescence intensity; WT, wild-type.
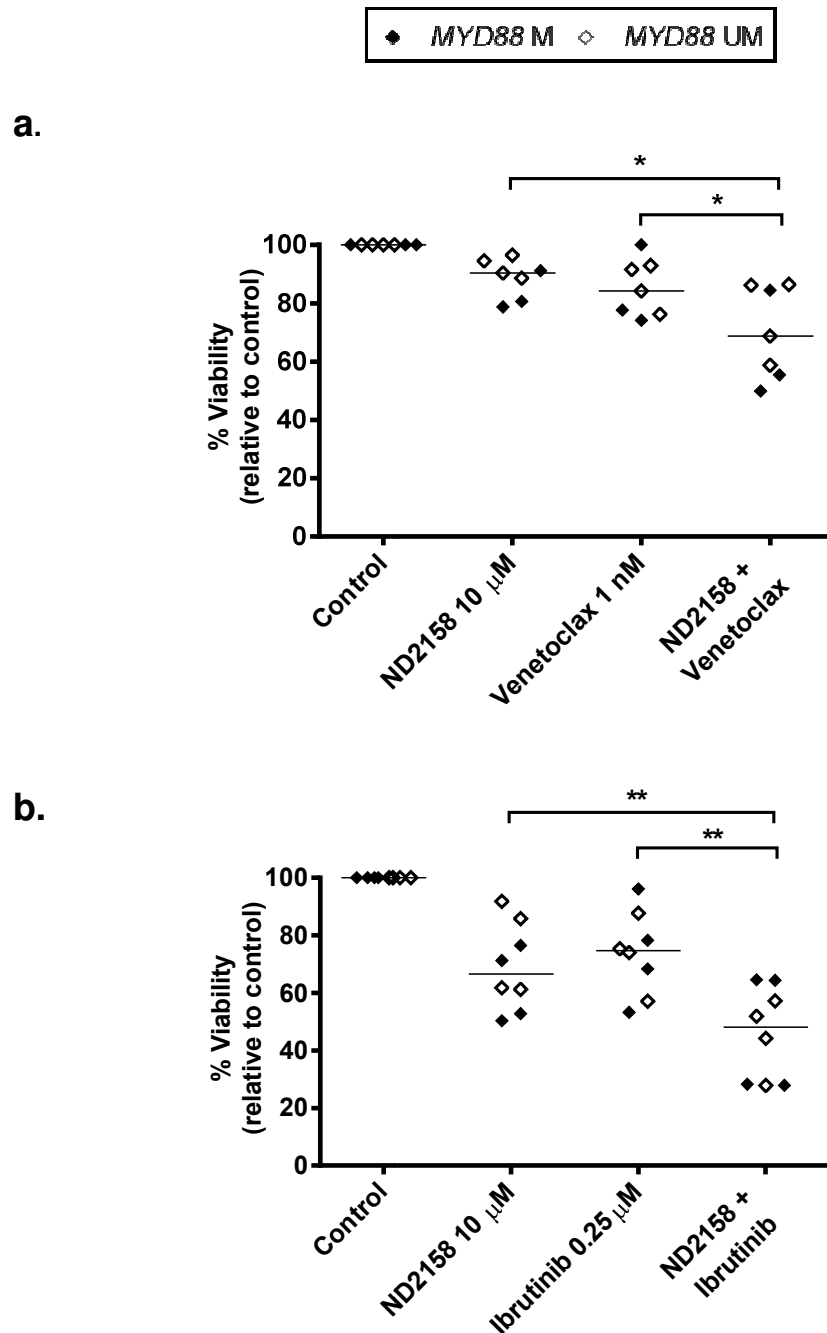
Figure S20. Combinatory effects of ND2158 and venetoclax or ibrutinib. CLL cells were stimulated *in vitro* with TLR agonist mix for 30 min, before 10 μM ND2158, 1 nM venetoclax or 0.25 μM Ibrutinib were added to the cultures as indicated. Percentage of viable cells was measured as CD19+Annexin-V- cells by flow cytometry and normalized to untreated control samples. **a)** Single treatment with ND2158 or venetoclax or their combination was measured after 48 h of incubation of CLL cells from *MYD88*-mutated (n=3) and *MYD88*-unmutated (n=4) patients (IGHV-mutated). **b)** Single treatment with ND2158 or ibrutinib or their combination was measured after 6 days of incubation of CLL cells from *MYD88*-mutated (n=4) and *MYD88*-unmutated (n=4) patients (IGHV-mutated). Wilcoxon signed-rank test was used for statistical analysis. *$P<0.05$, **$P<0.01$.

Article 2: Mutations in the RAS-BRAF-MAPK-ERK pathway define a specific subgroup of patients with adverse clinical features and provide new therapeutic options in chronic lymphocytic leukemia

Giménez N*, Martínez-Trillos A*, Montraveta A, Lopez-Guerra M, Rosich L, Nadeu F, Valero JG, Aymerich M, Magnano L, Rozman M, Matutes E, Delgado J, Baumann T, Gine E, González M, Alcoceba M, Terol MJ, Navarro B, Colado E, Payer AR, Puente XS, López-Otín C, Lopez-Guillermo A, Campo E, Colomer D[+], Villamor N[+]

ABSTRACT

Mutations in genes of the RAS-BRAF-MAPK-ERK pathway have not been fully explored in patients with chronic lymphocytic leukemia. We, therefore, analyzed the clinical and biological characteristics of chronic lymphocytic leukemia patients with mutations in this pathway and investigated the in vitro response of primary cells to BRAF and ERK inhibitors. Putative damaging mutations were found in 25 of 452 patients (5.5%). Among these, BRAF was mutated in nine patients (2.0%), genes upstream of BRAF (KITLG, KIT, PTPN11, GNB1, KRAS and NRAS) were mutated in 12 patients (2.6%), and genes downstream of BRAF (MAPK2K1, MAPK2K2, and MAPK1) were mutated in five patients (1.1%). The most frequent mutations were missense, subclonal and mutually exclusive. Patients with these mutations more frequently had increased lactate dehydrogenase levels, high expression of ZAP-70, CD49d, CD38, trisomy 12 and unmutated immunoglobulin heavy-chain variable region genes and had a worse 5-year time to first treatment (hazard ratio 1.8, P=0.025). Gene expression analysis showed upregulation of genes of the MAPK pathway in the group carrying RAS-BRAF-MAPK-ERK pathway mutations. The BRAF inhibitors vemurafenib and dabrafenib were not able to inhibit phosphorylation of ERK, the downstream effector of the pathway, in primary cells. In contrast, ulixertinib, a pan-ERK inhibitor, decreased phospho-ERK levels. In conclusion, although larger series of patients are needed to corroborate these findings, our results suggest that the RAS-BRAF-MAPK-ERK pathway is one of the core cellular processes affected by novel mutations in chronic lymphocytic leukemia, is associated with adverse clinical features and could be pharmacologically inhibited.

*Equally contribution

[+]Share senior authorship

ARTICLE

Ferrata Storti Foundation

Mutations in the RAS-BRAF-MAPK-ERK pathway define a specific subgroup of patients with adverse clinical features and provide new therapeutic options in chronic lymphocytic leukemia

Neus Giménez,[1,2]* Alejandra Martínez-Trillos,[1,3]* Arnau Montraveta,[1] Mónica Lopez-Guerra,[1,4] Laia Rosich,[1] Ferran Nadeu,[1] Juan G. Valero,[1] Marta Aymerich,[1,4] Laura Magnano,[1,4] Maria Rozman,[1,4] Estella Matutes,[4] Julio Delgado,[1,3] Tycho Baumann,[1,3] Eva Gine,[1,3] Marcos González,[5] Miguel Alcoceba,[5] M. José Terol,[6] Blanca Navarro,[6] Enrique Colado,[7] Angel R. Payer,[7] Xose S. Puente,[8] Carlos López-Otín,[8] Armando Lopez-Guillermo,[1,3] Elias Campo,[1,4] Dolors Colomer[1,4]** and Neus Villamor[1,4]**

[1]Institut d'Investigacions Biomèdiques August Pi i Sunyer (IDIBAPS), CIBERONC, Barcelona; [2]Anaxomics Biotech, Barcelona; [3]Hematology Department and [4]Hematopathology Unit, Hospital Clinic, Barcelona; [5]Hematology Department, University Hospital- IBSAL, and Institute of Molecular and Cellular Biology of Cancer, University of Salamanca, CIBERONC; [6]Hematology Department, Hospital Clínico Universitario, Valencia: [7]Hematology Department, Hospital Universitario Central de Asturias, Oviedo, and [8]Departamento de Bioquímica y Biología Molecular, Instituto Universitario de Oncología, Universidad de Oviedo, CIBERONC, Spain.

*NG and AM-T contributed equally to the study.

**DC and NV share senior authorship of the manuscript.

Correspondence:

DOLORS COLOMER
dcolomer@clinic.cat

ABSTRACT

Mutations in genes of the RAS-BRAF-MAPK-ERK pathway have not been fully explored in patients with chronic lymphocytic leukemia. We, therefore, analyzed the clinical and biological characteristics of chronic lymphocytic leukemia patients with mutations in this pathway and investigated the *in vitro* response of primary cells to BRAF and ERK inhibitors. Putative damaging mutations were found in 25 of 452 patients (5.5%). Among these, *BRAF* was mutated in nine patients (2.0%), genes upstream of *BRAF* (*KITLG, KIT, PTPN11, GNB1, KRAS* and *NRAS*) were mutated in 12 patients (2.6%), and genes downstream of *BRAF* (*MAPK2K1, MAPK2K2,* and *MAPK1*) were mutated in five patients (1.1%). The most frequent mutations were missense, subclonal and mutually exclusive. Patients with these mutations more frequently had increased lactate dehydrogenase levels, high expression of ZAP-70, CD49d, CD38, trisomy 12 and unmutated immunoglobulin heavy-chain variable region genes and had a worse 5-year time to first treatment (hazard ratio 1.8, *P*=0.025). Gene expression analysis showed upregulation of genes of the MAPK pathway in the group carrying RAS-BRAF-MAPK-ERK pathway mutations. The BRAF inhibitors vemurafenib and dabrafenib were not able to inhibit phosphorylation of ERK, the downstream effector of the pathway, in primary cells. In contrast, ulixertinib, a pan-ERK inhibitor, decreased phospho-ERK levels. In conclusion, although larger series of patients are needed to corroborate these findings, our results suggest that the RAS-BRAF-MAPK-ERK pathway is one of the core cellular processes affected by novel mutations in chronic lymphocytic leukemia, is associated with adverse clinical features and could be pharmacologically inhibited.

109

Introduction

The clinical course of patients with chronic lymphocytic leukemia (CLL) is highly heterogeneous.[1,2] The mutational status of the immunoglobulin heavy-chain variable-region genes (IGHV) and deletions/mutations of 11q/*ATM/BIRC3* and 17p/*TP53* are important determinants of the clinical outcome of patients with CLL.[3-6] Whole genome sequencing and whole exome sequencing have identified recurrent acquired mutations in the coding and non-coding regions of several genes. A few of them are mutated with moderate/low frequencies (11-15%), whereas the majority are mutated at much lower frequencies (2-5%).[7-10] This mutational landscape highlights the patients' heterogeneity. Several of the mutations, including some with a low incidence, have been reported to be associated with particular clinical features and disease evolution.[9,11-13]

BRAF is a member of the serine-threonine kinase RAF family, comprising RAF-1/CRAF, ARAF, and BRAF. In normal cells, BRAF functions as a mitotic signal transporter in the RAS/RAF/mitogen-extracellular signal-regulated kinase 1/2 (MEK1/2)/ extracellular signal-regulated kinase 1/2 (ERK1/2)/mitogen activated protein kinase (MAPK) pathway. This pathway plays a pivotal role in regulating embryogenesis, cell proliferation, differentiation, migration, and survival.[14] In the last decade, a high frequency of *BRAF* point mutations has been identified in melanoma and other human cancers.[15,16] *BRAF* mutations are also a characteristic of hairy cell leukemia (HCL), being detected in 95% to 100% of patients with this type of leukemia.[17,18] The most common *BRAF* mutation leads to the substitution of a valine for glutamic acid at amino acid 600 (V600E) in the kinase domain of the protein. This substitution mimics the phosphorylation of the activation loop, thereby leading to its constitutive activation and phosphorylation of MEK1 and MEK2, which in turn phosphorylate and activate the effector kinases ERK1 and ERK2.[19] ERK proteins target numerous substrates, such as protein kinases, transcription factors, and cytoskeletal or nuclear proteins. Moreover, they are able to affect protein functions either by phosphorylating proteins in the cytoplasm or by translocating them into the nucleus where they activate transcription factors that regulate proliferation- and cell survival-associated genes.[20]

BRAF mutations have been recurrently reported in CLL patients with a frequency of approximately 3%;[21-24] most of these mutations cluster within or near the activation loop. Recently, novel CLL drivers (*NRAS, KRAS, NRAS* and *MAP2K1*) of the RAS-BRAF-MAPK-ERK pathway have also been described.[9-24] However, the impact of *BRAF* mutations and other mutations in the RAS-BRAF-MAPK-ERK pathway in CLL is not well established.

We analyzed the clinical and biological characteristics and the impact of mutations in genes of the RAS-BRAF-MAPK-ERK pathway in CLL patients, the functional implications of these mutations and the *in vitro* response to different MAPK inhibitors.

Methods

Patients

Four hundred fifty-two patients (276 males/176 females) diagnosed with CLL according to the World Health Organization criteria[25] and included in the International Cancer Genome Consortium for CLL (ICGC-CLL)[7] were analyzed. All patients gave informed consent to inclusion in this study, according to the guidelines of the ICGC-CLL project and the local ethics committees. The study was conducted in accordance with the Declaration of Helsinki.

Primary chronic lymphocytic leukemia cells

CLL cells were isolated, cryopreserved and stored in the Hematopathology collection registered at the Biobank (Hospital Clínic-IDIBAPS; R121004-094) (*Online Supplementary Methods*). Functional studies were done in all patients with mutations in genes of the RAS-BRAF-MAPK-ERK pathway for whom cryopreserved material was available.

Mutational analysis

Whole exome sequencing or whole genome sequencing was performed in 452 CLL patients. DNA from purified CLL cells (>95% tumor cells) was obtained before administration of any treatment, as described elsewhere.[7] The median interval between diagnosis and sample analysis was 36 months (range, 0-300 months). Mutations in genes of the RAS-BRAF-MAPK-ERK pathway according to the Kyoto Encyclopedia of Genes and Genomes (KEGG) database (*KITLG, KIT, SOS2, PTPN11, GNB1, KRAS, NRAS, BRAF, MAP2K1, MAP2K2* and *MAPK1*) were selected for further analysis. Clonal mutations were considered when the variant allele frequency (VAF) was ≥0.40 and subclonal when the VAF was <0.40. PolyPhen-2, SIFT and CADD algorithms were used for *in silico* prediction of the pathogenicity of the mutations. Coding mutations were considered pathogenic if they were reported as such by at least two algorithms (probably damaging by PolyPhen-2 and/or damaging by SIFT and/or with a phred-like score >20 by CADD).

Gene expression analysis

The gene expression profile of 143 purified CLL samples with unmutated IGHV genes (U-IGHV) from the CLL-ICGC project[7] was analyzed using the Gene Set Enrichment Analysis (GSEA) package version 2.0. Enrichment of the MAPK gene signature was investigated using the C2 Biocarta and C2 KEGG collection version 6.1 as reported in the *Online Supplementary Methods*. Gene sets with a P≤0.05, a false discovery rate (FDR) q-value ≤10% and a normalized enrichment score (NES) ≥1.5 were considered to be significantly enriched in the group with mutations in the RAS-BRAF-MAPK-ERK pathway.

Western blot analysis

Whole-cell protein extracts were obtained from CLL cells and peripheral blood mononuclear cells from healthy donors and western blot was performed with antibodies against phosphorylated-T202/Y204 ERK 1/2 and total ERK (Santa Cruz Biotechnology, Santa Cruz, CA, USA) (*Online Supplementary Methods*).

Analysis of viability

Vemurafenib, dabrafenib, and ulixertinib (BVD-523) were purchased from Selleckchem (Houston, TX, USA). Primary CLL cells were incubated for 24 or 48 h with the indicated doses of the drugs and then stained and analyzed as reported in the *Online Supplementary Methods*.

B-cell receptor stimulation and quantification of phosphorylated ERK by flow cytometry

B-cell receptors were stimulated by incubating CLL cells with 10 µg/mL of anti-IgM (Southern Biotech, Birmingham, AL, USA) and cells were stained for phospho (T202 and Y204)-ERK1/2-phyco-

N. Giménez *et al.*

erythrin (Becton Dickinson, Franklin Lakes, NJ, USA) (*Online Supplementary Methods*).

Statistical analysis

A Fisher test or non-parametric tests were used to correlate clinical and biological variables according to the presence of mutations in the RAS-BRAF-MAPK-ERK pathway. Time to first treatment (TTFT) was calculated from the date of sampling to the first treatment or last follow-up. Overall survival was calculated from the date of sampling to the date of death or last follow-up. All the analyses were conducted using SPSS 20 (www.ibm.com) software and are detailed in the *Online Supplementary Methods*. For primary cell cultures data are presented as the mean ± standard error of the mean. Comparisons between groups were evaluated with a Wilcoxon paired test using GraphPad Prism 4.0 software. Results were considered statistically significant when the *P*-value was ≤0.05.

Results

Clinical and biological impact of mutations in the RAS-BRAF-MAPK-ERK pathway

Four hundred fifty-two patients (276 males/176 females) with CLL were analyzed for the clinical and biological impact of mutations in genes of the RAS-BRAF-MAPK-ERK pathway (see *Online Supplementary Table S1* for the main characteristics of the series).

A total of 31 mutations affecting genes of the RAS-BRAF-MAPK-ERK pathway were observed in 30 of the 452 CLL patients (7%) (*Online Supplementary Figure S1* and Table 1). Mutations were missense (25/31; 81%) or non-coding mutations at the 3' or splice donor regions (6/31; 19%). The mean VAF for the 31 individual mutations was 0.36 ± 0.13. According to the results of the PolyPhen-2, SIFT and CADD algorithms used to predict the patho-

Table 1. Description of the mutations in genes of the RAS-BRAF-MAPK-ERK pathway in patients with chronic lymphocytic leukemia.

Case	Patient	Gene name	HGVS.p	Annotation	PolyPhen-2 prediction[a]	SIFT prediction[b]	CADD phred-like score[c]	VAF	IGHV	TP53	BIRC3	ATM
1	723	KITLG	n.a.	3' UTR	n.a.	n.a.	4.25	0.39	UM	UM	M	M
2	33	KIT	p.Val833Leu	missense	Probably damaging	Damaging	22.70	0.24	M	UM	UM	UM
3	1078	KIT	n.a.	3' UTR	n.a.	n.a.	5.91	0.55	UM	UM	UM	UM
4	850	SOS2	p.Pro7Ser	missense	Benign	Tolerated	10.21	0.50	M	UM	UM	UM
5	191	PTPN11	p.Ala72Val	missense	Probably damaging	Damaging	32.00	0.58	M	UM	UM	UM
6	677	PTPN11	p.Glu76Lys	missense	Probably damaging	Damaging	33.00	0.54	UM	M	UM	UM
7	1192	PTPN11	p.Asp61Val	missense	Probably damaging	Damaging	28.20	0.17	UM	UM	UM	UM
8	1226	PTPN11	p.Asp61Val	missense	Probably damaging	Damaging	28.20	0.50	UM	UM	UM	UM
9*	155	PTPN11	p.Ser502Pro	missense	Possibily damaging	Damaging	31.00	0.15	UM	UM	UM	UM
10	15	GNB1	p.Ile80Thr	missense	Probably damaging	Damaging	28.10	0.42	UM	UM	UM	UM
11	1564	GNB1	n.a.	3' UTR	n.a.	n.a.	1.21	0.31	UM	UM	UM	UM
12	398	KRAS	p.Gly12Val	missense	Probably damaging	Damaging	29.90	0.18	UM	UM	UM	UM
13	598	KRAS	p.Gln61His	missense	Benign	Damaging	23.50	0.42	UM	UM	UM	UM
9*	155	KRAS	p.Gly12Asp	missense	Possibily damaging	Damaging	25.30	0.30	UM	UM	UM	UM
14	1371	NRAS	p.Gln61Arg	missense	Benign	Damaging	23.10	0.22	UM	UM	UM	UM
15	27	BRAF	p.Glu501Lys	missense	Probably damaging	Damaging	34.00	0.15	UM	UM	UM	UM
16	100	BRAF	p.Lys601Glu	missense	Possibily damaging	Damaging	24.50	0.20	UM	UM	UM	UM
17	134	BRAF	p.Gly469Ala	missense	Probably damaging	Damaging	27.50	0.54	UM	UM	UM	UM
18	148	BRAF	p.Lys601Asn	missense	Possibily damaging	Damaging	24.30	0.38	UM	UM	UM	UM
19	279	BRAF	p.Asp594Gly	missense	Probably damaging	Damaging	29.70	0.49	UM	M	UM	UM
20	721	BRAF	p.Asn581Ser	missense	Probably damaging	Damaging	19.38	0.48	UM	UM	UM	UM
21	824	BRAF	p.Leu597Gln	missense	Probably damaging	Damaging	28.80	0.25	UM	UM	UM	UM
22	1079	BRAF	p.Val600Glu	missense	Probably damaging	Damaging	32.00	0.33	UM	UM	UM	UM
23	1431	BRAF	p.Gly534Arg	missense	Possibily damaging	Damaging	34.00	0.46	UM	UM	UM	UM
24	44	MAP2K1	p.Phe53Cys	missense	Probably damaging	Damaging	29.10	0.19	UM	UM	UM	UM
25	1365	MAP2K1	p.Gly128Asp	missense	Probably damaging	Damaging	32.00	0.29	UM	UM	UM	M
26	884	MAP2K2	n.a.	splice donor	n.a.	n.a.	23.30	0.39	M	UM	UM	UM
27	761	MAP2K2	p.Gln60Pro	missense	Probably damaging	Damaging	24.70	0.26	UM	UM	M	M
28	1477	MAP2K2	n.a.	3' UTR	n.a.	n.a.	11.64	0.43	M	UM	UM	UM
29	1568	MAP2K2	p.Tyr134Cys	missense	Probably damaging	Damaging	27.00	0.33	UM	M	UM	UM
30	442	MAPK1	n.a.	3' UTR	n.a.	n.a.	12.71	0.43	UM	UM	UM	UM

*CLL case with two mutations in genes of the RAS-BRAF-MAPK-ERK pathway; [a]Adzhubei I, Jordan DM, Sunyaev SR. Predicting functional effect of human missense mutations using PolyPhen-2. Curr Protoc Hum Genet. 2013; Chapter 7: Unit 7.20. [b]Ng PC, Henikoff S. SIFT: Predicting amino acid changes that affect protein function. Nucleic Acids Res. 2003 Jul 1;31(13):3812-4. cKircher M, Witten DM, Jain P, O'Roak BJ, Cooper GM, Shendure J. A general framework for estimating the relative pathogenicity of human genetic variants. Nat Genet. 2014;46(3):310-5. HGVS.p: Human Genome Variation Society protein sequence; PolyPhen-2: Polymorphism Phenotyping v2; SIFT: Sorting Intolerant From Tolerant; CADD: Combined Annotation-Dependent Depletion; VAF: variant allele frequency; IGVH: immunoglobulin variant heavy chain genes; 3'UTR: 3' untranslated region; n.a. not applicable; M: mutated, UM: unmutated.

111

genicity of the mutations, five mutations in the 3' untranslated region (cases 1, 3, 11, 28 and 30) and one missense mutation (case 4, *SOS2* gene) were discarded as not being pathogenic. We were able to demonstrate that the mutation in the 3' untranslated region of *KITLG* (case 1) was functional as we detected high levels of phosphorylated ERK, a surrogate marker of RAS-BRAF-MAPK-ERK pathway activation (Figure 3A). Due to the absence of cryopreserved material, we could not analyze the functionality of these mutations in the remaining cases. Therefore, considering only the putative functional mutations, a total of 26 functional mutations affecting genes of the RAS-BRAF-MAPK-ERK pathway were observed in 25 of 452 CLL patients (5.5%). In 11 of the 25 patients (44%) these mutations were clonal (VAF ≥0.40) and in the other 14 patients (56%) they were subclonal (VAF <0.40). Mutations were detected in genes upstream of *BRAF* (*KITLG*, *KIT*, *PTPN11*, *GNB1*, *KRAS* and *NRAS*) in 12/452 patients (2.6%), in *BRAF* in 9/452 patients (2.0%), and in genes downstream of *BRAF* (*MAP2K1* alias *MEK1*, *MAP2K2* alias *MEK2*) in 5/452 patients (1.1%). The most frequent single mutated gene was *BRAF* (n=9/26, 34.6%) followed by *PTPN11* (n=5/26, 19.2%), *MAP2K2* (n=3/26, 11.5%), *KRAS* (n=3/26, 11.5%), and *MAP2K1*, (2/26 cases, 7.7%); mutations of *GNB1*, *NRAS*, *KIT*, and *KITLG* were each found in one patient. One patient had concomitant mutations of *PTPN11* and *KRAS*. Interestingly, *BRAF* mutations were localized between exons 11 to 15 and most of them occurred in the activation loop (A-loop) near the V600 position or near the phosphate-binding loop (P-loop) at residues 464-469. Only in one case did the *BRAF* mutation correspond to V600E, the most common mutation described in a variety of human malignancies including HCL.[17]

Association of mutations in the RAS-BRAF-MAPK-ERK pathway with clinical and biological features

The main clinical and biological characteristics of the 25 patients with functional mutations in the RAS-BRAF-MAPK-ERK pathway are listed in Table 2.

The age, sex and clinical stage of the patients with mutations in the RAS-BRAF-MAPK-ERK pathway were similar to those of the patients without mutations. However, patients with mutations in RAS-BRAF-MAPK-ERK pathway genes more frequently had abnormal values of lactate dehydrogenase, high expression of ZAP-70, CD38 and CD49d, trisomy 12 and most of them had U-IGHV (21/24, 87%) (*P*≤0.05 in all comparisons) (Table 2). Patients with mutations in the RAS-BRAF-MAPK-ERK pathway more frequently had three or more driver mutations than patients without mutations in the pathway, but no differences were observed in the genes most frequently mutated in CLL (*NOTCH1*, *SF3B1*, *BIRC3*, *TP53* or *ATM*) (Table 2). Six cases contemporaneously carried mutations in *TP53*, *ATM* or *BIRC3*. As most patients with mutations in the RAS-BRAF-MAPK-ERK pathway had U-IGHV, we conducted a similar analysis including only the subgroup of U-IGHV patients. As seen in Table 3, only lactate dehydrogenase and trisomy 12 maintained statistical significance. Figure 1 shows a brick-plot of concomitant gene mutations/cytogenetic aberrations for cases with RAS-BRAF-MAPK-ERK pathway mutations.

Patients with mutations in the RAS-BRAF-MAPK-ERK pathway required treatment more frequently, considering both the whole group (88% *versus* 43%; *P*<0.001) and

within the U-IGHV subgroup (95% *versus* 75%; *P*<0.048). There were no differences in the type of treatment received or the response achieved according to the presence or absence of mutations in the pathway (Table 2). Five-year TTFT of patients with Binet A or B disease was 82% [95% confidence interval (95% CI): 66-98%] in patients with mutations in the RAS-BRAF-MAPK-ERK pathway *versus* 50% (95% CI: 42-58%) in the unmutated group; *P*<0.001]. The comparison between clonal and subclonal mutated cases showed that the 5-year TTFT was

Table 2. Main clinical and biological characteristics of patients according to mutations in the RAS-BRAF-MAPK-ERK pathway.

Parameter	Category	Unmutated (n=427)	Mutated (n=25)	P-value
Gender	Male (%)	257 (60%)	19 (76%)	ns
Age (years), median (range)		61 (18-93)	61 (44-84)	ns
Binet stage	A	366 (87%)	21 (88%)	ns
	B	47 (11%)	1 (4%)	
	C	8 (2%)	2 (8%)	
Rai stage	0	278 (66%)	13 (54%)	ns
	I-II	130 (31%)	9 (38%)	
	III-IV	12 (3%)	2 (8%)	
Lymphocytes count (x10⁹/L), median (range)		11 (1-203)	11 (1-75)	ns
Absolute CLL cell count (x10⁹/L), median (range)		8 (0.4-192)	6 (0.7-83)	ns
Hemoglobin (g/L), median (range)		141 (45-177)	147 (125-159)	ns
Platelets (x10⁹/L), median (range)		204 (49-791)	170 (99-315)	ns
B₂ microglobulin	UNV*	119/373 (32%)	7/18 (39%)	ns
Lactate dehydrogenase	UNV*	26/407 (6%)	6/19 (32%)	0.002
IGHV	Unmutated	145/421 (34%)	21/24 (87%)	<0.001
CD49d	>30%	92/290 (32%)	9/13 (69%)	0.012
CD38	>30%	96/403 (24%)	10/23 (43%)	0.046
ZAP-70	≥20%	98/394 (25%)	14/21 (67%)	<0.001
Genetics	del(13q)(q14.3)	148/308 (48%)	3/13 (23%)	ns
	Trisomy 12	48/308 (16%)	6/13 (46%)	0.011
	del(11q)(q22.3)	26/307 (8%)	0/13 (0%)	ns
	del(17p)(p13.1)	11/308 (4%)	1/13 (8%)	ns
Driver mutations	≥3	159/427 (37%)	17/25 (68%)	0.003
NOTCH1	Mutated	52/427 (12%)	5/25 (20%)	ns
SF3B1	Mutated	38/427 (9%)	1/25 (4%)	ns
TP53	Disrupted	21/397 (5%)	2/23 (9%)	ns
BIRC3	Disrupted	38/427 (9%)	2/25 (8%)	ns
ATM	Disrupted	47/427 (11%)	3/25 (12%)	ns
Treated		184/427 (43%)	22/25 (88%)	<0.001
Response to treatment*	CR	102 (55%)	12 (57%)	ns
	PR	48 (26%)	4 (19%)	
	Failure	13 (7%)	3 (14%)	
5-year TTFT (95% CI)*	A&B	50% (42-58)	82% (66-98)	<0.001
5-year OS (95% CI)	All	80% (74-86)	78% (60-96)	ns
5-year t-DLBCL	All	2% (1-3)	11% (0-25)	0.080

*It was not possible to assess the response to treatment in 21/184 (11%) of the unmutated patients and in 2/21 (9%) of the mutated patients. CLL: chronic lymphocytic leukemia; UNV: above normal value; CR: complete response, PR: partial response; TTFT: time to first treatment; OS: overall survival; 95% CI: 95% confidence interval; t-DLBCL: transformation into diffuse large B-cell lymphoma (Richter syndrome); ns: not significant.

112

N. Giménez *et al.*

92% (95 CI: 76-100%) for patients with subclonal mutations, 70% (95 CI: 42-98%) for patients with clonal mutations, and 51% (95% CI: 42-60%; $P \leq 0.001$) for those without mutations. The adverse effect of mutations in genes of the RAS-BRAF-MAPK-ERK pathway was observed independently of the mutated gene (*Online Supplementary Figure S2*). Overall, patients with mutations in the RAS-BRAF-MAPK-ERK pathway had a worse TTFT than that of patients without mutations ($P<0.001$) (Figure 2A). However, when other adverse mutations (*TP53, ATM* or *BIRC3*)[26,27] were taken into account, patients with mutations in both the RAS-BRAF-MAPK-ERK pathway and in *TP53, ATM* or *BIRC3* (n=6, 1%) had the shortest 5-year TTFT (100%) followed by patients with mutations in *TP53, ATM* or *BIRC3* [n=64,15%; 5-year TTFT of 83% (CI 95%: 71-95%)], patients with mutations only in the RAS-BRAF-MAPK-ERK pathway [n=16, 4%; 5-year TTFT of 75% (CI 95%: 54-96%)], and patients without mutations [n=337, 79%; 5-year TTFT of 44% (CI 95%: 34-54%)]

($P \leq 0.001$) (Figure 2B). In the subgroup of patients with Binet A or B CLL with U-IGHV, those patients with adverse gene mutations concomitantly with mutations in RAS-BRAF-MAPK-ERK pathway genes (n=6, 4%) again had a worse 5-year TTFT (all treated) than patients with only mutations in *TP53, ATM* or *BIRC3* (n=45, 30%; 5-year TTFT: 87%, CI 95%: 77-97%), patients with only mutations in RAS-BRAF-MAPK-ERK pathway genes (n=13, 8%; 5-year TTFT: 85%, CI 95%: 65-100%), and patients without mutations in these genes (n=88, 56%; 5-year TTFT: 71%, CI: 95%: 60-82%) ($P=0.001$) (Figure 2C). A multivariate analysis including IGHV status, mutations in RAS-BRAF-MAPK-ERK pathway genes, and mutations in *TP53, ATM* or *BIRC3* in a final model with 418 patients showed an independent impact on TTFT for IGHV status [hazard risk (HR) 3.4 (95% CI: 2.5-4.8), $P<0.001$], mutations in the RAS-BRAF-MAPK-ERK pathway [HR 1.8 (95% CI: 1.1- 3), $P=0.016$] and adverse mutations [HR 2.0 (95% CI: 1.5-2.8), $P<0.001$].

Table 3. Main clinical and biological characteristics of patients according to the presence or absence of mutations in genes of the RAS-BRAF-MAPK-ERK pathway in the subgroup with unmutated IGHV chronic lymphocytic leukemia.

Parameter	Category	Unmutated (n=145)	Mutated (n=21)	P-value
Gender	Male (%)	94 (65%)	16 (76%)	ns
Age (years), median (range)		61 (18-93)	61 (44-78)	ns
Binet stage	A	105/142 (74%)	18/20 (90%)	ns
	B	32/142 (22%)	1/20 (5%)	
	C	5/142 (4%)	1/20 (5%)	
Rai stage	0	67/141 (47%)	11/20 (55%)	ns
	I-II	66/141 (47%)	8/20 (40%)	
	III-IV	8/141 (6%)	1/20 (5%)	
Lymphocytes count (x10⁹/L), median (range)		10.7 (1-106)	12 (1-26)	ns
Absolute CLL cells count (x10⁹/L), median (range)		8 (0.8-114)	7 (0.7-83)	ns
Hemoglobin (g/L), median (range)		140 (45-166)	149 (125-159)	ns
Platelets (x10⁹/L), median (range)		210 (49-470)	163 (99-315)	ns
B$_2$ microglobulin	UNV	57/128 (45%)	7/15 (47%)	ns
Lactate dehydrogenase	UNV	15/137 (11%)	6/16 (37%)	0.011
CD49d	>30%	42/89 (47%)	8/11 (73%)	ns
CD38	>30%	61/136 (45%)	10/19 (53%)	ns
ZAP-70	≥20%	77/1131 (59%)	13/18 (72%)	ns
Genetics	del(13q)(q14.3)	38/102 (37%)	1/10 (10%)	ns
	Trisomy 12	22/102 (22%)	6/10 (60%)	0.015
	del(11q)(q22.3)	21/102 (20%)	0/10 (9%)	ns
	del(17p)(p13.1)	5/102 (5%)	1/10 (10%)	ns
Driver mutations	≥3	96/145 (66%)	14/21 (67%)	ns
NOTCH1	Mutated	43/145 (30%)	5/21 (24%)	ns
SF3B1	Mutated	21/145 (15%)	1/21 (5%)	ns
TP53	Disrupted	9/134 (7%)	2/20 (10%)	ns
BIRC3	Disrupted	30/145 (21%)	2/21 (12%)	ns
ATM	Disrupted	38/145 (26%)	3/21 (14%)	ns
Treated		108/145 (75%)	20/21 (95%)	0.048
5-year TTFT (95% CI)	A&B	78% (68-88)	90% (76-100)	0.025
5-year OS (95% CI)	U-IGHV	70% (60-80)	84% (64-100)	0.020
5-year t-DLBCL	All	9% (5-13)	12% (0-26)	ns

TTFT: time to first treatment; OS: overall survival; 95% CI: 95% confidence interval; t-DLBCL: transformation into diffuse large B-cell lymphoma (Richter syndrome); ns: not significant; UNV: above normal value; 95% CI: 95% confidence interval; U-IGHV: unmutated IGHV genes

113

The overall survival of patients with mutations in RAS-BRAF-MAPK-ERK pathway genes was similar to that of patients without mutations in this pathway (Table 2). When mutations in *TP53*, *ATM* or *BIRC3* were taken into account, the overall survival of patients with mutations in genes of the RAS-BRAF-MAPK-ERK pathway alone was similar to that of patients without adverse mutations (Figure 2D) [5-year overall survival of patients without mutations, 84% (95% CI: 78-92%); with mutations only in the RAS-BRAF-MAPK-ERK pathway, 80% (95% CI: 64-99%); with adverse mutations only, 66% (95% CI: 53-79%); and with both abnormalities in RAS-BRAF-MAPK-ERK pathway genes and adverse mutations, 66% (95% CI: 45-100%), $P=0.003$]. Multivariate analysis including IGHV status, mutations in genes of the RAS-BRAF-MAPK-ERK pathway, and adverse mutations in a final model with 439 patients showed an independent impact on overall survival for IGHV status [HR 3.3 (95% CI: 1.9-5.9), $P<0.001$] and adverse mutations [HR 1.7 (95% CI: 1.1-2.8), $P=0.02$].

Functional and gene expression analysis

To assess the functional impact of these genomic alterations on the RAS-BRAF-MAPK-ERK pathway, we analyzed the phosphorylation status of ERK as a surrogate marker of activation of the pathway. Western blotting with an antibody that specifically recognizes the dually phosphorylated and active forms of ERK1 and ERK2 showed higher levels of endogenous ERK phosphorylation (3.3- to 4.4-fold induction) in CLL cases with mutations in *KITLG*, *BRAF*, *MAP2K2* and *MAP2K1* genes compared to U-IGHV CLL cases with no alterations in the MAPK/ERK pathway (Figure 3A). The same results were obtained when analyzing the phosphorylated forms of ERK by flow cytometry, labeling cells with phospho (T202/Y204)-ERK1/2-phycoerythrin. Figure 3B shows that cases with mutations in genes of the RAS-BRAF-MAPK-

ERK pathway (*PTPN11*, *BRAF*, and *MAP2K1* mutations) had higher basal levels of phosphorylated ERK than cases of U-IGHV CLL (5- to 10-fold).

To identify the differential biological characteristics of cells carrying mutations in the RAS-BRAF-MAPK-ERK pathway, we conducted a gene expression profiling study in CD19+ tumor CLL cells from 143 CLL cases, 17 of which carrying functional mutations according to PolyPhen-2, SIFT and CADD phred-like predictions. With the C2 Biocarta analysis, we detected 126 of 149 gene sets upregulated in the group carrying mutations in genes of the RAS-BRAF-MAPK-ERK pathway, including the Biocarta MAPK pathway (NES=1.90; $P<0.001$; FDR=0.013) (*Online Supplementary Table S2* and Figure 3C). Similar results were obtained when carrying out a C2 KEGG analysis. We detected 104 of 178 gene sets upregulated in the group carrying mutations in genes of the RAS-BRAF-MAPK-ERK pathway, including the KEGG MAPK signaling pathway (NES=1.85; $P<0.001$; FDR=0.013) (*Online Supplementary Table S3* and Figure 3D). Genes belonging to the Biocarta and KEGG MAPK pathways are listed in *Online Supplementary Tables S4 and S5*, respectively.

Response to MAPK pathway inhibitors

We next evaluated the effect of BRAF inhibitors (vemurafenib, a specific inhibitor of the BRAF V600E mutation, and dabrafenib, specific for BRAF V600E and V600K variants) in cells from 17 CLL cases, nine containing mutations in genes of the RAS-BRAF-MAPK-ERK pathway (*KITLG*, *PTPN11*, *KRAS*, *BRAF*, *MAPK1*, *MAP2K1* and *MAP2K2*) and eight U-IGHV CLL cases with no alterations in this pathway. Vemurafenib, at a dose of 2.5 μM, was not able to inhibit basal ERK phosphorylation or after anti-IgM stimulation in mutated cases, while a slight effect was observed after treatment with 2.5 μM of dabrafenib. Furthermore, upregulation of
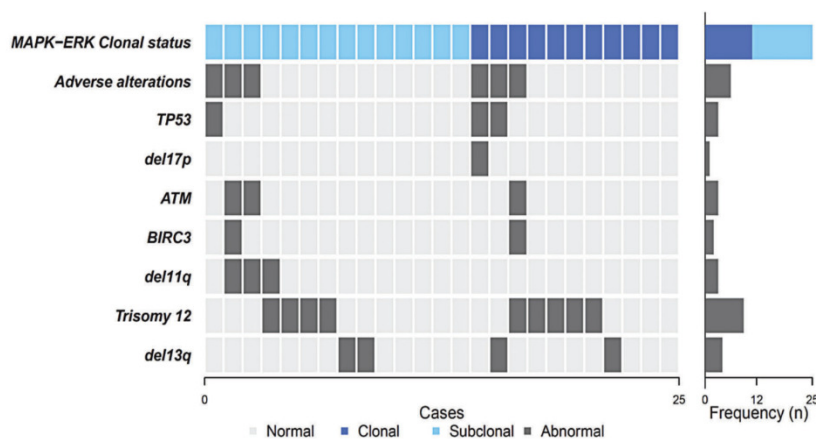
Figure 1. Brick-plot showing gene mutations, cytogenetic abnormalities and the type of RAS-BRAF-MAPK-ERK pathway mutations. Clonal mutations are labeled in dark blue, subclonal mutations in light blue, normal genes or chromosomal regions in light gray, and mutated/deleted genes or chromosomal regions in dark gray. Adverse alterations: *TP53*, *ATM* or *BIRC3*.

114

phosphorylated ERK, was observed in the U-IGHV CLL cases with no mutations in the RAS-BRAF-MAPK-ERK pathway after incubation with 2.5 μM of dabrafenib ($P<0.05$) (Figure 4A).

We next analyzed the cytotoxic effect of these drugs at different doses (0.5 to 5 μM) and times (24 h and 48 h): vemurafenib did not have any cytotoxic effect, while dabrafenib exerted some degree of cytotoxicity at the higher doses in both mutated RAS-BRAF-MAPK-ERK cases and U-IGHV CLL cases after 24 h of incubation ($P<0.05$) and at all doses after 48 h of incubation ($P<0.05$ at 0.5 μM and $P<0.01$ at 1-5 μM) (Figure 4B).

Finally, we compared the effect of the pan-ERK inhibitor ulixertinib (BVD-523) in six patients carrying mutations in the RAS-BRAF-MAPK-ERK pathway (*KITLG, PTPN11, BRAF, MAP2K1, MAP2K2* and *MAPK1*) and six U-IGHV CLL cases without mutations. In contrast to the lack of effect of vemurafenib and dabrafenib at 2.5 μM, ulixertinib was able to inhibit basal ERK phosphorylation (by 60%) in all cases with mutations in the RAS-BRAF-MAPK-ERK pathway at doses of 2.5 μM, and after stimulation with anti-IgM at much lower doses (100 nM) (Figure 4C). This effect was not observed in RAS-BRAF-MAPK-ERK pathway unmutated, U-IGHV cells.
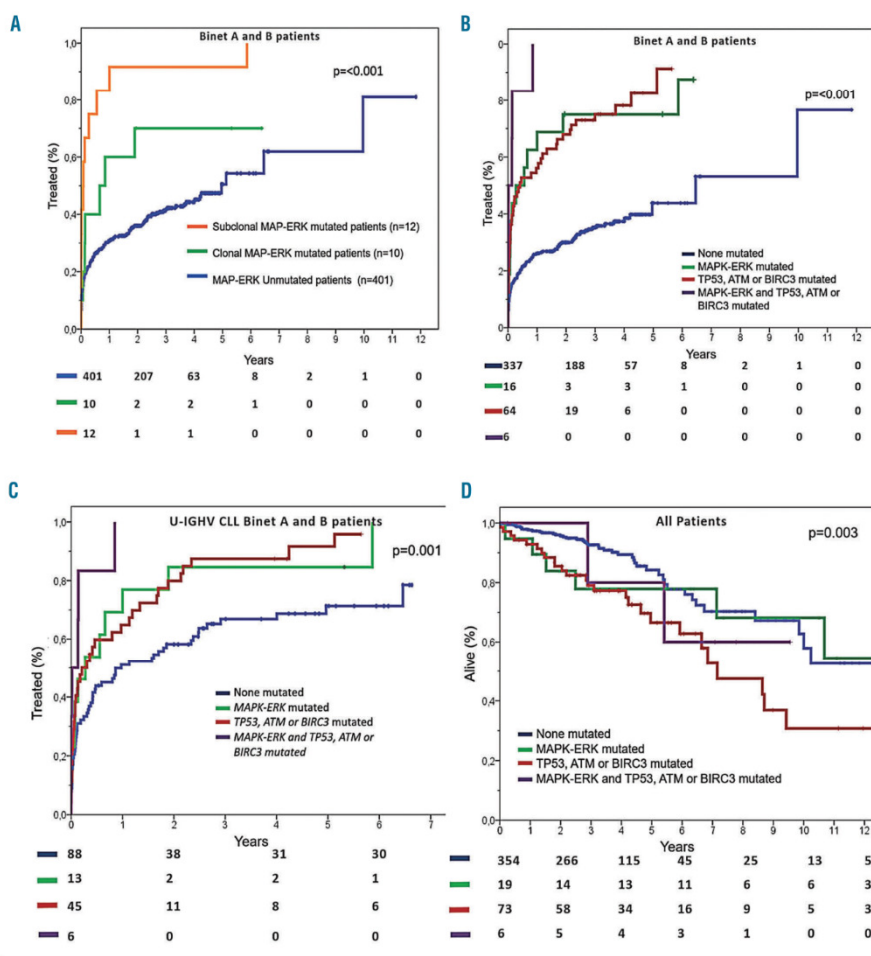
Figure 2. Outcome of patients according to mutations in genes of the RAS-BRAF-MAPK-ERK pathway. (A) Time to first treatment (TTFT) in Binet stage A and B patients according to mutations in the RAS-BRAF-MAPK-ERK pathway (the green line represents patients with clonal mutations, the orange line represents patients with subclonal mutations and the blue line represents patients with no mutations in the RAS-BRAF-MAPK-ERK pathway). (B) TTFT in Binet stage A and B patients according to the presence or absence of mutations in the RAS-BRAF-MAPK-ERK pathway and/or adverse mutations (*TP53, ATM* or *BIRC3*). (C) TTFT in U-IGHV CLL Binet A and B patients according to the presence or absence of mutations in the RAS-BRAF-MAPK-ERK pathway and/or adverse mutations (*TP53, ATM* or *BIRC3*). (D) Overall survival of all CLL patients according to the presence or absence of mutations in the RAS-BRAF-MAPK-ERK pathway and/or adverse mutations (*TP53, ATM* or *BIRC3*).

115

Discussion

CLL is characterized by a heterogeneous mutational landscape, with the presence of certain mutations being associated with progression of the disease and refractoriness to immuno-chemotherapy, which lead to a poor outcome.[6,13,28] Recently, it has been proposed that the MAPK–ERK pathway could be one of the cellular processes affected in CLL through mutations in novel CLL drivers such as *NRAS*, *KRAS*, *BRAF*, *PTPN11* and *MAP2K1*.[9,24] The RAS-BRAF-MAPK-ERK pathway plays a central role not only in regulating normal cellular processes involved in proliferation, growth, and differentiation, but also in oncogenesis,[29] and it is an important key dysregulated pathway in cancer.[30]

In our series, we observed mutations in genes belonging to the RAS-BRAF-MAPK-ERK pathway in 5% of CLL patients, a frequency similar to that already described.[13] When we evaluated each mutation specifically, *BRAF* mutations were detected in 2% of our CLL series, as previously reported.[9,21] *BRAF* mutations did not involve the canonical hotspot (V600E) seen in other malignancies,[17] which leads to constitutive activation of BRAF, but rather were clustered around the activation segment of the kinase domain.[9,23] Mutations in these positions confer variable but increased signaling and have oncogenic capacity.[31] Mutations in exon 15 of *BRAF* have been associated with refractoriness to fludarabine[22] although they do not seem to be selected during progression to refractory CLL.[21] Furthermore, the frequency of *BRAF* V600E mutations is higher in Richter syndrome than in untransformed CLL,[32] and this mutation could be acquired during the evolution of CLL. Recently, our group reported that the mere detection of a *BRAF* mutation, even at a very low frequency, had a prognostic impact on TTFT.[33] However, given the low frequency of mutations observed in CLL patients, larger series of patients are needed to corroborate these observations.

Mutations in genes upstream and downstream of *BRAF* were observed in 64% (16/25) of cases. *MAP2K1* mutations have already been described in HCL-variant and conventional HCL with rearranged IGHV4-34,[34] Langerhans cell histiocytosis,[35] and pediatric-type follicular lymphoma.[36] This mutation, similar to those of *BRAF*, leads to activation of the downstream target, ERK.[36] Moreover, we found mutations in additional genes of this pathway, such as *MAP2K2*, which encodes MEK2, and *PTPN11*, which encodes SHP-2. Both these proteins participate in the reg-
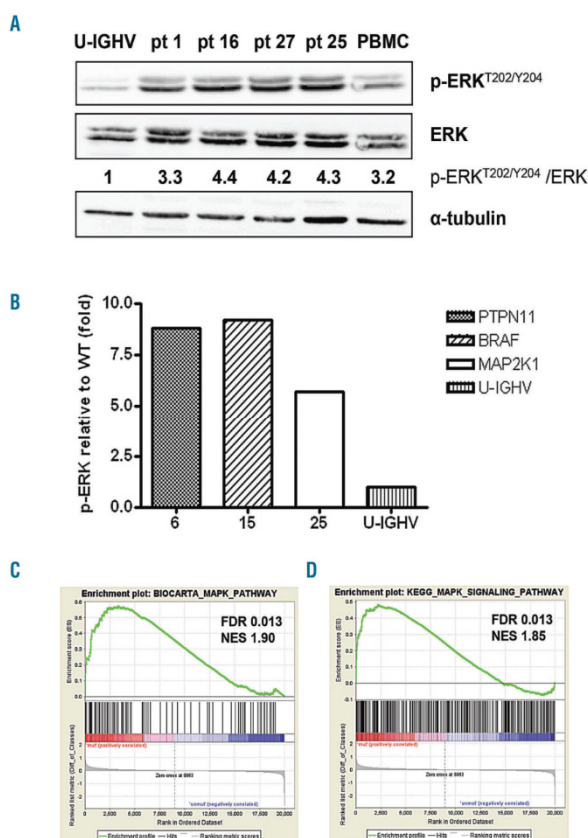
Figure 3. Activation of the RAS-BRAF-MAPK-ERK pathway. (A) Basal phosphorylated (p)-ERK and ERK levels analyzed by western blot in cases of chronic lymphocytic leukemia (CLL) with mutations in genes of the RAS-BRAF-MAPK-ERK pathway (case 1: *KITLG* mutation, case 16: *BRAF* mutation, case 27: *MAP2K2* mutation and case 25: *MAP2K1* mutation), in unmutated IGHV (U-IGHV) CLL and in peripheral blood mononuclear cells (PBMC). α-tubulin was used as a loading control. p-ERK/ERK levels were quantified relative to the U-IGHV case. (B) Basal p-ERK levels were analyzed by flow cytometry in CLL cases with mutations in genes of the RAS-BRAF-MAPK-ERK pathway (case 6: *PTPN11* mutation, case 15: *BRAF* mutation and case 25: *MAP2K1* mutation). Expression levels are relative to those in U-IGHV CLL. (C) Gene set enrichment analysis (GSEA) plots of the Biocarta-MAPK and KEGG MAPK signaling pathway gene sets regarding mutational status in genes of the RAS-BRAF-MAPK-ERK pathway in U-IGHV cases. The enrichment plot contains profiles of the running enrichment scores (ES) and positions of gene set members on the rank ordered list in GSEA (126 unmutated and 17 mutated CLL cases). NES, normalized enrichment score. FDR, false discovery rate.
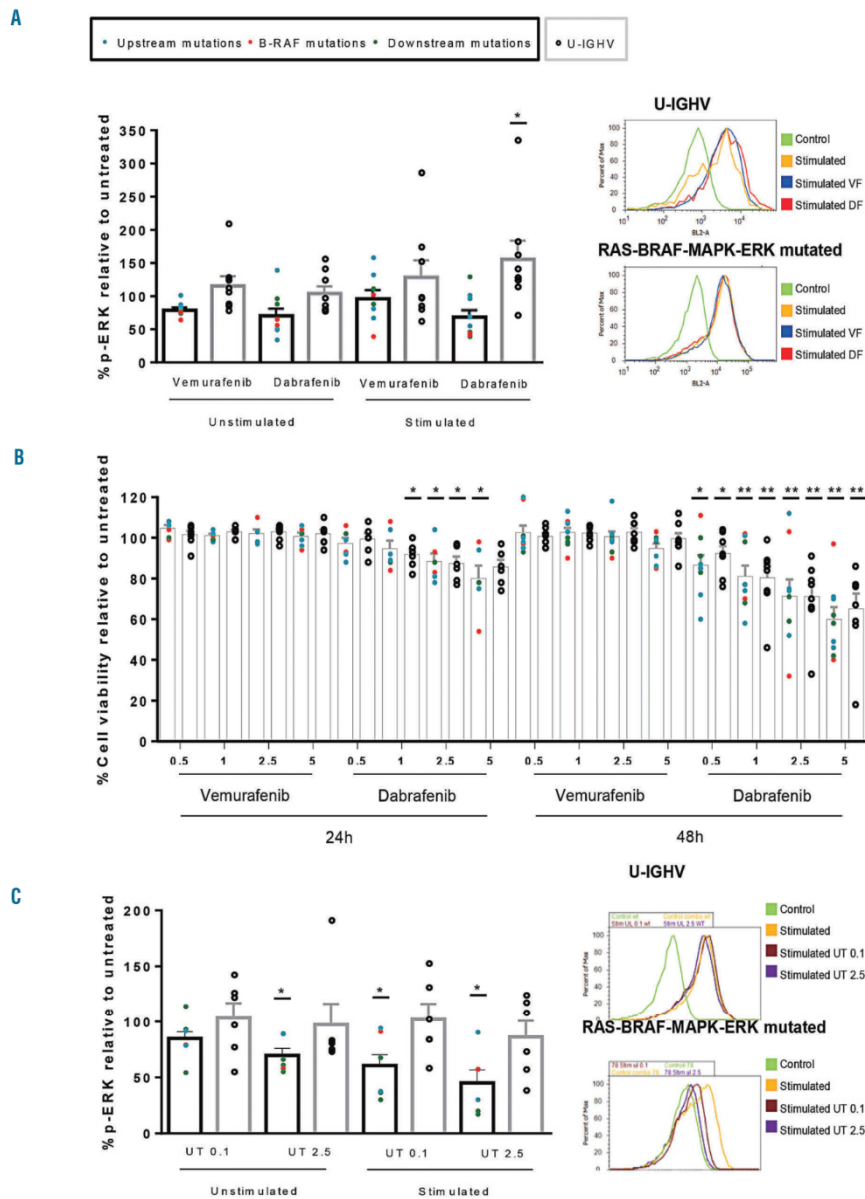
Figure 4. Effect of RAS-BRAF-MAPK-ERK inhibitors in cases of RAS-BRAF-MAPK-ERK-mutated and unmutated IGHV chronic lymphocytic leukemia. (A) Cells from 17 cases of chronic lymphocytic leukemia (CLL), nine containing mutations in the RAS-BRAF-MAPK-ERK pathway (*KITLG, PTPN11, KRAS, BRAF, MAPK1, MAP2K1, MAP2K2*) and eight with unmutated IGHV genes (U-IGHV) with no alterations in genes of the RAS-BRAF-MAPK-ERK pathway were treated with vemurafenib 2.5 μM or dabrafenib 2.5 μM. p-ERK levels were analyzed by flow cytometry after 1.5 h of treatment and expressed relative to untreated cells (Ct) at basal levels (unstimulated) or after stimulation with anti-IgM (stimulated) (*P<0.05). Histograms showing anti-IgM stimulation of ERK (T202/Y204) phosphorylation with and without vemurafenib or dabrafenib (2.5 μM) treatment in representative CLL cases (U-IGHV CLL and case 17 with a *BRAF* mutation). (B) Cell viability after treatment for 24 and 48 h with vemurafenib or dabrafenib at doses of 0.5-5 μM. Bars represent the mean ± standard error of the mean (SEM) of all samples analyzed (n=9 in the group of CLL cases with mutations in genes of the RAS-BRAF-MAPK-ERK pathway and n=8 in the unmutated CLL group) (*P<0.05; **P<0.01). (C) p-ERK levels after treatment with 0.1 or 2.5 μM ulixertinib (UT) relative to untreated (Ct) samples analyzed by flow cytometry at basal levels (unstimulated) or after stimulation with anti-IgM (stimulated). Bars represent the mean ± SEM of six samples analyzed in each group, six with mutations in genes of the RAS-BRAF-MAPK-ERK pathway (*KITLG, PTPN11, BRAF, MAP2K1, MAP2K2,* and *MAPK1*) and six U-IGHV CLL cases. Histograms showing anti-IgM stimulation of ERK (T202/Y204) phosphorylation and its inhibition by 100 nM and 2.5 μM ulixertinib (UT) in representative CLL cases (U-IGHV: CLL and case 15: *BRAF* mutation). Each patient is represented by a different color depending on the RAS-BRAF-MAPK-ERK mutational status and the mutation position relative to *BRAF*.

117

ulation of the RAS-BRAF-MAPK-ERK signaling pathway.[37] Mutations in this pathway seem to be mutually exclusive as only in one case were two different mutations observed simultaneously in the pathway. In this way, oncogene mutations that activate common downstream pathways often occur in a mutually exclusive fashion,[38] as has been reported for *BRAF* and *MAP2K1* in HCL-variant.[34]

The upregulation of genes of the MAPK pathway observed in the gene expression profiling analysis as well as the higher levels of phosphorylated ERK, a surrogate marker of MAPK pathway activation,[39] in cases with mutations in genes of the RAS-BRAF-MAPK-ERK pathway suggested the activation of this pathway in this subgroup of patients. Importantly, no ERK phosphorylation was observed in unmutated cases. Overall, these results agree with those found in other cancers, in which it has been postulated that the activation of RAS-RAF-MEK-ERK signaling can occur through mutations in several genes in the pathway.[40]

Our data suggest that mutations in the RAS-BRAF-MAPK-ERK pathway are associated with adverse biological features such as U-IGHV, high expression of ZAP-70, CD38 and CD49d, abnormal values of lactate dehydrogenase, and accumulation of three or more driver mutations. Importantly, mutated CLL cases had a 5-year TTFT similar to that of patients with adverse mutations (*TP53*, *ATM* or *BIRC3*), whereas patients carrying both types of mutations simultaneously had the worst 5-year TTFT, as reported by our group and others.[7,9,22,33] In our series of patients, the impact of mutations in genes of the RAS-BRAF-MAPK-ERK pathway on TTFT was independent of that of IGHV status and mutations in *TP53*, *ATM* or *BIRC3*. However, mutations in genes of the RAS-BRAF-MAPK-ERK pathway did not affect overall survival. Recently it was reported that *BRAF* mutations were associated with adverse overall survival, whereas *KRAS* and *NRAS* mutations were not.[24]

Vemurafenib (in 2011) and dabrafenib (in 2013) were the first selective BRAF inhibitors clinically approved for the treatment of melanoma with *BRAF* mutations.[30] MEK inhibitors have also shown efficacy in *BRAF*-mutant melanoma and in 2014 and 2015 the Food and Drug Administration approved the use of MEK inhibitors in combination with BRAF inhibitors as standard-of-care for *BRAF*-mutant advanced melanoma.[41] With these compounds, clinical response rates of around 50% and increased survival have been reported in *BRAF*-mutant melanoma[42] as well as in cases of HCL refractory to conventional therapy.[43,44] However, the majority of responses are transient and resistance is often associated with a plethora of different mechanisms that allow tumor cells to bypass BRAF/MEK inhibition and restore ERK-dependent signaling.[45] Our results showed that vemurafenib and dabrafenib were not able to decrease levels of ERK phosphorylation significantly in mutated cases, although a slight effect was observed after dabrafenib treatment which could be an off-target effect. Accordingly, a different spectrum of efficacy against non-V600 BRAF mutants has been described for vemurafenib and dabrafenib.[46] In contrast, activation of ERK was detected in unmutated CLL cases, potentially due to ERK activation by the B-cell receptor signaling complex as it has been described that

BRAF inhibitor-related ERK phosphorylation can be partially abrogated by blocking B-cell receptor signaling with SYK inhibitors.[47]

It has been postulated that cancer cells can dynamically rewire their signaling networks to restore ERK activity and override the actions of inhibitors that act upstream of ERK.[48] We, therefore, consider ERK itself as one of the "best" nodes for effective disruption of ERK signaling. Our results demonstrated that ulixertinib (BVD-523), a potent and highly selective inhibitor of ERK1/2, was able to inhibit ERK phosphorylation *in vitro* in all CLL cases with mutations in genes of the RAS-BRAF-MAPK-ERK pathway. Ulixertinib has shown activity in BRAF- and RAS-mutant cell lines. Results of phase I studies in solid tumors have documented a safe and well-tolerated effect in patients who harbored BRAF-, NRAS- and MEK-mutant solid tumors, supporting the ongoing development of ulixertinib for patients with MAPK-activating alterations.[49] Recently it was reported that CLL cells with trisomy 12 showed increased sensitivity to MEK and ERK inhibitors, pointing to an essential role for MEK/ERK signaling in CLL with trisomy 12.[50]

In conclusion, we showed that the RAS-BRAF-MAPK-ERK pathway is one of the cellular processes affected in CLL and identified novel CLL drivers. Patients with mutations in genes of the RAS-BRAF-MAPK-ERK pathway had adverse biological features and most of them required treatment. Furthermore, our results suggest that inhibition of ERK phosphorylation in this subgroup of mutated CLL patients can be achieved using new, specific ERK inhibitors that have recently entered clinical trials. Pharmacological inhibition of the RAS-BRAF-MAPK-ERK pathway may represent a therapeutic approach to improve responses in this subgroup of CLL patients.

References

1. Swerdlow SH, Campo E, Pileri SA, et al. The 2016 revision of the World Health Organization classification of lymphoid neoplasms. Blood. 2016;127(20):2375–2390.
2. Fabbri G, Dalla-Favera R. The molecular pathogenesis of chronic lymphocytic leukaemia. Nat Rev Cancer. 2016;16(3):145–162.
3. Delgado J, Salaverria I, Baumann T, et al. Genomic complexity and IGHV mutational status are key predictors of outcome of chronic lymphocytic leukemia patients with TP53 disruption. Haematologica. 2014;99(11):e231-234.
4. Zenz T, Eichhorst B, Busch R, et al. TP53 mutation and survival in chronic lymphocytic leukemia. J Clin Oncol. 2010;28(29):4473–4479.
5. Rossi D, Rasi S, Spina V, et al. Integrated mutational and cytogenetic analysis identifies new prognostic subgroups in chronic lymphocytic leukemia. Blood. 2013;121(8):1403–1412.
6. Baliakas P, Hadzidimitriou A, Sutton L-A, et al. Recurrent mutations refine prognosis in chronic lymphocytic leukemia. Leukemia. 2015;29(2):329–336.
7. Puente XS, Beà S, Valdés-Mas R, et al. Non-coding recurrent mutations in chronic lymphocytic leukaemia. Nature. 2015;526(7574):519–524.
8. Quesada V, Conde L, Villamor N, et al. Exome sequencing identifies recurrent mutations of the splicing factor SF3B1 gene in chronic lymphocytic leukemia. Nat Genet. 2012;44(1):47–52.
9. Landau DA, Tausch E, Taylor-Weiner AN, et al. Mutations driving CLL and their evolution in progression and relapse. Nature. 2015;526(7574):525–530.
10. Wang L, Lawrence MS, Wan Y, et al. SF3B1 and other novel cancer genes in chronic lymphocytic leukemia. N Engl J Med. 2011;365(26):2497–2506.
11. Landau DA, Carter SL, Stojanov P, et al. Evolution and impact of subclonal mutations in chronic lymphocytic leukemia. Cell. 2013;152(4):714–726.
12. Jeromin S, Weissmann S, Haferlach C, et al. SF3B1 mutations correlated to cytogenetics and mutations in NOTCH1, FBXW7, MYD88, XPO1 and TP53 in 1160 untreated CLL patient. Leukemia. 2014;28(1):108–117.
13. Nadeu F, Delgado J, Royo C, et al. Clinical impact of clonal and subclonal TP53, SF3B1, BIRC3, NOTCH1, and ATM mutations in chronic lymphocytic leukemia. Blood. 2016;127(17):2122–2130.
14. Lavoie H, Therrien M. Regulation of RAF protein kinases in ERK signalling. Nat Rev Mol Cell Biol. 2015;16(5):281–298.
15. Davies H, Bignell GR, Cox C, et al. Mutations of the BRAF gene in human cancer. Nature. 2002;417(6892):949–954.
16. Forbes SA, Beare D, Boutselakis H, et al. COSMIC: Somatic cancer genetics at high-resolution. Nucleic Acids Res. 2017;45(D1):D777–D783.
17. Tiacci E, Trifonov V, Schiavoni G, et al. BRAF mutations in hairy-cell leukemia. N Engl J Med. 2011;364(24):2305–2315.
18. Tiacci E, Pettirossi V, Schiavoni G, Falini B. Genomics of Hairy cell leukemia. J Clin Oncol. 2017;35(9):1002–1010.
19. Pakneshan S, Salajegheh A, Smith RA, Lam AK. Clinicopathological relevance of BRAF mutations in human cancer. Pathology. 2013;45(4):346–356.
20. Buscà R, Pouysségur J, Lenormand P. ERK1 and ERK2 map kinases: specific roles or functional redundancy? Front Cell Dev Biol. 2016;453.
21. Jebaraj BMC, Kienle D, Bühler A, et al. BRAF mutations in chronic lymphocytic leukemia. Leuk Lymphoma. 2013;54(6):1177–1182.
22. Pandzic T, Larsson J, He L, et al. Transposon mutagenesis reveals fludarabine-resistance mechanisms in chronic lymphocytic leukemia. Clin Cancer Res. 2016;22(24):6217–6227.
23. Damm F, Mylonas E, Cosson A, et al. Acquired initiating mutations in early hematopoietic cells of CLL patients. Cancer Discov. 2014;4(9):1088–1101.
24. Leeksma AC, Taylor J, Wu B, et al. Clonal diversity predicts adverse outcome in chronic lymphocytic leukemia. Leukemia. 2018 Jul 23. [Epub ahead of print]
25. Müller-Hermelink H, Montserrat E, Catovsky D et al. Chronic lymphocytic leukemia/small lymphocytic lymphoma. WHO classification of tumours of haematopoietic and lymphoid tissues. IARC: International Agency for Research on Cancer; Lyon, 2008; 4th edition. Pages 180-183.
26. Rossi D, Cerri M, Deambrogi C, et al. The prognostic value of TP53 mutations in chronic lymphocytic leukemia is independent of del17p13: Implications for overall survival and chemorefractoriness. Clin Cancer Res. 2009;15(3):995–1004.
27. Rossi D, Fangazio M, Rasi S, et al. Disruption of BIRC3 associates with fludarabine chemorefractoriness in TP53 wild-type chronic lymphocytic leukemia. Blood. 2012;119(12):2854–2862.
28. Lazarian G, Guièze R, Wu CJ. Clinical Implications of novel genomic discoveries in chronic lymphocytic leukemia. J Clin Oncol. 2017;35(9):984–993.
29. Downward J. Targeting RAS signalling pathways in cancer therapy. Nat Rev Cancer. 2003;3(1):11–22.
30. Imperial R, Toor OM, Hussain A, Subramanian J, Masood A. Comprehensive pancancer genomic analysis reveals (RTK)-RAS-RAF-MEK as a key dysregulated pathway in cancer: its clinical implications. Semin Cancer Biol. 2017 Nov 22. [Epub ahead of print].
31. Wan PTC, Garnett MJ, Roe SM, et al. Mechanism of activation of the RAF-ERK signaling pathway by oncogenic mutations of B-RAF. Cell. 2004;116(6):855–867.
32. Sellar RS, Fend F, Akarca AU, et al. BRAFV600E mutations are found in Richter syndrome and may allow targeted therapy in a subset of patients. Br J Haematol. 2015;170(2):282–285.
33. Nadeu F, Clot G, Delgado J, et al. Clinical impact of the subclonal architecture and mutational complexity in chronic lymphocytic leukemia. Leukemia. 2017;32(3):645-653.
34. Waterfall JJ, Arons E, Walker RL, et al. High prevalence of MAP2K1 mutations in variant and IGHV4-34-expressing hairy-cell leukemias. Nat Genet. 2014;46(1):8–10.
35. Brown NA, Furtado L V, Betz BL, et al. High prevalence of somatic MAP2K1 mutations in BRAF V600E-negative Langerhans cell histiocytosis. Blood. 2014;124(10):1655–1658.
36. Schmidt J, Ramis-Zaldivar JE, Nadeu F, et al. Mutations of MAP2K1 are frequent in pediatric-type follicular lymphoma and result in ERK pathway activation. Blood. 2017;130(3):323–327.
37. Yang SH, Sharrocks AD, Whitmarsh AJ. MAP kinase signalling cascades and transcriptional regulation. Gene. 2013;513(1):1–13.
38. Thomas RK, Baker AC, Debiasi RM, et al. High-throughput oncogene mutation profiling in human cancer. Nat Genet. 2007;39(3):347–351.
39. Warden DW, Ondrejka S, Lin J, Durkin L, Bodo J, Hsi ED. Phospho-ERK(THR202/Tyr214) is overexpressed in hairy cell leukemia and is a useful diagnostic marker in bone marrow trephine sections. Am J Surg Pathol. 2013;37(2):305–308.
40. Burotto M, Chiou VL, Lee J-M, Kohn EC. The MAPK pathway across different malignancies: a new perspective. Cancer. 2014;120(22):3446–3456.
41. Eroglu Z, Ribas A. Combination therapy with BRAF and MEK inhibitors for melanoma: latest evidence and place in therapy. Ther Adv Med Oncol. 2016;8(1):48–56.
42. Chapman PB, Hauschild A, Robert C, et al. Improved survival with vemurafenib in melanoma with BRAF V600E mutation. N Engl J Med. 2011;364(26):2507–2516.
43. Dietrich S, Glimm H, Andrulis M, et al. BRAF inhibition in refractory hairy-cell leukemia. N Engl J Med. 2012;366(21):2038–2040.
44. Follows GA, Sims H, Bloxham DM, et al. Rapid response of biallelic BRAF V600E mutated hairy cell leukaemia to low dose vemurafenib. Br J Haematol. 2013;161(1):150–153.
45. Shi H, Hugo W, Kong X, et al. Acquired resistance and clonal evolution in melanoma during BRAF inhibitor therapy. Cancer Discov. 2014;4(1):80–93.
46. Kordes M, Röring M, Heining C, et al. Cooperation of BRAF(F595L) and mutant HRAS in histiocytic sarcoma provides new insights into oncogenic BRAF signaling. Leukemia. 2016;30(4):937-946.
47. Yaktapour N, Meiss F, Mastroianni J, et al. BRAF inhibitor-associated ERK activation drives development of chronic lymphocytic leukemia. J Clin Invest. 2014;124(11):5074–5084.
48. Ryan MB, Der CJ, Wang-Gillam A, Cox AD. Targeting RAS-mutant cancers: Is ERK the key? Trends Cancer. 2015;1(3):183–198.
49. Sullivan RJ, Infante JR, Janku F, et al. First-in-class ERK1/2 inhibitor ulixertinib (BVD-523) in patients with MAPK mutant advanced solid tumors: results of a phase I dose-escalation and expansion study. Cancer Discov. 2018;8(2):184-195.
50. Dietrich S, Oleś M, Lu J, et al. Drug-perturbation-based stratification of blood cancer. J Clin Invest. 2018;128(1):427-445.

119

Chronic Lymphocytic Leukemia

Mutations in the RAS-BRAF-MAPK-ERK pathway define a specific subgroup of patients with adverse clinical features and provide new therapeutic options in chronic lymphocytic leukemia

Neus Giménez,[1,2]* Alejandra Martínez-Trillos,[1,3]* Arnau Montraveta,[1] Mónica Lopez-Guerra,[1,4] Laia Rosich,[1] Ferran Nadeu,[1] Juan G. Valero,[1] Marta Aymerich,[1,4] Laura Magnano,[1,4] Maria Rozman,[1,4] Estella Matutes,[4] Julio Delgado,[1,3] Tycho Baumann,[1,3] Eva Gine,[1,3] Marcos González,[5] Miguel Alcoceba,[5] M. José Terol,[6] Blanca Navarro,[6] Enrique Colado,[7] Angel R. Payer,[7] Xose S. Puente,[8] Carlos López-Otín,[8] Armando Lopez-Guillermo,[1,3] Elias Campo,[1,4] Dolors Colomer[1,4]** and Neus Villamor[1,4]**

[1]Institut d'Investigacions Biomèdiques August Pi i Sunyer (IDIBAPS), CIBERONC, Barcelona; [2]Anaxomics Biotech, Barcelona; [3]Hematology Department and [4]Hematopathology Unit, Hospital Clinic, Barcelona; [5]Hematology Department, University Hospital- IBSAL, and Institute of Molecular and Cellular Biology of Cancer, University of Salamanca, CIBERONC; [6]Hematology Department, Hospital Clínico Universitario, Valencia: [7]Hematology Department, Hospital Universitario Central de Asturias, Oviedo, and [8]Departamento de Bioquímica y Biología Molecular, Instituto Universitario de Oncología, Universidad de Oviedo, CIBERONC, Spain.

*NG and AM-T contributed equally to the study.

**DC and NV share senior authorship of the manuscript.

Supplemental data

Primary CLL cells

Cells were isolated from peripheral blood (PB) samples by Ficoll-Paque sedimentation (GE-Healthcare, Chicago, IL, USA). Thawed cells were cultured in fresh RPMI-1640 supplemented with 10% fetal bovine serum (FBS) (Life technologies; Carlsbad, CA, USA), 2 mM glutamine and 50 µg/mL penicillin-streptomycin (Life technologies) and cultured in a humidified atmosphere at 37ºC containing 5% carbon dioxide.

Gene expression analysis

Gene expression profile (GEP) of 143 purified U-IGHV CLL samples from the CLL-ICGC project[8] was analyzed. Cases with mutations in the RAS-BRAF-MAPK-ERK pathway versus those without mutations were compared using the gene set enrichment analysis (GSEA) package version 2.0. The enrichment of the MAPK gene signature was investigated using the C2 Biocarta and C2 KEGG collection version 6,1 with a two-class analysis, 1000 permutations of gene sets and weighted metrics. Gene sets with a p≤0.05 and a false discovery rate (FDR) q-value≤10% and a normalized enrichment score (NES) ≥1.5 were considered to be significantly enriched in the RAS-BRAF-MAPK-ERK mutated group. Sequencing, expression and genotyping array data have been deposited at the European Genome-Phenome Archive (EGA, http://www.ebi.ac.uk/ega/), which is hosted at the European Bioinformatics Institute (EBI), under accession number EGAS00000000092.

Western blot analysis

Whole-cell protein extracts were obtained by lysing primary CLL cells and peripheral blood mononuclear cells (PBMC) obtained from healthy donors (online with Triton buffer (20 mM Tris-HCL pH 7.6, 150 mM NaCl, 1 mM EDTA, and 1% Triton X-100) supplemented with protease and phosphatase inhibitors [10 µg/mL leupeptin, 10 µg/mL aprotinin, 1 mM PMSF (phenylmethanesulfonyl fluoride), 2 mM PHIC I (sodium pyrophosphate decahydrate), PHIC II (β-glycerol phosphate disodium salt pentahydrate), and 1 mM sodium orthovanadate (Sigma, Saint Louis, MO, USA)]. Proteins were quantified using Bio-Rad Protein Assay (Bio-Rad, Portland, ME, USA), separated in 12% SDS-PAGE and transferred to an Immobilon-P membrane (EMD Millipore, Billerica, MA, USA). Membranes were blocked with 2.5% phosphoBlocker Blocking Reagent (Cell Biolabs, San Diego, CA, USA) in Tris-Buffered Saline (TBS)-Tween 20, and probed with antibodies against phosphorylated- T202/Y204

ERK 1/2 and total ERK (Santa Cruz Biotechnology, Santa Cruz, CA, USA). Antibody binding was detected using secondary peroxidase-labeled anti-mouse and anti-rabbit antibodies (Sigma) and chemiluminescence was detected using a mini-LAS4000 Fujifilm device (Fujifilm. Tokyo, Japan). Equal protein loading was confirmed by probing membranes with α-tubulin antibody (Sigma).

Analysis of viability

Primary CLL cells were incubated for 24 or 48 hours with the indicated doses of the drugs and then stained with Annexin-V-Fluorescein isothiocyanate (FITC) and Propidium iodide (PI) (Ebiosciences, San Diego, CA, USA). Labeled samples were analyzed on an Attune focusing acoustic cytometer (Life Technologies). Viability (mean ± SEM) was calculated as the percentage of Annexin-V and PI negative cells in treated samples relative to the untreated ones.

BCR stimulation and quantification of p-ERK by flow cytometry

Primary CLL cells were starved for 1.5 hours in FBS-free RPMI ($5x10^6$ cells/mL) and preincubated with different doses of the drugs. Then, cells were stimulated for 2 minutes at 37°C with 10 μg/mL of anti-IgM (Southern Biotech, Birmingham, AL, USA) and 3.3 mM of hydrogen peroxide (Sigma), fixed for 1 hour with paraformaldehyde 2% and permeabilized by adding 70% ethanol overnight at –20°C. Intracellular unspecific staining was blocked with 10% mouse serum. Finally, cells were stained for phospho (T202 and Y204)-ERK1/2-phycoerythrin (PE) (Becton Dickinson, Franklin Lakes, NJ, USA) and 10000 cells were analyzed in an Attune acoustic cytometer (Life Technologies). Median fluorescence intensity (MFI) of the unstained sample was subtracted to respective p-ERK stained sample.

Statistical analysis

Time to first treatment (TTFT) was calculated from the date of sampling to the first treatment or last follow-up. Overall survival (OS) was calculated from the date of sampling to the date of death or last follow-up. All statistical tests were two-sided with a p-value of 0.05 to be considered significant. All the analyses were conducted using SPSS 20 (www.ibm.com) software.

Figure S1

RAS-BRAF-MAPK-ERK pathway
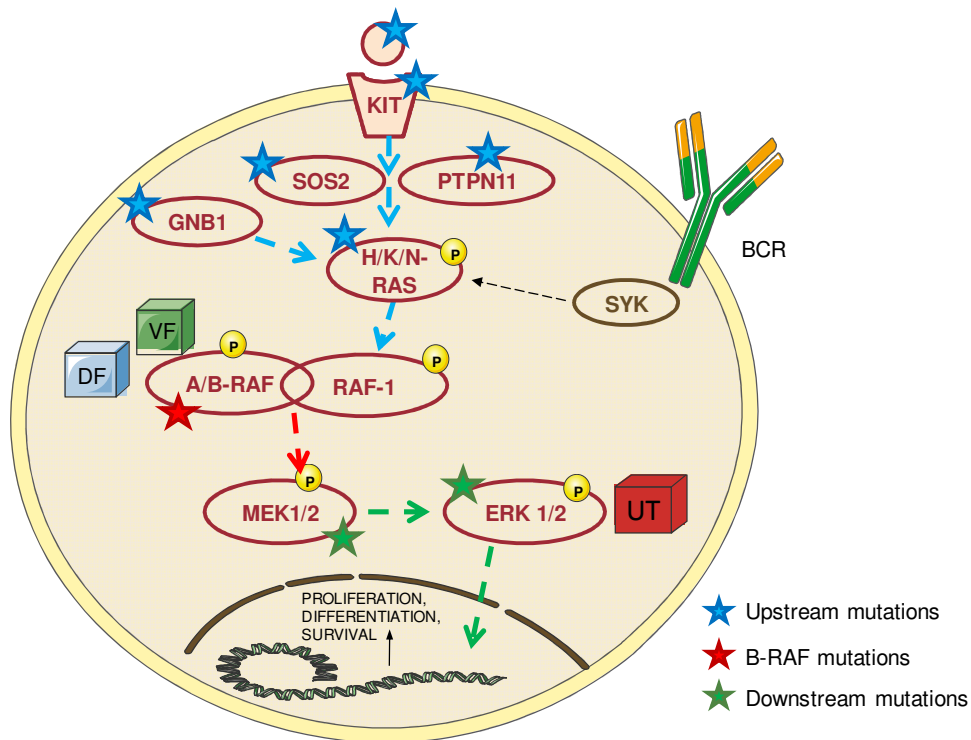
Figure S1. Scheme of the MAPK pathway with stars indicating the genes with mutations found in our cohort (detailed in Table 1). VF: vemurafenib, DF: dabrafenib, UT: ulixertinib.

Figure S2
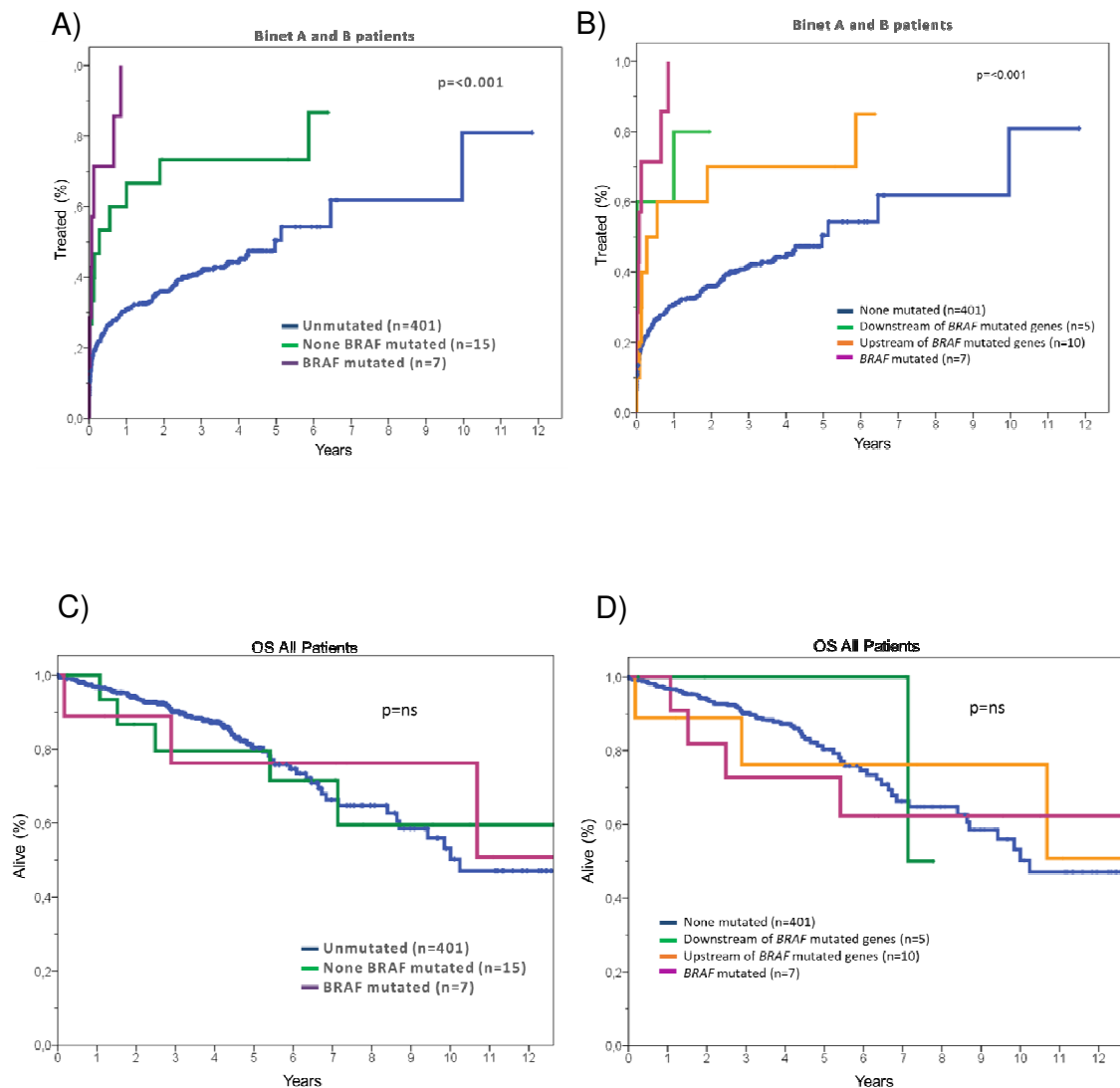
Figure S2. Outcome of patients according to the gene mutated and position of mutated genes in the RAS-BRAF-MAPK-ERK pathway. A) Time to first treatment in Binet A and B patients with mutations in *BRAF* (purple line), in genes different of *BRAF* (green line) or without mutations in RAS-BRAF-MAPK-ERK pathway (blue line). B) Time to first treatment in Binet A and B patients with mutations in *BRAF* (purple line), in genes upstream *BRAF* (orange line), downstream *BRAF* (green line), or without mutations in RAS-BRAF-MAPK-ERK pathway (blue line). C) Overall survival according to mutations in *BRAF* (purple line), in genes different of *BRAF* (green line) or without mutations in RAS-BRAF-MAPK-ERK pathway (blue line). D) Overall survival of patients according to mutations in *BRAF* (purple line), in genes upstream *BRAF* (orange line), downstream *BRAF* (green line), or without mutations in RAS-BRAF-MAPK-ERK pathway (blue line).

Table S1. Main clinical and biological characteristics of 452 patients included in the analysis.

Characteristic	
Age, median (range)	62 years (18-93 years)
Sex (Male/Female), n (%)	276 (61%) / 176 (49%)
Binet Stage (A/B/C/unknown), n (%)	387 (86%) / 48 (11%) / 10 (2%) / 7 (1%)
Elevated LDH, n/total (%)	32/426 (7%)
Elevated beta 2 microglobulin, n/total (%)	126/391 (32%)
CD38 ≥30%, n/total (%)	106/426 (25%)
CD49d ≥30%, n/total (%)	101/303 (33%)
ZAP-70 ≥20%, n/total (%)	112/415 (27%)
Unmutated IGHV (≥98% homology), n/total (%)	166/445 (37%)
Trisomy 12, n/total (%)	54/321 (16.8%)
Del(11q)(q22.3), n/total (%)	26/320 (8%)
Del(17p)(p13.1), n/total (%)	12/321 (3.7%)
Median follow-up (range)	3.1 years (0.1-14.8)
Patients treated, n (%)	206 (46%)
Treatment, n (%)	206 (46%)
Chlorambucil	40 (20%)
Purine analogs monotherapy	8 (4%)
Fludarabine based polychemotherapy w/o rituximab	25 (12%)
Fludarabine-based polychematherapy with rituximab	93 (45%)
CHOP-like regimens	7 (3%)
Others	33 (16%)

Table S2. Upregulated gene sets in cases with mutations in the RAS-BRAF-MAPK-ERK pathway with c2.cp.Biocarta analysis.

	NAME	SIZE	NES	NOM p-val	FDR q-val
1	BIOCARTA_CDMAC_PATHWAY	16	2.09	0.002	0.001
2	BIOCARTA_CARDIACEGF_PATHWAY	18	2.03	0.000	0.002
3	BIOCARTA_TCR_PATHWAY	43	1.94	0.000	0.015
4	BIOCARTA_MET_PATHWAY	37	1.93	0.000	0.012
5	BIOCARTA_ETS_PATHWAY	18	1.93	0.000	0.010
6	**BIOCARTA_MAPK_PATHWAY**	**86**	**1.90**	**0.000**	**0.013**
7	BIOCARTA_BCELLSURVIVAL_PATHWAY	16	1.86	0.000	0.021
8	BIOCARTA_ARF_PATHWAY	17	1.83	0.005	0.029
9	BIOCARTA_TOB1_PATHWAY	19	1.79	0.007	0.046
10	BIOCARTA_GLEEVEC_PATHWAY	23	1.72	0.002	0.091
11	BIOCARTA_KERATINOCYTE_PATHWAY	46	1.72	0.005	0.085
12	BIOCARTA_STRESS_PATHWAY	25	1.71	0.005	0.085
13	BIOCARTA_TNFR1_PATHWAY	29	1.69	0.007	0.098
14	BIOCARTA_EPO_PATHWAY	19	1.68	0.012	0.096
15	BIOCARTA_PDGF_PATHWAY	32	1.67	0.010	0.097
16	BIOCARTA_TPO_PATHWAY	24	1.67	0.016	0.095
17	BIOCARTA_TGFB_PATHWAY	19	1.67	0.015	0.091
18	BIOCARTA_CCR5_PATHWAY	16	1.66	0.014	0.088
19	BIOCARTA_EGF_PATHWAY	31	1.66	0.005	0.088
20	BIOCARTA_IL12_PATHWAY	21	1.64	0.023	0.097
21	BIOCARTA_CTCF_PATHWAY	23	1.64	0.012	0.096
22	BIOCARTA_ERYTH_PATHWAY	15	1.62	0.018	0.106
23	BIOCARTA_CD40_PATHWAY	15	1.61	0.025	0.108
24	BIOCARTA_TEL_PATHWAY	18	1.61	0.028	0.108
25	BIOCARTA_MTOR_PATHWAY	23	1.61	0.027	0.106
26	BIOCARTA_NO2IL12_PATHWAY	17	1.61	0.019	0.103
27	BIOCARTA_NGF_PATHWAY	18	1.60	0.018	0.101
28	BIOCARTA_IL6_PATHWAY	22	1.60	0.014	0.098
29	BIOCARTA_LAIR_PATHWAY	17	1.60	0.030	0.098
30	BIOCARTA_IGF1_PATHWAY	21	1.59	0.018	0.102
31	BIOCARTA_NTHI_PATHWAY	24	1.59	0.019	0.100
32	BIOCARTA_IL2_PATHWAY	22	1.58	0.028	0.099
33	BIOCARTA_41BB_PATHWAY	17	1.58	0.030	0.103
34	BIOCARTA_HCMV_PATHWAY	17	1.57	0.028	0.104
35	BIOCARTA_G1_PATHWAY	28	1.54	0.036	0.128
36	BIOCARTA_VEGF_PATHWAY	29	1.54	0.040	0.128
37	BIOCARTA_INSULIN_PATHWAY	21	1.53	0.040	0.128
38	BIOCARTA_IL1R_PATHWAY	32	1.52	0.040	0.140
39	BIOCARTA_BCR_PATHWAY	34	1.51	0.036	0.148
40	BIOCARTA_CXCR4_PATHWAY	24	1.51	0.043	0.144
41	BIOCARTA_NKCELLS_PATHWAY	19	1.50	0.050	0.145

42	BIOCARTA_P38MAPK_PATHWAY	39	1.49	0.038	0.148
43	BIOCARTA_TOLL_PATHWAY	37	1.49	0.043	0.148
44	BIOCARTA_RACCYCD_PATHWAY	26	1.49	0.030	0.148
45	BIOCARTA_IL17_PATHWAY	15	1.48	0.047	0.150
46	BIOCARTA_TNFR2_PATHWAY	18	1.48	0.056	0.147
47	BIOCARTA_AGR_PATHWAY	36	1.46	0.055	0.161
48	BIOCARTA_IL3_PATHWAY	15	1.45	0.080	0.166
49	BIOCARTA_PPARA_PATHWAY	55	1.44	0.041	0.173
50	BIOCARTA_FAS_PATHWAY	30	1.43	0.070	0.180
51	BIOCARTA_RAC1_PATHWAY	23	1.43	0.080	0.178
52	BIOCARTA_PML_PATHWAY	17	1.42	0.085	0.186
53	BIOCARTA_MAL_PATHWAY	19	1.41	0.095	0.191
54	BIOCARTA_IL7_PATHWAY	17	1.41	0.075	0.191
55	BIOCARTA_HIVNEF_PATHWAY	58	1.40	0.052	0.204
56	BIOCARTA_IL22BP_PATHWAY	16	1.38	0.113	0.221
57	BIOCARTA_RAS_PATHWAY	23	1.38	0.108	0.218
58	BIOCARTA_AKT_PATHWAY	22	1.38	0.100	0.217
59	BIOCARTA_IL2RB_PATHWAY	38	1.35	0.091	0.245
60	BIOCARTA_NKT_PATHWAY	28	1.35	0.100	0.242
61	BIOCARTA_RARRXR_PATHWAY	15	1.34	0.155	0.252
62	BIOCARTA_PROTEASOME_PATHWAY	28	1.34	0.115	0.249
63	BIOCARTA_INTRINSIC_PATHWAY	23	1.33	0.129	0.252
64	BIOCARTA_MEF2D_PATHWAY	18	1.31	0.158	0.273
65	BIOCARTA_HIF_PATHWAY	15	1.31	0.156	0.270
66	BIOCARTA_CSK_PATHWAY	22	1.31	0.144	0.276
67	BIOCARTA_WNT_PATHWAY	26	1.30	0.140	0.277
68	BIOCARTA_ATM_PATHWAY	20	1.30	0.164	0.278
69	BIOCARTA_CTLA4_PATHWAY	19	1.30	0.142	0.278
70	BIOCARTA_VIP_PATHWAY	26	1.28	0.155	0.289
71	BIOCARTA_CALCINEURIN_PATHWAY	18	1.28	0.161	0.293
72	BIOCARTA_HDAC_PATHWAY	27	1.28	0.159	0.291
73	BIOCARTA_RELA_PATHWAY	16	1.27	0.198	0.296
74	BIOCARTA_PTDINS_PATHWAY	23	1.26	0.169	0.303
75	BIOCARTA_CELLCYCLE_PATHWAY	23	1.26	0.165	0.301
76	BIOCARTA_GPCR_PATHWAY	34	1.25	0.173	0.304
77	BIOCARTA_IGF1MTOR_PATHWAY	20	1.23	0.204	0.340
78	BIOCARTA_FMLP_PATHWAY	35	1.22	0.190	0.341
79	BIOCARTA_AMI_PATHWAY	20	1.21	0.220	0.347
80	BIOCARTA_SPPA_PATHWAY	22	1.21	0.234	0.351
81	BIOCARTA_CARM_ER_PATHWAY	34	1.20	0.219	0.356
82	BIOCARTA_NFKB_PATHWAY	23	1.20	0.227	0.353
83	BIOCARTA_EIF4_PATHWAY	24	1.19	0.237	0.363
84	BIOCARTA_TID_PATHWAY	19	1.19	0.250	0.360
85	BIOCARTA_GATA3_PATHWAY	16	1.18	0.277	0.370
86	BIOCARTA_TH1TH2_PATHWAY	19	1.17	0.251	0.383

87	BIOCARTA_FCER1_PATHWAY	38	1.16	0.243	0.395
88	BIOCARTA_AT1R_PATHWAY	32	1.15	0.299	0.409
89	BIOCARTA_GCR_PATHWAY	19	1.10	0.335	0.475
90	BIOCARTA_EIF_PATHWAY	16	1.10	0.356	0.473
91	BIOCARTA_PYK2_PATHWAY	28	1.10	0.316	0.470
92	BIOCARTA_ERK_PATHWAY	28	1.10	0.328	0.466
93	BIOCARTA_GSK3_PATHWAY	27	1.09	0.345	0.475
94	BIOCARTA_ECM_PATHWAY	24	1.08	0.346	0.481
95	BIOCARTA_MTA3_PATHWAY	17	1.07	0.372	0.491
96	BIOCARTA_P53HYPOXIA_PATHWAY	22	1.05	0.406	0.519
97	BIOCARTA_ERK5_PATHWAY	17	1.03	0.441	0.548
98	BIOCARTA_PAR1_PATHWAY	37	1.03	0.402	0.543
99	BIOCARTA_INFLAM_PATHWAY	28	1.03	0.438	0.538
100	BIOCARTA_LONGEVITY_PATHWAY	15	1.03	0.426	0.537
101	BIOCARTA_G2_PATHWAY	24	1.02	0.443	0.549
102	BIOCARTA_STATHMIN_PATHWAY	19	1.01	0.463	0.548
103	BIOCARTA_CERAMIDE_PATHWAY	22	0.99	0.489	0.581
104	BIOCARTA_ALK_PATHWAY	37	0.99	0.463	0.576
105	BIOCARTA_ACH_PATHWAY	16	0.98	0.490	0.583
106	BIOCARTA_P53_PATHWAY	16	0.97	0.502	0.595
107	BIOCARTA_CYTOKINE_PATHWAY	20	0.96	0.525	0.604
108	BIOCARTA_CK1_PATHWAY	17	0.96	0.503	0.604
109	BIOCARTA_RHO_PATHWAY	31	0.96	0.522	0.601
110	BIOCARTA_EDG1_PATHWAY	27	0.93	0.566	0.637
111	BIOCARTA_CDC42RAC_PATHWAY	15	0.93	0.544	0.638
112	BIOCARTA_UCALPAIN_PATHWAY	18	0.90	0.605	0.678
113	BIOCARTA_CHEMICAL_PATHWAY	22	0.89	0.611	0.683
114	BIOCARTA_NFAT_PATHWAY	53	0.89	0.634	0.678
115	BIOCARTA_CASPASE_PATHWAY	23	0.87	0.630	0.705
116	BIOCARTA_TFF_PATHWAY	21	0.86	0.658	0.722
117	BIOCARTA_ACTINY_PATHWAY	19	0.85	0.657	0.722
118	BIOCARTA_CHREBP2_PATHWAY	42	0.85	0.692	0.718
119	BIOCARTA_GH_PATHWAY	27	0.85	0.669	0.719
120	BIOCARTA_DEATH_PATHWAY	33	0.84	0.714	0.717
121	BIOCARTA_INTEGRIN_PATHWAY	38	0.83	0.709	0.725
122	BIOCARTA_HER2_PATHWAY	22	0.78	0.778	0.801
123	BIOCARTA_HSP27_PATHWAY	15	0.68	0.888	0.916
124	BIOCARTA_NDKDYNAMIN_PATHWAY	16	0.66	0.873	0.927
125	BIOCARTA_CCR3_PATHWAY	23	0.65	0.919	0.925
126	BIOCARTA_BARRESTIN_SRC_PATHWAY	15	0.64	0.889	0.925

Table S3. Upregulated gene sets in cases with mutations in the RAS-BRAF-MAPK-ERK pathway with c2.cp.KEGG analysis.

	NAME	SIZE	NES	NOM p-val	FDR q-val
1	KEGG_COLORECTAL_CANCER	62	2.13	0.000	0.001
2	KEGG_ACUTE_MYELOID_LEUKEMIA	57	2.06	0.000	0.001
3	KEGG_T_CELL_RECEPTOR_SIGNALING_PATHWAY	107	1.91	0.000	0.011
4	KEGG_CHRONIC_MYELOID_LEUKEMIA	72	1.88	0.000	0.011
5	**KEGG_MAPK_SIGNALING_PATHWAY**	**264**	**1.85**	**0.000**	**0.013**
6	KEGG_B_CELL_RECEPTOR_SIGNALING_PATHWAY	75	1.83	0.000	0.016
7	KEGG_LEUKOCYTE_TRANSENDOTHELIAL_MIGRATION	113	1.79	0.000	0.021
8	KEGG_ALDOSTERONE_REGULATED_SODIUM_REABSORPTION	41	1.76	0.003	0.028
9	KEGG_NATURAL_KILLER_CELL_MEDIATED_CYTOTOXICITY	127	1.73	0.000	0.035
10	KEGG_MTOR_SIGNALING_PATHWAY	51	1.71	0.007	0.039
11	KEGG_SPLICEOSOME	124	1.71	0.000	0.036
12	KEGG_PANCREATIC_CANCER	70	1.70	0.002	0.036
13	KEGG_RENAL_CELL_CARCINOMA	70	1.68	0.005	0.040
14	KEGG_ENDOMETRIAL_CANCER	52	1.68	0.003	0.038
15	KEGG_TOLL_LIKE_RECEPTOR_SIGNALING_PATHWAY	98	1.66	0.000	0.045
16	KEGG_MELANOMA	71	1.61	0.011	0.069
17	KEGG_FC_GAMMA_R_MEDIATED_PHAGOCYTOSIS	91	1.58	0.006	0.080
18	KEGG_LEISHMANIA_INFECTION	68	1.58	0.008	0.078
19	KEGG_NON_SMALL_CELL_LUNG_CANCER	54	1.58	0.034	0.077
20	KEGG_HEMATOPOIETIC_CELL_LINEAGE	85	1.57	0.006	0.078
21	KEGG_CELL_CYCLE	123	1.57	0.001	0.075
22	KEGG_PATHWAYS_IN_CANCER	325	1.55	0.000	0.086
23	KEGG_SMALL_CELL_LUNG_CANCER	84	1.53	0.013	0.092
24	KEGG_ERBB_SIGNALING_PATHWAY	86	1.52	0.014	0.101
25	KEGG_PHOSPHATIDYLINOSITOL_SIGNALING_SYSTEM	76	1.50	0.013	0.110
26	KEGG_BLADDER_CANCER	42	1.50	0.027	0.106
27	KEGG_THYROID_CANCER	29	1.48	0.055	0.120
28	KEGG_PRION_DISEASES	35	1.44	0.057	0.159
29	KEGG_TGF_BETA_SIGNALING_PATHWAY	85	1.41	0.031	0.188
30	KEGG_GLIOMA	64	1.41	0.051	0.188
31	KEGG_ENDOCYTOSIS	180	1.40	0.017	0.185
32	KEGG_RIG_I_LIKE_RECEPTOR_SIGNALING_PATHWAY	69	1.40	0.061	0.186
33	KEGG_ADIPOCYTOKINE_SIGNALING_PATHWAY	66	1.39	0.066	0.186
34	KEGG_NOTCH_SIGNALING_PATHWAY	47	1.36	0.091	0.222
35	KEGG_PRIMARY_IMMUNODEFICIENCY	35	1.36	0.096	0.226
36	KEGG_INOSITOL_PHOSPHATE_METABOLISM	54	1.35	0.085	0.230
37	KEGG_REGULATION_OF_ACTIN_CYTOSKELETON	208	1.35	0.024	0.230
38	KEGG_ARRHYTHMOGENIC_RIGHT_VENTRICULAR_CARDIOMYOPATHY_ARVC	74	1.34	0.073	0.236
39	KEGG_STEROID_BIOSYNTHESIS	15	1.34	0.154	0.230
40	KEGG_NEUROTROPHIN_SIGNALING_PATHWAY	125	1.34	0.055	0.227
41	KEGG_PROSTATE_CANCER	88	1.30	0.084	0.267

42	KEGG_JAK_STAT_SIGNALING_PATHWAY	150	1.30	0.070	0.276
43	KEGG_OTHER_GLYCAN_DEGRADATION	16	1.29	0.182	0.274
44	KEGG_RIBOSOME	85	1.29	0.102	0.279
45	KEGG_WNT_SIGNALING_PATHWAY	150	1.27	0.086	0.308
46	KEGG_CYTOSOLIC_DNA_SENSING_PATHWAY	51	1.26	0.128	0.312
47	KEGG_SPHINGOLIPID_METABOLISM	38	1.22	0.180	0.377
48	KEGG_FOCAL_ADHESION	196	1.20	0.120	0.409
49	KEGG_ECM_RECEPTOR_INTERACTION	83	1.19	0.178	0.426
50	KEGG_EPITHELIAL_CELL_SIGNALING_IN_HELICOBACTER_PYLORI_INFECTION	68	1.19	0.197	0.422
51	KEGG_CELL_ADHESION_MOLECULES_CAMS	130	1.18	0.174	0.433
52	KEGG_FC_EPSILON_RI_SIGNALING_PATHWAY	76	1.17	0.211	0.449
53	KEGG_VEGF_SIGNALING_PATHWAY	73	1.16	0.225	0.466
54	KEGG_HYPERTROPHIC_CARDIOMYOPATHY_HCM	83	1.16	0.212	0.458
55	KEGG_FRUCTOSE_AND_MANNOSE_METABOLISM	34	1.14	0.303	0.481
56	KEGG_INSULIN_SIGNALING_PATHWAY	135	1.10	0.259	0.568
57	KEGG_CHEMOKINE_SIGNALING_PATHWAY	179	1.10	0.267	0.569
58	KEGG_RNA_DEGRADATION	57	1.09	0.315	0.565
59	KEGG_DILATED_CARDIOMYOPATHY	90	1.09	0.296	0.556
60	KEGG_LYSOSOME	120	1.08	0.310	0.571
61	KEGG_P53_SIGNALING_PATHWAY	67	1.08	0.332	0.574
62	KEGG_NOD_LIKE_RECEPTOR_SIGNALING_PATHWAY	62	1.08	0.338	0.565
63	KEGG_PENTOSE_PHOSPHATE_PATHWAY	27	1.06	0.360	0.589
64	KEGG_PROGESTERONE_MEDIATED_OOCYTE_MATURATION	84	1.05	0.368	0.618
65	KEGG_UBIQUITIN_MEDIATED_PROTEOLYSIS	134	1.03	0.401	0.647
66	KEGG_LYSINE_DEGRADATION	44	1.03	0.397	0.642
67	KEGG_APOPTOSIS	87	1.03	0.428	0.640
68	KEGG_TIGHT_JUNCTION	131	1.02	0.415	0.648
69	KEGG_BASAL_CELL_CARCINOMA	55	1.02	0.411	0.645
70	KEGG_TYPE_II_DIABETES_MELLITUS	46	1.02	0.418	0.637
71	KEGG_GLYCOLYSIS_GLUCONEOGENESIS	62	1.02	0.426	0.629
72	KEGG_RIBOFLAVIN_METABOLISM	16	1.01	0.454	0.629
73	KEGG_PYRIMIDINE_METABOLISM	93	1.01	0.438	0.625
74	KEGG_VIBRIO_CHOLERAE_INFECTION	54	1.01	0.416	0.620
75	KEGG_AMINOACYL_TRNA_BIOSYNTHESIS	41	0.97	0.516	0.708
76	KEGG_ADHERENS_JUNCTION	73	0.96	0.507	0.710
77	KEGG_GALACTOSE_METABOLISM	26	0.96	0.516	0.707
78	KEGG_PROTEASOME	44	0.96	0.533	0.701
79	KEGG_PANTOTHENATE_AND_COA_BIOSYNTHESIS	16	0.95	0.534	0.708
80	KEGG_PROTEIN_EXPORT	23	0.95	0.535	0.711
81	KEGG_NICOTINATE_AND_NICOTINAMIDE_METABOLISM	23	0.94	0.547	0.729
82	KEGG_CARDIAC_MUSCLE_CONTRACTION	74	0.94	0.574	0.724
83	KEGG_MATURITY_ONSET_DIABETES_OF_THE_YOUNG	24	0.93	0.562	0.734
84	KEGG_GLYCOSPHINGOLIPID_BIOSYNTHESIS_GANGLIO_SERIES	15	0.90	0.619	0.794
85	KEGG_GLYCEROPHOSPHOLIPID_METABOLISM	73	0.89	0.667	0.797

86	KEGG_REGULATION_OF_AUTOPHAGY	31	0.88	0.631	0.799
87	KEGG_PROXIMAL_TUBULE_BICARBONATE_RECLAMATION	23	0.88	0.631	0.791
88	KEGG_OOCYTE_MEIOSIS	110	0.88	0.705	0.784
89	KEGG_PHENYLALANINE_METABOLISM	18	0.87	0.644	0.809
90	KEGG_GLYCEROLIPID_METABOLISM	48	0.84	0.734	0.863
91	KEGG_GLYCOSAMINOGLYCAN_BIOSYNTHESIS_CHONDROITIN_SULFATE	22	0.82	0.720	0.884
92	KEGG_RNA_POLYMERASE	27	0.81	0.749	0.882
93	KEGG_CYSTEINE_AND_METHIONINE_METABOLISM	34	0.80	0.762	0.895
94	KEGG_ALZHEIMERS_DISEASE	158	0.79	0.895	0.907
95	KEGG_COMPLEMENT_AND_COAGULATION_CASCADES	67	0.77	0.842	0.925
96	KEGG_LONG_TERM_DEPRESSION	67	0.77	0.856	0.920
97	KEGG_TERPENOID_BACKBONE_BIOSYNTHESIS	15	0.76	0.769	0.915
98	KEGG_BASAL_TRANSCRIPTION_FACTORS	33	0.76	0.803	0.906
99	KEGG_LONG_TERM_POTENTIATION	70	0.74	0.906	0.934
100	KEGG_BASE_EXCISION_REPAIR	33	0.73	0.868	0.927
101	KEGG_ETHER_LIPID_METABOLISM	31	0.71	0.855	0.941
102	KEGG_DRUG_METABOLISM_OTHER_ENZYMES	42	0.69	0.925	0.948
103	KEGG_CITRATE_CYCLE_TCA_CYCLE	30	0.68	0.907	0.950
104	KEGG_AXON_GUIDANCE	129	0.66	0.990	0.952

Table S4. Genes of the Biocarta-MAPK pathway

	GENE SYMBOL	GENE_TITLE	CORE ENRICHMENT
1	ARAF	v-raf murine sarcoma 3611 viral oncogene homolog	Yes
2	ATF2	activating transcription factor 2	No
3	BRAF	v-raf murine sarcoma viral oncogene homolog B1	No
4	CEBPA	CCAAT/enhancer binding protein (C/EBP), alpha	No
5	CHUK	conserved helix-loop-helix ubiquitous kinase	Yes
6	CREB1	cAMP responsive element binding protein 1	No
7	DAXX	death-associated protein 6	No
8	ELK1	ELK1, member of ETS oncogene family	No
9	FOS	v-fos FBJ murine osteosarcoma viral oncogene homolog	Yes
10	GRB2	growth factor receptor-bound protein 2	No
11	HRAS	v-Ha-ras Harvey rat sarcoma viral oncogene homolog	Yes
12	IKBKB	inhibitor of kappa light polypeptide gene enhancer in B-cells, kinase beta	No
13	JUN	jun oncogene	Yes
14	MAP2K1	mitogen-activated protein kinase kinase 1	No
15	MAP2K2	mitogen-activated protein kinase kinase 2	Yes
16	MAP2K3	mitogen-activated protein kinase kinase 3	Yes
17	MAP2K4	mitogen-activated protein kinase kinase 4	No
18	MAP2K5	mitogen-activated protein kinase kinase 5	Yes
19	MAP2K6	mitogen-activated protein kinase kinase 6	Yes
20	MAP2K7	mitogen-activated protein kinase kinase 7	No
21	MAP3K1	mitogen-activated protein kinase kinase kinase 1	Yes
22	MAP3K10	mitogen-activated protein kinase kinase kinase 10	No
23	MAP3K11	mitogen-activated protein kinase kinase kinase 11	No
24	MAP3K12	mitogen-activated protein kinase kinase kinase 12	Yes
25	MAP3K13	mitogen-activated protein kinase kinase kinase 13	No
26	MAP3K14	mitogen-activated protein kinase kinase kinase 14	No
27	MAP3K2	mitogen-activated protein kinase kinase kinase 2	No
28	MAP3K3	mitogen-activated protein kinase kinase kinase 3	No
29	MAP3K4	mitogen-activated protein kinase kinase kinase 4	Yes
30	MAP3K5	mitogen-activated protein kinase kinase kinase 5	No
31	MAP3K6	mitogen-activated protein kinase kinase kinase 6	No
32	MAP3K7	mitogen-activated protein kinase kinase kinase 7	Yes
33	MAP3K8	mitogen-activated protein kinase kinase kinase 8	Yes
34	MAP3K9	mitogen-activated protein kinase kinase kinase 9	No
35	MAP4K1	mitogen-activated protein kinase kinase kinase kinase 1	No
36	MAP4K2	mitogen-activated protein kinase kinase kinase kinase 2	Yes
37	MAP4K3	mitogen-activated protein kinase kinase kinase kinase 3	Yes
38	MAP4K4	mitogen-activated protein kinase kinase kinase kinase 4	Yes
39	MAP4K5	mitogen-activated protein kinase kinase kinase kinase 5	No
40	MAPK1	mitogen-activated protein kinase 1	No
41	MAPK10	mitogen-activated protein kinase 10	No
42	MAPK11	mitogen-activated protein kinase 11	No

43	MAPK12	mitogen-activated protein kinase 12	No
44	MAPK13	mitogen-activated protein kinase 13	No
45	MAPK14	mitogen-activated protein kinase 14	No
46	MAPK3	mitogen-activated protein kinase 3	No
47	MAPK4	mitogen-activated protein kinase 4	Yes
48	MAPK6	mitogen-activated protein kinase 6	Yes
49	MAPK7	mitogen-activated protein kinase 7	No
50	MAPK8	mitogen-activated protein kinase 8	No
51	MAPK9	mitogen-activated protein kinase 9	No
52	MAPKAPK2	mitogen-activated protein kinase-activated protein kinase 2	No
53	MAPKAPK3	mitogen-activated protein kinase-activated protein kinase 3	No
54	MAPKAPK5	mitogen-activated protein kinase-activated protein kinase 5	Yes
55	MAX	MYC associated factor X	No
56	MEF2A	MADS box transcription enhancer factor 2, polypeptide A (myocyte enhancer factor 2A)	No
57	MEF2C	MADS box transcription enhancer factor 2, polypeptide C (myocyte enhancer factor 2C)	No
58	MEF2D	MADS box transcription enhancer factor 2, polypeptide D (myocyte enhancer factor 2D)	Yes
59	MKNK1	MAP kinase interacting serine/threonine kinase 1	No
60	MKNK2	MAP kinase interacting serine/threonine kinase 2	Yes
61	MYC	v-myc myelocytomatosis viral oncogene homolog (avian)	Yes
62	NFKB1	nuclear factor of kappa light polypeptide gene enhancer in B-cells 1 (p105)	Yes
63	NFKBIA	nuclear factor of kappa light polypeptide gene enhancer in B-cells inhibitor, alpha	No
64	PAK1	p21/Cdc42/Rac1-activated kinase 1 (STE20 homolog, yeast)	Yes
65	PAK2	p21 (CDKN1A)-activated kinase 2	No
66	RAC1	ras-related C3 botulinum toxin substrate 1 (rho family, small GTP binding protein Rac1)	Yes
67	RAF1	v-raf-1 murine leukemia viral oncogene homolog 1	No
68	RAPGEF2	Rap guanine nucleotide exchange factor (GEF) 2	No
69	RELA	v-rel reticuloendotheliosis viral oncogene homolog A, nuclear factor of kappa light polypeptide gene enhancer in B-cells 3, p65 (avian)	Yes
70	RIPK1	receptor (TNFRSF)-interacting serine-threonine kinase 1	Yes
71	RPS6KA1	ribosomal protein S6 kinase, 90kDa, polypeptide 1	No
72	RPS6KA2	ribosomal protein S6 kinase, 90kDa, polypeptide 2	No
73	RPS6KA3	ribosomal protein S6 kinase, 90kDa, polypeptide 3	No
74	RPS6KA4	ribosomal protein S6 kinase, 90kDa, polypeptide 4	Yes
75	RPS6KA5	ribosomal protein S6 kinase, 90kDa, polypeptide 5	Yes
76	RPS6KB1	ribosomal protein S6 kinase, 70kDa, polypeptide 1	Yes
77	RPS6KB2	ribosomal protein S6 kinase, 70kDa, polypeptide 2	No
78	SHC1	SHC (Src homology 2 domain containing) transforming protein 1	Yes
79	SP1	Sp1 transcription factor	Yes
80	STAT1	signal transducer and activator of transcription 1, 91kDa	No
81	TGFB1	transforming growth factor, beta 1 (Camurati-Engelmann disease)	Yes
82	TGFB2	transforming growth factor, beta 2	No
83	TGFB3	transforming growth factor, beta 3	No
84	TGFBR1	transforming growth factor, beta receptor I (activin A receptor type II-like kinase, 53kDa)	Yes
85	TRADD	TNFRSF1A-associated via death domain	No
86	TRAF2	TNF receptor-associated factor 2	Yes

Table S5. Genes of the KEGG-MAPK SIGNALING pathway

	GENE SYMBOL	GENE_TITLE	CORE ENRICHMENT
1	AKT1	v-akt murine thymoma viral oncogene homolog 1	No
2	AKT2	v-akt murine thymoma viral oncogene homolog 2	No
3	AKT3	v-akt murine thymoma viral oncogene homolog 3 (protein kinase B, gamma)	Yes
4	ARRB1	arrestin, beta 1	No
5	ARRB2	arrestin, beta 2	Yes
6	ATF2	activating transcription factor 2	No
7	ATF4	activating transcription factor 4 (tax-responsive enhancer element B67)	Yes
8	BDNF	brain-derived neurotrophic factor	No
9	BRAF	v-raf murine sarcoma viral oncogene homolog B1	No
10	CACNA1A	calcium channel, voltage-dependent, P/Q type, alpha 1A subunit	No
11	CACNA1B	calcium channel, voltage-dependent, L type, alpha 1B subunit	No
12	CACNA1C	calcium channel, voltage-dependent, L type, alpha 1C subunit	No
13	CACNA1D	calcium channel, voltage-dependent, L type, alpha 1D subunit	No
14	CACNA1E	calcium channel, voltage-dependent, alpha 1E subunit	No
15	CACNA1F	calcium channel, voltage-dependent, alpha 1F subunit	No
16	CACNA1G	calcium channel, voltage-dependent, alpha 1G subunit	No
17	CACNA1H	calcium channel, voltage-dependent, alpha 1H subunit	No
18	CACNA1I	calcium channel, voltage-dependent, alpha 1I subunit	No
19	CACNA1S	calcium channel, voltage-dependent, L type, alpha 1S subunit	No
20	CACNA2D1	calcium channel, voltage-dependent, alpha 2/delta subunit 1	No
21	CACNA2D2	calcium channel, voltage-dependent, alpha 2/delta subunit 2	No
22	CACNA2D3	calcium channel, voltage-dependent, alpha 2/delta 3 subunit	No
23	CACNA2D4	calcium channel, voltage-dependent, alpha 2/delta subunit 4	Yes
24	CACNB1	calcium channel, voltage-dependent, beta 1 subunit	No
25	CACNB2	calcium channel, voltage-dependent, beta 2 subunit	Yes
26	CACNB3	calcium channel, voltage-dependent, beta 3 subunit	No
27	CACNB4	calcium channel, voltage-dependent, beta 4 subunit	No
28	CACNG1	calcium channel, voltage-dependent, gamma subunit 1	No
29	CACNG2	calcium channel, voltage-dependent, gamma subunit 2	No
30	CACNG3	calcium channel, voltage-dependent, gamma subunit 3	No
31	CACNG4	calcium channel, voltage-dependent, gamma subunit 4	No
32	CACNG5	calcium channel, voltage-dependent, gamma subunit 5	No
33	CACNG6	calcium channel, voltage-dependent, gamma subunit 6	No
34	CACNG7	calcium channel, voltage-dependent, gamma subunit 7	No
35	CACNG8	calcium channel, voltage-dependent, gamma subunit 8	No
36	CASP3	caspase 3, apoptosis-related cysteine peptidase	No
37	CD14	CD14 molecule	Yes
38	CDC25B	cell division cycle 25B	No
39	CDC42	cell division cycle 42 (GTP binding protein, 25kDa)	No
40	CHP	-	No

41	CHP2	-	No
42	CHUK	conserved helix-loop-helix ubiquitous kinase	Yes
43	CRK	v-crk sarcoma virus CT10 oncogene homolog (avian)	No
44	CRKL	v-crk sarcoma virus CT10 oncogene homolog (avian)-like	No
45	DAXX	death-associated protein 6	No
46	DDIT3	DNA-damage-inducible transcript 3	Yes
47	DUSP1	dual specificity phosphatase 1	Yes
48	DUSP10	dual specificity phosphatase 10	Yes
49	DUSP14	dual specificity phosphatase 14	No
50	DUSP16	dual specificity phosphatase 16	No
51	DUSP2	dual specificity phosphatase 2	Yes
52	DUSP3	dual specificity phosphatase 3 (vaccinia virus phosphatase VH1-related)	No
53	DUSP4	dual specificity phosphatase 4	No
54	DUSP5	dual specificity phosphatase 5	Yes
55	DUSP6	dual specificity phosphatase 6	Yes
56	DUSP7	dual specificity phosphatase 7	No
57	DUSP8	dual specificity phosphatase 8	Yes
58	DUSP9	dual specificity phosphatase 9	No
59	ECSIT	ECSIT homolog (Drosophila)	Yes
60	EGF	epidermal growth factor (beta-urogastrone)	No
61	EGFR	epidermal growth factor receptor (erythroblastic leukemia viral (v-erb-b) oncogene homolog, avian)	No
62	ELK1	ELK1, member of ETS oncogene family	No
63	ELK4	ELK4, ETS-domain protein (SRF accessory protein 1)	No
64	FAS	Fas (TNF receptor superfamily, member 6)	No
65	FASLG	Fas ligand (TNF superfamily, member 6)	No
66	FGF1	fibroblast growth factor 1 (acidic)	No
67	FGF10	fibroblast growth factor 10	No
68	FGF11	fibroblast growth factor 11	No
69	FGF12	fibroblast growth factor 12	No
70	FGF13	fibroblast growth factor 13	No
71	FGF14	fibroblast growth factor 14	No
72	FGF16	fibroblast growth factor 16	No
73	FGF17	fibroblast growth factor 17	No
74	FGF18	fibroblast growth factor 18	No
75	FGF19	fibroblast growth factor 19	No
76	FGF2	fibroblast growth factor 2 (basic)	Yes
77	FGF20	fibroblast growth factor 20	No
78	FGF21	fibroblast growth factor 21	No
79	FGF22	fibroblast growth factor 22	No
80	FGF23	fibroblast growth factor 23	No
81	FGF3	fibroblast growth factor 3 (murine mammary tumor virus integration site (v-int-2) oncogene homolog)	No
82	FGF4	fibroblast growth factor 4 (heparin secretory transforming protein 1, Kaposi sarcoma oncogene)	No

83	FGF5	fibroblast growth factor 5	No
84	FGF6	fibroblast growth factor 6	No
85	FGF7	fibroblast growth factor 7 (keratinocyte growth factor)	No
86	FGF8	fibroblast growth factor 8 (androgen-induced)	No
87	FGF9	fibroblast growth factor 9 (glia-activating factor)	No
88	FGFR1	fibroblast growth factor receptor 1 (fms-related tyrosine kinase 2, Pfeiffer syndrome)	No
89	FGFR2	ffer syndrome, Jackson-Weiss syndrome)	No
90	FGFR3	fibroblast growth factor receptor 3 (achondroplasia, thanatophoric dwarfism)	No
91	FGFR4	fibroblast growth factor receptor 4	No
92	FLNA	filamin A, alpha (actin binding protein 280)	No
93	FLNB	filamin B, beta (actin binding protein 278)	Yes
94	FLNC	filamin C, gamma (actin binding protein 280)	No
95	FOS	v-fos FBJ murine osteosarcoma viral oncogene homolog	Yes
96	GADD45A	growth arrest and DNA-damage-inducible, alpha	No
97	GADD45B	growth arrest and DNA-damage-inducible, beta	Yes
98	GADD45G	growth arrest and DNA-damage-inducible, gamma	No
99	GNA12	guanine nucleotide binding protein (G protein) alpha 12	No
100	GNG12	guanine nucleotide binding protein (G protein), gamma 12	No
101	GRB2	growth factor receptor-bound protein 2	No
102	HRAS	v-Ha-ras Harvey rat sarcoma viral oncogene homolog	Yes
103	HSPA1A	heat shock 70kDa protein 1A	No
104	HSPA1B	heat shock 70kDa protein 1B	Yes
105	HSPA1L	heat shock 70kDa protein 1-like	No
106	HSPA2	heat shock 70kDa protein 2	No
107	HSPA6	heat shock 70kDa protein 6 (HSP70B')	No
108	HSPA8	heat shock 70kDa protein 8	Yes
109	HSPB1	heat shock 27kDa protein 1	No
110	IKBKB	inhibitor of kappa light polypeptide gene enhancer in B-cells, kinase beta	No
111	IKBKG	inhibitor of kappa light polypeptide gene enhancer in B-cells, kinase gamma	No
112	IL1A	interleukin 1, alpha	No
113	IL1B	interleukin 1, beta	No
114	IL1R1	interleukin 1 receptor, type I	No
115	IL1R2	interleukin 1 receptor, type II	No
116	JUN	jun oncogene	Yes
117	JUND	jun D proto-oncogene	Yes
118	KRAS	v-Ki-ras2 Kirsten rat sarcoma viral oncogene homolog	Yes
119	MAP2K1	mitogen-activated protein kinase kinase 1	No
120	MAP2K2	mitogen-activated protein kinase kinase 2	Yes
121	MAP2K3	mitogen-activated protein kinase kinase 3	Yes
122	MAP2K4	mitogen-activated protein kinase kinase 4	No
123	MAP2K5	mitogen-activated protein kinase kinase 5	Yes
124	MAP2K6	mitogen-activated protein kinase kinase 6	No
125	MAP2K7	mitogen-activated protein kinase kinase 7	No

126	MAP3K1	mitogen-activated protein kinase kinase kinase 1	Yes
127	MAP3K11	mitogen-activated protein kinase kinase kinase 11	No
128	MAP3K12	mitogen-activated protein kinase kinase kinase 12	Yes
129	MAP3K13	mitogen-activated protein kinase kinase kinase 13	No
130	MAP3K14	mitogen-activated protein kinase kinase kinase 14	No
131	MAP3K2	mitogen-activated protein kinase kinase kinase 2	No
132	MAP3K3	mitogen-activated protein kinase kinase kinase 3	No
133	MAP3K4	mitogen-activated protein kinase kinase kinase 4	Yes
134	MAP3K5	mitogen-activated protein kinase kinase kinase 5	No
135	MAP3K6	mitogen-activated protein kinase kinase kinase 6	No
136	MAP3K7	mitogen-activated protein kinase kinase kinase 7	No
137	MAP3K8	mitogen-activated protein kinase kinase kinase 8	Yes
138	MAP4K1	mitogen-activated protein kinase kinase kinase kinase 1	No
139	MAP4K2	mitogen-activated protein kinase kinase kinase kinase 2	No
140	MAP4K3	mitogen-activated protein kinase kinase kinase kinase 3	Yes
141	MAP4K4	mitogen-activated protein kinase kinase kinase kinase 4	Yes
142	MAPK1	mitogen-activated protein kinase 1	No
143	MAPK10	mitogen-activated protein kinase 10	No
144	MAPK11	mitogen-activated protein kinase 11	No
145	MAPK12	mitogen-activated protein kinase 12	No
146	MAPK13	mitogen-activated protein kinase 13	No
147	MAPK14	mitogen-activated protein kinase 14	No
148	MAPK3	mitogen-activated protein kinase 3	No
149	MAPK7	mitogen-activated protein kinase 7	No
150	MAPK8	mitogen-activated protein kinase 8	No
151	MAPK8IP1	mitogen-activated protein kinase 8 interacting protein 1	No
152	MAPK8IP2	mitogen-activated protein kinase 8 interacting protein 2	No
153	MAPK8IP3	mitogen-activated protein kinase 8 interacting protein 3	Yes
154	MAPK9	mitogen-activated protein kinase 9	No
155	MAPKAPK2	mitogen-activated protein kinase-activated protein kinase 2	No
156	MAPKAPK3	mitogen-activated protein kinase-activated protein kinase 3	No
157	MAPKAPK5	mitogen-activated protein kinase-activated protein kinase 5	Yes
158	MAPT	microtubule-associated protein tau	No
159	MAX	MYC associated factor X	No
160	MECOM	-	No
161	MEF2C	MADS box transcription enhancer factor 2, polypeptide C (myocyte enhancer factor 2C)	No
162	MKNK1	MAP kinase interacting serine/threonine kinase 1	No
163	MKNK2	MAP kinase interacting serine/threonine kinase 2	No
164	MOS	v-mos Moloney murine sarcoma viral oncogene homolog	No
165	MRAS	muscle RAS oncogene homolog	No
166	MYC	v-myc myelocytomatosis viral oncogene homolog (avian)	Yes
167	NF1	neurofibromin 1 (neurofibromatosis, von Recklinghausen disease, Watson disease)	Yes
168	NFATC2	nuclear factor of activated T-cells, cytoplasmic, calcineurin-dependent 2	No

169	NFATC4	nuclear factor of activated T-cells, cytoplasmic, calcineurin-dependent 4	No
170	NFKB1	nuclear factor of kappa light polypeptide gene enhancer in B-cells 1 (p105)	Yes
171	NFKB2	nuclear factor of kappa light polypeptide gene enhancer in B-cells 2 (p49/p100)	No
172	NGF	-	No
173	NLK	nemo-like kinase	No
174	NR4A1	nuclear receptor subfamily 4, group A, member 1	Yes
175	NRAS	neuroblastoma RAS viral (v-ras) oncogene homolog	No
176	NTF3	neurotrophin 3	No
177	NTF4	null	No
178	NTRK1	neurotrophic tyrosine kinase, receptor, type 1	No
179	NTRK2	neurotrophic tyrosine kinase, receptor, type 2	No
180	PAK1	p21/Cdc42/Rac1-activated kinase 1 (STE20 homolog, yeast)	Yes
181	PAK2	p21 (CDKN1A)-activated kinase 2	No
182	PDGFA	platelet-derived growth factor alpha polypeptide	Yes
183	PDGFB	platelet-derived growth factor beta polypeptide (simian sarcoma viral (v-sis) oncogene homolog)	No
184	PDGFRA	platelet-derived growth factor receptor, alpha polypeptide	No
185	PDGFRB	platelet-derived growth factor receptor, beta polypeptide	No
186	PLA2G10	phospholipase A2, group X	No
187	PLA2G12A	phospholipase A2, group XIIA	No
188	PLA2G12B	phospholipase A2, group XIIB	No
189	PLA2G1B	phospholipase A2, group IB (pancreas)	No
190	PLA2G2A	phospholipase A2, group IIA (platelets, synovial fluid)	No
191	PLA2G2C	phospholipase A2, group IIC	No
192	PLA2G2D	phospholipase A2, group IID	No
193	PLA2G2E	phospholipase A2, group IIE	No
194	PLA2G2F	phospholipase A2, group IIF	No
195	PLA2G3	phospholipase A2, group III	No
196	PLA2G4A	phospholipase A2, group IVA (cytosolic, calcium-dependent)	No
197	PLA2G4E	phospholipase A2, group IVE	No
198	PLA2G5	phospholipase A2, group V	No
199	PLA2G6	phospholipase A2, group VI (cytosolic, calcium-independent)	No
200	PPM1A	protein phosphatase 1A (formerly 2C), magnesium-dependent, alpha isoform	No
201	PPM1B	protein phosphatase 1B (formerly 2C), magnesium-dependent, beta isoform	Yes
202	PPP3CA	protein phosphatase 3 (formerly 2B), catalytic subunit, alpha isoform (calcineurin A alpha)	No
203	PPP3CB	protein phosphatase 3 (formerly 2B), catalytic subunit, beta isoform (calcineurin A beta)	No
204	PPP3CC	protein phosphatase 3 (formerly 2B), catalytic subunit, gamma isoform (calcineurin A gamma)	No
205	PPP3R1	protein phosphatase 3 (formerly 2B), regulatory subunit B, 19kDa, alpha isoform (calcineurin B, type I)	No
206	PPP3R2	protein phosphatase 3 (formerly 2B), regulatory subunit B, 19kDa, beta isoform (calcineurin B, type II)	No
207	PPP5C	protein phosphatase 5, catalytic subunit	Yes
208	PRKACA	protein kinase, cAMP-dependent, catalytic, alpha	No
209	PRKACB	protein kinase, cAMP-dependent, catalytic, beta	No

210	PRKACG	protein kinase, cAMP-dependent, catalytic, gamma	No
211	PRKCA	protein kinase C, alpha	Yes
212	PRKCB	-	No
213	PRKCG	protein kinase C, gamma	No
214	PRKX	protein kinase, X-linked	No
215	PTPN5	protein tyrosine phosphatase, non-receptor type 5 (striatum-enriched)	No
216	PTPN7	protein tyrosine phosphatase, non-receptor type 7	Yes
217	PTPRR	protein tyrosine phosphatase, receptor type, R	No
218	RAC1	ras-related C3 botulinum toxin substrate 1 (rho family, small GTP binding protein Rac1)	Yes
219	RAC2	ras-related C3 botulinum toxin substrate 2 (rho family, small GTP binding protein Rac2)	No
220	RAC3	ras-related C3 botulinum toxin substrate 3 (rho family, small GTP binding protein Rac3)	No
221	RAF1	v-raf-1 murine leukemia viral oncogene homolog 1	No
222	RAP1A	RAP1A, member of RAS oncogene family	No
223	RAP1B	RAP1B, member of RAS oncogene family	Yes
224	RAPGEF2	Rap guanine nucleotide exchange factor (GEF) 2	No
225	RASA1	RAS p21 protein activator (GTPase activating protein) 1	Yes
226	RASA2	RAS p21 protein activator 2	Yes
227	RASGRF1	Ras protein-specific guanine nucleotide-releasing factor 1	No
228	RASGRF2	Ras protein-specific guanine nucleotide-releasing factor 2	No
229	RASGRP1	RAS guanyl releasing protein 1 (calcium and DAG-regulated)	No
230	RASGRP2	RAS guanyl releasing protein 2 (calcium and DAG-regulated)	No
231	RASGRP3	RAS guanyl releasing protein 3 (calcium and DAG-regulated)	No
232	RASGRP4	RAS guanyl releasing protein 4	No
233	RELA	v-rel reticuloendotheliosis viral oncogene homolog A, nuclear factor of kappa light polypeptide gene enhancer in B-cells 3, p65 (avian)	Yes
234	RELB	v-rel reticuloendotheliosis viral oncogene homolog B, nuclear factor of kappa light polypeptide gene enhancer in B-cells 3 (avian)	Yes
235	RPS6KA1	ribosomal protein S6 kinase, 90kDa, polypeptide 1	No
236	RPS6KA2	ribosomal protein S6 kinase, 90kDa, polypeptide 2	No
237	RPS6KA3	ribosomal protein S6 kinase, 90kDa, polypeptide 3	No
238	RPS6KA4	ribosomal protein S6 kinase, 90kDa, polypeptide 4	No
239	RPS6KA5	ribosomal protein S6 kinase, 90kDa, polypeptide 5	No
240	RPS6KA6	ribosomal protein S6 kinase, 90kDa, polypeptide 6	No
241	RRAS	related RAS viral (r-ras) oncogene homolog	No
242	RRAS2	related RAS viral (r-ras) oncogene homolog 2	No
243	SOS1	son of sevenless homolog 1 (Drosophila)	No
244	SOS2	son of sevenless homolog 2 (Drosophila)	No
245	SRF	serum response factor (c-fos serum response element-binding transcription factor)	No
246	STK3	serine/threonine kinase 3 (STE20 homolog, yeast)	No
247	STK4	serine/threonine kinase 4	No
248	STMN1	stathmin 1/oncoprotein 18	No
249	TAB1	-	No
250	TAB2	-	No
251	TAOK1	TAO kinase 1	No

252	TAOK2	TAO kinase 2	No
253	TAOK3	TAO kinase 3	Yes
254	TGFB1	transforming growth factor, beta 1 (Camurati-Engelmann disease)	Yes
255	TGFB2	transforming growth factor, beta 2	No
256	TGFB3	transforming growth factor, beta 3	No
257	TGFBR1	transforming growth factor, beta receptor I (activin A receptor type II-like kinase, 53kDa)	Yes
258	TGFBR2	transforming growth factor, beta receptor II (70/80kDa)	No
259	TNF	tumor necrosis factor (TNF superfamily, member 2)	Yes
260	TNFRSF1A	tumor necrosis factor receptor superfamily, member 1A	Yes
261	TP53	tumor protein p53 (Li-Fraumeni syndrome)	Yes
262	TRAF2	TNF receptor-associated factor 2	Yes
263	TRAF6	TNF receptor-associated factor 6	No
264	ZAK	-	No

Article 3: Network-based drug discovery guided *in vitro* screening defines statins as a therapy to combine with current treatments in chronic lymphocytic leukemia

Giménez N, Tripathy R, Giró A, Mas JM, Rosich L, López-Guerra M, Perez-Galan P, Campo E, Farrés J[+], Colomer D[+]

In preparation

ABSTRACT

Chronic lymphocytic leukemia (CLL) is a B chronic lymphoid malignancy highly dependent on microenvironment. Although recently new targeted therapies such as ibrutinib and venetoclax has been introduced, progression and relapses remain an issue. By using a systems biology approach, we identified several motives to define CLL, being the microenvironment one of the most representatives. With the aim to identify drugs likely to be beneficial in CLL treatment by targeting the microenvironment, we have used a custom compound library composed of bioactive compounds (drug-like molecules) and approved drugs identified and prioritized using a platform for drug discovery based on systems biology and artificial intelligence. Initially we built molecular maps and unbiased proteomic data to identify key molecules. We screened these maps with a selection of drugs in CLL cell lines and we validated the selected drugs in primary CLL cells. Our results suggested that statins target CLL microenvironment and that statins might enhance the effect of ibrutinib or venetoclax in CLL cells.

[+]Share senior authorship

INTRODUCTION

Chronic lymphocytic leukemia (CLL) is a monoclonal disorder characterized by a progressive accumulation of mature functionally incompetent B cell lymphocytes (CD19^{+}) in which microenvironmental signals play a critical role in ontogeny and evolution.1 Recently new targeted therapies have been approved for CLL such as ibrutinib, a BTK inhibitor targeting the B cell receptor (BCR) signaling and venetoclax, a BCL2 inhibitor, both having significantly prolonged progression-free survival (PFS).[2] Ibrutinib in addition to interfering with BCR signaling pathways as its primary mechanism of action, ibrutinib appears to block survival signals delivered by the microenvironment, which may include cell–cell contact and cytokines that modulate cell migration, trafficking, and proliferation.[3, 4] The microenvironment in the bone marrow (BM) and in the secondary lymphoid organs plays a crucial role in sustaining the viability of CLL cells and still represent a major obstacle to achieve curative responses.[5]

Most of the approaches to develop anticancer therapies include selectively targeting tumor cells and inhibition of supportive signals from the microenvironment. One of the major goals is to identify new targets for therapeutic intervention. Systems biology presents a natural complement to ongoing efforts in cell biology integrating information about the parts (e.g., genes, proteins) of a complex biological system to predicting the behaviour of the whole. In the same manner this type of analysis can evaluate the pleiotropic effect of large compound libraries and existing drugs.[6]

With the aim of targeting the microenvironment effect on B-cells and with no commercial chemical library available for this purpose we have used a custom compound library composed of bioactive compounds and drugs identified and prioritized using a systems biology-based approach.[7] On the bases of the existing molecular knowledge on CLL microenvironment effects and the existing knowledge of the interactors of these proteins we have built a human protein network. Bioactive compounds with known targets and existing drugs have been screened *in silico* for their potential of affecting the CLL microenvironment network built. These compounds were tested in CLL cell lines alone and in the presence of stromal cells to mimic the microenvironment. Then selected drugs were validated in primary CLL cells alone and in the presence of stromal cells.

MATERIALS AND METHODS

Identification of key molecules involved in microenvironment of CLL cells

The molecular characterization of 'CLL microenvironment' has been performed through manual curation of the literature to identify proteins (effectors) with a known role on the microenvironment effect on CLL (Supplemental Table S2). The final selected set streams from 152 full-length articles in PubMed published until 2012 (Supplemental Table S1). To narrow down the analysis a subset of proteins "Key Proteins" with a higher probability of having a larger effect on the microenvironment as a whole when their pathological function is counteracted have been identified using a combination of systems biology-based metrics. Effector proteins are evaluated in the context of human functional protein network. The network structure assembled significantly constrains but does not uniquely determine the dependency relationships among proteins. On the bases this network we have applied different mathematical modelling strategies. Models were trained using a collection of drug - indication relationships. Drug targets and indications where obtained from DrugBank, the molecular description of the indications was retrieved from BED (Biological Effectors Database, Anaxomics Biotech) a hand-curated collection of scientific knowledge relating biological processes (indications) to their molecular effectors (key proteins with a functional role in the biological processes).

Two different mathematical modelling strategies were used:

i) Modelling based on Artificial Neural Network (ANN),[7] infers the probability of the existence of a specific relationship between sets of proteins on the bases of the topology of the network. The likelihood of the individual effectors of CLL Microenvironment Motive of affecting the whole motive has been measured using this approach. Proteins that are closer to a higher number of other proteins in the microenvironment motive have more chances to be a good target.

ii) Modelling based on sampling methods,[8] infers the most plausible network interactions and information flow linking a set of input proteins with a set of output proteins. Two different measurements have been done using this modelling strategy to priorize CLL Microenvironment effectors. In a first place we have used the model to identify the effectors that its modulation is going to affect the larger number of other effectors, that is those with a higher coverage. In a second place we have measured the effect on the whole when the signal of an effector is reverted. Those with higher impact on the whole response when their action in disease stage is reverted have been selected.

146

The proteins that showed the highest scores in the three measurements (one based on ANN and two different metrics from the sampling methods) were selected as key proteins of CLL microenvironment and have been used for further screenings (Supplemental Table S3).

Compound library selection and combination therapies

BindingDB (version 2016-m6) was selected as the source of information for biochemical active compounds and their targets. Most of the compounds are reported to affect several targets. Only compounds reported to affect human targets with less than 6 reported targets and with potential purchasable identifiers have been taken into consideration, which gave rise to 332,029 feasible compounds for screening. As BindingDB does not include all the marketed drugs, DrugBank (4,500 drugs) was also included in the analysis.

A repurposing network-based mathematical model based on ANN (described above) has been used to select compounds with the best target combination to affect the larger number of Key Proteins as possible; the effect on the entire CLL Microenvironment motive has also been measured. Compounds were selected based on three criteria: i) the predictive value has an associated p-value lower than 0.05 (Prediction values above 78 have an associated p-value< 0.05), ii) they have a link to a drug supplier and iii) compounds fulfilling the previous criteria with the same target profile the one with best reported binding constants has been selected. Finally, due to availability and easy of purchase, the number of compounds moved forward to the phenotypic screening was 54 bioactive compounds and 11 drugs (Supplemental Table S4).

The screening for drugs combining with simvastatin to treat CLL has been done using the same ANN modelling strategy.7 The potential effect of targeted drugs used for CLL treatment L has been measured first alone and then in combination with simvastatin The molecular description of CLL was done by as previously described for CLL microenvironment by a manual review of the literature. This characterization was performed in two steps: first identifying the main pathophysiological processes involved in CLL (referred to as motives) being the microenvironment one of them and second the characterization at the protein level; resulting in a set of 300 effector proteins. Only combinations with a prediction value corresponding to a p-value lower than 0.1 and with prediction value for the combination greater than the individual ones have been selected.

Cell lines and primary cells culture

CLL cell lines HG3 (ACC 765) and MEC-1 (ACC 497) were obtained from German Collection of Microorganisms and Cell Cultures (DSMZ). The human bone-marrow derived

stromal cell line HS-5 (CRL-11882) were obtained from the American Type Culture Collection (ATCC). Mycoplasma contamination in cell lines were routinely tested for Mycoplasma infection by PCR. The identification of all cell lines was done by using GenePrint (R) kit (Promega, Madison, WI, USA). CLL cell lines were cultured in RPMI 1640 complemented with 10% fetal bovine serum (FBS), 2 mM L-glutamine and 50 µg/mL penicillin/streptomycin (Life Technologies, Carlsbad, CA, USA) and grown in a humidified atmosphere at 37°C with 5% CO2. Peripheral blood mononuclear cells (PBMCs) from patients diagnosed with CLL according to the World Health Organization criteria1 and from healthy donors were used in this study. Clinical and biological data of each patient are detailed in Supplemental Table S5. Primary cells were isolated from peripheral blood (PB) by Ficoll-Paque sedimentation (GE-Healthcare, Munich, Germany), cryopreserved and stored within the Hematopathology collection of our institution registered at the Biobank from Hospital Clinic-IDIBAPS (R121004-094). The ethical approval for this project including the informed consent of the patients was granted following the guidelines of the Hospital Clinic Ethics Committee and the Declaration of Helsinki.

Thawed cells were cultured in fresh RPMI-1640 supplemented with 10% FBS, 2 mM glutamine and 50 µg/mL penicillin-streptomycin and cultured in a humidified atmosphere at 37ºC containing 5% CO2.

Analysis of cytotoxicity

HG3 and MEC-1 CLL cell lines (200.000 cells/mL) and primary CLL cells (with ☐90% tumor B cells (2x10^6 cells/mL) were incubated alone or in coculture with HS5 cells (50.000 cells/mL) for 48 h with the compounds at doses ranging from 15 to 0.1 µM. Cell cytotoxicity was quantified by double staining with Annexin-V conjugated to fluoresce in isothiocyanate (FITC) and propidium iodide (PI) (eBiosciences, San Diego, USA). For the comparative analysis of response in PB CLL cells and normal B and T lymphocytes from healthy donors, PBMCs were labeled simultaneously with anti-CD3-FITC, anti-CD19-Phycoeritrin (PE; Becton Dickinson) antibodies, and Annexin V-Pacific Blue (Life Technologies). Labeled samples were analyzed on an Attune focusing acoustic cytometer (Life Technologies). Cytotoxicity values were represented relative to untreated control.

Active Metabolic Activity (MTT) assay

Viable cells in culture were determined by using the MTT Assay based on quantitation of intracellular MTT levels. Primary CLL cells were incubated with the compounds for 48 h prior metabolically active cells were measured. Data was represented relative to the untreated control.

In vitro CLL proliferation assay

CLL primary cells (10^7 cells) were labeled with 0.5 µM carboxyfluoresceinsuccinimidyl ester (CFSE Life Technologies, Eugene, OR, USA), seeded in 96-well plates (Falcon; Costar) at a density of 10^5 cells/200 µl, and cultured for 6 days in an enriched RPMI-1640 medium (Gibco) used for long-term cultures, supplemented with 15 ng/mL recombinant human IL-15 (R&D systems, Minneapolis, MN, USA) to sustain survival and with 0.2 µM CpG DNA TLR-9 ligand (ODN-2006; Invivogen) to induce cell proliferation.[9] The percentage of divided cells was determined as the percentage of CD19+(PE)/Annexin-V- (Pacific Blue) cells showing a decrease in CFSE staining on flow cytometry.[10, 11] Fluorescence-minus-one (FMO) was used as a negative control. Data analysis was performed using FlowJow 10.0.7 software (FlowJo, Ashland, OR, USA).

Chemotaxis assay

CLL cells were washed twice and maintained in serum-starved in FBS-free RPMI during the whole experiment. When indicated, TLR agonist mix was added 30 min before ND2158 treatment. Three hours after treatment cells were diluted to 5×10^6 cells/mL with 0.5% bovine serum albumin (BSA; Sigma-Aldrich) in PBS. One hundred microliters of the cell suspension (5×10^5 cells) were added to the top chamber of a Transwell culture polycarbonate insert with 6.5 mm diameter and 5 µm pore size (Corning, Corning, NY, USA). Transwell inserts had been previously coated with ICAM (Peprotech, Rocky Hill, NJ, USA) overnight, washed twice with PBS, and transferred to 24-well culture plates containing 600 µL of RPMI with 0.5% BSA with or without 200 ng/mL of human recombinant CXCL12 and CXCL13 (Peprotech) per well. After 3 h of incubation, 100 µL from each lower chamber of the transwell plate were collected in triplicate and viable cells counted on a cytometer for 12 s under a constant flow rate of 500 µL/min. Values are presented as the ratio of migrating cells and total viable cells, relative to the untreated control.

Cell Confluence Proliferation Assay methodology

HG3 cells were plated at 200.000 cells/mL (100 µL per well) into a 96-well flat bottom plate. In a day 1 the cell confluence is approximately 10%. HS5 cells were plated at 50.000 cells/mL (100 µL per well) into a 96-well flat bottom plate.

Cell growth was monitored for 48 h by recording phase images using the IncuCyte ZOOM® live cell imaging system (Sartorius, Germany) and confluence algorithm.

Statistical analysis

Statistical data analysis was performed using Prism 6.01 Graphpad software (San Diego, CA. Results are expressed as mean±SEM. Non-parametric Wilcoxon matched-pairs signed rank test was used to compare the median of a set of samples against a hypothetical median. Comparison between two paired groups of samples was evaluated by the nonparametric Wilcoxon matched-pairs signed-rank test. The nonparametric Mann-Whitney test was used to compare two unpaired groups of data. Statistical significance was considered when P-value < 0.05 (*P < 0.05, **P < 0.01, ***P < 0.001). Receiver (or Relative) operating characteristic (ROC) curves were constructed and the area under ROC curves (AUC) was calculated to evaluate sensitivity and specificity of both metabolic rate and cytotoxicity for each compound tested. Cut-off points on the ROC curves with higher AUC and P < 0.05 were used as selection criteria of effective drugs.

RESULTS

Capitalizing in the existing knowledge on microenvironment effect on CLL, existing tools for *in silico* screening based in systems biology approaches and a solid coculture screening system we have identified *in silico* compounds with potential to counteract the microenvironment effect in CLL and screened and validated some of them *in vitro* assays. The main steps of the overall experimental procedure is summarized in Figure 1.

Identification of key molecular enclaves involved in microenvironment effects on CLL

A molecular description of CLL microenvironment was obtained by the identification of proteins (from now called "effectors") with a known role on CLL microenvironment from PubMed publications. A total of 139 unique proteins were selected to describe "CLL microenvironment motive" (Supplemental Table S2 and Figure 2A). The known functional protein–protein associations of these proteins with other human proteins where retrieved from public data bases, building a network around the known proteins related with CLL microenvironment effect. The contributions of close neighbors to the effector proteins are also taken into consideration when analyzing the effects of compounds. In this way, proteins that may have an important role in CLL microenvironment but have not previously been acknowledged may be taken into consideration (Figure 2B).

To narrow down the analysis a combination of different systems biology measures has been used to measure the likelihood of each individual effector protein of affecting a larger number of other proteins in the motive when its pathological function is counteracted. This

analysis has identified a subset 57 proteins, now on referred as "key proteins" (Supplemental Table S3).

Compound library selection

A network-based mathematical model based on artificial neural networks has been used to select compounds with the best target combination to affect the larger number of Key Proteins or effectors of the CLL microenvironment as possible. BindingDB (version 2016-m6) was selected as the source of information for biochemical active compounds and their targets (332,029 bioactive compounds). Most of the compounds are reported to affect several targets. Only compounds reported to affect human targets, less than 6 targets and with potential purchasable identifiers have been taken into consideration, which gave rise to 332,029 feasible compounds for screening. As BindingDB does not include all the marketed drugs, DrugBank (4,500 drugs) was also included in the analysis.

Compounds were selected based on three criteria: i) the predictive value has an associated p-value lower than 0.05 (Prediction values >78 have an associated p-value < 0.05), ii) they have a link to a drug supplier and iii) compounds fulfilling the previous criteria with the same target profile the one with best reported binding constants has been selected. Finally, due to availability and ease of purchase the number of compounds moved forward to the phenotypic screening was 54 bioactive compounds and 11 drugs (Supplementary Table S4), a total of 65 compounds to conform the library. The number of targets affected by the selected compounds is shown in Figure 2C.

Compound library screening in CLL cells

HG3 cell line, derived from a CLL patient with an unmutated IGHV phenotype,[12] was used to test the effect of the 65 compounds selected. MTT analysis was performed after incubation of cells for 48 h with 15 µM of the different compounds (Figure 3A). In order to define the best threshold to discriminate the effect of the compounds, a ROC analysis was performed (Supplemental Figure S1). The best cut off for MTT assay was 50%. MTT was analyzed in HG3 and HS5, a human stromal cell line, and according to the threshold determined by ROC, only 8 compounds were affecting metabolic activity (color dot). Cytotoxicity was also analyzed by Annexin-V/PI staining in HG3 alone or in coculture with the stromal cell line HS5 (Figure 3B). With a 20% cut off, defined by ROC analysis (Supplemental Figure 1B), 6 compounds were cytotoxic for CLL cells. One of the compounds (A5) was a false positive due to its autofluorescence. Similar results were obtained when HG3 cells were cocultured with HS5 cells. Two compounds (A1 and A2) exerted a cytotoxic effect (MTT analysis) but with no effect on viability (Annexin V/PI staining). Similar results were observed in the MEC-1 CLL cell line (Supplemental Figure 2A).

Then, with the 8 compounds selected, a dose response (1 to 15 µM) was performed in the HG3 and HS5 cell lines. At all the concentrations used, the CLL cell line was more sensitive to these compounds in a dose dependent manner by MTT (Figure 3C) or Annexin-V analysis (Figure 3D) than the stromal HS5 cell line. Compound D1 exerted a huge cytotoxic effect in all cell lines even at the lowest doses used.

Compound library screening in primary CLL cells

A dose response screening of these 8 compounds selected was performed in primary CLL cells with doses from 0.1 to 2.5 µM. As expected, compounds A1 and A2 didn't exert any cytotoxic effect regardless the dose used. Compound A12 and C11 also didn't exert t at these doses. Compounds C5, C7, D1 and F1 exerted a significant dose-dependent cytotoxic effect (Figure 4A).

Then these 4 compounds (C5, C7, D1 and F1) were analyzed in primary CLL cells in the presence of HS5 in order to mimic the microenvironment. Compound D1 was discarded as had a high cytotoxic effect on HS5 cells, being the effect not selective for tumoral CLL cells. Compound C7 and F1 were selective for tumoral CLL cells even with the presence of HS5 cells at all the tested doses. In contrast, compound C5 only exert a significant (p<0.05) and selective effect at the dose of 2.5 µM (Figure 4B).

We also analyzed if these compounds had any effect on CLL proliferation. CFSE-labeled primary CLL cells were induced to proliferate by incubating them with a medium containing the CpG oligonucleotide ODN2006, which triggers growth and cell division in the proliferative centers of CLL patients, and the inflammation-linked cytokine IL-15, which is constitutively produced by stromal cells[9,13] for 6 days. As it is showed in Figure 4C, ODN2006 plus IL15 induced the increase of the mean percentage of CFSE[low] viable CLL cells indicative of increase on cell proliferation. All compounds tested (C5, C7 and F1) decreased the percentage of CFSE[low] viable CLL cells, indicating that these compounds are inducing a significant decrease on CLL proliferation. Ibrutinib 0.25 µM was used as a positive control to inhibit proliferation of CLL cells under these conditions.

In order to analyze if cytotoxicity of these compounds was specific for CLL cells, we incubated PBMCs from healthy donors with these compounds at the same doses used in primary CLL cells. The effect on normal B (CD19^{+}) and T (CD3^{+}) lymphocytes was analyze by flow cytometry. Compound C7 and F1 were selective for CLL cells at all doses used. In contrast, compound C5 lost the selectivity using the highest dose (2.5 µM) (Figure 4D).

Target validation of selected compounds

According to the experimental *in vitro* results, our compounds of interest were C7 and F1. One of the main targets of compound C7 was NOD1 (nucleotide-binding oligomerization domain-containing protein 1) (Supplemental Table S6). NOD1 is an innate immune receptor, that together with NOD2 recognize intra-cellular bacterial components.[14] As NOD1 is a target of other effective compounds (A1, A12 and C5) we compared the cytotoxic effect of these compounds with 5 currently available commercial NOD inhibitors (Supplemental Table S6): BDBM62265, BDBM54356, NOD-IN-1 and noditinib (NOD1 inhibitors) and GSK583 (inhibitor of RIP2, a downstream effector of NOD1/2).[15] Any of these specific inhibitors exert a cytotoxic effect analyzed by MTT analysis in the CLL cell lines (HG3, MEC-1) and the stromal HS5 cell line (Figure 5A). We confirmed by AnnexinV/PI staining that these inhibitors were not cytotoxic for HG3 alone or in coculture with HS5 cells (Figure 5B). Therefore, we considered that NOD1 is not the main target responsible of the effects seen for C7. We cannot discard NOD1 contributing a pleiotropic effect with the other identified targets for this compound, As going from a promising compound to an approved drug is still a complicated and long process we concentrated further efforts on further screening compound F1.

According to our data (Supplemental Table S4), F1 corresponded to simvastatin, a well-known statin. This drug inhibits the synthesis of cholesterol in the liver by the enzyme HMG-CoA reductase.[16] Then, we compared the effect of simvastatin with other commercially available stains (lovastatin, fluvastatin and rosuvastatin) with different IC50 (Supplemental Table S7 and Supplemental Figure 4). As it has been reported that statins also inhibit LFA-1,[17] we also tested two specific LFA-1 inhibitors (lifitegrast and BDBM50199033). We observed that all statins exerted a cytotoxic effect, analyzed by MTT (Figure 5C) and AnnexinV/PI staining (Figure 5D), although F1 (simvastatin) was the statin with the highest effect. In contrast, LFA-1 inhibitors didn't show any cytotoxic effect. Again, we cannot discard a possible contribution of LFA-1 when combined with HMG-CoA reductase in the effects seen. we hypothesize that statins by inhibiting the pathway of cholesterol synthesis might participate in the decrease of cell survival and proliferation. But, on the other hand by inhibiting LFA-1 might have also a role in cellular adhesion (Figure 5E-F). But, on the other hand, by inhibiting LFA-1 might have a role in cellular adhesion (Figure 5E-F).

To validate this hypothesis, first we recorded the confluence of cell culture of HG3 alone, HG3 in coculture with HS5 and HS5 alone treated with simvastatin 1 µM for 48 h. We observed that simvastatin induced a dramatic decrease on cell proliferation in HG3 alone and in coculture with HS5. In contrast, no effect was observed in HS5 alone (Figure 6A).

We next analysed the effect of statins and LFA-1 inhibitors on ICAM-mediated adhesion and migration of CLL cells triggered by CXCL12 and CXCL13, key chemokines for CLL cell homing to lymphoid tissues.[18] All different statins and the specific LFA-1 inhibitors induced a significant ($p<0.05$) reduction on CLL adhesion/invasion induced by CXCL12 (Figure 6B) and CXCL13 (Figure 6C). We also confirmed by CFSE staining that all statins tested reduced significantly ($p<0.05$) the proliferation of CLL cells induced by incubation of cells with ODN2006 plus IL15 by 6 days (Figure 6D). A representative experiment is showed in Figure 6E, where the stains were able to decrease the percentage of CFSE^{low} CLL cells.

To further study the effect of statins in CLL cells, we incubated primary CLL cells alone or in coculture with the stromal cell line HS5 with these different drugs. As observed in Figure 7A, all statins tested induced a cytotoxic effect on CLL cells, and this effect was not protected by incubating the cells with the stromal cell line HS5. Furthermore, this effect is selective for CLL cells, as no effect was observed in the HS5 cells at the low doses tested (0.1 and 1 µM; Figure 7A).

The effect of these statins was also analyzed in PBMCs from healthy donors (Figure 7B). Statins exerted a significant selective cytotoxic effect in CLL cells compared to B (CD19^{+}) and T (CD3^{+}) cells from healthy donors at the doses of 0.1 and 1 µM.

Systems biology analysis of possible combination therapies

We tried if statins could benefit of the current cancer therapies and we might increase the benefits on CLL treatment when combined. To identify the best combination therapies, we have used the same strategy based on network-based mathematical model strategy used to select the compound library. The effect of the individual drugs and the combination has been measured over the whole description of the CLL. Drugs have been selected when the prediction score for the combination was superior to the individual ones and the p-value associated to the prediction score was lower than 0.1. As simvastatin already gives a high prediction score for CLL (75) it has been more difficult to identify compounds that would increase the individual action. We tested several targeted drugs used for CLL treatment (22 drugs tested) 8 of them showed a probability for the combination above threshold but only for two drugs, ibrutinib and venetoclax, the combination score was higher than the individual ones (Supplemental Table S8).

Validation *in vitro* of possible combination therapies

According to the systems biology prediction, we tested the combination of statins with ibrutinib and venetoclax. We incubated CLL cells in the presence of ODN2006 plus IL15 and viability was analyzed in CD19^{+} CLL cells by AnnexinV staining after 6 days. We observed that incubation of cells with the different statins and Ibrutinib (0.1 µM) reduced significantly

CLL cell viability (Figure 8A). Furthermore, proliferation of CLL cells decreased after ibrutinib and statins alone and this decrease on CLL proliferation is significantly higher when combining statins with ibrutinib (Figure 8B).

We tested *in vitro* the combination of venetoclax and statins at the dose of 1 nM and 0.1 µM, respectively. The addition of statins to venetoclax potentiated the cytotoxic effect (Figure 8C) significantly ($p<0.05$).

As using the systems biology approach, we observed also that the venetoclax combinatory score with statins was also high (75.7), we tested this combination *in vitro*. Venetoclax and statins alone at the dose of 1 nM and 0.1 µM respectively, induced a decrease on cell viability ($p<0.05$). The addition of statins to venetoclax potentiated the cytotoxic effect (Figure 8C).

DISCUSSION

CLL is an antigen-experienced mature B lymphocytes malignancy, in which microenvironmental signals play a critical role in ontogeny and evolution.[19] In the recent years, tremendous progress regarding the therapy of CLL has been achieved by introducing small molecule kinase inhibitors, targeting the B cell receptor (BCR). Recently it has been proposed that these inhibitors are also disrupting the dialogue of tumor B cells with the microenvironment giving further support to the importance of the microenvironment.

In the present study we have coupled a systems biology approach to prioritize bioactive molecules and approved drugs with a functional phenotypic screen emulating the microenvironment effect on CLL to identify drugs and targets that can overcome the supportive effect of the tissue microenvironment on CLL cell survival.

We have screened not only approved drugs but also bioactive compounds giving access to a greater portion of the different chemical structures to improve the chances of success. Of the 65 compounds tested 8 of them showed promising results either for their cytotoxicity or viability effects or in many instances for both effects. The positive compounds also showed minimal change in their effects when analysed in co-culture, thus their action may overturn, at least partially, the supportive effect of the microenvironment. The in silico screening performed has provided a significant enrichment compared with what combinatorial studies without computational prioritization would have given starting from spare evidences on the microenvironment effects on CLL and a large battery of possible drug-like molecules and commercial drugs.

A more extensive screening of dose-response, primary cell lines and CLL specificity has highlighted 2 compounds a drug-like molecule (C7) and a commercial drug, simvastatin. In spite of the promising results shown for C7 we concentrated further screening to simvastatin as the advantages of drug repositioning[20] over new developments are overriding.

Simvastatin is a statin that interferes in the synthesis of cholesterol in the liver by inhibiting the enzyme 3-hydroxy-3-methylglutaryl coenzyme A reductase (HMGCR) in the mevalonate pathway, thus blocking the synthesis of mevalonate and preventing cholesterol formation.[16] Statins can be divided into two groups depending on their origin: type-1 includes statins that have been produced by fermentation products of cettain funghi such as mevastatin, lovastatin, pravastatin and simvastatin. And type-2 are statins manufactured by chemical syntheses such as fluvastatin, atorvastatin, cerivastatin and pivastatin.[21] Multiple analysis have reported that statins showed antitumor activity in monotherapy and in combination with several anticancer agents and their involvement in cancer risk and prevention.[22] The antitumor effect of statins results in the inhibition of proliferation, migration, invasion, survival and stemness.[21, 23]

Particularly, statins promote apoptosis in several hematological malignancies[24-26] and epidemiologic studies suggest improved outcomes in some hematological malignancies in the statins users.[27, 28] Particularly in CLL and lymphoma cells, statins induced apoptosis.[29, 30] It has been reported in lymphoma cells that statins induced apoptosis by promoting ROS generation and regulating Akt, Erk and p38 signals via suppression of mevalonate pathway.[31] Simvastatin has shown cytotoxicity against CLL cells.[31]

Also it has been reported that Fluvastatin showed higher cytotoxicity against lymphoma cells than atorvastatin and simvastatin.[31] Recently an association between low-potency lipophilic statin (lovastatin and fluvastatin) use and reduced CLL risk, with a possible dose-response effect was reported in a nested case-control study in Manitoba, Canada analyzing 1385 cases.[32]

Simvastatin also targets the integrin lymphocyte function-associated antigen-1 (LFA-1).[17] This protein is an heterodimeric integral membrane protein composed of an alpha chain (ITGAL) and a beta chain (ITGB2) which is expressed on all leukocytes.[33] LFA-1 plays a central role in leukocyte intercellular adhesion through interactions with its receptive counterpart intercellular adhesion molecule 1 (ICAM-1).[34] LFA-1 is one of the most important adhesion molecules that mediate contact between tumoral cells and stromal cells. Furthermore, cell adhesion has been considered one of the major causes of primary drug resistance in tumors.[35]

Our results showed that the statins (simvastatin, lovastatin, fluvastatin and rosuvastatin) exerted a cytotoxic effect, while no effect was observed using LFA-1 inhibitors (lifitegrast and BDBM50199033). Furthermore, all statins tested reduced significantly the proliferation of CLL cells. When we analysed the effect of statins and LFA-1 inhibitors on ICAM-mediated adhesion and migration of CLL cells triggered by CXCL12 and CXCL13, key chemokines for CLL cell homing to lymphoid tissues,[18] all statins and the LFA-1 inhibitors induced a significant reduction on CLL adhesion/invasion induced by CXCL12 and CXCL13. With these results and the two putative targets of statins, HMGCR and LFA-1, we can hypothesize that statins by inhibiting the pathway of cholesterol synthesis might participate in the decrease of cell survival and proliferation and on the other hand, by inhibiting LFA-1 we are targeting cellular adhesion, confirming that the mechanism of action of statins might involve HMGCR inhibition-dependent and –independent inhibitory effects on the adhesive function of LFA-1.[17]

The *in silico* screening for potentially synergistic CLL treatments with simvastatin highlighted Ibrutinib and venetoclax as synergistic combinations that we have experimentally validated.

The statins have been shown to downregulate the anti-apoptotic protein BCL2 in some leukemias.[31] Venetoclax, a selective BCL2 inhibitor was recently approved for CLL treatment. Furthermore, complete remission rate in CLL is increased when simvastatin is combined with venetoclax.[36]

In summary, we propose that systems biology approach is useful to find new drugs for CLL treatment and to predict new and efficient combinations. Our results propose that statins might enhance the cytotoxic effect of ibrutinib or venetoclax by blockade of cell proliferation and lymphocyte homing.

ACKNOWLEDGEMENTS

CONFLICT OF INTERESTS

NG, JMM and JF have competing interests on ANAXOMICS systems biology analysis.

RT, AG, LR, MLG, EC and DC don't have any competing financial interests.

REFERENCES

1. Puente,XS., Jares,P., & Campo,E. Chronic lymphocytic leukemia and mantle cell lymphoma: crossroads of genetic and microenvironment interactions. Blood 131, 2283-2296 (2018).

2. Bosch,F. & la-Favera,R. Chronic lymphocytic leukaemia: from genetics to treatment. Nature Reviews. Clinical Oncology [Epub ahead of print], (2019).

3. Ponader,S. et al. The Bruton tyrosine kinase inhibitor PCI-32765 thwarts chronic lymphocytic leukemia cell survival and tissue homing in vitro and in vivo. Blood 119, 1182 (2012).

4. de Rooij,M.F.M. et al. The clinically active BTK inhibitor PCI-32765 targets B-cell receptorGÇô and chemokine-controlled adhesion and migration in chronic lymphocytic leukemia. Blood 119, 2590 (2012).

5. Herishanu,Y., Katz,B.Z., Lipsky,A., & Wiestner,A. Biology of chronic lymphocytic leukemia in different microenvironments: clinical and therapeutic implications. Hematol Oncol Clin North Am 27, 173-206 (2013).

6. Pujol,A., Mosca,R., Farr+®s,J., & Aloy,P. Unveiling the role of network and systems biology in drug discovery. Trends in Pharmacological Sciences 31, 115-123 (2010).

7. Romeo-Guitart,D. et al. Neuroprotective Drug for Nerve Trauma Revealed Using Artificial Intelligence. Sci Rep 8, 1879-1894 (2018).

8. Guillen-Gomez et al. Urinary Proteome Analysis Identified Neprilysin and VCAM as Proteins Involved in Diabetic Nephropathy. J Diabetes Res 2018, 1-12 (2018).

9. Mongini,P.K. et al. TLR-9 and IL-15 Synergy Promotes the In Vitro Clonal Expansion of Chronic Lymphocytic Leukemia B Cells. J. Immunol. 195, 901-923 (2015).

10. Gimenez,N. et al. Targeting IRAK4 disrupts inflammatory pathways and delays tumor development in chronic lymphocytic leukemia. Leukemia [Epub ahead of print], (2019).

11. Lee-Verges,E. et al. Selective BTK inhibition improves bendamustine therapy response and normalizes immune effector functions in chronic lymphocytic leukemia. Int. J. Cancer 144, 2762-2773 (2019).

12. Rosen,A. et al. Lymphoblastoid cell line with B1 cell characteristics established from a chronic lymphocytic leukemia clone by in vitro EBV infection. OncoImmunology 1, 18-27 (2012).

13. Gupta R, Yan XJ, Barrientos J, Kolitz JE, Allen SL, Rai K, et al. Mechanistic Insights into CpG DNA and IL-15 Synergy in Promoting B Cell Chronic Lymphocytic Leukemia Clonal Expansion. J Immunol. 2018;201:1570-85.

14. Velloso,F., Trombetta-Lima,M., Anschau,V., Sogayar,M., & Correa,R. NOD-like receptors: major players (and targets) in the interface between innate immunity and cancer. Biosci. Rep 39, BSR20181709 (2019).

15. Magalhaes,J.G. et al. Essential role of Rip2 in the modulation of innate and adaptive immunity triggered by Nod1 and Nod2 ligands. Eur. J. Immunol. 41, 1445-1455 (2011).

16. Plosker,G.L. & McTavish,D. Simvastatin. A reappraisal of its pharmacology and therapeutic efficacy in hypercholesterolaemia. Drugs 50, 334-363 (1995).

17. Schramm,R. et al. Statins inhibit lymphocyte homing to peripheral lymph nodes. Immunology 120, 315-324 (2007).

18. Davids,M.S. & Burger,J.A. Cell Trafficking in hronic Lymphocytic Leukemia. Open. J. Hematol. 3, 1-13 (2012).

19. Ten,H.E. & Burger,J.A. Microenvironment interactions and B-cell receptor signaling in Chronic Lymphocytic Leukemia: Implications for disease pathogenesis and treatment. Biochim. Biophys. Acta 1863, 401-413 (2016).

20. Pantziarka,P. et al. The Repurposing Drugs in Oncology (ReDO) Project. Ecancermedicalscience 8, 442 (2014).

21. Federica,I. et al. Targeting Mevalonate Pathway in Cancer Treatment: Repurposing of Statins. Recent Patents. on Anti. -Cancer Drug Discovery 13, 184-200 (2018).

22. Pisanti,S., Picardi,P., Ciaglia,E., DGÇÖAlessandro,A., & Bifulco,M. Novel prospects of statins as therapeutic agents in cancer. Pharmacological Research 88, 84-98 (2014).

23. Gazzerro,P. et al. Pharmacological Actions of Statins: A Critical Appraisal in the Management of Cancer. Pharmacol Rev 64, 102 (2012).

24. Minden,M.D., Dimitroulakos,J., Nohynek,D., & Penn,L.Z. Lovastatin Induced Control of Blast Cell Growth in an Elderly Patient with Acute Myeloblastic Leukemia. Leukemia & Lymphoma 40, 659-662 (2001).

25. Dimitroulakos,J. et al. Increased Sensitivity of Acute Myeloid Leukemias to Lovastatin-Induced Apoptosis: A Potential Therapeutic Approach. Blood 93, 1308 (1999).

26. Bockorny,B. & Dasanu,C.A. HMG-CoA reductase inhibitors as adjuvant treatment for hematologic malignancies: what is the current evidence? Annals. of Hematology 94, 1-12 (2015).

27. Yi,X., Jia,W., Jin,Y., & Zhen,S. Statin use is associated with reduced risk of haematological malignancies: evidence from a meta-analysis. PLoS One 9; e87019, 1-8 (2014).

28. Sanfilippo,K.M. et al. Statins Are Associated With Reduced Mortality in Multiple Myeloma. JCO. 34, 4008-4014 (2016).

29. Chapman-Shimshoni,D., Yuklea,M., Radnay,J., Shapiro,H., & Lishner,M. Simvastatin induces apoptosis of B-CLL cells by activation of mitochondrial caspase 9. Experimental Hematology 31, 779-783 (2003).

30. Qi,X.F. et al. HMG-CoA reductase inhibitors induce apoptosis of lymphoma cells by promoting ROS generation and regulating Akt, Erk and p38 signals via suppression of mevalonate pathway. Cell Death. & Amp; Disease 4, e518 (2013).

31. Chong,P.H., Seeger,J.D., & Franklin,C. Clinically relevant differences between the statins: implications for therapeutic selection. The American Journal of Medicine 111, 390-400 (2001).

32. Righolt,C.H. et al. Statin Use and Chronic Lymphocytic Leukemia Incidence: A Nested Case-Control Study in Manitoba, Canada. Cancer Epidemiology Biomarkers Prevention [Epub ahead of print], (2019).

33. Arnaout,M.A. Structure and Function of the Leukocyte Adhesion Molecules CD11/CD18. Blood 75, 1037-1050 (1990).

34. Kim,M., Carman,C.V., Yang,W., Salas,A., & Springer,T.A. The primacy of affinity over clustering in regulation of adhesiveness of the integrin a. J Cell Biol 167, 1241 (2004).

35. Hazlehurst,L.A., Landowski,T.H., & Dalton,W.S. Role of the tumor microenvironment in mediating de novo resistance to drugs and physiological mediators of cell death. Oncogene 22, 7396-7402 (2003).

36. Lee,J.S. et al. Statins enhance efficacy of venetoclax in blood cancers. Science Translational Medicine 10, eaaq1240 (2018).

FIGURES
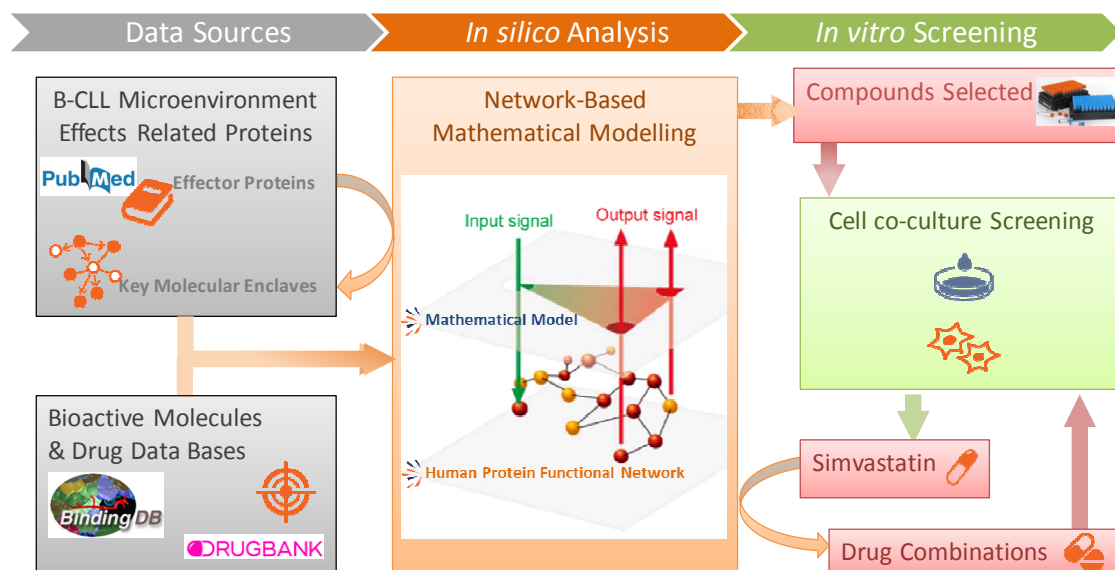
Figure 1. Overall experimental procedure.

(1) Data sources. Retrieve molecular description of CLL microenvironment effects from literature and mapping in a human protein functional network. Retrieve bioactive compounds and drugs with known protein target profile.

(2) *In silico* analysis. Different metrics derived from network-based mathematical models have served in a first instance to select key molecular enclaves in the network around know effector proteins CLL microenvironment. In a second place to identify compounds with a potential effect around the key proteins. In a third instance to identify antineoplastic agents that could have synergistic effect with simvastatin

(3) *In vitro* screening. Compound library identified previously is screened in *vitro* co-culture CLL System as well as the combination therapies identified for simvastatin (the drug that showed the best results in the initial *in vitro* screen

A

B

C
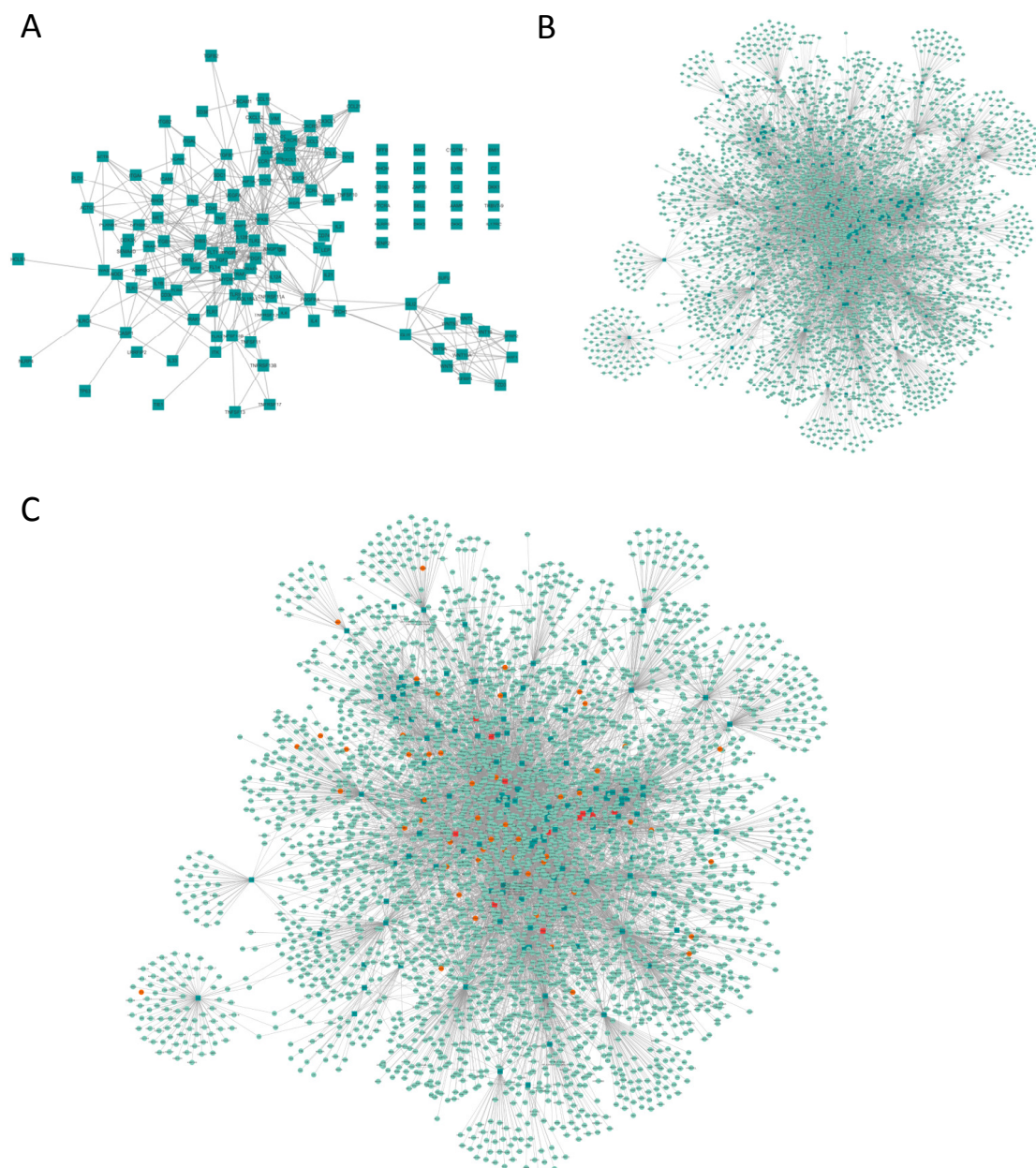
Figure 2. Molecular description of B-CLL microenvironment and targets.
A) 139 proteins (effectors) selected as descriptors of the CLL microenvironment and the relations between them. B) The selected descriptors of the CLL microenvironment and proteins directly related to them. C) Extract of the network build around the selected effectors of the microenvironment that contains the targets for the 65 compounds screened. Dark green square: CLL microenvironment selected descriptors; Light green round: Proteins directly related with selected CLL microenvironment descriptors; Orange, round: Protein targets of the 65 compounds screened that lay within the network described by the microenvironment effector proteins and close neighbours; Red square: Proteins that are at the same time effectors and targets.
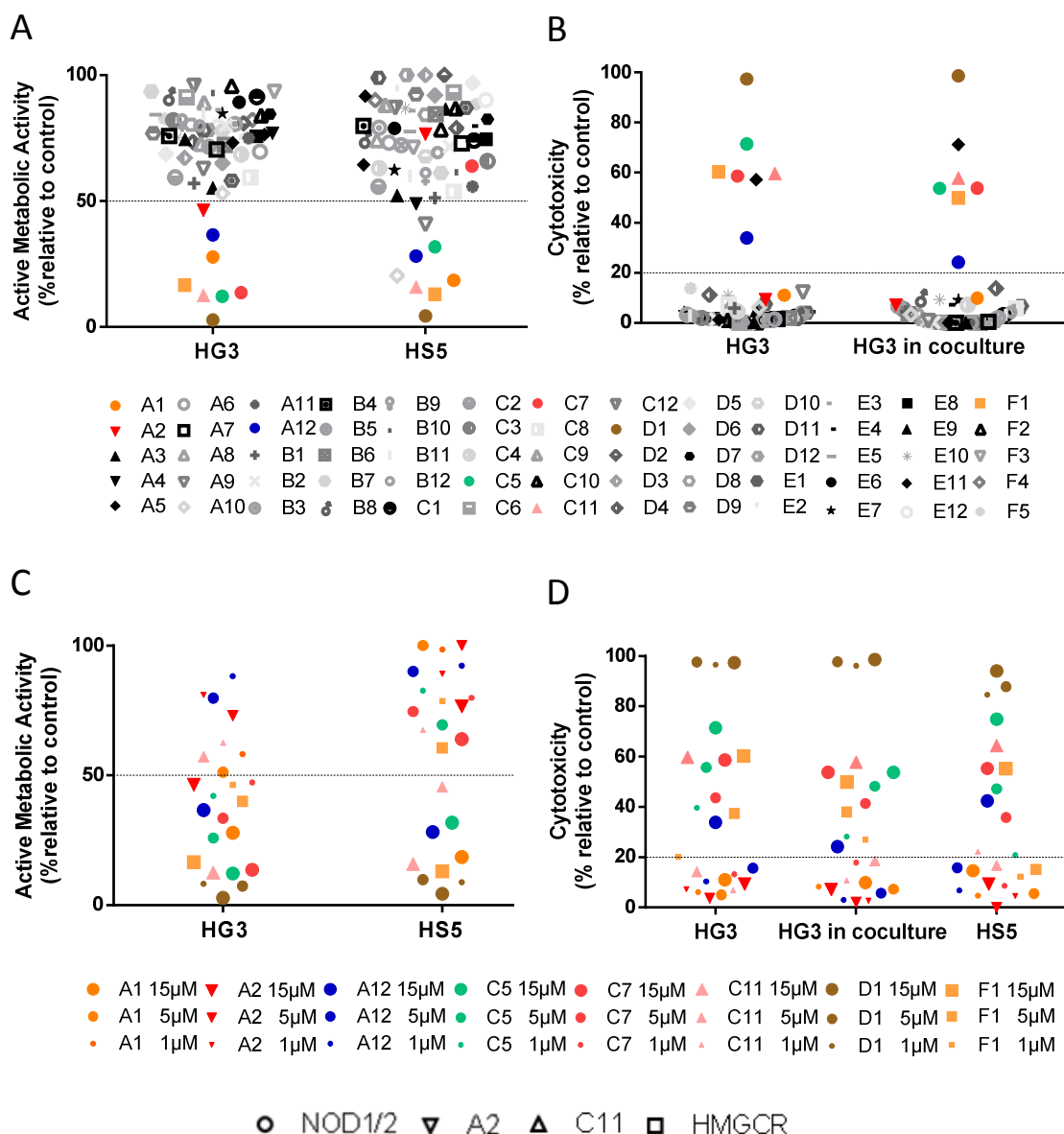
Figure 3. Compound library screening in HG3 and HS5 cell lines.
Cells were treated for 48 h with the compounds at concentrations from 1 to 15 µM. Each dot represents de mean of 3 independent experiments in different days. Dotted line indicates the threshold to discriminate the effect of the compounds. The cut off for MTT is 50% and for cytotoxicity is 20%. Active metabolic activity of CLL cells was measured using the MTT assay, and is depicted relative to untreated control. Cytotoxicity was defined as the increase in Annexin-V$^+$/PI$^+$ cells compared to untreated control. A) Active metabolic activity of cells treated with the compounds at the concentration of 15 µM in the HG3 and HS5 cell lines. B) Cytotoxicity of the compounds at 15 µM concentration in HG3 alone and in co-culture with HS5. C) Active metabolic activity of cells treated with the compounds at the concentrations of 1-5-15 µM in the HG3 and HS5 cell lines. D) Cytotoxicity of the compounds at 1-5-15 µM concentration in HG3 alone, HG3 in co-culture with HS5 and in HS5 alone. Round dots: compounds that target NOD1/2; Triangle down-pointing dots: A2; Triangle up-pointing dots: C11; Square dots: compounds that target HMGCR and LFA-1.
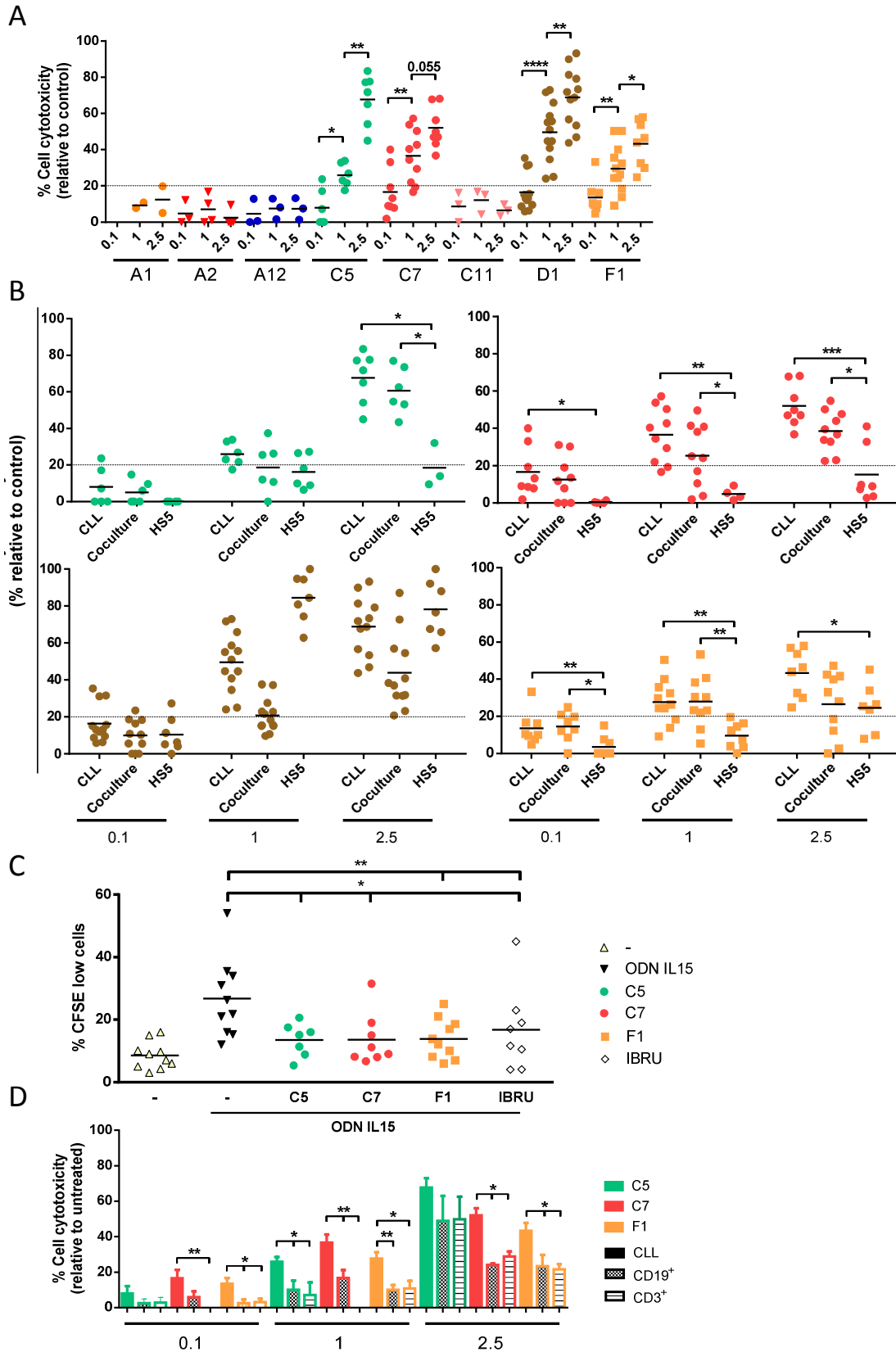
Figure 4. Screening of selected compounds in primary CLL cells.
CLL cells or CD19^{+} B cells and CD3^{+} T cells from healthy donors were treated for 48 h with the compounds at concentrations from 0.1 to 2,5 µM. Dotted line indicate the threshold to discriminate the effect of the compounds. The cut off for cytotoxicity is 20%. Cytotoxicity was defined as the increase in Annexin-V[+]/PI^{+} cells compared to untreated control.

A) Cytotoxicity of the compounds at 0.1-1-2.5 µM concentration in primary CLL cells (n=2-13). Horizontal bars represent population means. B) Cytotoxicity of the compounds at 0.1-1-2.5 µM concentration in primary CLL cells, primary CLL in co-culture with HS5 in HS5 alone (n=6-13). Horizontal bars represent population means. C) Percentage of proliferating CD19^{+} CLL cells after ODN2006+IL15 stimulation (30 min before treatment) and treatment with different compounds at the dose of 1 µM (C5, C7 and F1) or 0.25 µM (Ibrutinib) for 6 days measured by CFSE dilution (n=10). Horizontal bars represent population means. D) Cytotoxicity of the compounds at 0.1-1-2.5 µM concentration in primary CLL cells and CD19^{+} B cells and CD3^{+} T cells from healthy donors (n=8). Bars represent the mean ± SEM of all samples analyzed. Non-parametric Wilcoxon matched-pairs signed rank test was used for statistical analysis. *P<0.05*, **P<0.01*, ***P<0.001*, ****P<0.0001*.Round dots: compounds that target NOD1/2; Triangle down-pointing dots: A2; Triangle up-pointing dots: C11; Square dots: compounds that target HMGCR and LFA-1.
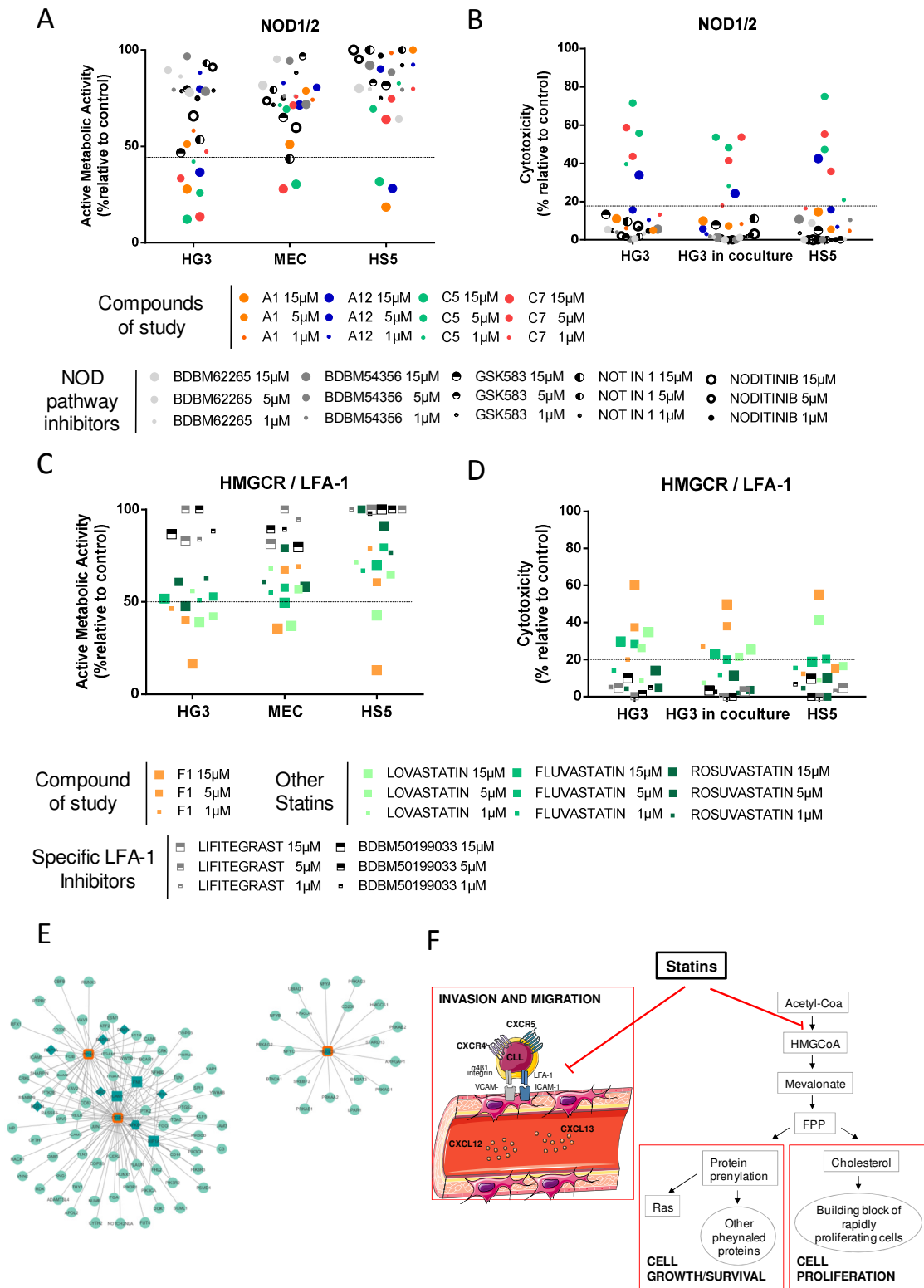
Figure 5. HMGCR/LFA-1 targets were validated for CLL treatment, but not NOD1/2.
Cells were treated for 48 h with the compounds at concentrations from 1 to 15 μM. Each dot represents de mean of 3 independent experiments in different days. Dotted line indicates the threshold to discriminate the effect of the compounds. The cut off for MTT is 50% and for cytotoxicity is 20%. Active metabolic activity of CLL cells was measured using the MTT assay, and is depicted relative to untreated control. Cytotoxicity was defined as the increase in Annexin-V$^+$/PI$^+$ cells compared to untreated control.

A) Active metabolic activity of cells treated with the selected compounds from the library and NOD1/2 specific inhibitors in the HG3, MEC and HS5 cell lines. B) Cytotoxicity of the selected compounds from the library and NOD1/2 specific inhibitors in HG3 alone, HG3 in co-culture with HS5 and in HS5 alone. C) Active metabolic activity of cells treated with the F1 compound and different statins and specific LFA-1 inhibitors in the HG3, MEC and HS5 cell lines. D) Cytotoxicity of the F1 compound and different statins and specific LFA-1 inhibitors in HG3 alone, HG3 in co-culture with HS5 and in HS5 alone. Round dots: compounds that target NOD1/2; Square dots: compounds that target HMGCR and LFA-1; Grey dots: specific inhibitors for each target.
E) Molecular description of F1 targets. Dark green square: CLL microenvironment selected descriptors; Dark green diamond: CLL microenvironment identified key proteins, Dark green, hexagon: Proteins that are at the same time descriptors and key; Light green, round: Proteins directly related with selected CLL microenvironment descriptors; Frame orange: Protein F1 targets. F) Schematic description of statins mechanism of action.
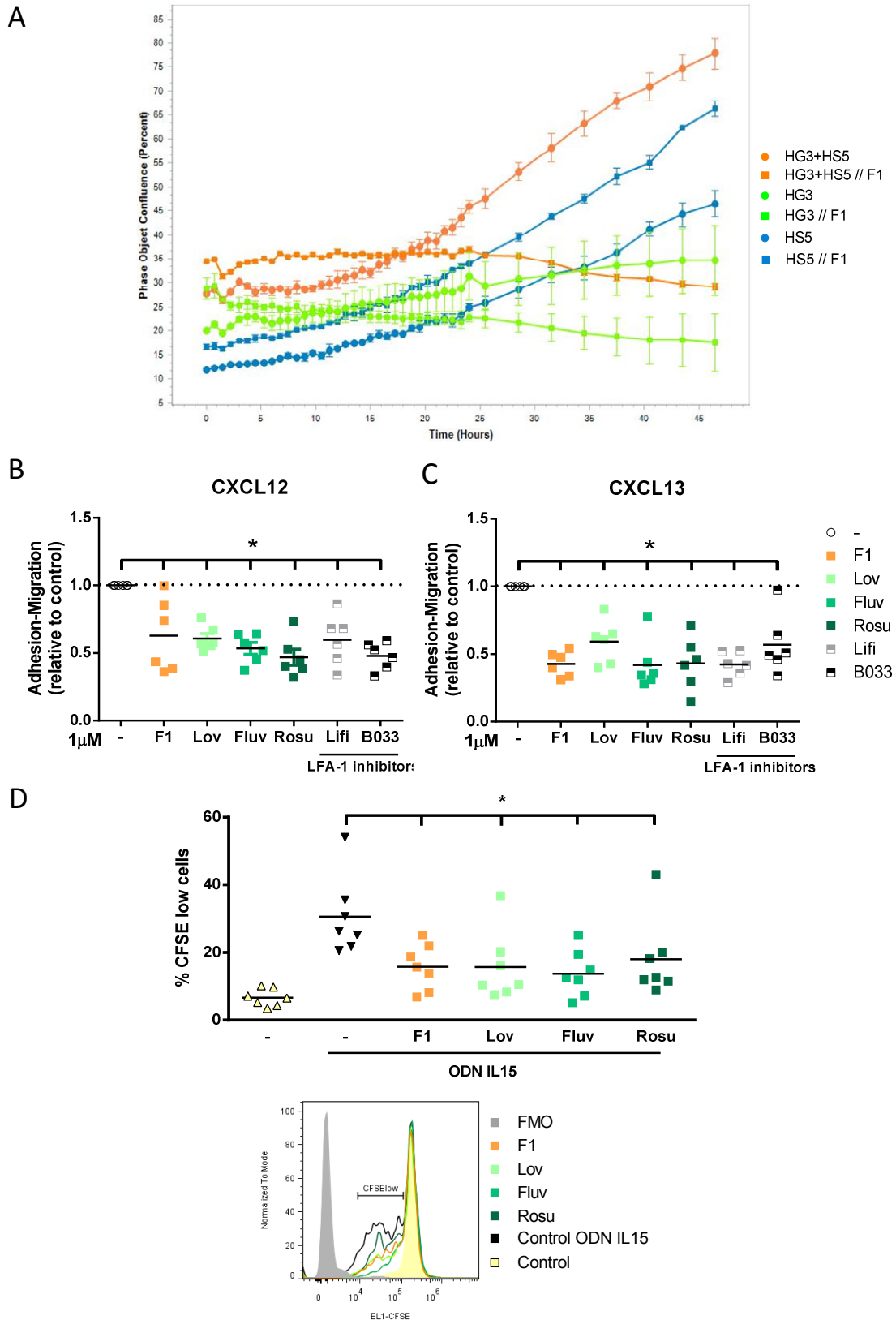
Figure 6. HMGCR/LFA-1 inhibition is effective to reduce CLL migration, proliferation and viability.

Cells were treated for 48 h with the compounds at concentrations of 1 µM.

A) Cell phase object confluence after F1 treatment was monitored for 48 h by recording phase images using the IncuCyte® Live Cell Analysis Imaging System in HG3, HS5 and co-culture of HG3 and HS5 cells (n=3). Bars represent the ± SD of all samples analyzed. B) Migration of cells treated with statins or LFA-1 inhibitors for 3 h towards CXCL12 analyzed by transwell assays. Values are presented as the ratio of migrating cells and total viable cells, relative to the untreated control. Dotted line indicates the untreated control reference. Horizontal bars represent population means. C) Migration of cells treated with statins or LFA-1 inhibitors for 3 h towards CXCL13 analyzed by transwell assays. Values are presented as the ratio of migrating cells and total viable cells, relative to the untreated control. Dotted line indicates the untreated control reference. Horizontal bars represent population means. D) **Upper panel**: Percentage of proliferating CD19$^+$ CLL cells after ODN2006+IL15 stimulation (30 min before treatment) and treatment with different for 6 days measured by CFSE dilution (n=7). Horizontal bars represent population means. **Lower panel**: Flow cytometry histograms of a CLL representative case (#4) show the percentages of proliferating cells (gated on viable CD19$^+$ cells) after 6 days of ODN2006 and IL15 stimulation. A decrease in CFSE signal is indicative for cells that have divided. FMO, fluorescence-minus-one. Non-parametric Wilcoxon matched-pairs signed rank test was used for statistical analysis. *P<0.05*.
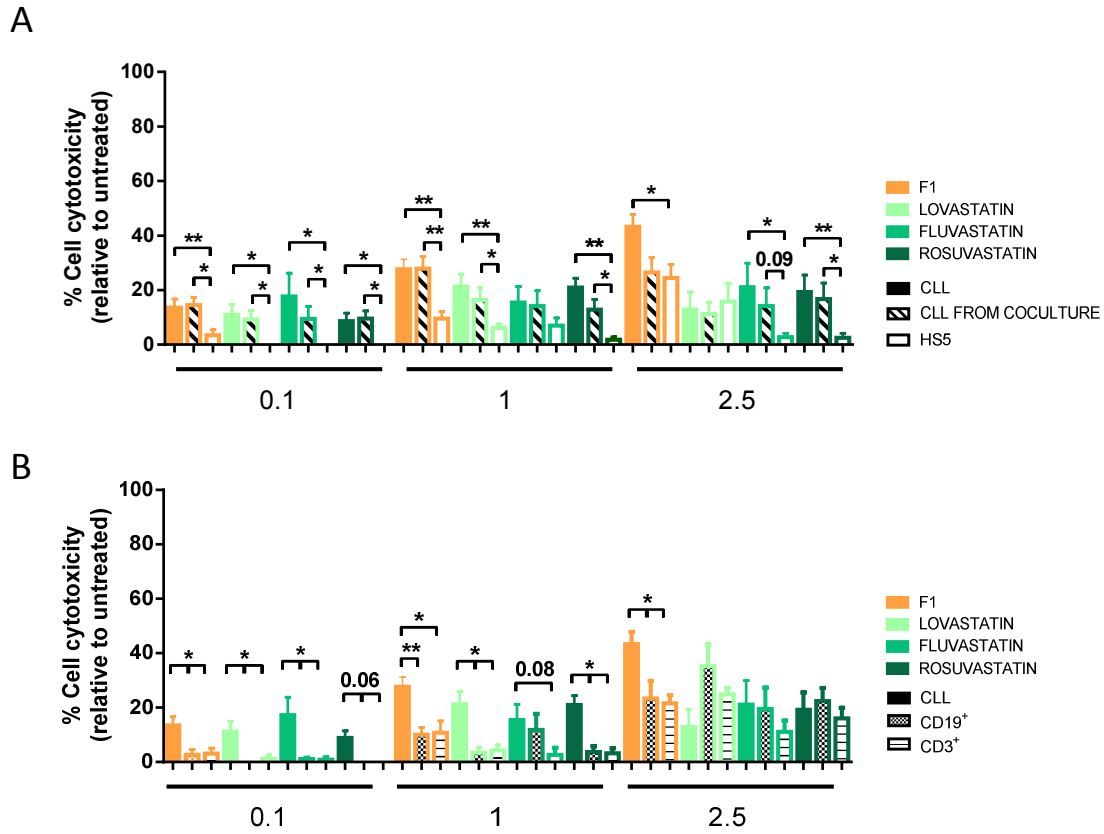
Figure 7. Statins exert a cytotoxic effect in primary CLL cells alone or in coculture with stromal cells, which is higher than in healthy B or T cells.
CLL cells or CD19^{+} B cells and CD3^{+} T cells from healthy donors were treated for 48 h with the statins at concentrations from 0.1 to 2.5 µM. Cytotoxicity was defined as the increase in Annexin-V[+]/PI^{+} cells compared to untreated control. A) Cytotoxicity of statins in primary CLL cells alone, in coculture with HS5 or in HS5 alone (n=6). B) Cytotoxicity of statins in primary CLL cells and CD19^{+} B cells and CD3^{+} T cells from healthy donors (n=8). The selected compounds exerted a preferential cytotoxic effect in CLL cells compared to their counterparts CD19^{+} or CD3^{+} cells. Bars represent the mean ± SEM of all samples analyzed. Non-parametric Wilcoxon matched-pairs signed rank test was used for statistical analysis. *P<0.05, **P<0.01.
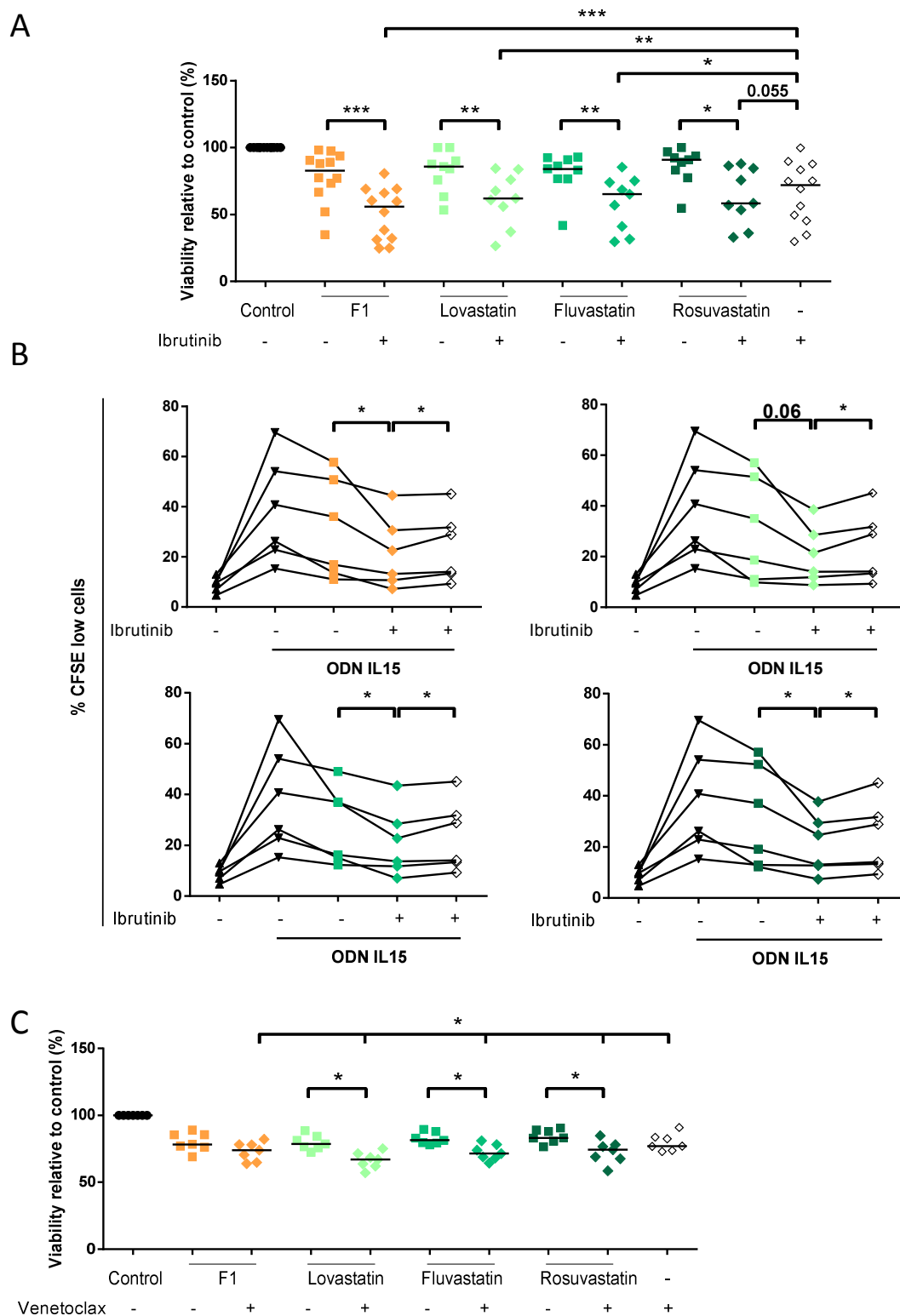
Figure 8. Combinatory effects of statins and venetoclax or ibrutinib.
Primary CLL cells were treated with 0.1 µM statins, 1 nM venetoclax and/or 0.1 µM ibrutinib. Percentage of viable cells was measured as CD19$^+$Annexin-V$^-$ cells by flow cytometry and normalized to untreated control samples.

A) Viability of CD19$^+$ cells after statins and or ibrutinib treatment for 6 days (n=9-12). Horizontal bars represent the mean of the population. B) Percentage of proliferating CD19$^+$ CLL cells after ODN2006+IL15 stimulation (30 min before treatment) and treatment with statins and or ibrutinib for 6 days measured by CFSE dilution (n=6). C) Viability of CD19$^+$ cells after statins and or venetoclax treatment for 48 h (n=7). Horizontal bars represent the mean of the population. Non-parametric Wilcoxon matched-pairs signed rank test was used for statistical analysis. *P<0.05*, **P<0.01*, ***P<0.001*.

Supplementary information

Compounds purchased

Compounds were purchased from Mcule Inc. (Palo Alto, CA, USA). The complete list is presented in supplementary Table S3. Other compounds selected from the 1st round screening were: BDBM62265 (Vitas-M Laboratory (Moscow, CA, Russia); BDBM54356: enamine (Monmouth Jct., NJ USA); GSK583, Lovastatin, Fluvastatin, Rosuvastatin, ML130 (nodinitib-1) from SelleckChem (Houston, TX USA), Lifitegrast and NOD-IN-1 (MedChemExpress; Monmouth Junction, NJ USA); and BDBM50199033 (KeyOrganics/Bionet; Cornwall, United Kingdom, PL329RA).

Compounds preparation

The compounds were purchased at 20 mM. The compounds purchased for target validation were bought or reconstituted to 10 mM.

As in some compounds, its direct dilution in aqueous media causes precipitation, we prepared the dilutions from stock solutions with a dilution 1:1 in aqueous media:DMSO

We checked by colorimetry and cytometry if the color compounds interfered with the analysis done.

SUPPLEMENTARY TABLES

Table S1. PMDIs of full-length articles in PubMed curated to identify proteins (effectors) with a known role on the microenvironment effect on CLL

	PMID		PMID		PMID		PMID
1	1709244	47	16270354	93	20357260	139	22151263
2	3048446	48	16423993	94	20382847	140	22160019
3	6537890	49	16517754	95	20454844	141	22289918
4	7520409	50	16621959	96	20473358	142	22333038
5	9159168	51	16699949	97	20488224	143	22397722
6	9207409	52	16785782	98	20495622	144	22446006
7	9470818	53	16832815	99	20501831	145	22457367
8	9720719	54	17080020	100	20530793	146	22474251
9	10025901	55	17082584	101	20544350	147	22475052
10	10233382	56	17241660	102	20606160	148	22475215
11	10329920	57	17447063	103	20618428	149	22521894
12	10393705	58	17508001	104	20620968	150	22593611
13	10545994	59	17654059	105	20643953	151	22623161
14	10979972	60	17928052	106	20671131	152	22672427
15	11248324	61	17984179	107	20687794		
16	11380405	62	18160669	108	20716767		
17	11460888	63	18223168	109	20809501		
18	11699221	64	18271063	110	20863894		
19	11700386	65	18358929	111	20883788		
20	11867687	66	18423023	112	20956327		
21	11981828	67	18470728	113	20981323		
22	11986954	68	18474259	114	21054149		
23	12351399	69	18765431	115	21078912		
24	12411322	70	18818986	116	21093051		
25	12470418	71	19036098	117	21209908		
26	12673718	72	19050243	118	21242190		
27	12688308	73	19074837	119	21347514		
28	12693719	74	19074885	120	21401803		
29	12857600	75	19278964	121	21417823		
30	12901966	76	19293181	122	21443542		
31	14504101	77	19383907	123	21465189		
32	14523464	78	19395025	124	21474673		
33	14687619	79	19547714	125	21487463		
34	14726163	80	19582829	126	21519633		
35	15001469	81	19604237	127	21524353		
36	15074015	82	19616847	128	21543761		
37	15109528	83	19654311	129	21546901		
38	15142527	84	19685493	130	21569005		
39	15176301	85	19934331	131	21595749		
40	15182336	86	19956173	132	21709686		
41	15184877	87	19956559	133	21765022		
42	15325098	88	19960063	134	21768328		
43	15860672	89	19965686	135	21876768		
44	15887227	90	20018914	136	21940819		
45	15927846	91	20159608	137	22130798		
46	16227675	92	20339095	138	22144129		

Table S2. CLL microenvironment motive

	Uniprot ID	Protein (Name)	Protein	Reference
1	Q13685	Angio-associated migratory cell protein	AAMP	
2	A1L0T0	Acetolactate synthase-like protein	ILVBL	
3	P60709	Actin, cytoplasmic 1	ACTB	[1]PMID: 19278964 [2] PMID: 20687794
4	P51617	Interleukin-1 receptor-associated kinase 1	IRAK1	PMID: 21642962
5	P63261	Actin, cytoplasmic 2	ACTG1	PMID: 19278964
6	P13612	Integrin alpha-4 // VLA-4 // CD49d	ITGA4	[1] PMID: 21876768 [2] PMID: 20687794 [3] PMID: 22160019
7	Q15848	Adiponectin	ADIPOQ	[1] PMID: 19960063 [2] PMID: 20454844 [3] PMID: 18818986
8	P20701	Integrin alpha-L	ITGAL // LFA-1	[1] PMID: 20687794 [2] PMID: 19293181 [3] PMID: 3048446 [4] PMID: 19934331
9	P03950	Angiogenin	ANG	[1] PMID: 16832815 [2] PMID: 15182336 [3] PMID: 15182336
10	P05556	Integrin beta-1 // VLA-4 // CD29	ITGB1	[1] PMID: 21876768 [2] PMID: 21093051 [3] PMID: 20687794 [4] PMID: 22160019
11	O15123	Angiopoietin-2	ANGPT2	[1] PMID: 20671131 [2] PMID: 17928052 [3] PMID: 20382847
12	P05107	Integrin beta-2	ITGB2	[1] PMID: 20687794 [2] PMID: 19293181 [3] PMID: 3048446
13	P35226	Polycomb complex protein BMI-1	BMI1	PMID: 22130798
14	Q08881	Tyrosine-protein kinase ITK/TS	ITK	PMID: 25730880
15	Q9BXJ1	Complement1q tumor necrosis factor-related protein1	C1QTNF1	
16	P35968	Vascular endothelial growth factor receptor 2	KDR // VEGFR2	PMID: 19965686
17	P06681	Complement C2	C2	
18	Q9UJU2	Lymphoid enhancer-binding factor 1	LEF1	PMID: 22446006
19	P10643	Complement component C7	C7	
20	P41159	Leptin	LEP	[1] PMID: 20454844 [2] PMID: 20643953 [3] PMID: 17080020 [4] PMID: 11460888
21	P29466	Caspase-1	CASP1	
22	Q9Y608	Leucine-rich repeat flightless-interacting protein 2	LRRFIP2	
23	Q92583	C-C motif chemokine 17	CCL17	[1] PMID: 20883788 [2] PMID: 21709686 [3] PMID: 20883788
24	P08581	Hepatocyte growth factor receptor	MET	[1] PMID: 20809501 [2] PMID: 10979972
25	Q99731	C-C motif chemokine 19	CCL19	[1] PMID: 20883788 [2]PMID: 20687794 [3] PMID: 17082584 [4] PMID: 15184877
26	P14780	Matrix metalloproteinase-9	MMP9	[1] PMID: 21569005 [2] PMID: 20159608 [3] PMID: 19965686 [4] PMID: 15109528
27	P13500	C-C motif chemokine 2	CCL2	[1] PMID: 22397722 [2] PMID: 19074885 [3] PMID: 20981323
28	Q99836	Myeloid differentiation primary response protein MyD88	MYD88	[1] PMID: 19050243 [2] PMID: 22150006
29	O00585	C-C motif chemokine 21	CCL21	[1] PMID: 20883788 [2]PMID: 20687794 [3] PMID: 17082584 [4] PMID: 15184877
30	Q96MN2	NACHT, LRR and PYD domains-containing protein 4	NALP4	

	Uniprot ID	Protein (Name)	Protein	Reference
31	O00626	C-C motif chemokine 22	CCL22	[1] PMID: 11981828 [2] PMID: 12688308 [3] PMID: 20883788
32	P59047	NACHT, LRR and PYD domains-containing protein 5	NALP5	
33	P10147	C-C motif chemokine 3	CCL3	PMID: 20883788
34	P19838	Nuclear factor NF-kappa-B p105 subunit	NFKB1	[1] PMID: 20863894 [2] PMID: 20148715
35	P13236	C-C motif chemokine 4	CCL4	PMID: 20883788
36	O00221	NF-kappa-B inhibitor epsilon	NFKBIE	PMID: 22675518
37	P32246	C-C chemokine receptor type 1	CCR1	[1] PMID: 19383907 [2] PMID: 20883788 [3] PMID: 15001469
38	Q9NPP4	NLR family CARD domain-containing protein 4	NLRC4	
39	P51679	C-C chemokine receptor type 4	CCR4	[1]PMID: 20883788 [2] PMID: 21443542
40	Q9Y239	Nucleotide-binding oligomerization domain-containing protein 1	NOD1	PMID: 19036098
41	P51681	C-C chemokine receptor type 5	CCR5	[1] PMID: 19383907 [2] PMID: 20883788
42	P04085	Platelet-derived growth factor subunit A	PDGFA	[1] PMID: 20606160 [2] PMID: 16227675
43	P32248	C-C chemokine receptor type 7	CCR7	[1] PMID: 21347514 [2] PMID: 20883788
44	P01127	Platelet-derived growth factor subunit B	PDGFB	[1] PMID: 20606160 [2] PMID: 16227675
45	Q86VB7	Scavenger receptor cysteine-rich type 1 protein M130	CD163	
46	P16234	Platelet-derived growth factor receptor alpha	PDGFRA	[1] PMID: 20606160 [2] PMID: 16227675
47	P16671	Platelet glycoprotein 4	CD36	
48	P16284	Platelet endothelial cell adhesion molecule	PECAM1 // CD31	[1] PMID: 12673718 [2] PMID: 19956559 [3] PMID: 16621959
49	P28907	ADP-ribosyl cyclase 1	CD38	[1] PMID: 20620968 [2] PMID: 22289918 [3] PMID: 21765022
50	Q13393	Phospholipase D1	PLD1	PMID: 19934331
51	P25942	Tumor necrosis factor receptor superfamily 5	CD40	[1] PMID: 20687794 [2] PMID: 22160019 [3] PMID: 22593611 [4] PMID: 22475052
52	O43157	Plexin-B1	PLXNB1	PMID: 22446006
53	P29965	CD40 ligand // CD154	CD40LG	[1] PMID: 20687794 [2] PMID: 22160019 [3] PMID: 22593611 [4] PMID: 22475052
54	Q13635	Protein patched homolog 1	PTCH1	PMID: 22130798
55	P04233	HLA class II histocompatibility antigen gamma chain	CD74	[1] PMID: 20357260 [2] PMID: 21417823
56	Q6ISU1	Pre T-cell antigen receptor alpha	PTCRA	[1] PMID: 20620968 [2] PMID: 21078912 [3] PMID: 17984179
57	P39060	Collagen alpha-1(XVIII) chain // Endostatin	COL18A1	[1] PMID: 17654059 [2] PMID: 12693719 [3] PMID: 12857600
58	P63000	Ras-related C3 botulinum toxin substrate 1	RAC1	[1] PMID: 19934331 [2] PMID: 20687794 [3] PMID: 21940819 [4] PMID: 21474673
59	P78423	Fractalkine	CX3CL1	[1] PMID: 21546901 [2] PMID: 22457367
60	P61586	Transforming protein RhoA	RHOA	[1] PMID: 22474251 [2] PMID: 20488224 [3] PMID: 19934331
61	P49238	CX3C chemokine receptor 1	CX3CR1	[1] PMID: 21546901 [2] PMID: 15325098 [3] PMID: 22457367
62	Q15669	Rho-related GTP-binding protein RhoH	RHOH	[1] PMID: 22474251 [2] PMID: 20687794

178

	Uniprot ID	Protein (Name)	Protein	Reference
63	P48061	Stromal cell-derived factor 1	CXCL12	[1] PMID: 20687794 [2] PMID: 22160019 [3] PMID: 19934331 [4] PMID: 20883788
64	P18827	Syndecan-1	SDC1	[1] PMID: 9470818 [2] PMID: 18470728
65	O43927	C-X-C motif chemokine 13	CXCL13	PMID: 20883788
66	P14151	L.-selectin	SELL // CD62L	[1]PMID: 11699221 [2] PMID: 10233382 [3] PMID: 19654311 [4] PMID: 1709244 [5] PMID: 7520409
67	P19875	C-X-C motif chemokine 2	CXCL2	[1] PMID: 22397722 [2] PMID: 19074885
68	Q92854	Semaphorin-4D	SEMA4D//CD100	PMID: 22446006
69	Q07325	C-X-C motif chemokine 9	CXCL9	PMID: 20981323
70	Q9HC62	Sentrin-specific protease 2	SENP2	
71	P49682	C-X-C chemokine receptor type 3	CXCR3	[1] PMID: 20687794 [2] PMID: 10393705
72	Q8N474	Secreted frizzled-related protein 1	SFRP1	PMID: 16423993;PMID: 22672427
73	P61073	C-X-C chemokine receptor type 4	CXCR4	[1] PMID: 22160019 [2] PMID: 20687794
74	Q96HF1	Secreted frizzled-related protein 2	SFRP2	PMID; 20495622
75	P32302	C-X-C chemokine receptor type 5	CXCR5	PMID: 20883788
76	Q9UMX1	Suppressor of fused homolog	SUFU	PMID: 19074837
77	O00571	ATP-dependent RNA helicase DDX3X	DDX3X	PMID: 22150006
78	P04435	T-cell receptor beta chain V region CTL-L17	TCRB	[1] PMID: 20620968 [2] PMID: 21078912 [3] PMID: 17984179
79	O76075	DNA fragmentation factor subunit beta	DFF2	
80	P01137	Transforming growth factor beta-1	TGFB1	[1] PMID: 9207409 [2] PMID: 9720719 [3] PMID: 9159168 [4] PMID: 15927846
81	O94907	Dickkopf-related protein 1	DKK1	PMID: 20618428
82	P61812	Transforming growth factor beta-2	TGFB2	PMID: 16785782
83	Q9UBU2	Dickkopf-related protein 2	DKK2	PMID: 22672427
84	P07996	Thrombospondin-1	THBS1 // TSP1	[1] PMID: 19604237 [2] PMID: 18423023 [3] PMID: 10329920 [4] PMID: 10545994
85	Q9UBP4	Dickkopf-related protein 3	DKK3	PMID: 22672427
86	P35590	Tyrosine-protein kinase receptor Tie-1	TIE1	[1] PMID: 16832815 [2] PMID: 11248324
87	P09038	Fibroblast growth factor-2	FGF2	[1] PMID: 19960063 [2] PMID: 17241660 [3] PMID: 11380405 [4] PMID: 11700386
88	P58753	Toll/interleukin-1 receptor domain-containing adapter protein	TIRAP/MAL	
89	P17948	Vascular endothelial growth factor receptor 1	FLT1 // VGFR1	PMID: 11986954
90	Q15399	Toll-like receptor 1	TLR1	[1] PMID: 19036098 [2] PMID: 19685493 [3] PMID: 19036098
91	P35916	Vascular endothelial growth factor receptor 2	FLT4 // VEGFR3	PMID: 14687619
92	O60603	Toll-like receptor 2	TLR2	[1] PMID: 22521894 [2] PMID: 19685493 [3] PMID: 19036098
93	P02751	Fibronectin	FN1	[1] PMID: 10025901 [2] PMID: 20501831 [3] PMID: 11867687
94	O60602	Toll-like receptor 5	TLR5	
95	Q9NPG1	Frizzled-3	FZD3	PMID: 22446006

	Uniprot ID	Protein (Name)	Protein	Reference
96	Q9Y2C9	Toll-like receptor 6	TLR6	[1] PMID: 19685493 [2] PMID: 19036098
97	P08151	Zinc finger protein GLI1	GLI1	PMID: 22130798
98	Q9NYK1	Toll-like receptor 7	TLR7	PMID: 19685493
99	P10070	Zinc finger protein GLI2	GLI2	PMID: 19074837
100	Q9NR96	Toll-like receptor 9	TLR9	[1] PMID: 20339095 [2] PMID: 19685493 [3] PMID: 18474259 [4] PMID: 19050243
101	P14317	Hematopoietic lineage cell-specific protein	HCLS1	[1] PMID: 17508001 [2] PMID: 22333038 [3] PMID: 20530793
102	P01375	Tumor necrosis factor	TNF	[1] PMID: 21242190 [2] PMID: 12901966 [3] PMID: 22144129 [4] PMID: 21487463
103	P14210	Hepatocyte growth factor	HGF	[1] PMID: 20809501 [2] PMID: 10979972
104	O14788	Tumor necrosis factor receptor superfamily 11A	TNFRSF11A // RANK	PMID: 16270354
105	Q16665	Hypoxia-inducible factor 1-alpha	HIF1A	[1] PMID: 18423023 [2] PMID: 21401803 [3] PMID: 20018914
106	O14836	Tumor necrosis factor receptor superfamily 13B	TNFRSF13B // TACI	[1] PMID: 22160019 [2] PMID: 15860672
107	P05362	Intercellular adhesion molecule 1	ICAM1	[1] PMID: 20687794 [2] PMID: 15142527
108	Q96RJ3	Tumor necrosis factor receptor superfamily 13C	TNFRSF13C // BAFFR	[1] PMID: 22160019 [2] PMID: 20956327 [3] PMID: 19395025 [4] PMID: 14504101
109	P22301	Interleukin-10	IL10	[1] PMID: 19956173 // [2] PMID: 21242190
110	Q02223	Tumor necrosis factor receptor superfamily 17	TNFRSF17 // BCMA	[1] PMID: 22160019 [2] PMID: 15860672
111	P29460	Interleukin-12 subunit beta	IL12AB	[1] PMID: 15176301 [2] PMID: 12470418
112	P50591	Tumor necrosis factor ligand superfamily 10	TNFSF10 // TRAIL	[1] PMID: 19547714 [2] PMID: 18160669 [3] PMID: 16699949 [4] PMID: 15887227
113	P29459	Interleukin-12 subunit alpha	IL12B	[1] PMID: 15176301 [2] PMID: 12470418
114	Q9Y6Q6	Tumor necrosis factor ligand superfamily 11	TNFSF11 // RANKL	PMID: 16270354
115	Q8NAC3	Interleukin-17 receptor C	IL17RC	
116	O75888	Tumor necrosis factor ligand superfamily 13	TNFSF13 // APRIL	[1] PMID: 22160019 [2] PMID: 21543761 [3] PMID: 21595749 [4] PMID: 15860672
117	P01584	Interleukin-1	IL1B	[1] PMID: 18271063 [2] PMID: 9470818 [3] PMID: 15074015
118	Q9Y275	Tumor necrosis factor ligand superfamily 13B	TNFSF13B // BAFF	[1] PMID: 22160019 [2] PMID: 20956327 [3] PMID: 19395025 [4] PMID: 15860672
119	P60568	Interleukin-2	IL2	[1] PMID: 16517754 [2] PMID: 22623161 [3] PMID: 20544350 [4] PMID: 19582829
120	Q9H3D4	Tumor protein 63	TP63	[1] PMID: 20357260 [2] PMID: 21417823
121	Q9HBE4	Interleukin-21	IL21	PMID: 17447063
122	Q13077	TNF receptor-associated factor 1	TRAF1	[1] PMID: 12411322 [2] PMID: 21524353
123	O95760	Interleukin-33	IL33	
124	Q12933	TNF receptor-associated factor 2	TRAF2	[1] PMID: 20863894 [2] PMID: 12411322 [3] PMID: 21524353
125	P05112	Interleukin-4	IL4	[1] PMID: 20687794 [2] PMID: 21768328 [3] PMID: 20716767

	Uniprot ID	Protein (Name)	Protein	Reference
126	P19320	Vascular cell adhesion protein 1	VCAM1	PMID: 22160019
127	P05231	Interleukin-6	IL6	[1] PMID: 22475215 [2] PMID: 21465189 [3] PMID: 15176301
128	P15692	Vascular endothelial growth factor A	VEGFA	[1] PMID: 19616847 [2] PMID: 18423023 [3] PMID: 21519633 [4] PMID: 21054149
129	P10145	Interleukin-8	IL8 // CXCL8	[1] [2] PMID: 16270354
130	P08670	Vimentin	VIM	[1] PMID: 20620968 [2] PMID: 6537890 [3] PMID: 21209908
131	P42768	Wiskott-Aldrich syndrome protein	WAS	[1] PMID: 20687794 [2] PMID: 12351399 [3] PMID: 18223168
132	Q9Y5W5	Wnt inhibitory factor 1	WIF1	[1] PMID: 18765431 [2] PMID: 18765431
133	Q9GZT5	Protein Wnt-10a	WNT10A	PMID: 20473358
134	Q9UBV4	Protein Wnt-16	WNT16	PMID: 22446006
135	P56703	Proto-oncogene Wnt-3	WNT3	PMID: 14523464
136	Q9H1J7	Protein Wnt-5b	WNT5B	PMID: 20473358
137	Q9Y6F9	Protein Wnt-6	WNT6	PMID: 20473358
138	O14904	Protein Wnt-9a	WNT9A // WNT14	PMID: 22446006
139	P43403	Tyrosine-protein kinase ZAP-70	ZAP70	[1] PMID: 20687794 [2] PMID: 18358929 [3] PMID: 14726163 [4] PMID: 22151263

Table S3. CLL microenvironment Key Proteins (Uamb-KeyProts)

	Uniprot	[1]Causative Effect		Uniprot	[1]Causative Effect
1	O43566	1	30	P14210	-1
2	P12931	-1	31	P19838	-1
3	P25105	-1	32	P19875	-1
4	P61224	1	33	P32246	-1
5	P62834	1	34	P48061	-1
6	Q15139	1	35	P49238	-1
7	Q9UL17	1	36	P78423	-1
8	P40763	-1	37	Q02223	-1
9	Q04206	-1	38	Q07325	-1
10	P31994	1	39	Q08881	-1
11	O00206	-1	40	Q15389	-1
12	O00585	-1	41	Q15399	-1
13	O14625	-1	42	Q15848	1
14	O14788	-1	43	Q86VB7	-1
15	O14904	-1	44	Q92583	-1
16	O15123	-1	45	Q92854	-1
17	O60602	-1	46	Q99731	-1
18	O60603	-1	47	Q99836	-1
19	O75888	-1	48	Q9BXR5	-1
20	P01127	-1	49	Q9GZT5	-1
21	P01375	-1	50	Q9H1J7	-1
22	P02778	-1	51	Q9HB19	-1
23	P04085	-1	52	Q9UBP4	1
24	P05771	-1	53	Q9UBU2	1
25	P09038	-1	54	Q9Y275	-1
26	P10145	-1	55	Q9Y2C9	-1
27	P10147	-1	56	Q9Y608	-1
28	P13236	-1	57	Q9Y6F9	-1
29	P13500	-1			

[1]Causative effect referers to the state of the protein (more active +1, less active -1) that contributes to produce CLL

Table S4. Compounds purchased

#	Internal ID	Mcule ID	Systematic name	Common Name
1	A1	2510363079	N-(4-methyl-5-{2-[(3-nitrophenyl)amino]-1,3-thiazol-4-yl}-1,3-thiazol-2-yl)acetamide	N.A.
2	A2	8191036162	2-(3,4-dihydroxyphenyl)-5-hydroxy-7-{[(2S,3R,4S,5S,6R)-3,4,5-trihydroxy-6-(hydroxymethyl)oxan-2-yl]oxy}-4H-chromen-4-one	N.A.
3	A3	8792621521	1-(4-acetylphenyl)-3-{2-[3-(prop-1-en-2-yl)phenyl]propan-2-yl}urea	N.A.
4	A4	6000022702	3-{3-[4-(dimethylamino)phenyl]prop-2-enoyl}-4-hydroxy-2H-chromen-2-one	N.A.
5	A5	7249710756	1-(4-methylbenzenesulfonyl)-1H-1,3-benzodiazol-2-amine	N.A.
6	A6	8365251586	N-{3,5-dimethyl-1-[(2-methylphenyl)methyl]-1H-pyrazol-4-yl}-4H,5H-naphtho[2,1-d][1,2]oxazole-3-carboxamide	N.A.
7	A7	3618750171	[(4-carbamoylphenyl)carbamoyl]methyl 3-(2H-1,3-benzodioxol-5-yl)prop-2-enoate	N.A.
8	A8	9291497335	3-amino-2-(2-{[5-(2H-1,3-benzodioxol-5-yl)-1,3,4-oxadiazol -2-yl]sulfanyl}acetyl)but-2-enenitrile	N.A.
9	A9	9607341619	1-[2,5-dimethyl-1-(prop-2-en-1-yl)-1H-pyrrol-3-yl]-2-[(6-methyl-2-nitropyridin-3-yl)oxy]ethan-1-one	N.A.
10	A10	6560812611	3-(4-hydroxyphenyl)-1-phenylprop-2-en-1-one	N.A.
11	A11	2266778062	5,5-dimethyl-2-{[(pyridin-3-yl)amino]methylidene}cyclohexane-1,3-dione	N.A.
12	A12	9723270257	3-cyano-3-[(2Z)-2,3-dihydro-1H-1,3-benzodiazol-2-ylidene]-2-oxopropyl 2-[(4-bromo-2-methylphenyl)sulfanyl]acetate	N.A.
13	B1	7885672138	6,7-dihydroxy-4-({[5-(3,4,5-trimethoxyphenyl)-1,3,4-oxadiazol-2-yl]sulfanyl}methyl)-2H-chromen-2-one	N.A.
14	B2	6680323146	N-(2-methylphenyl)-5-[(oxan-2-ylmethyl)sulfanyl]-1,3,4-thiadiazol-2-amine	N.A.
15	B3	4044779367	4-(3-methoxypropyl)-4H-1,2,4-triazole-3-thiol	N.A.
16	B4	9334292863	2-{4-[5-methyl-2-(propan-2-yl)phenoxymethyl]phenyl}-1,3,4-oxadiazole	N.A.
17	B5	1772644300	2-chloro-5H,6H,7H,8H,9H,10H-cyclohepta[b]indole-6-carboxamide	N.A.
18	B6	5533294331	(1S,2R,13R,14S,17R,18S)-17-ethynyl-2,18-dimethyl-7-oxa-6-azapentacycloicosa-4(8),5,9-trien-17-ol	Danazol
19	B7	3157000542	3-(4-chlorophenyl)-6-(4-fluorophenyl)-5-methylpyrazolo[1,5-a]pyrimidin-7-amine	N.A.
20	B8	2559361853	1-[(4-methoxyphenyl)methyl]-2-(2-phenylethenyl)-1H-1,3-benzodiazole	N.A.
21	B9	2997420086	N-(3-chloro-4-methylphenyl)-2-[3-chloro-5-(trifluoromethyl)pyridin-2-yl]acetamide	N.A.
22	B10	4158159239	ethyl 2-[(propan-2-yl)carbamoyl]-3-{[3-(trifluoromethyl)phenyl]carbamoyl}cyclopropane-1-carboxylate	N.A.
23	B11	9091986717	2-phenyl-5-(1H-pyrazol-3-yl)-1,3-thiazole	PHENYL-5- (1H-PYRAZOL-3-YL)-1,3-THIAZOLE
24	B12	6640334579	4-methyl-N-(quinoxalin-6-yl)benzamide	N.A.
25	C1	5893043131	propanedioic acid	Malonic acid
26	C2	2979302446	5,7-dihydroxy-3-(4-methoxyphenyl)-6,8-bis(piperidin-1-ylmethyl)-4H-chromen-4-one	N.A.
27	C3	9740144074	2-(3-benzoylphenyl)propanoic acid	Ketoprofen
28	C4	5948863568	3,5-diamino-N-carbamimidoyl-6-chloropyrazine-2-carboxamide hydrochloride	Amipramidin Amiloride
29	C5	7734253699	5-chloro-7-{[4-(pyridin-2-yl)piperazin-1-yl]methyl}quinolin-8-ol	N.A.
30	C6	3879834235	[3,4,5-tris(acetyloxy)-6-sulfanyloxan-2-yl]methyl acetate	Auranofin
31	C7	7254287531	2-[4-(dimethylamino)phenyl]-3,6-dimethyl-1,3-benzothiazol-3-ium chloride	N.A.
32	C8	5620960445	methylsulfanylmethanethioyamino(1-phenylethylidene)amine	N.A.

#	Internal ID	Mcule ID	Systematic name	Common Name
33	C9	8575702894	N-(2-phenylphenyl)thiophene-2-carboxamide	N.A.
34	C10	8679857296	1-(3-chlorophenyl)-3-[4-(dimethylamino)phenyl]urea	N.A.
35	C11	6627172552	N-{10,13-dioxa-4-thia-6-azatricyclo[7.4.0.0]trideca-1,3(7),5,8-tetraen-5-yl}-2-methoxybenzamide	N.A.
36	C12	2208162052	2-(4-ethylphenyl)-2-oxoethyl 3-{4-methyl-1,3-dioxo-1H,2H,3H-pyrrolo[3,4-c]quinolin-2-yl}benzoate	N.A.
37	D1	7541888215	(4E)-6-(chloromethyl)-4-[(naphthalen-2-yl)imino]-4,5-dihydro-1,3,5-triazin-2-amine	N.A.
38	D2	3296821986	2-(4-propoxyphenyl)imidazo[1,2-a]pyridine	N.A.
39	D3	5608953652	10-amino-3-azatricyclo[7.3.1.0]trideca-1(13),5,7,9,11-pentaene-2,4-dione	6-AMINO-BENZO[DE]ISOQUINOLINE-1,3-DIONE
40	D4	9880228788	N-[(1E)-amino({[(2E)-2,3-dihydro-1,3-benzothiazol-2-ylidene]amino})methylidene]-3-methylbutanamide	N.A.
41	D5	7960548249	5-oxo-1H,2H,3H,4H,5H-chromeno[3,4-b]pyridin-4-ium-9-olate	N.A.
42	D6	6404224369	N-(5-benzyl-1,3-thiazol-2-yl)thiophene-2-carboxamide	N.A.
43	D7	3721465696	4-[3-(4-aminophenoxy)phenoxy]aniline	N.A.
44	D8	7823638137	2-(4-tert-butylphenyl)-1,3-benzothiazole	N.A.
45	D9	9761380121	1-(2H-1,3-benzodioxol-5-yl)-3-[(2-bromophenyl)amino]prop-2-en-1-one	N.A.
46	D10	1144303704	N-(4-fluorophenyl)-5-nitropyridin-2-amine	N.A.
47	D11	2502936802	17-{[(3-hydroxyphenyl)methylidene]amino}-17-azapentacyclo[6.6.5.0]nonadeca-2,4,6,9(14),10,12-hexaene-16,18-dione	N.A.
48	D12	5228315948	1-(2,5-dimethylphenyl)-3-[2-(1H-indol-3-yl)ethyl]thiourea	N.A.
49	E1	5990662836	N-(6-chloro-1,3-benzothiazol-2-yl)furan-2-carboxamide	N.A.
50	E2	3379988083	N-(2-methoxyphenyl)-4-(thiophen-2-yl)-1,3-thiazol-2-amine	N.A.
51	E3	2521803878	3-methoxy-N-(4-methylphenyl)benzamide	N.A.
52	E4	4381636893	1-(4-phenylbenzoyl)-3-(2,4,6-trimethylphenyl)thiourea	N.A.
53	E5	6212734898	5-[(2-phenoxyethyl)sulfanyl]-1-phenyl-1H-1,2,3,4-tetrazole	N.A.
54	E6	5694794398	N-[4-(diethylamino)phenyl]-7-(difluoromethyl)-5-methyl-[1,2,4]triazolo[1,5-a]pyrimidine-2-carboxamide	N.A.
55	E7	3199876315	4-benzyl-2-[N-(2-hydroxy-5-methylphenyl)carboximidoyl]-6-nitrophenol	N.A.
56	E8	1048848056	2-aminoacetamide hydrochloride	Glycinamid
57	E9	7690742955	1,3-diethyl-5-[(1-methyl-1H-indol-3-yl)methylidene]-2-sulfanylidene-1,3-diazinane-4,6-dione	N.A.
58	E10	3097873461	6-[(4,6-dimethylpyrimidin-2-yl)sulfanyl]-4-methyl-8-oxa-3,5-diazatricyclo[7.4.0.0?,?]trideca-1(13),2(7),3,5,9,11-hexaene	N.A.
59	E11	6327754946	2-(2,6-dioxopiperidin-3-yl)-2,3-dihydro-1H-isoindole-1,3-dione	Thalidomide
60	E12	5734283547	2-(methylamino)pentanoic acid	N-Methylleucine
61	F1	8390617062	(1S,3R,7S,8S,8aR)-8-{2-[(2R,4R)-4-hydroxy-6-oxooxan-2-yl]ethyl}-3,7-dimethyl-1,2,3,7,8,8a-hexahydronaphthalen-1-yl 2,2-dimethylbutanoate	Simvastatin
62	F2	3065255051	5-benzoyl-2,3-dihydro-1H-pyrrolizine-1-carboxylic acid	ROX-888
63	F3	5698614065	2-[(3R,11S,17S,20S,25aS)-11-(4-carbamimidamidobutyl)-3-carbamoyl-20-(1H-indol-3-ylmethyl)-1,9,12,15,18,21-hexaoxo-docosahydro-1H-pyrrolo[2,1-g]1,2-dithia-5,8,11,14,17,20-hexaazacyclotricosan-17-yl]acetic acid	Eptifibatide
64	F4	3466233504	ethyl 2-cyano-4-(1-ethyl-1,2-dihydroquinolin-2-ylidene)but-2-enoate	N.A.
65	F5	4334386251	5-[2-(4-hydroxyphenyl)ethenyl]benzene-1,3-diol	SRT501/resveratrol

N.A. Not aplicable.

Table S5. Clinical and biological features of CLL patients

# Patient	Gender/ Age at diagnosis	[a]%Tumor cells[a]	[b]Binet/Rai stage	[c]IGHV	Previous treatment	[d]Cytogenetic alterations	[e]Recurrent mutations	Previous statins treatment
CLL 01	M/43	90	B/II	M	Chlorambucil	13Q	MYD88	
CLL 02	F/53	96	B/II	UM	2CDA, CHOP, ALOTPH	11Q, TRISOMY 12		
CLL 03	M/28	91	B/II	UM	NO	N	NO	No
CLL 04	M/60	90	B/I	M	NO	TRISOMY12	NO	Simvastatin
CLL 05	M/58	95	B/II	M	RFCM	13Q, 17P	NO	No
CLL 06	F/61	92		UM	RFCM	N		
CLL 07	M/66	95	C/IV	M	No	13Q	NO	No
CLL 08	F/43	95	A/0	M	No	13Q	NO	?
CLL 09	M/69	98	A/0	M	No	N	NO	No
CLL 10	F/69	98	A/0	M	Chlorambucil	N	CHD2	No
CLL 11	F/52	92	B/II	M	No	TRISOMY12	NO	No
CLL 13	M/59	95	B/II	M	No	13Q	NFKBIA	No
CLL 14	M/67	95	B/II	UM	Fludarabine, chlorambucil, ofatumumab	13Q		
CLL 15	F/77	92	A/0	M	NO	N		
CLL 16	M/67	95	A/1	M	NO	13Q	NO	No
CLL 17	F/61	49	A/0	M	NO	13Q		
CLL 18	F/62	96	A/0	M	NO	11Q, TRISOMY 12	NO	No
CLL 19	M/58	86	B/II	UM	NO	13Q	BRAF	No
CLL 20	M/49	96	C/IV	M	NO	13Q	MYD88, CHD2	No
CLL 21	F/43	97	B/II	UM	FCM	N	NO	No
CLL 22	M/49	82	B/I	UM	NO	13Q		
CLL 23	M/54	94	A/0	M	NO	13Q, 17P	TP53	
CLL 24	F/62	96	A/0	M	NO	13Q	NO	

Abbreviations: M, male; F, female; ND, not determined; m, mutated; um, unmutated; N, normal; del, deletion; T, treated; U, untreated.
[a] Percentage of tumoral cells was quantified by flow cytometry labeling of CD5+/CD19+ cells and light chain restriction.
[b] According to Rai and Binet's classification: Early (Rai 0, Binet A), intermediate (Rai I/II, Binet B) and advanced (Rai III/IV, Binet C) stage disease.
[c] *IGVH* gene was sequenced following RT-PCR, and aligned to NCBI IgBlast. Mutated status was assigned when >2% deviation from germline IGHV sequence was present.
[d] Cytogenetic alterations were assessed by FISH.
[e] Recurrent mutations were identified by exome-sequencing analysis within the ICGC project.

Table S6. Selected compounds that target NOD

Compound	Uniprot AC	UniProt Target	UniProt (SwissProt) Recommended Name of Target Chain	IC50 (nM)
A1	Q07820	MCL1_HUMAN	Induced myeloid leukemia cell differentiation protein Mcl-1	902
	P01375	TNFA_HUMAN	Tumor necrosis factor	1,11E+04
	Q9HC29	NOD2_HUMAN	Nucleotide-binding oligomerization domain-containing protein 2	8,61E+03
	Q9Y239	NOD1_HUMAN	Nucleotide-binding oligomerization domain-containing protein 1	9,40E+03
A12	P01375	TNFA_HUMAN	Tumor necrosis factor	>2.00E+4
	P05186	PPBT_HUMAN	Alkaline phosphatase, tissue-nonspecific isozyme	2,41E+04
	P09923	PPBI_HUMAN	Intestinal-type alkaline phosphatase	1,34E+04
	P10696	PPBN_HUMAN	Alkaline phosphatase, placental-like	2,55E+04
	Q9HC29	NOD2_HUMAN	Nucleotide-binding oligomerization domain-containing protein 2	2,00E+04
	Q9Y239	NOD1_HUMAN	Nucleotide-binding oligomerization domain-containing protein 1	2,00E+04
C5	~~Q13285~~	STF1_HUMAN	Steroidogenic factor 1	6,65E+03
	P01375	TNFA_HUMAN	Tumor necrosis factor	6,23E+03
	P34949	MPI_HUMAN	Mannose-6-phosphate isomerase	5,00E+04
	Q9HC29	NOD2_HUMAN	Nucleotide-binding oligomerization domain-containing protein 2	4,88E+03
	Q9Y239	NOD1_HUMAN	Nucleotide-binding oligomerization domain-containing protein 1	4,58E+03
C7	Q9Y239	NOD1_HUMAN	Nucleotide-binding oligomerization domain-containing protein 1	556
	P01375	TNFA_HUMAN	Tumor necrosis factor	762
	P05067	A4_HUMAN	Amyloid beta A4 protein	116-9,000
	P06276	CHLE_HUMAN	Cholinesterase	3.620
	P22303	ACES_HUMAN	Acetylcholinesterase	1,000-5,000

Table S7. Compounds purchased to validate the targets

Internal ID	Targets	IC50 (nM)	Supplier	Catalog number
BDBM62265	NOD1	32	MoltPort-Vitas-M Laboratory	STK299594
	TNFA	216		
BDBM54356	NOD1	4800	ENAMINE	Z19669458
	TNFA	45,6		
	NOD2	36		
GSK583	RIP2	5	Selleck	S8261
	RIP3	16		
NOD IN 1	NOD1	5740	Medchem express	HY-100691
	NOD2	6450		
NODITINIB	NOD1	560	Selleck	ML130
Lovastatin	HMDH	20-20000	Selleck	S2061
	ITGAL / CD11A / LFA-1A	12900 KD		
Fluvastatin	HMDH	28	Selleck	S1909
Rosuvastatin	HMDH	3--6	Selleck	S2169
Lifitegrast	ITGAL / CD11A / LFA-1A	3	Medchem express	HY-19344
BDBM50199033	ITGAL / CD11A / LFA-1A	18-280	BIONET/Key Organics	BMS-587101 / HE-0001

Table S8. Simvastatin combination cancer therapies identified by a systems biology approach

Drug Name A	Probability A	Drug Name B	Probability B	Combination Probability
Simvastatin	75	Sorafenib	84	83
		Ibrutinib	73	82
		Alemtuzumab	85	79
		Imiquimod	78	77
		Rituximab	84	77
		Ofatumumab	84	77
		Venetoclax	68	76
		Idelalisib	60	73

Prediction values > 78 have an associated *P < 0.05*; values between 78 and 71 have a *P < 0.1*.

SUPPLEMENTARY FIGURES

A
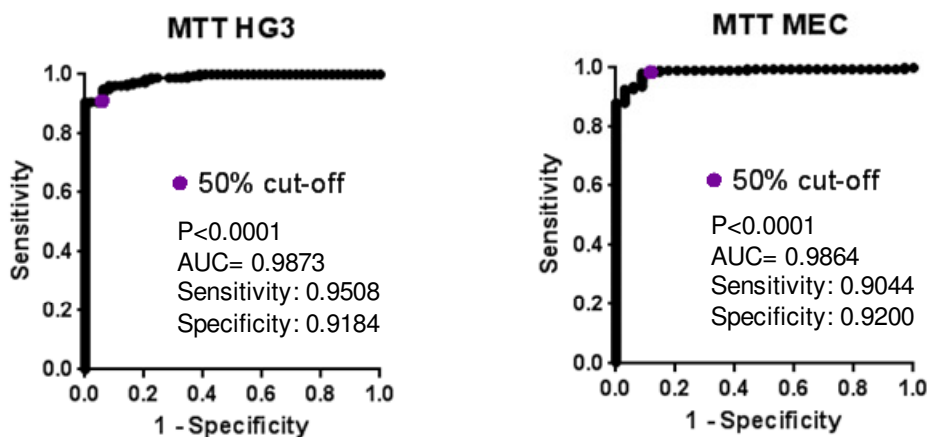
B
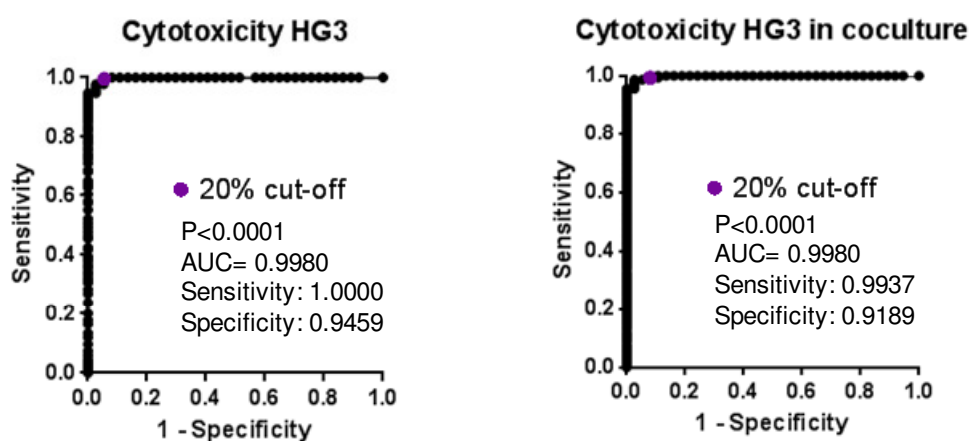
Figure S1. ROC analysis defines the threshold to discriminate the effect of the compounds.
ROC analysis of the Figure 1 data to define the best discrimination threshold. A) MTT ROC analysis in HG3 and MEC cell lines. B) Cytotoxicity ROC analysis in HG3 alone and in co-culture with HS5 cell line. ****$P < 0.0001$. AUC: Area under the curve.

A
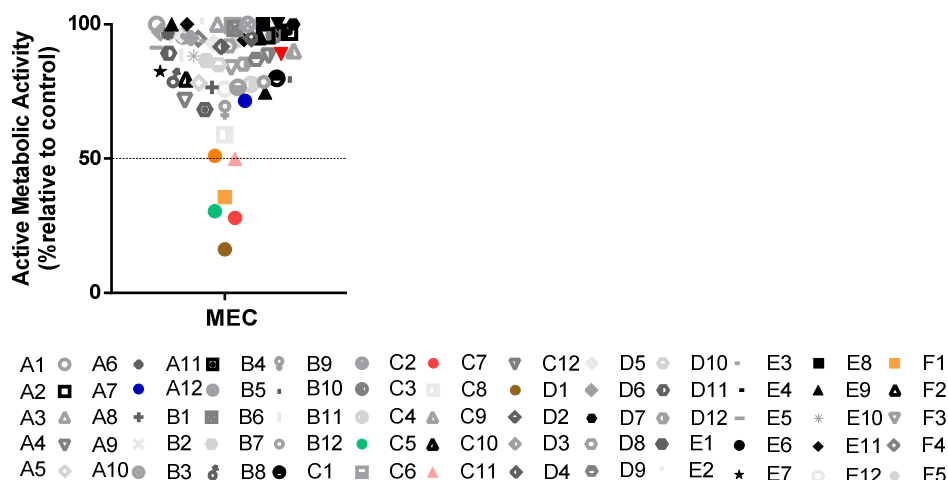
B
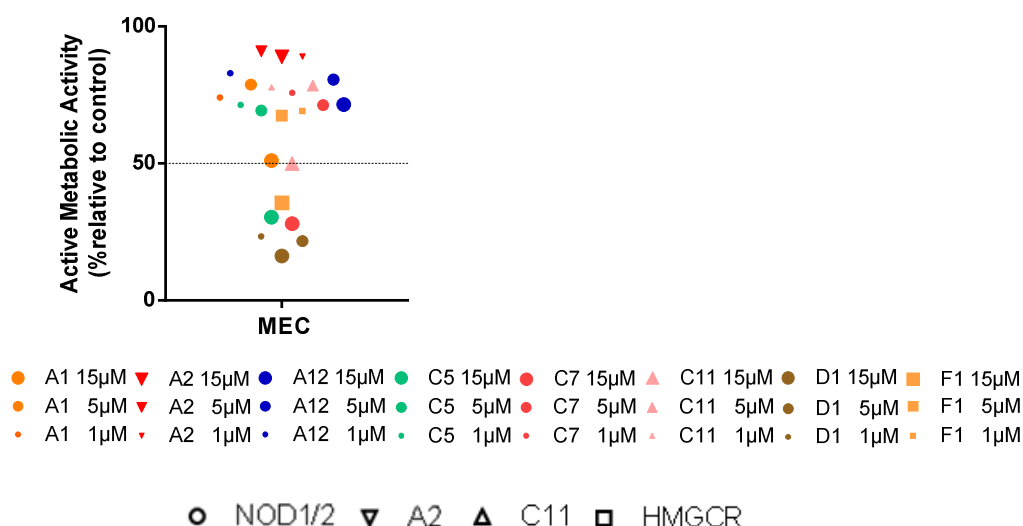
Figure S2. Compound library screening in MEC-1 cell line.
Cells were treated for 48 h with the compounds at concentrations from 1 to 15 µM. Each dot represents de mean of 3 independent experiments in different days. Dotted line indicates the threshold to discriminate the effect of the compounds. The cut off for MTT is 50% and for cytotoxicity is 20%. Active metabolic activity of CLL cells was measured using the MTT assay, and is depicted relative to untreated control. Cytotoxicity was defined as the increase in Annexin-V$^+$/PI$^+$ cells compared to untreated control. A) Active metabolic activity of cells treated with the compounds at the concentration of 15 µM in MEC-1 cell line. B) Active metabolic activity of cells treated with the compounds at the concentrations of 1-5-15 µM in the MEC-1 cell line. Round dots: compounds that target NOD1/2; Triangle down-pointing dots: A2; Triangle up-pointing dots: C11; Square dots: compounds that target HMGCR.

F1	
TARGET	**IC$_{50}$ (nM)**
HMGCR	11-49
LFA-1	Not detailed

LOVASTATIN	
TARGET	**IC$_{50}$ (nM)**
HMGCR	20-20100
LFA-1	12900

FLUVASTATIN	
TARGET	**IC$_{50}$ (nM)**
HMGCR	28
LFA-1	NA

ROSUVASTATIN	
TARGET	**IC$_{50}$ (nM)**
HMGCR	3.1-5.4
LFA-1	NA

LIFITEGRAST	
TARGET	**IC$_{50}$**
LFA-1	9-74

BDBM50199033	
TARGET	**IC$_{50}$**
LFA-1	18-280

Figure S4. Chemical structures and IC50 of main targets of statins and LFA-1 inhibitors used.

DISCUSSION

CLL is a malignancy of antigen-experienced mature B lymphocytes, in which microenvironmental signals play a critical role in their survival and proliferation.[20] CLL is an incurable disease with a heterogeneous clinical course. During the past 5 years, the knowledge of the genetic lesions underpinning CLL, along with the advent of novel drugs, has shifted the treatment strategy in patients with CLL from universal chemoimmunotherapy to more individualized approaches based on diagnostic stratification.[10, 14, 196]

Nowadays, standard chemotherapeutic agents, such as fludarabine, chlorambucil, bendamustine, and cyclophosphamide can only be used in patients without *TP53* alterations.[109, 110] Chemotherapy induces DNA-damage that can manifest as more aggressive and refractory phenotypes.[197] Avoiding alkylators and purine analogues also prevents prolonged cytopenias and the recurrent fatal infections seen after therapy with these agents.[198] Novel agents, like ibrutinib, idelalisib, and venetoclax, do not exert their antileukemic activity through genotoxic mechanisms, and are therefore active irrespective of *TP53* dysfunction.[199] These novel agents are able to increase the complete remissions rates observed with standard immune-chemotherapy.[103]
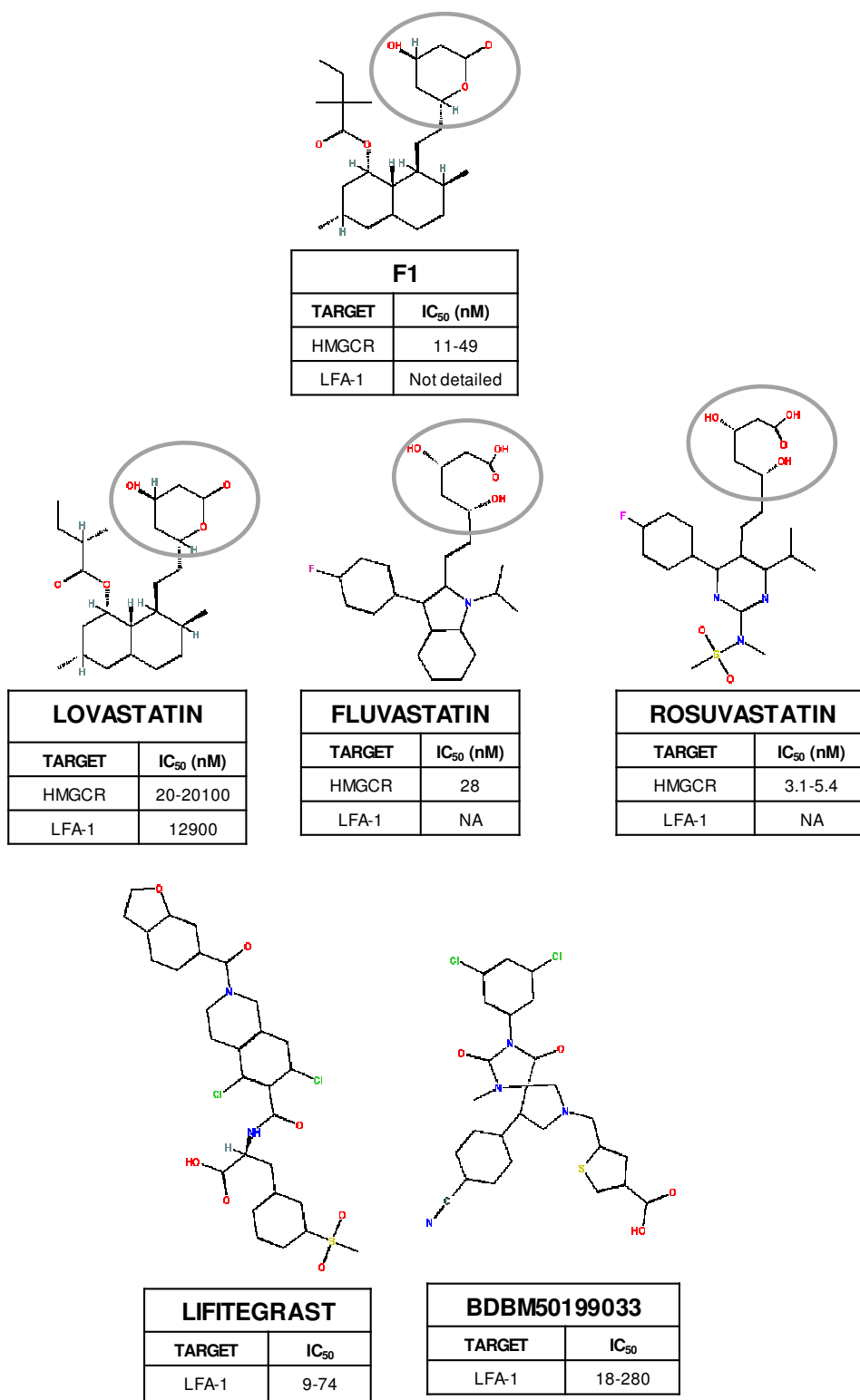
This is paralleled by substantial increase in understanding the disease genetics owing to major advances in the next generation sequencing (NGS) technology.[130, 200] NGS efforts have identified somatic mutations in the coding and non-coding regions of several genes in CLL patients with frequencies up to 15%.[34] CLL harbors a high degree of genetic variability and intratumoral heterogeneity, rather than a single driver mutation.[24, 34, 35, 40] The most frequent mutation in CLL is *NOTCH1* (13-15%) followed by *ATM* (9-11%), *SF3B1* (9%) and *BIRC3* (9%). Other mutations occur in lower frequencies like *TP53* (5%), *MYD88* (4%), *POT1* (2-3%) or *BRAF* (2%).[23, 24, 40] Some mutations are specific of the IGHV mutational status (e.g., *MYD88* in IGHV M or *BRAF* in IGHV UM cells) and others are present in both subsets (e.g.,*SF3B1,* although with different frequencies).[23, 24, 41]

The mutational status of the IGHV is important to define the clinical course of the disease, but there are other important determinants of the clinical outcome of the patients, like deletions/mutations of 11q/*ATM/BIRC3* and 17p/*TP53*.[16, 58, 201, 202] Several somatic mutations, including some with a low incidence, have been reported to be associated with particular clinical features and disease evolution.[23, 42, 203, 204] Although a lot of effort is being deputed to define specific subgroups before treatment, the only genetic factor that affects the treatment decision, a part from the IGHV mutational status, is *TP53*.[102]

Exploring the molecular pathways involved in disease pathogenesis enables to propose new genes which could be targeted for therapeutic purposes.[205] Given the growing number of new targeted agents, the management of CLL will conceivably be revised and early

intervention may also become an option. In this changing scenario, there is increasing interest in the use of prognostic markers that may guide the management of patients from the early phases of the disease.[206, 207]

The best pathway studied involved in CLL pathogenesis is the BCR pathway. Different aspects of the BCR have been recognized as prognostic markers in CLL (such as IGHV mutational status or the IGH stereotypes).[102] The BCR is key for the fate of B cells and plays an important role in the survival of CLL cells. The BCR is connected to a network of kinases, like BTK or PI3K, that lead to downstream activation of NF-κB.[208, 209] In the past two decades BCR associated kinases (BAKs) inhibitors have been studied and have entered to clinics for CLL treatment with impressing results.[210, 211] Since BAKs are expressed in multiple cell types, they seem to disrupt the dialogue between malignant B cells and the TME. This concept also explains the typical response to BAKs inhibitors treatment, characterized by a long-lasting increase of PB lymphoid cells, due to redistribution from the lymphoid homing compartments.[10, 210]

Ibrutinib, the first BTK inhibitor approved for first-line treatment in CLL,[210] has achieved unprecedented response rates and excellent outcomes,[111] but toxicities may limit ibrutinib use. Reports of its use in community-based cohorts have estimated discontinuation rates as high as 40% in the first year of therapy.[212] The most relevant side effects were viral infections, pneumonitis, bleeding, atrial fibrillation and neutropenia.[212] *BTK* and distinct *PLCγ* (*phospholipase-C gamma*) mutations were identified *the novo* in 85% of patients with relapse after ibrutinib treatment, leading to a constitutive BCR activation.[131-133]

PI3K inhibitors, like idelalisib (a PI3Kδ inhibitor) reduces survival signals derived from the BCR or from NLC, and inhibits BCR-, AKT-, and MAPK- activation.[213] It is approved in CLL in combination with the anti-CD20 antibody rituximab. Unfortunately, PI3Kδ inhibition has been associated with a particular toxicity profile characterized by autoimmune complications and an increased risk of opportunistic infections, particularly in treatment- naive patients.[214]

More recently, BCL2 inhibitors appear in the clinical scenario as an alternative[215] or a combinatory option to BAKs inhibitors.[216] Proteins in the BCL2 family are key regulators of the apoptotic process and consist of proapoptotic and prosurvival proteins. The intrinsic apoptotic pathway is universally dysregulated in CLL due to overexpression of antiapoptotic proteins (such as BCL2).[19]

Venetoclax, a BCL2 inhibitor, acts as a BH3-mimetic, displacing the BH3-only protein (proapoptotic protein) from BCL2 thereby inducing apoptosis in BCL2 dependent lymphoid cells. Toxic effects included mild diarrhea, upper respiratory tract infection, nausea, neutropenia and tumor lysis syndrome. Venetoclax monotherapy is active and well tolerated

in R/R CLL patients presenting del17p13, providing a new therapeutic option for this poor prognosis population.[19] A recent study also propose the combination of venetoclax plus the monoclonal antibody obinutuzumab in R/R or previously untreated CLL patients.[217]

Inspite of all the advances and the huge number of highly active novel agents, there is not a cure for CLL, and all treatments still have adverse effects. In this thesis we explore new therapeutic purposes for CLL based on the mutated genes found to be driver mutations in this disease. We have focused in the TLR-MYD88 and RAS-BRAF-MAPK-ERK pathways. Furthermore, we used a systems biology method to find compounds on reprofiling drugs to target CLL microenvironment.

TLRs PATHWAY (Article 1: Targeting IRAK4 disrupts inflammatory pathways and delay tumor development in CLL)

The persistence of CLL cells despite virtually complete inhibition of BTK and tumor proliferation suggest that BTK-independent pathways can maintain tumor viability.[218] We focused on the role of TLRs signaling in CLL pathogenesis and specifically, whether it can be inhibited by ND2158, an IRAK4 inhibitor.

TLRs are the third essential signal to complete B-cell activation,[159] along with BCR activation[219, 220] and interactions with helper T cells.[221] The recognition of invading pathogens and endogenous molecules from damaged tissues by TLRs triggers protective self-defense mechanisms.[222] However, excessive TLRs activation disrupts the immune homeostasis by sustained pro-inflammatory cytokines and chemokines production and consequently contributes to the development of many inflammatory and autoimmune diseases,[223] as well as some types of cancers.[224, 225] Autoantigens and bacterial components recognized by B cells via BCR and TLRs are described to drive CLL.[219] Moreover, CLL patients are associated with an increased frequency and severity of infectious and autoimmune complications.[226]

When TLRs are activated by PAMPS/DAMPS or somatic gain-of-function mutations, the adaptor protein MYD88 is recruited. The signal is propagated through the activation of IRAKs-TRAF6 and the IKK complex, culminating in the activation of transcription factors such as NF-κB.[225] We and others have identified recurrent mutations in the *MYD88* gene in 2-10% of CLL patients.[23, 24, 35, 40, 203] The most common of these mutations is the L265P, as found in other lymphoid malignancies, like WM (~90% of cases), extranodal subtypes of DLBCL such as primary DLBCL of the CNS (70%), cutaneous DLBCL, leg-type (54%) and testicular (74%) DLBCL, and in significant portions of ABC-DLBCL (24%).[170]

MYD88 mutations are predominantly clonal and considered drivers in CLL, highlighting the relevance of TLRs-MYD88 pathway in this disease.[23, 44, 203, 225] As described by Puente *et al.*[34] and Martinez-Trillos *et al.*,[173, 227] *MYD88* M cases have a different expression profile than *MYD88* UM ones, related to its NF-κB overactivation. *MYD88* M cases are associated with the lower-risk IGHV M CLL subset [34, 173, 201, 204, 225, 228] and with a favorable outcome.[173] There is controversy about the prognosis value of this mutation[176, 228] due to its low incidence in CLL, giving rise to statistical and practical limitations in these studies.

Using the same initial CLL cohort analyzed by Martinez-Trillos *et al.*,[173] enriched with 80 new cases sequenced, we found that gene expression profiles of *MYD88* M cases, compared to *MYD88* UM ones, were enriched with genes related to the NF-κB and JAK-STAT pathways, similar to the results previously published in ABC-DLBCL.[166] These results are in

controversy with a new study in a CLL cohort, published this year, that reported no enrichment of the NF-κB pathway in *MYD88* M cases.[228] At biological level we validated an increase of JAK-STAT and NF-κB canonical activity, and cytokine expression and secretion in *MYD88* mutated cases compared to unmuted ones.

B cells exhibit constitutively high levels of specific TLRs,[229-231] which are not developmentally regulated during the B-cell differentiation process.[232] A total of 13 TLRs have been identified, among which TLRs 1–10 are expressed in human, although the function of TLR10 is still unclear.[157] CLL cells were shown to have a similar expression pattern of TLRs as normal B cells.[231, 233, 234] Furthermore, we did not observe differences in TLRs expression between *MYD88* M and *MYD88* UM, indicating that the TLRs signaling framework is similar in both groups.

Previous studies suggested the involvement of TLRs signaling in CLL cell survival[234] and its contribution to NF-κB activity and inflammatory micromilieu in CLL.[69] TLRs gene signature is higher expressed in LN–resident CLL cells compared with CLL cells from PB.[235-237] This finding corroborates the idea that CLL cells in the microenvironment behave differently than CLL cells in circulation. Notably, the TLRs gene signature is part of an overall activation signature expressed in lymph node resident CLL cells that is also highly enriched in genes regulated by BCR, NF-κB, and JAK/STAT pathways, the latter indicative of cytokine signaling, suggesting CLL cells are more antigen exposed in the microenvironment.[69] As validated in our results, CpG-dependent activation of TLRs signaling *in vitro* recapitulate activation of NF-κB and upregulation of IL10 with consequent activation STAT1 and STAT3 and improved CLL cell survival. Thus, TLRs and concurrent cytokine signaling are activated within the tissue microenvironment and, in agreement with a prior *in vitro* study, may cooperate to improve CLL cell survival.[238] Similarly, TLR9 activation suggests that CLL cells in the LN may be exposed to increased levels of microbial DNA (known to contain CpG motifs).[235]

TLRs ligands such as bacterial cell membrane components or unmethylated DNA are potent stimulators of immune cells, activate the NF-κB pathway, and may cooperate with BCR signals to overcome the anergy of autoreactive B cells.[239] Responses to BCR and TLRs stimulation depends on biological features of patients.[240] IGHV mutational status and BCR stereotypes are described to be involved in BCR and TLRs stimulation sensitivity.[241] IGHV UM CLL cells are more responsive to BCR activation than those with IGHV M CLL. This is mirrored by TLRs activation.[242] Similarly, the two subtypes demonstrate differential responses to CpG stimulation *in vitro*. In contrast, IGHV M CLL cells are more likely to enter an apoptotic state when stimulated with CpG *in vitro*, in the absence of concurrent BCR activation or coculture with cytokines.[238, 242] These observations raise the possibility that

such costimulatory signals may sustain survival of IGHV M CLL cells *in vivo*. In support, although there is a difference in the magnitude of TLRs activation, both IGHV UM and IGHV M patients display an overrepresentation of TLRs signature genes in the LN.[235]

We observed that the response to TLRs stimulation is very variable between CLL patients. To avoid these heterogeneous responses when activating TLRs signaling in CLL cells, we used a mix of the most effective TLRs agonists in CLL cells, which stimulated TLR1, TLR2, TLR6, and TLR9; from now "TLRs agonists mix". This mix allowed us to mimic the mechanisms of activation of CLL cells in the LN microenvironment regardless biological patient's characteristics.

As previously reported, the *in vitro* stimulation of TLRs in CLL cells[235] activates the NF-κB and JAK-STAT signaling pathways, leading to an increase in NF-κB canonical activity,[34] cytokines secretion,[34, 69, 231-233, 243] and cell proliferation.[238, 243] Furthermore, we observed that TLRs stimulation enhanced CLL cell migration. These results highlight the relevance of TLRs signaling in CLL pathobiology.

It has been predicted that TLRs signaling inhibition could be an effective therapeutic strategy to suppress unwanted, disease-associated inflammatory responses.[168] Despite many efforts have been done in developing inhibitors targeting this pathway, unfortunately very few compounds are currently available for clinical uses.[244]

In general, TLRs inhibition can be achieved by two major strategies: (1) blocking the binding of TLRs ligands to the receptor; (2) interfering the intracellular signaling pathways, which are carried on by SMIs, antibodies, oligonucleotides, lipid-A analogs, microRNAs, and new emerging nano-inhibitors.[168]

There are two clinical trials inhibiting the TLRs pathway in CLL, both by IRAK inhibitors. The NCT03601819 clinical trial uses an IRAK1 inhibitor (pacritinib)[245] in R/R lymphoproliferative disorders. The NCT03328078 clinical trial studies an IRAK4 inhibitor (CA-4948) in R/R hematologic malignancies.

In this work, we have analyzed the effect in CLL cells of a small molecule inhibitor against IRAK4: ND2158. This drug exhibited robust activity against ABC-DLBCL with *MYD88* mutations in preclinical mouse models.[245]

The *in vitro* cytotoxic effect of ND2158 in CLL cells, albeit significant, was modest. ND2158 reduced CLL cell viability independently of *MYD88* mutational status, at concentrations that did not impact on normal B- and T-cells survival. The *in vitro* concentration used (10 µM) is similar to the ones used in others studies with ND2158 in ABC-DLBCL[172] and CLL.[228]

In contrast to its modest apoptotic effect, we demonstrated that ND2158 was capable of completely inhibiting tumor proliferation promoted by the TLRs agonists mix. These observations suggest that similarly to ibrutinib effect,[246, 247] inhibition of cell proliferation, rather than apoptosis induction, is one of the primary effects of ND2158 against CLL leukemic cells.

In accordance with Improgo et al,[228] we show that IRAK4 inhibition disrupts MYD88 signaling in CLL, resulting in blockade of NF-κB signaling and attenuating levels of downstream cytokine production, consistent with pathway inhibition.[166] ND2158 also reduced STAT3 activity and cell adhesion-migration, which were enhanced upon TLRs activation.

Monocytes, which are known to support survival of CLL cells,[248] express all TLRs of which TLRs 1, 2, and 4 are present at high levels.[249, 250] We confirmed that monocytes respond to TLRs stimulation and inhibition. ND2158 was able to reduce the release of inflammatory factors from monocytes, leading to a dual inhibition: directly on CLL cells and in the myeloid bystander cells, reducing their tumor-protective activity.

To test the therapeutically potential of ND2158 in vivo, we used the Eμ-TCL1 AT mouse model of CLL. As there are not available mouse models that recapitulates MYD88 mutations in an immunocompetent microenvironment, we used the Eμ-TCL1 AT model, although it is a model of aggressive CLL,[85] with no somatic mutations in the IGHV gene,[86, 88, 251] unlike MYD88 M human CLL cases. As ND2158 is a potential drug for all CLL cases, regardless IGHV mutational status, the results of this model are of great interest.

The Eμ-TCL1 mouse model is the most accepted for CLL studies since it recapitulates many features of human CLL, including alterations in the tumor microenvironment.[252, 253] This mouse model is immunocompetent, so it is appropriate to study the effect of the drugs evaluating its pharmacokinetics, being the only CLL animal model that can be used to test drugs whose mechanism of action depends on or interferes with the influence of the microenvironment. As the development of CLL in the Eμ-TCL1 mouse occurs approximately after 15 months, and has a heterogenous course of disease, we used an adoptive transfer model (Eμ-TCL1 AT), which develops the disease more homogenously and faster.[86] In these mice, development of CLL is associated with a systemic inflammatory cytokine milieu and alterations within the distribution and activity of myeloid cells,[252] in accordance with the phenotype described in human CLL.[254, 255] Monocytes are skewed toward pro-tumorigenic phenotypes, including the release of tumor-supportive cytokines and the expression of immunosuppressive molecules.[252]

ND2158 slowed down leukemia progression in *Eµ*-TCL1 AT mice reducing the tumor load in secondary lymphoid organs compared to control mice. This was accompanied with a decrease in monocytes number, as well as in their activation and cytokine secretion. Previous studies have shown that depletion of monocytes delays CLL in the *Eµ*-TCL1 AT model, as well as in a xenotransplantation approach using the MEC-1 CLL cell line.[252, 256] Thus, the reduction and functional impairment of monocytes by ND2158 and its impact on the inflammatory milieu might reduce microenvironment-mediated support of CLL cells, and likely contributes to the observed delay in tumor progression.

T-cell responses play a major role in controlling tumor growth. CD8^{+} tumor-specific effector T cells are the subset responsible to control CLL development.[257] Without T cells, CLL develops much faster, as seen when *Eµ*-TCL1 leukemia is adoptively transferred into a B and T cells deficient mice (Rag2^{-/-}).[257] In CLL, these CD8^{+} effector T cells fail to fully eradicate the malignant cells, resulting in failure of antitumor immunity and increased susceptibility to infections.[258] They rather show signs of activation-induced exhaustion including enhanced expression of inhibitory receptors like PD-1, CD244, CD160, and LAG3 and decreased proliferation and rendered incapable of attacking the malignant clone, both in mouse models[257, 259] and CLL patients.[258, 260] This T-cell exhaustion has also been described in other hematological malignancies, like adult T-cell leukemia/lymphoma,[261] chronic myeloid leukemia,[262] and acute myeloid leukemia.[263]

Furthermore, T cells from the *Eµ*-TCL1 mouse model exhibit comparable changes in gene and protein expression, and T-cell function, to that seen in human CLL patients.[264, 265] A further feature of both the human disease and the mouse model is that there is an expansion of the number of circulating CD8^{+} T cells, which show evidence of chronic activation.[264, 266]

Our results show that ND2158 impacted CD8^{+} T-cell activity and expansion, both *in vivo* and *in vitro*. We observed a lower number of CD8^{+} effector T-cells with reduced expression of proliferation and activation markers (CD25, CD28 and CD137), and higher expression of exhaustion markers, including the inhibitory receptor PD-1. This exhaustion phenotype of CD8^{+} effector T-cells leads to a reduction on their anti-tumor activity and could be an explanation for the only moderate effect of ND2158 on tumor load in our *in vivo* study.

Knowing that ND2158 is mainly acting by inhibiting the TLR-MYD88 pathway in B-cells, we were interested in the mechanism of action in T-cells, where the TLRs pathway is also active. T cells express all TLRs at low levels with the exception of TLR5, which is present abundantly,[249, 267] and are sensitive to CpG-ODN.[249] Our data suggest that perhaps the

activity of ND2158 on CD8$^+$ T cells is independent of MYD88/IRAK4. An unbiased analysis to determine which kinases are inhibited by ND2158 showed that besides effectively targeting IRAK4 (100% inhibition at 10 µM), ND2158 also inhibits other kinases with lower efficacy, including proteins that are of functional relevance in T cells (e.g., > 70% inhibition of DYRK1, TXK and LCK at 10 µM).[249]

As ND2158 treatment of mice inhibits CD8$^+$ effector T-cell expansion and increases their exhaustion, an inferior tumor control by these cells is expected. Therefore, the positive antitumor effects of ND2158 on tumor cells and monocytes seems to be counteracted by its negative impact on the T-cell compartment, which might at least partly explain the modest effects ND2158 has in controlling leukemia development in the TCL1 mouse model.

In addition, to overcome the negative impact of ND2158 on T cells, we propose to consider its combination with drugs that improve T-cell function and avoid their rapid exhaustion. As we observed increased expression of several inhibitory receptors on CD8$^+$ T cells in ND2158-treated mice, including PD-1 and TIGIT, blocking these receptors with antibodies might be a successful strategy to overcome the loss of T-cell function and improve therapy outcome (Figure 28). In this sense, a clinical trial (NCT02420912) demonstrated synergy of ibrutinib and nivolumab in CLL (an anti-PD-1 monoclonal antibody).[129]

The development of more selective IRAK4 inhibitors and therefore the reduced negative impact on T cells should be considered to improve therapeutic targeting of the TLRs pathway in CLL and other diseases. Ideally, such drugs should not compromise the patients' immune system, and decrease their risk of infections, which is a frequent adverse effect in treated CLL patients.[268, 269]
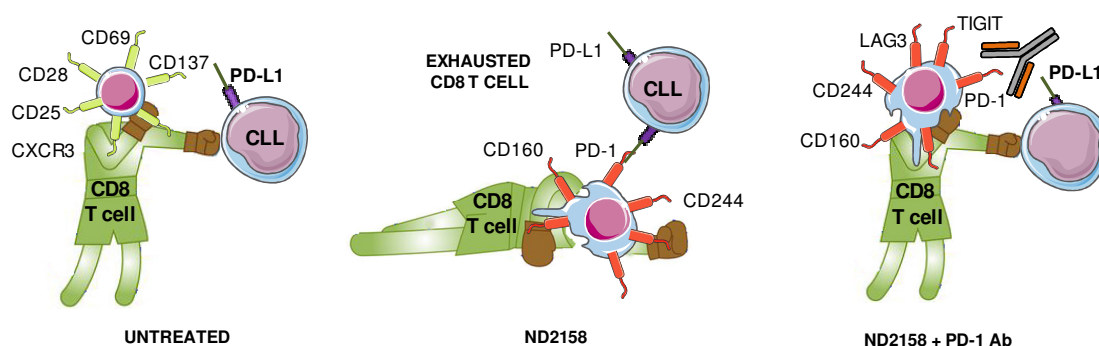
Figure 28. Scheme of overcoming T-cell exhaustion by combining ND2158 and a PD-1 antibody.

Crosstalk between BCR and TLRs pathways has been implicated in aggressive lymphoma and in the activation of normal B cells, as well as CLL cells.[239, 270] Dadashian *et al*[235] concluded that ibrutinib can effectively inhibit BCR signaling but only partially TLRs signaling, which is consistent with the clinical experience with ibrutinib in WM.[271] Also, similar to CLL, although sustained on continuous therapy, most WM responses are partial with lingering tumor cells for the duration of treatment.[271] Overall, the persistence of residual disease in WM patients with activated TLRs signaling on ibrutinib is further indication that BTK inhibition alone is insufficient to completely block prosurvival signals. We tested the combination of ibrutinib with the IRAK4 inhibitor ND2158 to try to achieve maximal apoptosis of cells through BCR and TLRs inhibition. In agreement with previous studies,[172, 235] we observed a superior antitumor activity whit the combination.

Furthermore, as ND2158 is not reducing the high levels of BCL2 in CLL, we tried the combination of this IRAK4 inhibitor with the BCL2 inhibitor venetoclax. We observed that ND2158 also increased the cytotoxic effect of venetoclax.

In conclusion, our data warrants further investigation of a combination of TLRs and BTK or BCL2 inhibitors in CLL. A role of TLRs signaling in the pathogenesis of lymphoma, WM, and CLL is supported by the presence of gain-of-function mutations in *MYD88*.[34, 166, 272]

The mechanistic studies presented in our work confirm that IRAK4 inhibition could be a novel target for CLL treatment. Although inhibition of TLR-MYD88 signaling with ND2158 blocks survival and proliferation of CLL cells and reduces the tumor-supportive inflammatory milieu, the effect is partially counteracted by T-cell negative effect. Considering our findings in the TCL1 mouse model, combining the IRAK4 inhibitor ND2158 with immune checkpoint therapy might result in enhanced treatment efficacies.

RAS-BRAF-MAPK-ERK PATHWAY (Article 2: Mutations in the RAS-BRAF-MAPK-ERK pathway define a specific subgroup of patients with adverse clinical features and provide new therapeutic options in chronic lymphocytic leukemia)

The RAS-BRAF-MAPK-ERK pathway is one of the four common oncogenic mutated pathways in most tumor types along with PI3K-AKT-mTOR, cell cycle and p53–DNA repair pathways.[273] Interestingly this pathway was altered in ~50% of the tumors with variable frequencies across different types.[274] The RAS-BRAF-MAPK-ERK pathway is affected in CLL through mutations in novel CLL drivers such as *NRAS, KRAS, BRAF, PTPN11 and MAP2K1*.[23, 275] The RAS-BRAF-MAPK-ERK pathway plays a central role not only in regulating normal cell proliferation, differentiation, migration, and survival,[180] but also in oncogenesis,[276] and it is an important key dysregulated pathway in cancer.[277]

The RAS-BRAF-MAPK-ERK pathway is activated by extra-cellular ligand binding of growth factors to RTKs which results in the recruitment of RAS to the cell membrane. RAS in turn leads to downstream activation of several different pathways, including the serine/threonine kinase RAF.[183] The downstream targets of RAF are few and include MEK1 and MEK2, which phosphorylate ERK, a downstream effector of many pathways.[178] As a result of this specificity, a "bottleneck" within the pathway occurs.

RAS is an oncogene mutated in more than 30% of all cancers.[185] *BRAF* mutations have been described in HCL (100%), melanoma (50–60%), thyroid (30–50%), colorectal (10%) and non-small cell lung cancer (3%).[186, 187] The *BRAF^V600E* mutation is the most common *BRAF* mutation.[180] *MEK* mutations have been mainly identified in melanoma.[188] Generally, all of the upstream mutations are shown to confer constitutive activation of the downstream effector ERK, which is related to modulation of anti-apoptotic molecules such as BCL2, linked to drug resistance in some types of cancers.[183]

In our cohort, we observed mutations in genes belonging to the RAS-BRAF-MAPK-ERK pathway in 5% of CLL patients, a frequency similar to previous studies.[204] In these mutated cases, gene expression profile analysis showed an upregulation of genes of the MAPK pathway. Furthermore, higher levels of phosphorylated ERK, a surrogate marker of MAPK pathway activation,[278] were also observed in the RAS-BRAF-MAPK-ERK mutated cases compared to the unmutated ones, suggesting the activation of this pathway in this subgroup of patients. These results agree with those found in other cancers, in which the activation of RAS-RAF-MEK-ERK signaling can occur through mutations in several genes in the pathway.[274]

BRAF mutations were detected in 2% of our CLL series, as previously reported.[23, 190] The BRAF mutations found, were not the typical *BRAF^V600E* seen in other malignancies,[279] but

rather were clustered around the activation segment of the kinase domain.[23, 280] Mutations in these positions confer variable but increased signaling and have oncogenic capacity[281] and are associated with refractoriness to fludarabine.[282] Apart from BRAF mutations, we found mutations in genes upstream of BRAF (KITLG, KIT, PTPN11, GNB1, KRAS and NRAS) and in genes downstream of BRAF (MAP2K1 alias MEK1, MAP2K2 alias MEK2). MAP2K1 mutations were already described in HCL-variant and conventional HCL with rearranged IGHV4-34,[283] Langerhans cell histiocytosis,[284] and pediatric-type follicular lymphoma.[285] As reported in HCL-variant,[283] mutations in this pathway seem to be mutually exclusive, as only one case had concomitant mutations of PTPN11 and KRAS.

In accordance with a recent study published,[286] our data suggest that mutations in the RAS-BRAF-MAPK-ERK pathway are associated with adverse biological features such as high expression of ZAP-70, CD38 and CD49d and IGHV UM. Furthermore, a recent study[286] pinpointed a higher frequency of mutations in members of the RAS-BRAF-MAPK-ERK pathway in CLL cases with specific clinico-biological features,[287] including the presence of trisomy 12, a cytogenetic aberration associated with a unique pathophysiology among CLL.[288, 289]

In our series of patients, CLL with mutations in genes of the RAS-BRAF-MAPK-ERK pathway had a 5-year TTFT similar to that of patients with adverse mutations (*TP53, ATM* or *BIRC3*), whereas patients carrying both types of mutations simultaneously had the worst 5-year TTFT, as previously reported.[23, 24, 42, 282] Nadeu *et al*[44] described that BRAF mutation have a prognostic impact on TTFT even at a very low frequency detection. In our cohort, mutations in genes of the RAS-BRAF-MAPK-ERK pathway did not affect OS, which could be explained by the recent publication which reported that although *BRAF* mutations were associated with adverse OS, *KRAS* and *NRAS* mutations were not.[275] Larger cohorts should be studied to define these parameters.

Given the ubiquitous expression and the numerous mutations in many malignancies described in this pathway, coupled with the "bottleneck" nature of downstream signaling,[285] the MAPK pathway provides an attractive platform for anti-cancer targeting.[290] Substantial efforts in the past decades have led to the clinical success of drugs that target MEK, RAF and upstream RTK proteins,[277] although due to the huge cancer heterogeneity and genomic instability, many acquired resistance occured.[183] Currently, there are no FDA-approved therapies that specifically target RAS mutations.[277]

To develop RAS inhibitors is challeging until now, there are not clinically effective molecules. This difficulty is firstly attributed to the tertiary structure of RAS protein, which is very smooth and floppy, thus hardly providing a binding pocket for small molecule inhibitors. The affinity

of mutant RAS proteins for GTP (guanosine triphosphate) is very high, and as a result, it is almost impossible to develop a competitive binding strategy.[192]

Among the three RAF isoforms, CRAF was first identified as an oncogene and considered a potential target, which lead to numerous pre-clinical compounds, like sorafenib, which later was identified as a multikinase inhibitor.[291] Many studies have highlighted the potential of targeting BRAF for the treatment of BRAF-mutant cases.[292]

BRAF and MEK inhibitors have shown clinical benefits in cancers harboring oncogenic mutations in this pathway. For example, competitive BRAFi such as vemurafenib (specific for BRAF^{V600E} mutated cases) and dabrafenib (specific for mutations in BRAF^{600}), have clinical response rates around 50% in patients with these mutations, and showed a survival increase in BRAF-mutant melanoma[292] as well as in cases of HCL refractory to conventional therapy.[293, 294] However, due to the extend duration of the treatment and the extremely high frequency of emergence of drug resistance eventually leads to failure of the treatments using these inhibitors.[193, 194, 295, 296] Although the mechanism of resistance is still unclear, many potential mechanisms have been suggested. These include gene mutations occurring in the targeted proteins, MAPK signaling interaction with PI3K pathway, loss of functions in MAPK signaling feedback control and abnormal alterations of tumor suppressor genes.[183] Allosteric MEKi, such as trametinib, selumetinib, cobimetinib, and binimetinib, have antitumor activities in melanoma, including those with/without NRAS mutations. Recently, the acquisition of MEK1 mutations have been proposed as a mechanism for MEKi and BRAFi resistance.[297, 298]

The convergence of multiple mechanisms to reactivate the MAPK pathway provided a strong rational for combined BRAF and MEK targeting to overcome BRAFi resistance, a strategy that is supplanting single-agent BRAFi therapy.[299, 300]

Particularly in CLL, treatment with the multikinase inhibitor, sorafenib, induced cell death in mutated BRAF and the unmutated BRAF subgroups, while treatment with the BRAF inhibitor, PLX4720, the vemurafenib (PLX4032) progenitor, failed to produce a significant effect on the *BRAF* mutant cells *in vitro*.[190] This suggests the importance of testing BRAF mutations to adjust the best treatment for these patients.

As expected, our results demonstrated that vemurafenib and dabrafenib were not able to significantly decrease ERK phosphorylation in RAS-BRAF-MAK-ERK mutated cases, although a slight effect was observed after dabrafenib treatment, which could be an off-target effect. In contrast, in cases without RAS-BRAF-MAK-ERK mutation, an ERK rephosphorylation was observed after BRAFi treatment, potentially due to ERK activation by

BCR signaling complex. It was previously described that this BRAFi-related ERK phosphorylation can be partially abrogated by blocking BCR signaling with SYK inhibitors.[301]

The RAS-BRAF-MAPK-ERK cascade is under control by feedback loops. For instance, activated ERK inhibits phosphorylation of their upstream factors (MEK, RAF, SOS and RTKs).[181] These feedback loops play an essential role in maintaining cellular homeostasis in physiological conditions[183] and need to be considered in the drug resistance mechanisms.

In our work, we have used an ERK inhibitor. ERK inhibitors (ERKi) can reverse the abnormal activation of MAPK pathway induced by upstream mutations and are able to overcome the acquired drug resistance induced by upstream kinases inhibitors (maybe by escaping the feedback loops). As such, combinational usage of ERKi and upstream inhibitors has become an important strategy to overcome acquired resistance and optimize therapeutic efficacy. In our work we used the ERKi ulixertinib. This drug has been used in a phase II clinical trial in acute myeloid leukemia, solid tumors and melanoma.[183, 195]

As it has been postulated that cancer cells can rewire their signaling networks to restore ERK activity and override the actions of inhibitors that act upstream of ERK,[302] we tested the selective ERK1/2 inhibitor ulixertinib capacity to disrupt ERK signaling compared to the BRAFi vemurafenib and dabrafenib. Our results demonstrated that ulixertinib was able to inhibit ERK phosphorylation *in vitro* in all CLL cases with mutations in genes of the RAS-BRAF-MAPK-ERK pathway. Recently it was reported that CLL cells with trisomy 12 showed increased sensitivity to MEK and ERK inhibitors, pointing to an essential role for MEK/ERK signaling in CLL with trisomy 12.[286, 303]

Our work showed that the RAS-BRAF-MAPK-ERK pathway patients with mutations in the RAS-BRAF-MAPK-ERK pathway had adverse biological features and most of them required treatment. Furthermore, our results suggest that in this subgroup of mutated CLL patients ERK inhibitors could be a useful therapeutic strategy.

MYD88, BTK and ERK are closely related proteins (Article 1 and 2)

It has been postulated that MYD88 might prevent ERK inactivation, thereby amplifying the activation of the canonical RAS pathway. The relevance of this mechanism to human neoplasia was suggested by the finding that MYD88 was overexpressed and interacted with activated ERK in primary human cancer tissues.[304] Collectively, these results show that in addition to its role in inflammation, MYD88 plays a crucial direct role in RAS signaling, cell-cycle control, and cell transformation (Figure 29).
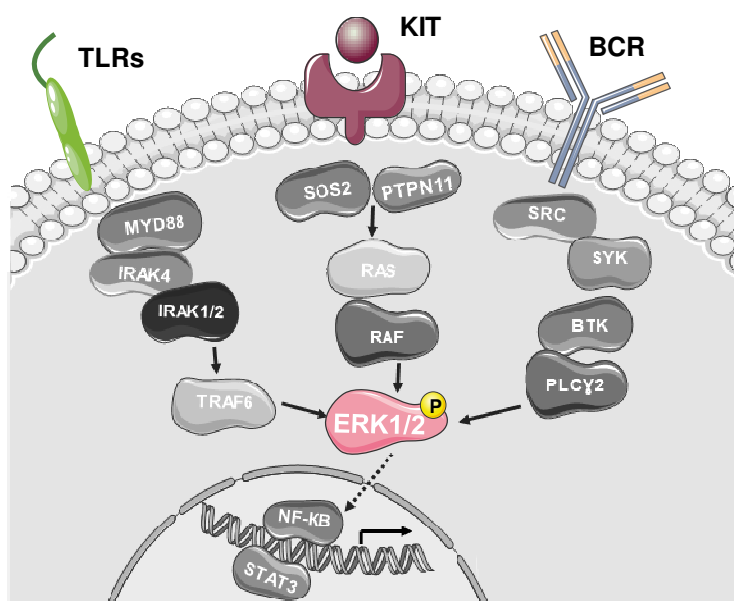
Figure 29. BCR, TLR and MAPK pathways cooperate to regulate cell survival

In the same way, ERK is a downstream effector of the BTK signaling (Figure 29). With BTK inhibitors, like ibrutinib, ERK phosphorylation is significantly decreased.[235] Dadashian *et al*,[235] showed only modest reduction of ERK phosphorylation after the IRAK1/4 inhibitor 407601 from EMD Millipore. This study could also be done with the IRAK4 inhibitor used in our work, ND2158, which had very promising results.

Acquired ibrutinib resistance due to BTK[Cys481Ser] mutations occurs in B-cell malignancies, including those with *MYD88* mutations, and show higher levels of ERK phosphorylation compared to unmutated- BTK[Cys481Ser]. The use of ERK1/2 inhibitors triggered apoptosis in BTK[Cys481Ser] expressing cells and showed synergistic cytotoxicity with ibrutinib. ERK1/2 re-activation in ibrutinib treated BTK[Cys481Ser] cells was accompanied by release of many pro-survival and inflammatory cytokines, including IL-6 and IL-10 that were also blocked by ERK1/2 inhibition.[305]

So, after the work exposed in this thesis, we can propose to study the ERK pathway in CLL patients with mutations in BTK or TLRs-MYD88 pathway to find new possible combination strategies for those patients.

SYSTEMS BIOLOGY DRUG SCREENING (Article 3 : Network-based drug discovery guided *in vitro* screening defines statins as a therapy to combine with current treatments in chronic lymphocytic leukemia)

Most of the approaches to develop anticancer therapies include selectively targeting tumor cells and inhibition of supportive signals from the microenvironment. The hope of the rapid translation of 'genes to drugs' has foundered on the reality that disease biology is complex, and that drug development must be driven by insights into biological responses. Systems biology aims to describe and to understand the operation of complex biological systems and ultimately to develop predictive models of human disease.

Automation of complex primary human cell–based assay systems designed to capture emergent properties can now integrate a broad range of disease-relevant human biology into the drug discovery process, informing target and compound validation, lead optimization, and clinical indication selection.[306] Better models of human disease biology, including more integrated network-based models that can accommodate multiple omics data types, as well as more relevant experimental systems leads to the identification of novel targets, which has been an important application of omics technologies in pharmaceutical research. Early during the post-genomic era, there was substantial focus on differentially regulated genes for new target identification. Thus, studies related to drug mechanisms of action and those that support drug development goals, such as clinical indication selection and patient stratification, are of particular interest.[307]

Identification of novel targets has been an important application of omics technologies in pharmaceutical research. Early during the post-genomic era, there was substantial focus on differentially regulated genes for new target identification. However, this focus did not account for the relatively poor correlation of gene expression with protein expression and the fact that many valuable drug targets are not differentially expressed. More recent approaches organize gene expression data along with other information into networks to identify key nodes controlling important disease pathways based on network topology.[307]

In this work, we used systems biology for integrating "omics" from the available literature to predicting possible drug candidates that can overcome the supportive effect of the tissue microenvironment on CLL cell survival. We have screened not only approved drugs but also bioactive compounds giving access to a greater portion of the different chemical structures to improve the chances of success. A library of 65 compounds emerged from this analysis.

The effect of the different compounds was tested in CLL cells alone and in a co-culture system with mesenchymal stromal cells, that have proved effective in partially mimicking the microenvironment and has been proposed as better screening systems to test drugs that target the proliferative and drug resistant CLL cells.[308]

Our results highlighted a drug-like molecule (C7) and the commercial drug simvastatin as the more effective and selective out of the 65 compounds tested for cytotoxicity. Despite the promising results shown for C7 we concentrated further screening on simvastatin as the advantages of drug repositioning[309] over new developments are overriding. A previous study also reported the cytotoxic effect of simvastatin in CLL cells.[310]

Simvastatin, as all statins, act by inhibiting the 3-hydroxy-3-methylglutaryl coenzyme A reductase (HMGCR). This is a key regulator enzyme of the metabolic pathway responsible for the endogenous production of cholesterol.[311] Multiple analysis have reported that statins showed antitumor activity in monotherapy and in combination with several anticancer agents and their involvement in cancer risk and prevention.[312] The antitumor effect of statins results in the inhibition of proliferation, migration, invasion, survival and stemness.[313, 314] Particularly, statins promote apoptosis in several hematological malignancies[315-317] and epidemiologic studies suggest improved outcomes in some hematological malignancies in the statins users.[318, 319] Particularly in CLL and lymphoma cells, statins induced apoptosis.[320, 321] Recently an association between statins use and reduced CLL risk, was reported.[322]

Apart from the main target (HMGCR), simvastatin also targets the integrin lymphocyte function-associated antigen-1 (LFA-1).[323] This protein, expressed on all leukocytes, is composed of an alpha chain (integrin alpha L; ITGAL) and a beta chain (integrin beta chain-2; ITGB2).[324] LFA-1 is one of the most important adhesion molecules that mediate contact between tumoral cells and stromal cells through interactions with its receptive counterpart intercellular adhesion molecule 1 (ICAM-1).[325] Furthermore, cell adhesion has been considered one of the major causes of primary drug resistance in tumors.[326]

We observed a significant cytotoxic effect in the four statins tested (simvastatin, lovastatin, fluvastatin and rosuvastatin), while no effect was observed using LFA-1 inhibitors (lifitegrast and BDBM50199033). Furthermore, statins reduced significantly the proliferation of CLL cells. Statins and LFA-1 inhibitors, reduced significantly CLL adhesion/invasion induced by CXCL12 and CXCL13, key chemokines for CLL cell homing to lymphoid tissues.[327]

Our results showed that there are two putative targets of statins, HMGCR and LFA-1, which inhibition induces cell cytotoxicity and a reduction of cell proliferation and cell homing, which could be useful for CLL treatment.

Systems biology highlighted ibrutinib and venetoclax as possible synergistic combinations for CLL treatment. We validated *in vitro* that statins potentiated the antiproliferative effect of ibrutnib and the cytotoxic effect of venetoclax. Furthermore, a new clinical study showed that complete remission rate in CLL is increased when simvastatin is combined with venetoclax.[328]

CONCLUSIONS

CONCLUSIONS

The main conclusions derived from this thesis are as follows:

First study: To study the TLRs pathway in CLL blocking IRAK4 (a key kinase in the TLRs signal transduction), with a new inhibitor (ND2158).

1. TLRs stimulation induces cytokine secretion, NF-κB -activation and cell proliferation of CLL cells.

2. ND2158 blocks survival and proliferation of CLL cells.

3. ND2158 impacts on the tumor-supportive inflammatory milieu, by reducing cytokine secretion in malignant and bystander cells.

4. ND2158 enhances CD8^{+} effector T-cell exhaustion which seems to counteract the positive anti-tumor effects of ND2158 on tumor cells and monocytes.

5. ND2158 shows a superior anti-tumor activity when combined with ibrutinib or venetoclax.

6. Combining ND2158 with immune checkpoint therapy might result in enhanced treatment efficacies.

Second study: To analyze the clinical impact of mutations in the RAS-BRAF-MAPK-ERK pathway in CLL and the possibility to target them.

7. RAS-BRAF-MAPK-ERK mutations are associated with adverse clinical features in CLL.

8. CLL cases with RAS-BRAF-MAPK-ERK mutations show and upregulation of genes of the MAPK pathway and higher levels of phosphorylated ERK, suggesting the activation of this pathway in this subset of patients.

9. The ERK inhibitor ulixertinib is able to significantly decrease ERK phosphorylation in cases with mutations in RAS-BRAF-MAPK-ERK.

Third Study: To find new compounds on reprofiling drugs to target CLL by systems biology.

10. Simvastatin was selected among the compounds proposed by the CLL - *in silico* model to target CLL.

11. Several statins block survival, proliferation and adhesion/migration of CLL cells.

12. Combination of statins and ibrutinib or venetoclax shows superior anti-tumor activity.

BIBLIOGRAPHY

1. Scott,D.W. & Gascoyne,R.D. The tumour microenvironment in B cell lymphomas. *Nat. Rev. Cancer* **14**, 517-534 (2014).

2. World Health Organization *WHO classification of tumours of haematopoietic and lymphoid tissues. (*2008).

3. Swerdlow SH et *al.* The 2016 revision of the World Health Organization classification of lymphoid neoplasms. *Blood* **127**, 2375-2390 (2016).

4. Yatim,K.M. & Lakkis,F.G. A brief journey through the immune system. *Clin J Am Soc Nephrol* **10**, 1274-1281 (2015).

5. ten Hacken,E., Gounari,M., Ghia,P., & Burger,J.A. The importance of B cell receptor isotypes and stereotypes in chronic lymphocytic leukemia. *Leukemia* **33**, 287-298 (2019).

6. Puente,XS., Jares,P., & Campo,E. Chronic lymphocytic leukemia and mantle cell lymphoma: crossroads of genetic and microenvironment interactions. *Blood* **131**, 2283-2296 (2018).

7. Xu,Z., Zan,H., Pone,E.J., Mai,T., & Casali,P. Immunoglobulin class-switch DNA recombination: induction, targeting and beyond. *Nat. Rev. Immunol.* **12**, 517-531 (2012).

8. Seifert,M., Scholtysik,R., & Kuppers,R. Origin and Pathogenesis of B Cell Lymphomas in *Lymphoma: Methods and Protocols* (ed. Kuppers,R.) 1-25 (Humana Press, Totowa, NJ, 2013).

9. Basso,K. & la-Favera,R. Germinal centres and B cell lymphomagenesis. *Nature Reviews Immunology* **15**, 172-184 (2015).

10. Kipps,T.J. *et al.* Chronic lymphocytic leukaemia. *Nat. Rev. Dis. Primers.* **3**, 1-21 (2017).

11. Nabhan,C. & Rosen,S.T. Chronic lymphocytic leukemia: a clinical review. *JAMA* **312**, 2265-2276 (2014).

12. Fabbri,G. & la-Favera,R. The molecular pathogenesis of chronic lymphocytic leukaemia. *Nature Reviews Cancer* **16**, 145-162 (2016).

13. Hallek,M. *et al.* Guidelines for the diagnosis and treatment of chronic lymphocytic leukemia: a report from the International Workshop on Chronic Lymphocytic Leukemia updating the National Cancer Institute-Working Group 1996 guidelines. *Blood* **111**, 5446-5456 (2008).

14. Bosch,F. & la-Favera,R. Chronic lymphocytic leukaemia: from genetics to treatment. *Nature Reviews. Clinical Oncology* **[Epub ahead of print]**, (2019).

15. Seifert,M. *et al.* Cellular origin and pathophysiology of chronic lymphocytic leukemia. *J. Exp. Med* **209**, 2183-2198 (2012).

16. Rossi,D. *et al.* Integrated mutational and cytogenetic analysis identifies new prognostic subgroups in chronic lymphocytic leukemia. *Blood* **121**, 1403-1412 (2013).

17. Damle,R.N. *et al.* Ig V gene mutation status and CD38 expression as novel prognostic indicators in chronic lymphocytic leukemia. *Blood* **94**, 1840-1847 (1999).

18. Hamblin,T.J., Davis,Z., Gardiner,A., Oscier DG., & Stevenson,F.K. Unmutated Ig V(H) genes are associated with a more aggressive form of chronic lymphocytic leukemia. *Blood* **94**, 1848-1854 (1999).

19. Cimmino,A. *et al.* miR-15 and miR-16 induce apoptosis by targeting BCL2. *Proc Natl Acad Sci U S A* **102**, 13944-13949 (2005).

20. Ten,H.E. & Burger,J.A. Microenvironment interactions and B-cell receptor signaling in Chronic Lymphocytic Leukemia: Implications for disease pathogenesis and treatment. *Biochim. Biophys. Acta* **1863**, 401-413 (2016).

21. Queiros,A.C. *et al.* A B-cell epigenetic signature defines three biologic subgroups of chronic lymphocytic leukemia with clinical impact. *Leukemia* **29**, 598-605 (2015).

22. Sutton,L.A. *et al.* Different spectra of recurrent gene mutations in subsets of chronic lymphocytic leukemia harboring stereotyped B-cell receptors. *Haematologica* **101**, 959-967 (2016).

23. Landau,D.A. *et al.* Mutations driving CLL and their evolution in progression and relapse. *Nature* **526**, 525-530 (2015).

24. Puente,X.S. *et al.* Non-coding recurrent mutations in chronic lymphocytic leukaemia. *Nature* **526**, 519-524 (2015).

25. Deaglio,S. *et al.* CD38 and ZAP-70 are functionally linked and mark CLL cells with high migratory potential. *Blood* **110**, 4012-4021 (2007).

26. Deaglio,S. *et al.* CD38 is a signaling molecule in B-cell chronic lymphocytic leukemia cells. *Blood* **102**, 2146-2155 (2003).

27. Gobessi,S. *et al.* ZAP-70 enhances B-cell-receptor signaling despite absent or inefficient tyrosine kinase activation in chronic lymphocytic leukemia and lymphoma B cells. *Blood* **109**, 2032-2039 (2007).

28. Zucchetto,A. *et al.* CD38/CD31, the CCL3 and CCL4 chemokines, and CD49d/vascular cell adhesion molecule-1 are interchained by sequential events sustaining chronic lymphocytic leukemia cell survival. *Cancer Res* **69**, 4001-4009 (2009).

29. Dohner,H. *et al.* Genomic aberrations and survival in chronic lymphocytic leukemia. *N. Engl. J. Med.* **343**, 1910-1916 (2000).

30. Rossi,D. *et al.* Disruption of BIRC3 associates with fludarabine chemorefractoriness in TP53 wild-type chronic lymphocytic leukemia. *Blood* **119**, 2854-2862 (2012).

31. Le Garff-Tavernier,M. *et al.* Functional assessment of p53 in chronic lymphocytic leukemia. *Blood Cancer Journal* **1**, 1-3 (2011).

32. Campo,E. *et al.* TP53 aberrations in chronic lymphocytic leukemia: an overview of the clinical implications of improved diagnostics. *Haematologica* **103**, 1956-1968 (2018).

33. Stankovic,T. *et al.* Inactivation of ataxia telangiectasia mutated gene in B-cell chronic lymphocytic leukaemia. *The Lancet* **353**, 26-29 (1999).

34. Puente,X.S. *et al.* Whole-genome sequencing identifies recurrent mutations in chronic lymphocytic leukaemia. *Nature* **475**, 101-105 (2011).

35. Quesada,V. *et al.* Exome sequencing identifies recurrent mutations of the splicing factor SF3B1 gene in chronic lymphocytic leukemia. *Nat. Genet.* **44**, 47-52 (2011).

36. Fabbri,G. *et al.* Analysis of the chronic lymphocytic leukemia coding genome: role of NOTCH1 mutational activation. *J Exp Med* **208**, 1389-1401 (2011).

37. Rossi,D. *et al.* Mutations of NOTCH1 are an independent predictor of survival in chronic lymphocytic leukemia. *Blood* **119**, 521-529 (2012).

38. Villamor,N. *et al.* NOTCH1 mutations identify a genetic subgroup of chronic lymphocytic leukemia patients with high risk of transformation and poor outcome. *Leukemia* **27**, 1100-1106 (2013).

39. Landau,D.A. & Wu,C.J. Chronic lymphocytic leukemia: molecular heterogeneity revealed by high-throughput genomics. *Genome Med* **5**, 1-13 (2013).

40. Wang,L. *et al.* SF3B1 and Other Novel Cancer Genes in Chronic Lymphocytic Leukemia. *N. Engl. J. Med* **365**, 2497-2506 (2011).

41. Guieze,R. *et al.* Presence of multiple recurrent mutations confers poor trial outcome of relapsed/refractory CLL. *Blood* **126**, 2110 (2015).

42. Nadeu,F. *et al.* Clinical impact of clonal and subclonal TP53, SF3B1, BIRC3, NOTCH1, and ATM mutations in chronic lymphocytic leukemia. *Blood* **127**, 2122-2130 (2016).

43. Lionetti,M. *et al.* High-throughput sequencing for the identification of NOTCH1 mutations in early stage chronic lymphocytic leukaemia: biological and clinical implications. *Br. J Haematol.* **165**, 629-639 (2014).

44. Nadeu,F. *et al.* Clinical impact of the subclonal architecture and mutational complexity in chronic lymphocytic leukemia. *Leukemia* **32**, 645-653 (2018).

45. Oakes,C.C. *et al.* DNA methylation dynamics during B cell maturation underlie a continuum of disease phenotypes in chronic lymphocytic leukemia. *Nat. Genet.* **48**, 253-264 (2016).

46. Chen,C. & Puvvada,S. Prognostic Factors for Chronic Lymphocytic Leukemia. *Current Hematologic Malignancy Reports* **11**, 37-42 (2016).

47. Parikh,S.A. Chronic lymphocytic leukemia treatment algorithm 2018. *Blood Cancer Journal* **8**, 93 (2018).

48. Smolewski,P., Witkowska,M., & Korycka-Wolowiec,A. New insights into biology, prognostic factors, and current therapeutic strategies in chronic lymphocytic leukemia. *ISRN Oncol* **2013**, 1-7 (2013).

49. Oken,M.M. *et al.* Toxicity and response criteria of the Eastern Cooperative Oncology Group. *Am. J. Clin. Oncol.* **5**, 649-655 (1982).

50. Hallek,M. Prognostic factors in chronic lymphocytic leukemia. *Ann. Oncol* **19**, 51-53 (2008).

51. Molica,S. & Alberti,A. Prognostic value of the lymphocyte doubling time in chronic lymphocytic leukemia. *Cancer* **60**, 2712-2716 (1987).

52. Bulian,P. *et al.* CD49d is the strongest flow cytometry-based predictor of overall survival in chronic lymphocytic leukemia. *J Clin. Oncol* **32**, 897-904 (2014).

53. Dal,B.M. *et al.* Microenvironmental interactions in chronic lymphocytic leukemia: the master role of CD49d. *Semin. Hematol.* **51**, 168-176 (2014).

54. Rassenti,L.Z. *et al.* ZAP-70 compared with immunoglobulin heavy-chain gene mutation status as a predictor of disease progression in chronic lymphocytic leukemia. *N. Engl. J Med* **351**, 893-901 (2004).

55. Crespo,M. *et al.* ZAP-70 expression as a surrogate for immunoglobulin-variable-region mutations in chronic lymphocytic leukemia. *N. Engl. J Med* **348**, 1764-1775 (2003).

56. Hamblin,T.J. *et al.* CD38 expression and immunoglobulin variable region mutations are independent prognostic variables in chronic lymphocytic leukemia, but CD38 expression may vary during the course of the disease. *Blood* **99**, 1023-1029 (2002).

57. Fischer,K. *et al.* Long-term remissions after FCR chemoimmunotherapy in previously untreated patients with CLL: updated results of the CLL8 trial. *Blood* **127**, 208-215 (2016).

58. Zenz,T. *et al.* TP53 mutation and survival in chronic lymphocytic leukemia. *J. Clin. Oncol.* **28**, 4473-4479 (2010).

59. Rigolin,G.M. *et al.* In CLL, comorbidities and the complex karyotype are associated with an inferior outcome independently of CLL-IPI. *Blood* **129**, 3495-3498 (2017).

60. Jain,N. & O'Brien,S. Targeted therapies for CLL: Practical issues with the changing treatment paradigm. *Blood Reviews* **30**, 233-244 (2016).

61. Eichhorst,B. *et al.* Chronic lymphocytic leukaemia: ESMO Clinical Practice Guidelines for diagnosis, treatment and follow-up. *Annals. of Oncology* **26**, 78-84 (2015).

62. Jain,N. *et al.* Ibrutinib, fludarabine, cyclophosphamide, and obinutuzumab (GA101) (iFCG) for previously untreated patients with chronic lymphocytic leukemia (CLL) with mutated IGHV and non-del (17p). *Journal of Clinical Oncology* **35** [15_suppl], 7522 (2017). Ref Type: Abstract

63. Bittolo,T. *et al.* Mutations in the 3' untranslated region of NOTCH1 are associated with low CD20 expression levels chronic lymphocytic leukemia. *Haematologica* **102**, 305-309 (2017).

64. Stilgenbauer,S. *et al.* Gene mutations and treatment outcome in chronic lymphocytic leukemia: results from the CLL8 trial. *Blood* **123**, 3247-3254 (2014).

65. Rai K.R *et al.* Clinical staging of chronic lymphocytic leukemia. *Blood* **46**, 219-234 (1975).

66. Rai,K.R. & Jain,P. Advances in the clinical staging of chronic lymphocytic leukemia. *Clin Chem* **57**, 1771-1772 (2011).

67. Binet JL *et al.* A new prognostic classification of chronic lymphocytic leukemia derived from a multivariate survival analysis. *Cancer* **48**, 198-206 (1981).

68. International CLL-IPI working group An international prognostic index for patients with chronic lymphocytic leukaemia (CLL-IPI): a meta-analysis of individual patient data. *Lancet Oncol.* **17**, 779-790 (2016).

69. Herishanu,Y. *et al.* The lymph node microenvironment promotes B-cell receptor signaling, NF-kappaB activation, and tumor proliferation in chronic lymphocytic leukemia. *Blood* **117**, 563-574 (2011).

70. Herreros,B. *et al.* Proliferation centers in chronic lymphocytic leukemia: the niche where NF-kappaB activation takes place. *Leukemia* **24**, 872-876 (2010).

71. Burger,J.A. *et al.* High-level expression of the T-cell chemokines CCL3 and CCL4 by chronic lymphocytic leukemia B cells in nurselike cell cocultures and after BCR stimulation. *Blood* **113**, 3050-3058 (2009).

72. Ye,J. *et al.* TLR8 signaling enhances tumor immunity by preventing tumor-induced T-cell senescence. *EMBO Mol Med* **6**, 1294-1311 (2014).

73. Catovsky,D., Miliani,E., Okos,A., & Galton,D.A.G. Clinical significance of T-cells in chronic lymphocytic leukaemia. *The Lancet* **304**, 751-752 (1974).

74. Nunes,C. *et al.* Expansion of a CD8+PD-1+ Replicative Senescence Phenotype in Early Stage CLL Patients Is Associated with Inverted CD4:CD8 Ratios and Disease Progression. *Clin. Cancer Res.* **18**, 678-687 (2011).

75. Rosner Philipp M *et al.* Exhausted PD-1 T-Cells Are Enriched in Secondary Lymphoid Organs of CLL Patients. *Blood* **130**, 4281 (2017).

76. Lutzny,G. *et al.* Protein kinase c-beta-dependent activation of NF-kappaB in stromal cells is indispensable for the survival of chronic lymphocytic leukemia B cells in vivo. *Cancer Cell* **23**, 77-92 (2013).

77. Nguyen,P.H. *et al.* LYN Kinase in the Tumor Microenvironment Is Essential for the Progression of Chronic Lymphocytic Leukemia. *Cancer Cell* **30**, 610-622 (2016).

78. Paggetti,J. *et al.* Exosomes released by chronic lymphocytic leukemia cells induce the transition of stromal cells into cancer-associated fibroblasts. *Blood* **126**, 1106-1117 (2015).

79. Nicholas,N.S., Apollonio,B., & Ramsay,A.G. Tumor microenvironment (TME)-driven immune suppression in B cell malignancy. *Biochim. Biophys. Acta* **1863**, 471-482 (2016).

80. Lagneaux,L., Delforge,A.F., Bron,D.F., De Bruyn,C.F., & Stryckmans,P. Chronic lymphocytic leukemic B cells but not normal B cells are rescued from apoptosis by contact with normal bone marrow stromal cells. *Blood* **91**, 2387-2396 (1998).

81. Oldreive,C.E. *et al.* T-cell number and subtype influence the disease course of primary chronic lymphocytic leukaemia xenografts in a lymphoid mice. *Dis Model Mech* **8**, 1401-1412 (2015).

82. Crassini,K.R., Best,O.G., & Mulligan,S.P. Immune failure, infection and survival in chronic lymphocytic leukemia. *Haematologica* **103**, 330-303 (2018).

83. Boissard,F., Fourni+®,J.J., Quillet-Mary,A., Ysebaert,L., & Poupot,M. Nurse-like cells mediate ibrutinib resistance in chronic lymphocytic leukemia patients. *Blood Cancer Journal* **5**, e355 (2015).

84. Crassini,K., Shen,Y., Mulligan,S., & Giles,B.O. Modeling the chronic lymphocytic leukemia microenvironment in vitro. *Leuk. Lymphoma* **58**, 266-279 (2017).

85. Simonetti,G., Bertilaccio,M.T., Ghia,P., & Klein,U. Mouse models in the study of chronic lymphocytic leukemia pathogenesis and therapy. *Blood* **124**, 1010-1019 (2014).

86. Bichi,R. *et al.* Human chronic lymphocytic leukemia modeled in mouse by targeted TCL1 expression. *Proc Natl Acad Sci USA* **99**, 6955-6960 (2002).

87. Yin,S. *et al.* A murine model of chronic lymphocytic leukemia based on B cell-restricted expression of Sf3b1 mutation and Atm deletion. *Cancer Cell* **35**, 283-296 (2019).

88. Herling,M. *et al.* TCL1 shows a regulated expression pattern in chronic lymphocytic leukemia that correlates with molecular subtypes and proliferative state. *Leukemia* **20**, 280-285 (2006).

89. Michael A. Teitell. The TCL1 family of oncoproteins: co-activators of transformation. *Nature Reviews Cancer* **5**, 640–648 (2005).

90. Bertilaccio,M.T. *et al.* Xenograft models of chronic lymphocytic leukemia: problems, pitfalls and future directions. *Leukemia* **27**, 534-540 (2013).

91. Shimoni,A. *et al.* A Model for Human B-Chronic Lymphocytic Leukemia in Human /Mouse Radiation Chimera: Evidence for Tumor-Mediated Suppression of Antibody Production in Low-Stage Disease. *Blood* **89**, 2210 (1997).

92. Durig,J. *et al.* A Novel Nonobese Diabetic/Severe Combined Immunodeficient Xenograft Model for Chronic Lymphocytic Leukemia Reflects Important Clinical Characteristics of the Disease. *Cancer Res* **67**, 8653 (2007).

93. Bagnara,D. *et al.* A novel adoptive transfer model of chronic lymphocytic leukemia suggests a key role for T lymphocytes in the disease. *Blood* **117**, 5463 (2011).

94. Kikushige,Y. *et al.* Self-Renewing Hematopoietic Stem Cell Is the Primary Target in Pathogenesis of Human Chronic Lymphocytic Leukemia. *Cancer Cell* **20**, 246-259 (2011).

95. Chen,S.S. Method for Generating a Patient-Derived Xenograft Model of CLL in *Chronic Lymphocytic Leukemia: Methods and Protocols* (ed. Malek,S.N.) 165-171 (2019).

96. Lee,C.L.Y., Uniyal,S., Fernandez,L.A., Lee,S.H.S., & Ghose,T. Growth and Spread in Nude Mice of Epstein-Barr Virus Transformed B-Cells from a Chronic Lymphocytic Leukemia Patient. *Cancer Res* **46**, 2497 (1986).

97. Kawata,A. *et al.* Establishment and characterization of the tumors of chronic lymphocytic leukemia cell line in nude and SCID mice. *Leuk. Res* **17**, 883-894 (1993).

98. Loisel,S. *et al.* Establishment of a novel human B-CLL-like xenograft model in nude mouse. *Leukemia Research* **29**, 1347-1352 (2005).

99. Bertilaccio,M.T.S. *et al.* A novel Rag2-xenograft model of human CLL. *Blood* **115**, 1605 (2010).

100.Vaisitti,T. *et al.* Novel Richter Syndrome Xenograft Models to Study Genetic Architecture, Biology, and Therapy Responses. *Cancer Res* **78**, 3413 (2018).

101.Burger,J.A. & O'Brien,S. Evolution of CLL treatment-from chemoimmunotherapy to targeted and individualized therapy. *Nature Reviews Clinical Oncology* **15**, 510-527 (2018).

102.Hallek,M. Chronic lymphocytic leukemia: 2017 update on diagnosis, risk stratification, and treatment. *Am. J. Hematol.* **92**, 946-965 (2017).

103.Hallek,M. *et al.* iwCLL guidelines for diagnosis, indications for treatment, response assessment, and supportive management of CLL. *Blood* **131**, 2745-2760 (2018).

104.Gribben,J.G. & O'Brien,S. Update on therapy of chronic lymphocytic leukemia. *J Clin Oncol* **29**, 544-550 (2011).

105.Natural history of stage A chronic lymphocytic leukaemia untreated patients. French Cooperative Group on Chronic Lymphocytic Leukaemia. *Br. J. Haematol.* **76**, 45-57 (1990).

106.Effects of chlorambucil and therapeutic decision in initial forms of chronic lymphocytic leukemia (stage A): results of a randomized clinical trial on 612 patients. The French Cooperative Group on Chronic Lymphocytic Leukemia. *Blood* **75**, 1414-1421 (1990).

107.Rossi,D. *et al.* The prognostic value of TP53 mutations in chronic lymphocytic leukemia is independent of del17p13: Implications for overall survival and chemorefractoriness. *Clin. Cancer Res.* **15**, 995-1004 (2009).

108.Rossi,D. *et al.* Clinical impact of small TP53 mutated subclones in chronic lymphocytic leukemia. *Blood* **123**, 2139-2147 (2014).

109.Hallek,M. *et al.* Addition of rituximab to fludarabine and cyclophosphamide in patients with chronic lymphocytic leukaemia: a randomised, open-label, phase 3 trial. *The Lancet* **376**, 1164-1174 (2010).

110.Eichhorst,B. *et al.* First-line chemoimmunotherapy with bendamustine and rituximab versus fludarabine, cyclophosphamide, and rituximab in patients with advanced chronic lymphocytic leukaemia (CLL10): an international, open-label, randomised, phase 3, non-inferiority trial. *Lancet Oncol* **17**, 928-942 (2016).

111.Farooqui,M.Z. *et al.* Ibrutinib for previously untreated and relapsed or refractory chronic lymphocytic leukaemia with TP53 aberrations: a phase 2, single-arm trial. *Lancet Oncol.* **16**, 169-176 (2014).

112.Stilgenbauer,S. *et al.* Venetoclax in relapsed or refractory chronic lymphocytic leukaemia with 17p deletion: a multicentre, open-label, phase 2 study. *The Lancet Oncology* **17**, 768-778 (2016).

113.Jain,N. *et al.* Ibrutinib and Venetoclax for First-Line Treatment of CLL. *N. Engl. J. Med* **380**, 2095-2103 (2019).

114.Tam,C.S. *et al.* Long-term results of first salvage treatment in CLL patients treated initially with FCR (fludarabine, cyclophosphamide, rituximab). *Blood* **[Epub ahead of print]**, (2014).

115. Thompson,P.A. *et al*. Fludarabine, cyclophosphamide, and rituximab treatment achieves long-term disease-free survival in IGHV-mutated chronic lymphocytic leukemia. *Blood* **127**, 303-309 (2016).

116. Rossi,D. *et al.* Molecular prediction of durable remission after first-line fludarabine-cyclophosphamide-rituximab in chronic lymphocytic leukemia. *Blood* **126**, 1921-1924 (2015).

117. Laurenti,L. *et al.* Bendamustine in combination with rituximab for elderly patients with previously untreated B-cell chronic lymphocytic leukemia: A retrospective analysis of real-life practice in Italian hematology departments. *Leuk. Res* **39**, 1066-1070 (2015).

118. Hillmen,P. *et al.* Chlorambucil plus ofatumumab versus chlorambucil alone in previously untreated patients with chronic lymphocytic leukaemia (COMPLEMENT 1): a randomised, multicentre, open-label phase 3 trial. *The Lancet* **385,** 1873-1883 (2015).

119. Owen,C.J. & Stewart,D.A. Obinutuzumab for the treatment of patients with previously untreated chronic lymphocytic leukemia: overview and perspective. *Ther Adv Hematol* **6**, 161-170 (2015).

120. Goede,V. *et al.* Obinutuzumab plus Chlorambucil in Patients with CLL and Coexisting Conditions. *N. Engl. J. Med* **370**, 1101-1110 (2014).

121. Woyach,J.A. *et al.* Ibrutinib Regimens versus Chemoimmunotherapy in Older Patients with Untreated CLL. *N. Engl. J. Med* **379**, 2517-2528 (2018).

122. O'Brien,S. *et al.* Single-agent ibrutinib in treatment-naive and relapsed/refractory chronic lymphocytic leukemia: a 5-year experience. *Blood* **131**, 1910-1919 (2018).

123. Moreno,C. *et al.* Ibrutinib plus obinutuzumab versus chlorambucil plus obinutuzumab in first-line treatment of chronic lymphocytic leukaemia (iLLUMINATE): a multicentre, randomised, open-label, phase 3 trial. *The Lancet Oncology* **20**, 43-56 (2019).

124. Shanafelt,T.D. *et al.* A Randomized Phase III Study of Ibrutinib (PCI-32765)-Based Therapy Vs. Standard Fludarabine, Cyclophosphamide, and Rituximab (FCR) Chemoimmunotherapy in Untreated Younger Patients with Chronic Lymphocytic Leukemia (CLL): A Trial of the ECOG-ACRIN Cancer Research Group (E1912). *Blood* **132**, LBA-4 (2018).

125. Furman,R.R. *et al.* Idelalisib and Rituximab in Relapsed Chronic Lymphocytic Leukemia. *N. Engl. J. Med* **370**, 997-1007 (2014).

126. Brown,J.R. *et al.* Extended follow-up and impact of high-risk prognostic factors from the phase 3 RESONATE study in patients with previously treated CLL/SLL. *Leukemia* **32**, 83-91 (2018).

127. Seymour,J.F. *et al.* Venetoclax + Rituximab in Relapsed or Refractory Chronic Lymphocytic Leukemia. *N. Engl. J. Med* **378**, 1107-1120 (2018).

128. Byrd,J.C. *et al.* Targeting BTK with Ibrutinib in Relapsed Chronic Lymphocytic Leukemia. *N. Engl. J. Med* **369**, 32-42 (2013).

129. Freeman,C.L. & Gribben,J.G. Immunotherapy in Chronic Lymphocytic Leukaemia (CLL). *Current Hematologic Malignancy Reports* **11**, 29-36 (2016).

130. Guieze,R. & Wu,C.J. Genomic and epigenomic heterogeneity in chronic lymphocytic leukemia. *Blood* **126**, 445-453 (2015).

131. Woyach,J.A. *et al.* Resistance Mechanisms for the Bruton's Tyrosine Kinase Inhibitor Ibrutinib. *N. Engl. J. Med* **370**, 2286-2294 (2014).

132. Quinquenel,A. *et al.* Prevalence of BTK and PLCG2 mutations in a reallife CLL cohort still on ibrutinib after three years: a FILO group study. *Blood* **134**, 641-644 (2019).

133. Burger,J.A. *et al.* Clonal evolution in patients with chronic lymphocytic leukaemia developing resistance to BTK inhibition. *Natu commun* **7**, 1-13 (2016).

134. June,C.H. & Sadelain,M. Chimeric Antigen Receptor Therapy. *N. Engl. J. Med* **379**, 64-73 (2018).

135. Grywalska,E., Pasiarski,M., Gozdz,S., & Rolinski,J. Immune-checkpoint inhibitors for combating T-cell dysfunction in cancer. *Onco Targets Ther* **11**, 6505-6524 (2018).

136. Robak,T. et al. Randomized phase 2 study of otlertuzumab and bendamustine versus bendamustine in patients with relapsed chronic lymphocytic leukaemia. *Br. J Haematol* **176**, 618-628 (2017).

137. Skoetz,N. *et al.* Alemtuzumab for patients with chronic lymphocytic leukaemia. *Cochrane Database Syst Rev* **2012**, 1-91 (2012).

138. Beckwith,K.A., Byrd,J.C., & Muthusamy,N. Tetraspanins as therapeutic targets in hematological malignancy: a concise review. *Front Physiol* **6**, 1-13 (2015).

139. Zhao,Y. *et al.* The immunological function of CD52 and its targeting in organ transplantation. *Inflammation Research* **66**, 571-578 (2017).

140. Cuesta-Mateos,C., caraz-Serna,A., Somovilla-Crespo,B., & Muñoz-Calleja,C. Monoclonal Antibody Therapies for Hematological Malignancies: Not Just Lineage-Specific Targets. *Frontiers in Immunology* **8**, 1936-1969 (2018).

141. Stamatopoulos,B. *et al.* AMD3100 disrupts the cross-talk between chronic lymphocytic leukemia cells and a mesenchymal stromal or nurse-like cell-based microenvironment: pre-clinical evidence for its association with chronic lymphocytic leukemia treatments. *Haematologica* **97**, 608-615 (2012).

142. Andritsos,L.A. *et al.* A multicenter phase 1 study of plerixafor and rituximab in patients with chronic lymphocytic leukemia. *Leukemia & Lymphoma* **[Epub ahead of print]**, 1-9 (2019).

143. Byrd,J.C. *et al.* Acalabrutinib (ACP-196) in Relapsed Chronic Lymphocytic Leukemia. *N. Engl. J. Med* **374**, 323-332 (2016).

144. Awan FT *et al.* Acalabrutinib monotherapy in patients with chronic lymphocytic leukemia who are intolerant to ibrutinib. *Blood adv* **3**, 1553-1562 (2019).

145. Khan,Y. & O'Brien,S. Acalabrutinib and its use in treatment of Chronic lymphocytic leukemia. *Future Oncology* **15**, 579-589 (2019).

146. Walter HS *et al.* Long-term follow-up of patients with CLL treated with the selective Bruton's tyrosine kinase inhibitor ONO/GS-4059. *Blood* **129**, 2808-2810 (2017).

147. Munakata,W. *et al.* Phase I study of tirabrutinib (ONO-4059/GS-4059) in patients with relapsed or refractory B-cell malignancies in Japan. *Cancer Sci.* **110**, 1686-1694 (2019).

148. Li,Y. *et al.* Population pharmacokinetics and exposure response assessment of CC-292, a potent BTK inhibitor, in patients with chronic lymphocytic leukemia. *J Clin Pharmacol* **57**, 1279-1289 (2017).

149. Lee-Verges,E. *et al.* Selective BTK inhibition improves bendamustine therapy response and normalizes immune effector functions in chronic lymphocytic leukemia. *Int. J. Cancer* **144**, 2762-2773 (2019).

150. Tam,C.S.L. *et al.* Phase 1 study of selective BTK inhibitor zanubrutinib in B-cell malignancies and safety and efficacy evaluation in CLL. *Blood* **[Epub ahead of print]**, (2019).

151. Burris,H.A., III *et al.* Umbralisib, a novel PI3Kdelta and casein kinase-1epsilon inhibitor, in relapsed or refractory chronic lymphocytic leukaemia and lymphoma: an open-label, phase 1, dose-escalation, first-in-human study. *Lancet Oncol.* **19**, 486-496 (2018).

152. Frustaci,A.M. *et al.* Duvelisib: a new phosphoinositide-3-kinase inhibitor in chronic lymphocytic leukemia. *Future Oncology* **15**, 2227-2239 (2019).

153. Vangapandu,H.V., Jain,N., & Gandhi,V. Duvelisib: a phosphoinositide-3 kinase inhibitor for chronic lymphocytic leukemia. *Expert Opin Investig Drugs* **26**, 625-632 (2017).

154. Brown,J.R. *et al.* Phase I Trial of the Pan-PI3K Inhibitor Pilaralisib (SAR245408/XL147) in Patients with Chronic Lymphocytic Leukemia (CLL) or Relapsed/Refractory Lymphoma. *Clin. Cancer Res.* **21**, 3160-3169 (2015).

155. Assouline,S. *et al.* A Phase II Clinical Trial of the Pan PI3K Inhibitor, Buparlisib, for the Treatment of Relapsed and Refractory Chronic Lymphocytic Leukemia: Canadian Cancer Trials Group IND.216. *Blood* **130**, 4319 (2017).

156. Sharman,J. *et al.* An open-label phase 2 trial of entospletinib (GS-9973), a selective spleen tyrosine kinase inhibitor, in chronic lymphocytic leukemia. *Blood* **125**, 2336-2343 (2015).

157. Kawasaki,T. & Kawai,T. Toll-like receptor signaling pathways. *Frontiers in Immunology* **5**, 1-8 (2014).

158. Rolls,A. *et al.* Toll-like receptors modulate adult hippocampal neurogenesis. *Nature Cell Biology.* **9**, 1081-1088 (2007).

159. Ruprecht,C.R. & Lanzavecchia,A. Toll-like receptor stimulation as a third signal required for activation of human naive B cells. *Eur. J. Immunol.* **36**, 810-816 (2006).

160. Rawlings,D.J., Schwartz,M.A., Jackson,S.W., & Meyer-Bahlburg,A. Integration of B cell responses through Toll-like receptors and antigen receptors. *Nat. Rev. Immunol.* **12**, 282-294 (2012).

161. Cole,J.E., Georgiou,E., & Monaco,C. The expression and functions of toll-like receptors in atherosclerosis. *Mediators Inflamm* **2010**, 1-18 (2010).

162. Liu,G. & Zhao,Y. Toll-like receptors and immune regulation: their direct and indirect modulation on regulatory CD4+ CD25+ T cells. *Immunology* **122**, 149-156 (2007).

163. Kawai,T. & Akira,S. TLR signaling. *Cell Death. & Differentiation* **13**, 816-825 (2006).

164. Li,M., Zhou,Y., Feng,G., & Su,S.B. The critical role of Toll-like receptor signaling pathways in the induction and progression of autoimmune diseases. *Curr. Mol. Med* **9**, 365-374 (2009).

165. Gay,N.J., Symmons,M.F., Gangloff,M., & Bryant,C.E. Assembly and localization of Toll-like receptor signalling complexes. *Nat. Rev. Immunol.* **14**, 546-558 (2014).

166. Ngo,V.N. *et al.* Oncogenically active MYD88 mutations in human lymphoma. *Nature* **470**, 115-119 (2011).

167. Balka,K.R. & De,N.D. Understanding early TLR signaling through the Myddosome. *J. Leukoc. Biol.* **105**, 339-351 (2019).

168. Gao,W., Xiong,Y., Li,Q., & Yang,H. Inhibition of Toll-Like Receptor Signaling as a Promising Therapy for Inflammatory Diseases: A Journey from Molecular to Nano Therapeutics. *Frontiers in Physiology* **8**, 1-20 (2017).

169. Mogensen,T.H. Pathogen recognition and inflammatory signaling in innate immune defenses. *Clin Microbiol Rev* **22**, 240-273 (2009).

170. Yu,X. *et al.* MYD88 L265P Mutation in Lymphoid Malignancies. *Cancer Res* **78**, 2457-2462 (2018).

171. Lim,K.H., Romero,D.L., Chaudhary,D., Robinson,S.D., & Staudt,L.M. IRAK4 Kinase As A Novel Therapeutic Target in the ABC Subtype of Diffuse Large B Cell Lymphoma. Blood 120[21], 62. 2012. Ref Type: Abstract

172. Kelly,P.N. *et al.* Selective interleukin-1 receptor-associated kinase 4 inhibitors for the treatment of autoimmune disorders and lymphoid malignancy. *J Exp Med* **212**, 2189-2201 (2015).

173. Martinez-Trillos,A. *et al.* Mutations in TLR/MYD88 pathway identify a subset of young chronic lymphocytic leukemia patients with favorable outcome. *Blood* **123**, 3790-3796 (2014).

174. Rousseau,S. & Martel,G. Gain-of-Function Mutations in the Toll-Like Receptor Pathway: TPL2-Mediated ERK1/ERK2 MAPK Activation, a Path to Tumorigenesis in Lymphoid Neoplasms? *Frontiers in Cell and Developmental Biology* **4**, 1-10 (2016).

175. Dunleavy,K. *et al.* Differential efficacy of bortezomib plus chemotherapy within molecular subtypes of diffuse large B-cell lymphoma. *Blood* **113**, 6069-6076 (2009).

176. Baliakas,P. *et al.* Prognostic relevance of MYD88 mutations in CLL: the jury is still out. *Blood* **126**, 1043-1044 (2015).

177. Dajon,M., Iribarren,K., & Cremer,I. Toll-like receptor stimulation in cancer: A pro- and anti-tumor double-edged sword. *Immunobiology* **222**, 89-100 (2017).

178. McCain,J. The MAPK (ERK) Pathway: Investigational Combinations for the Treatment of BRAF-Mutated Metastatic Melanoma. *P T* **38**, 96-108 (2013).

179. Lavoie,H. & Therrien,M. Regulation of RAF protein kinases in ERK signalling. *Nat. Rev. Mol. Cell Biol.* **16**, 281-298 (2015).

180. Pakneshan S, Salajegheh A, Smith RA, & Lam AK Clinicopathological relevance of BRAF mutations in human cancer. *Pathology* **45**, 346-356 (2013).

181. Ramos,J.W. The regulation of extracellular signal-regulated kinase (ERK) in mammalian cells. *The International Journal of Biochemistry & Cell Biology* **40**, 2707-2719 (2008).

182. Caunt,C.J. & Keyse,S.M. Dual-specificity MAP kinase phosphatases (MKPs): shaping the outcome of MAP kinase signalling. *FEBS J* **280**, 489-504 (2013).

183. Liu,F., Yang,X., Geng,M., & Huang,M. Targeting ERK, an Achilles' Heel of the MAPK pathway, in cancer therapy. *Acta Pharm. Sin. B* **8**, 552-562 (2018).

184. Gonzalez-Hormazabal,P. *et al.* Polymorphisms in RAS/RAF/MEK/ERK Pathway Are Associated with Gastric Cancer. *Genes (Basel)* **10**, 20-29 (2018).

185. Hobbs,G.A., Der,C.J., & Rossman,K.L. RAS isoforms and mutations in cancer at a glance. *J. Cell Sci.* **129**, 1287-1292 (2016).

186. Davies,H. *et al.* Mutations of the BRAF gene in human cancer. *Nature* **417**, 949-954 (2002).

187. Arcaini,L. *et al.* The BRAFV600E mutation in hairy cell leukemia and other mature B-cell neoplasms. *Blood* **119**, 188-191 (2012).

188. Murugan,A.K., Dong,J., Xie,J., & Xing,M. MEK1 mutations, but not ERK2 mutations, occur in melanomas and colon carcinomas, but none in thyroid carcinomas. *Cell Cycle* **8**, 2122-2124 (2009).

189. Ping,N. *et al.* Absence of BRAF V600E mutation in hematologic malignancies excluding hairy-cell leukemia. *Leukemia & Lymphoma* **53**, 2498-2499 (2012).

190. Jebaraj,B.M.C. *et al.* BRAF mutations in chronic lymphocytic leukemia. *Leukemia & Lymphoma* **54**, 1177-1182 (2013).

191. Yang,S. & Liu,G. Targeting the Ras/Raf/MEK/ERK pathway in hepatocellular carcinoma. *Oncol Lett* **13**, 1041-1047 (2017).

192. Ledford,H. Cancer: The Ras renaissance. *Nature* **520**, 278-280 (2015).

193. Moriceau,G. *et al.* Tunable-Combinatorial Mechanisms of Acquired Resistance Limit the Efficacy of BRAF/MEK Cotargeting but Result in Melanoma Drug Addiction. *Cancer Cell* **27**, 240-256 (2015).

194. Shi,H. *et al.* Acquired resistance and clonal evolution in melanoma during BRAF inhibitor therapy. *Cancer Discov.* **4**, 80-93 (2014).

195. Sullivan,R.J. *et al.* First-in-Class ERK1/2 Inhibitor Ulixertinib (BVD-523) in Patients with MAPK Mutant Advanced Solid Tumors: Results of a Phase I Dose-Escalation and Expansion Study. *Cancer Discov.* **8**, 184-195 (2018).

196. Jaksic,O. *et al.* Guidelines for Diagnosis and Treatment of Chronic Lymphocytic Leukemia. Krohem B-Cll 2017. *Acta Clin Croat* **57**, 190-215 (2018).

197. Ibragimova,M.K., Tsyganov MM., & Litviakov,N.V. Natural and chemotherapy-induced clonal evolution of tumors. *Biochemistry (Mosch)* **82**, 413-425 (2017).

198. Nosari,A. Infectious complications in chronic lymphocytic leukemia. *Mediterr J Hematol Infect Dis* **4**, e2012070 (2012).

199. Anderson,M.A. *et al.* The BCL2 selective inhibitor venetoclax induces rapid onset apoptosis of CLL cells in patients via a TP53-independent mechanism. *Blood* **127**, 3215-3224 (2016).

200. Rossi,D. & Gaidano,G. The clinical implications of gene mutations in chronic lymphocytic leukaemia. *British. Journal Of Cancer* **114**, 849-854 (2016).

201. Baliakas,P. *et al.* Recurrent mutations refine prognosis in chronic lymphocytic leukemia. *Leukemia* **29**, 329-336 (2015).

202. Delgado,J. *et al.* Genomic complexity and IGHV mutational status are key predictors of outcome of chronic lymphocytic leukemia patients with TP53 disruption. *Haematologica* **99**, 231-234 (2014).

203. Landau,D.A. *et al.* Evolution and impact of subclonal mutations in chronic lymphocytic leukemia. *Cell* **152**, 714-726 (2013).

204. Jeromin,S. *et al.* SF3B1 mutations correlated to cytogenetics and mutations in NOTCH1, FBXW7, MYD88, XPO1 and TP53 in 1160 untreated CLL patients. *Leukemia* **28**, 108-117 (2014).

205. Rodriguez-Vicente,A.E. *et al.* Next-generation sequencing in chronic lymphocytic leukemia: recent findings and new horizons. *Oncotarget* **8**, 71234-71248 (2017).

206. Cheson,B.D. *et al.* Novel targeted agents and the need to refine clinical end points in chronic lymphocytic leukemia. *J Clin Oncol* **30**, 2820-2822 (2012).

207. Wiestner A. Emerging role of kinase-targeted strategies in chronic lymphocytic leukemia. *Blood* **120**, 4684-4691 (2012).

208. Stevenson,F.K., Krysov S - Davies,A., Davies AJ- Steele,A., Steele AJ, & Packham,G. B-cell receptor signaling in chronic lymphocytic leukemia. *Blood* **118**, 4313-4320 (2011).

209. Seda,V. & Mraz,Ma. B-cell receptor signalling and its crosstalk with other pathways in normal and malignant cells. *Eur. J. Immunol.* **94**, 193-205 (2015).

210. Nguyen,P.H., Niesen,E., & Hallek,M. New roles for B cell receptor associated kinases: when the B cell is not the target. *Leukemia* **33**, 576-587 (2019).

211. Ferrer,G. & Montserrat,E. Critical molecular pathways in CLL therapy. *BMC. Med.* **24**, 1-10 (2018).

212. Brown,J.R. How I treat CLL patients with ibrutinib. *Blood* **131**, 379-386 (2018).

213. Hoellenriegel,J. *et al.* The phosphoinositide 3'-kinase delta inhibitor, CAL-101, inhibits B-cell receptor signaling and chemokine networks in chronic lymphocytic leukemia. *Blood* **118**, 3603-3612 (2011).

214. Brown,J.R. *et al.* Idelalisib, an inhibitor of phosphatidylinositol 3-kinase, for relapsed/refractory chronic lymphocytic leukemia. *Blood* **123**, 3390 (2014).

215. Woyach,J.A. How I manage ibrutinib-refractory chronic lymphocytic leukemia. *Blood* **129**, 1270 (2017).

216. Jones,J. *et al.* Venetoclax (VEN) Monotherapy for Patients with Chronic Lymphocytic Leukemia (CLL) Who Relapsed after or Were Refractory to Ibrutinib or Idelalisib. *Blood* **128**, 637 (2016).

217. Flinn,I.W. *et al.* Phase 1b study of venetoclax-obinutuzumab in previously untreated and relapsed/refractory chronic lymphocytic leukemia. *Blood* **133**, 2765-2775 (2019).

218. Advani,R.H. *et al.* Bruton Tyrosine Kinase Inhibitor Ibrutinib (PCI-32765) Has Significant Activity in Patients With Relapsed/Refractory B-Cell Malignancies. *JCO.* **31**, 88-94 (2012).

219. Lau,C.M. *et al.* RNA-associated autoantigens activate B cells by combined B cell antigen receptor/Toll-like receptor 7 engagement. *J Exp Med* **202**, 1171-1177 (2005).

220. Chiorazzi,N. & Ferrarini,M. B cell chronic lymphocytic leukemia: lessons learned from studies of the B cell antigen receptor. *Annu Rev Immunol* **21**, 841-894 (2003).

221. Mills,D.M. & Cambier,J.C. B lymphocyte activation during cognate interactions with CD4+ T lymphocytes: molecular dynamics and immunologic consequences. *Semin. Immunol* **12**, 325-329 (2003).

222. Takeda,K. & Akira,S. Toll-like receptors in innate immunity. *Int. Immunol* **17**, 1-14 (2005).

223. Drexler,S.K. & Foxwell,B.M. The role of toll-like receptors in chronic inflammation. *Int. J. Biochem Cell Biol* **42**, 506-518 (2010).

224. Pradere,J.P., Dapito,D.H., & Schwabe,R.F. The Yin and Yang of Toll-like receptors in cancer. *Oncogene* **33**, 3485-3495 (2014).

225. Wang,J.Q., Jeelall,Y.S., Ferguson,L.L., & Horikawa,K. Toll-Like Receptors and Cancer: MYD88 Mutation and Inflammation. *Frontiers in Immunology* **5**, 1-10 (2014).

226. Riches,J.C. & Gribben,J.G. Understanding the Immunodeficiency in Chronic Lymphocytic Leukemia: Potential Clinical Implications. *Hematology. /Oncology Clinics. of North America.* **27**, 207-235 (2013).

227. Martinez-Trillos,A. *et al.* Clinical impact of MYD88 mutations in chronic lymphocytic leukemia. *Blood* **127**, 1611-1613 (2016).

228. Improgo,M.R. *et al.* MYD88 L265P mutations identify a prognostic gene expression signature and a pathway for targeted inhibition in CLL. *Br. J Haematol.* **184**, 925-936 (2019).

229. Yazawa N *et al.* CD19 regulates innate immunity by the toll-like receptor RP105 signaling in B lymphocytes. *Blood* **102**, 1374-1380 (2003).

230. M., Fonte,E., & Caligaris-Cappio,F. Toll-like Receptors in Chronic Lymphocytic Leukemia. *Mediterr J Hematol Infect Dis* **4**, e2012055; 1-10 (2012).

231. Rozkova,D. *et al.* Toll-like receptors on B-CLL cells: expression and functional consequences of their stimulation. *Int J Cancer* **126**, 1132-1143 (2010).

232. Mansson,A., Adner,M., Hockerfelt,U.F., & Cardell,L.O. A distinct Toll-like receptor repertoire in human tonsillar B cells, directly activated by PamCSK, R-837 and CpG-2006 stimulation. *Immunology* **118**, 539-548 (2006).

233. Arvaniti,E. *et al.* Toll-like receptor signaling pathway in chronic lymphocytic leukemia: distinct gene expression profiles of potential pathogenic significance in specific subsets of patients. *Haematologica* **96**, 1644-1652 (2011).

234. Muzio,M. *et al.* Expression and function of toll like receptors in chronic lymphocytic leukaemia cells. *Br. J Haematol.* **144**, 507-516 (2009).

235. Dadashian,E.L. *et al.* TLR Signaling Is Activated in Lymph Node Resident CLL Cells and Is Only Partially Inhibited by Ibrutinib. *Cancer Res* **79**, 360-371 (2019).

236. Shaffer,A.L. *et al.* A library of gene expression signatures to illuminate normal and pathological lymphoid biology. *Immunological Reviews* **210**, 67-85 (2006).

237. Bomben,R. *et al.* The miR-17-92 family regulates the response to Toll-like receptor 9 triggering of CLL cells with unmutated IGHV genes. *Leukemia* **26**, 1584-1593 (2012).

238. Mongini,P.K.A. *et al.* TLR-9 and IL-15 Synergy Promotes the In Vitro Clonal Expansion of Chronic Lymphocytic Leukemia B Cells. *J Immunol* **195**, 901-923 (2015).

239. Leadbetter,E.A. *et al.* Chromatin-IgG complexes activate B cells by dual engagement of IgM and Toll-like receptors. *Nature* **416**, 603-607 (2002).

240. Tromp,J.M. *et al.* Dichotomy in NF-kappaB signaling and chemoresistance in immunoglobulin variable heavy-chain-mutated versus unmutated CLL cells upon CD40/TLR9 triggering. *Oncogene* **29**, 5071-5082 (2010).

241. Ntoufa,S. *et al.* Distinct innate immunity pathways to activation and tolerance in subgroups of chronic lymphocytic leukemia with distinct immunoglobulin receptors. *Mol Med* **18**, 1281-1291 (2012).

242. Chatzouli,M. *et al.* Heterogeneous functional effects of concomitant B cell receptor and TLR stimulation in chronic lymphocytic leukemia with mutated versus unmutated Ig genes. *J. Immunol.* **192**, 4518-4524 (2014).

243. Decker,T. *et al.* Immunostimulatory CpG-oligonucleotides cause proliferation, cytokine production, and an immunogenic phenotype in chronic lymphocytic leukemia B cells. *Blood* **95**, 999-1006 (2000).

244. Ntoufa,S., Vilia,M.G., Stamatopoulos,K., Ghia,P., & Muzio,M. Toll-like receptors signaling: A complex network for NF-kappaB activation in B-cell lymphoid malignancies. *Semin. Cancer Biol.* **39**, 15-25 (2016).

245. Singer,J.W. *et al.* Comprehensive kinase profile of pacritinib, a nonmyelosuppressive Janus kinase 2 inhibitor. *J Exp Pharmacol* **8**, 11-19 (2016).

246. Herman,S.E.M. *et al.* Bruton tyrosine kinase represents a promising therapeutic target for treatment of chronic lymphocytic leukemia and is effectively targeted by PCI-32765. *Blood* **117**, 6287-6296 (2011).

247. Herman,S.E.M. *et al.* Ibrutinib inhibits BCR and NF-kB signaling and reduces tumor proliferation in tissue-resident cells of patients with CLL. *Blood* **123**, 3286-3295 (2014).

248. Hanna,B.S., Ozturk,S., & Seiffert,M. Beyond bystanders: Myeloid cells in chronic lymphocytic leukemia. *Blood* **110**, 77-87 (2017).

249. Hornung,V. *et al.* Quantitative Expression of Toll-Like Receptor 1-10 mRNA in Cellular Subsets of Human Peripheral Blood Mononuclear Cells and Sensitivity to CpG Oligodeoxynucleotides. *J. Immunol.* **168**, 4531-4537 (2002).

250. Ozinsky,A. *et al.* The repertoire for pattern recognition of pathogens by the innate immune system is defined by cooperation between Toll-like receptors. *Proc Natl Acad Sci USA* **97**, 13766-13771 (2000).

251. Bresin A, *et al.* TCL1 transgenic mouse model as a tool for the study of therapeutic targets and microenvironment in human B-cell chronic lymphocytic leukemia. *Cell Death Dis* **7**, e2171 1-11 (2016).

252. Hanna,B.S. *et al.* Depletion of CLL-associated patrolling monocytes and macrophages controls disease development and repairs immune dysfunction in vivo. *Leukemia* **30**, 570-579 (2016).

253. McClanahan,F. *et al.* PD-L1 checkpoint blockade prevents immune dysfunction and leukemia development in a mouse model of chronic lymphocytic leukemia. *Blood* **126**, 203-211 (2015).

254. Seiffert,M. *et al.* Soluble CD14 is a novel monocyte-derived survival factor for chronic lymphocytic leukemia cells, which is induced by CLL cells in vitro and present at abnormally high levels in vivo. *Blood* **116**, 4223-4230 (2010).

255. Schulz,A. *et al.* Inflammatory cytokines and signaling pathways are associated with survival of primary chronic lymphocytic leukemia cells in vitro: a dominant role of CCL2. *Haematologica* **96**, 408-416 (2011).

256. Galletti,G. *et al.* Targeting Macrophages Sensitizes Chronic Lymphocytic Leukemia to Apoptosis and Inhibits Disease Progression. *Cell Rep.* **14**, 1748-1760 (2016).

257. Hanna,B.S. *et al.* Control of chronic lymphocytic leukemia development by clonally-expanded CD8(+) T-cells that undergo functional exhaustion in secondary lymphoid tissues. *Leukemia* **33**, 625-637 (2019).

258. Riches,J.C. *et al.* T cells from CLL patients exhibit features of T-cell exhaustion but retain capacity for cytokine production. *Blood* **121**, 1612-1621 (2013).

259. McClanahan,F.A. *et al.* Mechanisms of PD-L1/PD-1-mediated CD8 T-cell dysfunction in the context of aging-related immune defects in the Eu-TCL1 CLL mouse model. *Blood* **126**, 212-221 (2015).

260. Ramsay,A.G. *et al.* Chronic lymphocytic leukemia T cells show impaired immunological synapse formation that can be reversed with an immunomodulating drug. *J Clin Invest* **118**, 2427-2437 (2008).

261. Kozako,T. *et al.* PD-1/PD-L1 expression in human T-cell leukemia virus type 1 carriers and adult T-cell leukemia/lymphoma patients. *Leukemia* **23**, 375-382 (2008).

262. Mumprecht,S., Schurch,C., Schwaller,J., Solenthaler,M., & Ochsenbein,A.F. Programmed death 1 signaling on chronic myeloid leukemia–specific T-cells results in T-cell exhaustion and disease progression. *Blood* **114**, 1528-1536 (2009).

263. Zhou,Q. *et al.* Coexpression of Tim-3 and PD-1 identifies a CD8+ T-cell exhaustion phenotype in mice with disseminated acute myelogenous leukemia. *Blood* **117**, 4501-4510 (2011).

264. Hofbauer,J.P. *et al.* Development of CLL in the TCL1 transgenic mouse model is associated with severe skewing of the T-cell compartment homologous to human CLL. *Leukemia* **25**, 1452-1458 (2011).

265. Gorgun,G. *et al.* Eu-TCL1 mice represent a model for immunotherapeutic reversal of chronic lymphocytic leukemia-induced T-cell dysfunction. *Proc Natl Acad Sci USA* **106**, 6250-6255 (2009).

266. Van den Hove,L.E. *et al.* Peripheral blood lymphocyte subset shifts in patients with untreated hematological tumors: Evidence for systemic activation of the T cell compartment. *Leukemia Research* **22**, 175-184 (1998).

267. Gelman,A.E., Zhang,J., Choi,Y., & Turka,L.A. Toll-Like Receptor Ligands Directly Promote Activated CD4+ T Cell Survival. *J. Immunol.* **172**, 6065-6073 (2004).

268. Voo,K.S. *et al.* Targeting of TLRs Inhibits CD4+ Regulatory T Cell Function and Activates Lymphocytes in Human Peripheral Blood Mononuclear Cells. *J. Immunol.* **193**, 627-634 (2014).

269. Davids,M.S. & Brown,J.R. Ibrutinib: a first in class covalent inhibitor of Bruton's tyrosine kinase. *Future Oncology* **10**, 957-967 (2014).

270. Ntoufa,S. *et al.* B Cell Anergy Modulated by TLR1/2 and the miR-17–92 Cluster Underlies the Indolent Clinical Course of Chronic Lymphocytic Leukemia Stereotyped Subset #4. *J. Immunol.* **196**, 4410-4417 (2016).

271. Treon,S.P. *et al.* Ibrutinib in Previously Treated Waldenstrom Macroglobulinemia. *N. Engl. J. Med* **372**, 1430-1440 (2015).

272. Treon,S.P. *et al.* MYD88 L265P Somatic Mutation in Waldenstr+Âm's Macroglobulinemia. *N. Engl. J. Med* **367**, 826-833 (2012).

273. Ciriello,G. *et al.* Emerging landscape of oncogenic signatures across human cancers. *Nature Genetics* **45**, 1127-1133 (2013).

274. Burotto,M., Chiou,V.L., Lee,J.M., & Kohn,E.C. The MAPK pathway across different malignancies: a new perspective. *Cancer* **120**, 3446-3456 (2014).

275. Leeksma,A.C. *et al.* Clonal diversity predicts adverse outcome in chronic lymphocytic leukemia. *Leukemia* **33**, 390-402 (2019).

276. Downward,J. Targeting RAS signalling pathways in cancer therapy. *Nat. Rev. Cancer* **3**, 11-22 (2003).

277. Imperial,R., Toor,O.M., Hussain,A., Subramanian,J., & Masood,A. Comprehensive pancancer genomic analysis reveals (RTK)-RAS-RAF-MEK as a key dysregulated pathway in cancer: Its clinical implications. *Semin. Cancer Biol* **54**, 14-28 (2019).

278. Warden,D.W. *et al.* Phospho-ERK(THR202/Tyr214) is overexpressed in hairy cell leukemia and is a useful diagnostic marker in bone marrow trephine sections. *Am. J. Surg. Pathol.* **37**, 305-308 (2013).

279.Tiacci,E. *et al.* BRAF mutations in hairy-cell leukemia. *N. Engl. J. Med.* **364**, 2305-2315 (2011).

280.Damm,F. *et al.* Acquired Initiating Mutations in Early Hematopoietic Cells of CLL Patients. *Cancer Discovery* **4**, 1088-1101 (2014).

281.Wan,P.T. *et al.* Mechanism of activation of the RAF-ERK signaling pathway by oncogenic mutations of B-RAF. *Cell* **116**, 855-867 (2004).

282.Pandzic,T. *et al.* Transposon Mutagenesis Reveals Fludarabine Resistance Mechanisms in CLL. *Clin. Cancer Res.* **22**, 6217-6227 (2016).

283.Waterfall,J.J. *et al.* High prevalence of MAP2K1 mutations in variant and IGHV4-34-expressing hairy-cell leukemias. *Nature Genetics* **46**, 8-10 (2014).

284.Brown,N.A. *et al.* High prevalence of somatic MAP2K1mutations in BRAFV600Enegative Langerhans cell histiocytosis. *Blood* **124**, 1655-1658 (2014).

285.Schmidt,J. *et al.* Mutations of MAP2K1 are frequent in pediatric-type follicular lymphoma and result in ERK pathway activation. *Blood* **130**, 323-327 (2017).

286.Vendramini,E. *et al.* KRAS, NRAS, and BRAF mutations are highly enriched in trisomy 12 chronic lymphocytic leukemia and are associated with shorter treatment-free survival. *Leukemia* **33**, 2111-2115 (2019).

287.Takahashi,K. *et al.* Clinical implications of cancer gene mutations in patients with chronic lymphocytic leukemia treated with lenalidomide. *Blood* **131**, 1820-1832 (2018).

288.Bulian,P. *et al.* Mutational status of IGHV is the most reliable prognostic marker in trisomy 12 chronic lymphocytic leukemia. *Haematologica* **102**, 443-446 (2017).

289.Zucchetto,A. *et al.* CD49d is overexpressed by trisomy 12 chronic lymphocytic leukemia cells: evidence for a methylation-dependent regulation mechanism. *Blood* **122**, 3317-3321 (2013).

290.Chin,L., Andersen,J.N., & Futreal,P.A. Cancer genomics: from discovery science to personalized medicine. *Nature Medicine* **17**, 297-303 (2011).

291.Wilhelm,S. *et al.* Discovery and development of sorafenib: a multikinase inhibitor for treating cancer. *Nature Reviews Drug Discovery* **5**, 835-844 (2006).

292.Chapman,P.B. *et al.* Improved survival with vemurafenib in melanoma with BRAF V600E mutation. *N. Engl. J. Med.* **364**, 2507-2516 (2011).

293.Dietrich,S. *et al.* BRAF inhibition in hairy cell leukemia with low-dose vemurafenib. *Blood* **127**, 2847-2855 (2016).

294.Follows,G.A. *et al.* Rapid response of biallelic BRAF V600E mutated hairy cell leukaemia to low dose vemurafenib. *Br. J. Haematol.* **161**, 150-153 (2013).

295.Villanueva,J., Vultur,A., & Herlyn,M. Resistance to BRAF inhibitors: unraveling mechanisms and future treatment options. *Cancer Res* **71**, 7137-7140 (2011).

296.Alcalá,A.M. & Flaherty,K.T. BRAF Inhibitors for the Treatment of Metastatic Melanoma: Clinical Trials and Mechanisms of Resistance. *Clin. Cancer Res.* **18**, 33-39 (2012).

297. Emery,C.M. *et al.* MEK1 mutations confer resistance to MEK and B-RAF inhibition. *Proc Natl Acad Sci USA* **106**, 20411-20416 (2009).

298. Wagle,N. *et al.* Dissecting Therapeutic Resistance to RAF Inhibition in Melanoma by Tumor Genomic Profiling. *JCO.* **29**, 3085-3096 (2011).

299. Ribas,A. & Flaherty,K.T. BRAF targeted therapy changes the treatment paradigm in melanoma. *Nature Reviews Clinical Oncology* **8**, 426-433 (2011).

300. Eroglu,Z. & Ribas,A. Combination therapy with BRAF and MEK inhibitors for melanoma: latest evidence and place in therapy. *Ther Adv Med Oncol* **8**, 48-56 (2016).

301. Yaktapour,N. *et al.* BRAF inhibitor-associated ERK activation drives development of chronic lymphocytic leukemia. *J. Clin. Invest* **124**, 5074-5084 (2014).

302. Ryan,M.B., Der,C.J., Wang-Gillam,A., & Cox,A.D. Targeting RAS-mutant cancers: is ERK the key? *Trends Cancer* **1**, 183-198 (2015).

303. Dietrich,S. *et al.* Drug-perturbation-based stratification of blood cancer. *J. Clin. Invest* **128**, 427-445 (2018).

304. Coste, I. *et al.* T Dual function of MyD88 in RAS signaling and inflammation, leading to mouse and human cell transformation. *J Clin Invest.* **120**, 3663-3667 (2010).

305. Chen,J.G. *et al.* BTKCys481Ser drives ibrutinib resistance via ERK1/2 and protects BTKwild-type MYD88-mutated cells by a paracrine mechanism. *Blood* **131**, 2047-2059 (2018).

306. Butcher,E.C., Berg,E.L., & Kunkel,E.J. Systems biology in drug discovery. *Nature Biotechnology* **22**, 1253-1259 (2004).

307. Berg,E.L. Systems biology in drug discovery and development. *Drug Discovery Today* **19**, 113-125 (2014).

308. Purroy,N. *et al.* Co-culture of primary CLL cells with bone marrow mesenchymal cells, CD40 ligand and CpG ODN promotes proliferation of chemoresistant CLL cells phenotypically comparable to those proliferating in vivo. *Oncotarget* **6**, 7632-7643 (2015).

309. Pantziarka,P. *et al.* The Repurposing Drugs in Oncology (ReDO) Project. *E.cancer medical science* **8**, 442 (2014).

310. Chong,P.H., Seeger,J.D., & Franklin,C. Clinically relevant differences between the statins: implications for therapeutic selection. *The American Journal of Medicine* **111**, 390-400 (2001).

311. Plosker,G.L. & McTavish,D. Simvastatin. A reappraisal of its pharmacology and therapeutic efficacy in hypercholesterolaemia. *Drugs* **50**, 334-363 (1995).

312. Pisanti,S., Picardi,P., Ciaglia,E., DΓÇÖAlessandro,A., & Bifulco,M. Novel prospects of statins as therapeutic agents in cancer. *Pharmacological Research* **88**, 84-98 (2014).

313. Gazzerro,P. *et al.* Pharmacological Actions of Statins: A Critical Appraisal in the Management of Cancer. *Pharmacol Rev* **64**, 102 (2012).

314. Federica,I. *et al.* Targeting Mevalonate Pathway in Cancer Treatment: Repurposing of Statins. *Recent Patents. on Anti. -Cancer Drug Discovery* **13**, 184-200 (2018).

315. Minden,M.D., Dimitroulakos,J., Nohynek,D., & Penn,L.Z. Lovastatin Induced Control of Blast Cell Growth in an Elderly Patient with Acute Myeloblastic Leukemia. *Leukemia & Lymphoma* **40**, 659-662 (2001).

316. Dimitroulakos,J. *et al.* Increased Sensitivity of Acute Myeloid Leukemias to Lovastatin-Induced Apoptosis: A Potential Therapeutic Approach. *Blood* **93**, 1308 (1999).

317. Bockorny,B. & Dasanu,C.A. HMG-CoA reductase inhibitors as adjuvant treatment for hematologic malignancies: what is the current evidence? *Annals. of Hematology* **94**, 1-12 (2015).

318. Yi,X., Jia,W., Jin,Y., & Zhen,S. Statin use is associated with reduced risk of haematological malignancies: evidence from a meta-analysis. *PLoS One* **9; e87019**, 1-8 (2014).

319. Sanfilippo,K.M. *et al.* Statins Are Associated With Reduced Mortality in Multiple Myeloma. *JCO.* **34**, 4008-4014 (2016).

320. Chapman-Shimshoni,D., Yuklea,M., Radnay,J., Shapiro,H., & Lishner,M. Simvastatin induces apoptosis of B-CLL cells by activation of mitochondrial caspase 9. *Experimental Hematology* **31**, 779-783 (2003).

321. Qi,X.F. *et al.* HMG-CoA reductase inhibitors induce apoptosis of lymphoma cells by promoting ROS generation and regulating Akt, Erk and p38 signals via suppression of mevalonate pathway. *Cell Death. &Amp; Disease* **4**, e518 (2013).

322. Righolt,C.H. *et al.* Statin Use and Chronic Lymphocytic Leukemia Incidence: A Nested Case–Control Study in Manitoba, Canada. *Cancer Epidemiology Biomarkers Prevention* **[Epub ahead of print]**, (2019).

323. Schramm,R. *et al.* Statins inhibit lymphocyte homing to peripheral lymph nodes. *Immunology* **120**, 315-324 (2007).

324. Arnaout,M.A. Structure and Function of the Leukocyte Adhesion Molecules CD11/CD18. *Blood* **75**, 1037-1050 (1990).

325. Kim,M., Carman,C.V., Yang,W., Salas,A., & Springer,T.A. The primacy of affinity over clustering in regulation of adhesiveness of the integrin aLB2. *J Cell Biol* **167**, 1241 (2004).

326. Hazlehurst,L.A., Landowski,T.H., & Dalton,W.S. Role of the tumor microenvironment in mediating de novo resistance to drugs and physiological mediators of cell death. *Oncogene* **22**, 7396-7402 (2003).

327. Davids,M.S. & Burger,J.A. Cell Trafficking in hronic Lymphocytic Leukemia. *Open. J. Hematol.* **3**, 1-13 (2012).

328. Lee,J.S. *et al.* Statins enhance efficacy of venetoclax in blood cancers. *Science Translational Medicine* **10**, eaaq1240 1-10 (2018).

ACKNOWLEDGEMENTS

Miro enrere i recordo perfectament el primer dia que vaig venir a visitar el laboratori. Era pels volts de Nadal, i vaig portar una flor de la sort, per desitjar que el següent any que començava (i amb ell, la meva tesi) fos molt fructífer. I fent valoració, puc dir que aquella flor va fer el seu efecte.

He de donar les gràcies perquè afortunadament aquest camí no l'he fet sola, sinó que han estat moltes les persones que m'han acompanyat i han contribuït a que fos possible. Han estat 3 anys en els que he après molt, i he crescut tant a nivell professional, com personal.

En primer lloc, et volia agrair **Dolors** per haver-me donat la oportunitat, perquè des del primer dia t'he sentit propera, per ensenyar-me i acompanyar-me en tots els moments. Perquè durant aquests anys he pogut comptar sempre amb la teva ajuda, sense importar els mil fronts oberts que tinguessis alhora. M'he sentit molt realitzada, i sobretot molt estimada. Considero que sóc molt afortunada d'haver picat a la porta del grup que lideres, ha estat un veritable plaer treballar amb tu.

Alhora, agrair a la **Judith**, i a tots els membres d'Anaxomics, sobretot la **Merche** i en **Xose**, per haver-me ajudat a dur a terme aquest Doctorat Industrial. Agrair sobretot la seva amabilitat, professionalitat i proximitat des del primer dia.

De la mateixa manera, agrair també al Dr. **Elias Campo** per haver estat tutor i codirector de la tesi, i també per les aportacions i revisions constructives dels nostres articles.

Patricia, gràcies per obrir cada dia el laboratori amb un somriure. Les teves idees i punts de vista científics, han enriquit el meu pas pel laboratori, però et vull agrair sobretot la teva energia, així com el relat de totes les peripècies domèstiques!

En especial gràcies al grup de recerca "*Apoptosis team.*" Primerament a la **Laia**, per tota la feina i lluita que hem fet juntes. Durant tres anys, hem pencat cada dia colze a colze, i realment ha estat un plaer. Has estat la meva mestra, consellera i confessora, senzillament gràcies. A les veteranes **Mònica i Eriong.** Amb caràcters ben diferents, totes dues m'heu ensenyat què vol dir fer recerca, i formar part d'un equip. Gràcies Mònica, perquè sempre m'he sentit acompanyada i recolzada per tu. Gràcies Eriong pels viatges compartits. **Irene,** basca médica mujer investigadora. Gracias por tu carácter, por enseñarme qué significa tener las ideas claras, y por tus ganas de trabajar, buscando el clon el perdido... es un placer trabajar contigo. Segur que en dos dies parles el català més correcte que nosaltres! A **l'Heribert** i la **Cèlia**, per tot l'entusiasme que m'heu transmès des del primer dia. Molta sort amb la tesi! A l'**Arnau,** per haver-me ajudat i ensenyat durant els primers mesos, i haver demostrat que els farmacèutics també podem fer recerca básica! I express my heartflet thanks to **Morihiro**, **Rupal** and **Berta**, who were part of our multi-cultural team. I loved it!

Jocabed i Ariadna, aconseguiu posar ordre dins el nostre caos, i així és un gust treballar. Gràcies Ariadna per ser la celíaca més divertida que conec, i explicar mil batalles que sempre arrenquen un somriure.

I am very thankful to **Ralph, Hanni, Selcen, Lavinia** and **Tina**, for warmly receiving me in their research team, and giving me the opportunity to gain invaluable experience and new insights to further shape my work.

Laura Llaó, gràcies per ser la millor companya que podia tenir a l'estada a Heidelberg. Per les hores de laboratori, pels caps de setmana de feina, per les confessions "fit for fun", i un miler de records que em vaig endur. Però sobretot, gràcies per la teva amistat.

El grup de la Patricia /Gael ha canviat molt, però agrair especialment a en **Juan**, per les seves idees boges, i l'entusiasme en tot allò que se li proposa. Agrair també a la Martina, la Neus, la Clara, en Fabián, l'Anna Vidal, l'Anna Esteve, l'Alba, l'Arantxa i la Vani, gràcies per acompanyar-me i fer pinya tot aquest temps.

Julio Delgado, Manel Juan i **Neus Villamor**, gràcies per la vostra ajuda i per totes les aportacions clíniques als treballs que hem compartit.

Marta Diví, gràcies per fer que la organització i la burocràcia semblessin fins i tot divertides.

Fora del laboratori, tinc la sort de tenir grans companys de vida, que m'acompanyen en totes les etapes que vaig construint:

A la meva família, per qui un "gràcies", es fa curt. Gràcies **mama** i **papa**, per ser-hi sempre. Per ser el meu punt de referència. Per quan tinc les idees clares, empènyer-me, i per quan dubto, agafar-me de la mà amb els millors consells. **Anna**, gràcies per ser el millor regal de Nadal que podia somniar, ets essència en cadascun dels meus dies. Als **avis**, per recordar-me la importància de la constància i el treball.

A en **Miquel**, l'amor de la meva vida. Senzillament gràcies per fer-me feliç cada dia. I a en **David** i la **Glòria**, per mimar-me i cuidar-me infinitament. Gràcies per fer-me sentir tan estimada.

Al meu grup d'amics de sempre, **Àlex, Alicia, Anna's, Carla, Cris, Elena, Eli, Georgina, Irene, Jovani, Laia, Lidia, Marina, Núria, Sandra, Xavi E i**, gràcies per creure en mi, i pels moments bojos que ens han fet créixer junts durant més de 20 anys. A la **Judit**, la **Dolo** i la **Marina**, per acompanyar-me durant tota la carrera, i seguir amb una amistat indescriptible. I a en **Jorge**, que ha acabat sent doctor abans que jo, gràcies per tot el recolzament!

Als **pacients**, les mostres dels quals han permès que es realitzi aquesta tesi doctoral.

Moltes gràcies a tots, sense vosaltres no ho hauria aconseguit.

ANNEXES

ANNEX I: WORKS PRESENTED AT NATIONAL AND INTERNATIONAL CONFERENCES DERIVED FROM THE THESIS

Title: Targeting IRAK4 disrupts inflammatory pathways and delays tumor development in chronic lymphocytic leukemia regardless *MYD88* mutational status

Authors: Laia Rosich, **Neus Giménez**, Ralph Schulz, Morihiro Higashi, Marta Aymerich, Neus Villamor, Julio Delgado, Manel Juan, Monica López-Guerra, Elias Campo, Martina Seiffert, Dolors Colomer

Type of participation: Poster

Congress: European Hematology Association (EHA) Annual Meeting. Amsterdam, June 2019

Title: Targeting IRAK4 disrupts inflammatory pathways and delays tumor development in chronic lymphocytic leukemia

Authors: Neus Giménez

Type of participation: Oral communication

Congress: 4th Lymphoid Neoplasm Program Scientific Retreat. Montserrat, Spain, March 2019

Title: IRAK4 com a diana terapèutica en la leucèmia limfàtica crònica

Authors: Neus Giménez

Type of participation: Oral communication

Congress: Hematopathology scientific sessions. Barcelona, Spain, February 2019

Title: Targeting IRAK4 disrupts inflammatory pathways and tumor microenvironment in chronic lymphocytic leukemia

Authors: <u>Neus Giménez</u>, Laia Rosich, Ralph Schulz, Morihiro Higashi, Marta Aymerich Monica Lopez-Guerra, Manel Juan, Martina Seiffert, Elias Campo, Dolors Colomer

Type of participation: Poster

Congress: 60th American Society of Hematology (ASH) Annual Meeting and Exposition. San Diego, USA, December 2018

Title: Targeting IRAK4 disrupts inflammatory pathways and tumor microenvironment in chronic lymphocytic leukemia

Authors: <u>Neus Giménez</u>

Type of participation: Oral communication

Congress: XIth International Workshop of the German CLL Study Group. Cologne, Germany, September 2018

Title: Targeting IRAK4 disrupts inflammatory pathways and tumor microenvironment in chronic lymphocytic leukemia regardless MYD88 mutational status

Authors: Laia Rosich, **<u>Neus Giménez</u>**, Ralph Schulz, Morihiro Higashi, Marta Aymerich, Monica López-Guerra, Manel Juan, Martina Seiffert, Elias Campo, Dolors Colomer

Type of participation: Poster

Congress: American Association for Cancer Researcher (AACR) Annual Meeting. Chicago, USA, April 2018

Title: Targeting TLR Signaling in Chronic Lymphocytic Leukemia with a Selective IRAK-4 Inhibitor

Authors: <u>Neus Giménez</u>, Laia Rosich, Ralph Schulz, Morihiro Higashi, Marta Aymerich, Monica López-Guerra, Martina Seiffert, Elias Campo, Dolors Colomer

Type of participation: Poster

Congress: II CIBERONC General Meeting. Madrid, Spain, February 2018

Title: Targeting CLL with a selective IRAK-4 inhibitor: ND2158

Authors: <u>Neus Giménez</u>

Type of participation: Oral Communication

Congress: DKFZ general session TP3. Heidelberg, Germany, December 2018

Title: Targeting TLR Signaling in Chronic Lymphocytic Leukemia with a Selective IRAK4 Inhibitor

Authors: <u>Neus Giménez</u>, Laia Rosich, Eriong Lee, Morihiro Higashi, Marta Aymerich, Monica López-Guerra, Elias Campo, Dolors Colomer

Type of participation: Poster

Congress: XVIIth International Workshop on Chronic Lymphocytic Leukemia. New York, USA, May 2017

Title: Targeting chronic lymphocytic leukemia with selective interleukin-1 receptor-associated kinase 4 (IRAK-4) inhibitor

Authors: <u>Neus Gimenez</u>, Laia Rosich, Arnau Montraveta, Eriong Lee-Vergés, Monica López-Guerra, Elias Campo, Dolors Colomer

Type of participation: Poster

Congress: Pittsburgh Conference & Exposition (Pittcon). Chicago, USA, March 2017

Title: Targeting chronic lymphocytic leukemia with selective interleukin-1 receptor-associated kinase 4 (IRAK-4) inhibitor

Authors: <u>Neus Giménez</u>, Laia Rosich, Arnau Montraveta, Eriong Lee-Vergés, Monica Lopez-Guerra, Elias Campo, Dolors Colomer

Type of participation: Poster

Congress: X[th] International Workshop on the occasion of the 20th anniversary of the German CLL Study Group. Cologne, Germany, Setember 2016

ANNEX II: PAPERS IN COLLABORATION

New drug discovery approaches targeting recurrent mutations
in chronic lymphocytic leukemia

Tripathi R, Lee-Verges E, Higashi M, **Giménez N**, Rosich L, Lopez-Guerra M, Colomer D.

Expert Opinion on Drug Discovery. **2017** Oct;12(10):1041-1052.

ABSTRACT

Next generation sequencing has provided a comprehensive understanding of the mutational landscape in chronic lymphocytic leukemia (CLL), and new drivers have been identified. Some of these drivers could be pharmacologically targeted to choose the most effective personalized therapy in each CLL patient. Areas covered: In this article, the authors uncover the potential role of new targeted therapies against the most recurrent mutations in CLL as well as the recently approved therapies. The authors also provide their expert opinion and give their perspectives for the future. Expert opinion: The development of more personalized therapies is of interest to clinicians as a system to enhance the duration of treatment response and to extend the survival and quality of life of CLL patients. The main challenge, however, will be to translate the preclinical results into the clinics. Therefore, the designing and execution of clinical trials focused on molecular drivers are the need of the hour.

REVIEW

Check for updates

New drug discovery approaches targeting recurrent mutations in chronic lymphocytic leukemia

Rupal Tripathi, Eriong Lee-Verges, Morihiro Higashi, Neus Gimenez, Laia Rosich, Monica Lopez-Guerra and Dolors Colomer

Experimental Therapeutics in Lymphoid Malignancies Group, Institut d'Investigacions Biomèdiques August Pi i Sunyer (IDIBAPS), Hematopathology Unit, Hospital Clinic, CIBERONC, Barcelona, Spain

ABSTRACT

Introduction: Next generation sequencing has provided a comprehensive understanding of the mutational landscape in chronic lymphocytic leukemia (CLL), and new drivers have been identified. Some of these drivers could be pharmacologically targeted to choose the most effective personalized therapy in each CLL patient.

Areas covered: In this article, the authors uncover the potential role of new targeted therapies against the most recurrent mutations in CLL as well as the recently approved therapies. The authors also provide their expert opinion and give their perspectives for the future.

Expert opinion: The development of more personalized therapies is of interest to clinicians as a system to enhance the duration of treatment response and to extend the survival and quality of life of CLL patients. The main challenge, however, will be to translate the preclinical results into the clinics. Therefore, the designing and execution of clinical trials focused on molecular drivers are the need of the hour.

Cyclin D1-CDK4 activity drives sensitivity to bortezomib in mantle cell lymphoma by blocking autophagy-mediated proteolysis of NOXA

Heine S, Kleih M, **Giménez N**, Böpple K, Ott G, Colomer D, Aulitzky WE, van der Kuip H, Silkenstedt E.

ABSTRACT

Background: Mantle cell lymphoma (MCL) is an aggressive B-non-Hodgkin lymphoma with generally poor outcome.MCL is characterized by an aberrantly high cyclin D1-driven CDK4 activity. New molecular targeted therapies such as inhibitors of the ubiquitin-proteasome system (UPS) have shown promising results in preclinical studies and MCL patients. Our previous research revealed stabilization of the short-lived pro-apoptotic NOXA as a critical determinant for sensitivity to these inhibitors. It is currently unclear how cyclin D1 overexpression and aberrant CDK4 activity affect NOXA stabilization and treatment efficacy of UPS inhibitors in MCL. Methods: The effect of cyclin D1-driven CDK4 activity on response of MCL cell lines and primary cells to proteasome inhibitor treatment was investigated using survival assays (Flow cytometry, AnnexinV/PI) and Western blot analysis of NOXA protein. Half-life of NOXA protein was determined by cycloheximide treatment and subsequent Western blot analysis. The role of autophagy was analyzed by LC3-II protein expression and autophagolysosome detection. Furthermore, silencing of autophagy-related genes was performed using siRNA and MCL cells were treated with autophagy inhibitors in combination with proteasome and CDK4 inhibition. Results: In this study, we show that proteasome inhibitor-mediated cell death in MCL depends on cyclin D1-driven CDK4 activity. Inhibition of cyclin D1/CDK4 activity significantly reduced proteasome inhibitor-mediated stabilization of NOXA protein, mainly driven by an autophagy-mediated proteolysis. Bortezomib-induced cell death was significantly potentiated by compounds that interfere with autophagosomal function. Combined treatment with bortezomib and autophagy inhibitors enhanced NOXA stability leading to super-induction of NOXA protein. In addition to established autophagy modulators, we identified the fatty acid synthase inhibitor orlistat to be an efficient autophagy inhibitor when used in combination with bortezomib. Accordingly, this combination synergistically induced apoptosis both in MCL cell lines and in patient samples. Conclusion: Our data demonstrate that CDK4 activity in MCL is critical for NOXA stabilization upon treatment with UPS inhibitors allowing preferential induction of cell death in cyclin D transformed cells. Under UPS blocked conditions, autophagy appears as the critical regulator of NOXA induction. Therefore, inhibitors of autophagy are promising candidates to increase the activity of proteasome inhibitors in MCL.

Journal of
Hematology & Oncology

RESEARCH

Open Access

Cyclin D1-CDK4 activity drives sensitivity to bortezomib in mantle cell lymphoma by blocking autophagy-mediated proteolysis of NOXA

Simon Heine[1,6]*[iD], Markus Kleih[1,6], Neus Giménez[2], Kathrin Böpple[1,6], German Ott[3], Dolors Colomer[2], Walter E. Aulitzky[4], Heiko van der Kuip[1,6]^ and Elisabeth Silkenstedt[1,4,5,6]

Abstract

Background: Mantle cell lymphoma (MCL) is an aggressive B-non-Hodgkin lymphoma with generally poor outcome. MCL is characterized by an aberrantly high cyclin D1-driven CDK4 activity. New molecular targeted therapies such as inhibitors of the ubiquitin-proteasome system (UPS) have shown promising results in preclinical studies and MCL patients. Our previous research revealed stabilization of the short-lived pro-apoptotic NOXA as a critical determinant for sensitivity to these inhibitors. It is currently unclear how cyclin D1 overexpression and aberrant CDK4 activity affect NOXA stabilization and treatment efficacy of UPS inhibitors in MCL.

Methods: The effect of cyclin D1-driven CDK4 activity on response of MCL cell lines and primary cells to proteasome inhibitor treatment was investigated using survival assays (Flow cytometry, AnnexinV/PI) and Western blot analysis of NOXA protein. Half-life of NOXA protein was determined by cycloheximide treatment and subsequent Western blot analysis. The role of autophagy was analyzed by LC3-II protein expression and autophagolysosome detection. Furthermore, silencing of autophagy-related genes was performed using siRNA and MCL cells were treated with autophagy inhibitors in combination with proteasome and CDK4 inhibition.

Results: In this study, we show that proteasome inhibitor-mediated cell death in MCL depends on cyclin D1-driven CDK4 activity. Inhibition of cyclin D1/CDK4 activity significantly reduced proteasome inhibitor-mediated stabilization of NOXA protein, mainly driven by an autophagy-mediated proteolysis. Bortezomib-induced cell death was significantly potentiated by compounds that interfere with autophagosomal function. Combined treatment with bortezomib and autophagy inhibitors enhanced NOXA stability leading to super-induction of NOXA protein. In addition to established autophagy modulators, we identified the fatty acid synthase inhibitor orlistat to be an efficient autophagy inhibitor when used in combination with bortezomib. Accordingly, this combination synergistically induced apoptosis both in MCL cell lines and in patient samples.

Conclusion: Our data demonstrate that CDK4 activity in MCL is critical for NOXA stabilization upon treatment with UPS inhibitors allowing preferential induction of cell death in cyclin D transformed cells. Under UPS blocked conditions, autophagy appears as the critical regulator of NOXA induction. Therefore, inhibitors of autophagy are promising candidates to increase the activity of proteasome inhibitors in MCL.

Keywords: Mantle cell lymphoma, Bortezomib, NOXA, CDK4, Autophagy

Specific NOTCH1 antibody targets DLL4-induced proliferation, migration, and angiogenesis in NOTCH1-mutated CLL cells

López-Guerra M, Xargay-Torrent S, Fuentes P, Roldán J, González-Farré B, Rosich L, Silkenstedt E, García-León MJ, Lee-Vergés E, **Giménez N**, Giró A, Aymerich M, Villamor N, Delgado J, López-Guillermo A, Puente XS, Campo E, Toribio ML, Colomer D.

ABSTRACT

Targeting Notch signaling has emerged as a promising therapeutic strategy for chronic lymphocytic leukemia (CLL), particularly in NOTCH1-mutated patients. We provide first evidence that the Notch ligand DLL4 is a potent stimulator of Notch signaling in NOTCH1-mutated CLL cells while increases cell proliferation. Importantly, DLL4 is expressed in histiocytes from the lymph node, both in NOTCH1-mutated and -unmutated cases. We also show that the DLL4-induced activation of the Notch signaling pathway can be efficiently blocked with the specific anti-Notch1 antibody OMP-52M51. Accordingly, OMP-52M51 also reverses Notch-induced MYC, CCND1, and NPM1 gene expression as well as cell proliferation in NOTCH1-mutated CLL cells. In addition, DLL4 stimulation triggers the expression of protumor target genes, such as CXCR4, NRARP, and VEGFA, together with an increase in cell migration and angiogenesis. All these events can be antagonized by OMP-52M51. Collectively, our results emphasize the role of DLL4 stimulation in NOTCH1-mutated CLL and confirm the specific therapeutic targeting of Notch1 as a promising approach for this group of poor prognosis CLL patients.

ARTICLE

Specific NOTCH1 antibody targets DLL4-induced proliferation, migration, and angiogenesis in *NOTCH1*-mutated CLL cells

Mónica López-Guerra[1,2,3] · Sílvia Xargay-Torrent[1] · Patricia Fuentes[4] · Jocabed Roldán[1,2,3] ·
Blanca González-Farré[2,3,5] · Laia Rosich[1,3] · Elisabeth Silkenstedt[1,6] · María J. García-León[7] · Eriong Lee-Vergés[1,3] ·
Neus Giménez[1,3] · Ariadna Giró[1,3] · Marta Aymerich[1,2,3] · Neus Villamor[2,3] · Julio Delgado[3,8] ·
Armando López-Guillermo[3,5,8] · Xose S. Puente [3,9] · Elias Campo [2,3,5] · María L. Toribio [4] ·
Dolors Colomer [1,2,3,5]

Abstract

Targeting Notch signaling has emerged as a promising therapeutic strategy for chronic lymphocytic leukemia (CLL), particularly in *NOTCH1*-mutated patients. We provide first evidence that the Notch ligand DLL4 is a potent stimulator of Notch signaling in *NOTCH1*-mutated CLL cells while increases cell proliferation. Importantly, DLL4 is expressed in histiocytes from the lymph node, both in *NOTCH1*-mutated and -unmutated cases. We also show that the DLL4-induced activation of the Notch signaling pathway can be efficiently blocked with the specific anti-Notch1 antibody OMP-52M51. Accordingly, OMP-52M51 also reverses Notch-induced *MYC*, *CCND1*, and *NPM1* gene expression as well as cell proliferation in *NOTCH1*-mutated CLL cells. In addition, DLL4 stimulation triggers the expression of protumor target genes, such as *CXCR4*, *NRARP*, and *VEGFA*, together with an increase in cell migration and angiogenesis. All these events can be antagonized by OMP-52M51. Collectively, our results emphasize the role of DLL4 stimulation in *NOTCH1*-mutated CLL and confirm the specific therapeutic targeting of Notch1 as a promising approach for this group of poor prognosis CLL patients.